OCRWM	MODEL COVER SHEET	1. QA: QA Page 1 of ~~142~~ 140 ERT 7-21-03

2. Type of Mathematical Model:

☐ Process Model ☒ Abstraction Model ☐ System Model

Describe Intended Use of Model:

Provides input to the TSPA-LA.

3. Title:

In-Package Chemistry Abstraction

4. DI (including Rev. No. and Change No., if applicable):

ANL-EBS-MD-000037 REV 02

5. Total Attachments:	6. Attachment Numbers - No. of Pages in Each:
Five (5)	I-1, II-1, III-4, IV-1, V-1 CD-ROM

	Printed Name	Signature	Date
7. Originator:	Paul S. Domski	SIGNATURE ON FILE	7/19/03
8. CSO:	David Stahl	SIGNATURE ON FILE	7/19/03
9. Checker:	Emma Thomas	SIGNATURE ON FILE	7/21/03
10. QER:	Judith E. Gebhart	SIGNATURE ON FILE	7/21/03
11. Responsible Manager/Lead:	Howard E. Adkins	SIGNATURE ON FILE	07-21-03
12. Responsible Manager:	Thomas W. Doering	SIGNATURE ON FILE	7.21.03

13. Remarks:

Sara Arthur and Pat Brady also contributed to this report.

The TBVs for the input status for the two reports (ANL-EBS-MD-000015 and ANL-WIS-MD-000004) will be resolved when this document is updated to reference the latest versions of those reports.

TER-02-042 has been corrected in the current revision.

TER-03-008 has been corrected in the current revision.

2. Title:

In-Package Chemistry Abstraction

3. DI (including Rev. No. and Change No., if applicable):

ANL-EBS-MD-000037 REV 02

4. Revision / Change Number:	5. Description of Revision/Change:
00	Initial Issue.
01	The entire abstraction model was revised to reflect updated inputs/outputs from the feed process model AMR (ANL-EBS-MD-000050 REV 01).
02	Complete revision to incorporate new conceptual model.

CONTENTS

Page

1. PURPOSE 15

2. QUALITY ASSURANCE 16

3. COMPUTER SOFTWARE AND MODEL USAGE 17
   3.1 COMPUTER SOFTWARE 17

4. INPUTS 18
   4.1 DATA AND PARAMETERS 18
      4.1.1 Data 18
      4.1.2 Parameters 20
      4.1.3 Other Input 22
   4.2 CRITERIA 28
   4.3 CODES AND STANDARDS 28

5. ASSUMPTIONS 29
   5.1 INERT WASTE PACKAGE COMPONENTS 29
   5.2 WATER FILM 29
   5.3 FILM THICKNESS 29
   5.4 TRANSLATION OF MODEL RESPONSE 30

6. MODEL 30
   6.1 OBJECTIVES 30
   6.2 FEATURES, EVENTS, AND PROCESSES 31
   6.3 BASE-CASE CONCEPTUAL MODEL 33
      6.3.1 Film versus the Bathtub Model 34
      6.3.2 Water Vapor Condensation Model 36
      6.3.3 Seepage Dripping Model 39
      6.3.4 Sensitivity Cases—Uncertainty Analyses 46
   6.4 ALTERNATIVE CONCEPTUAL MODELS 47
      6.4.1 Alternative Conceptual Model I 47
      6.4.2 Alternative Conceptual Model II 48
   6.5 BASE-CASE MODEL INPUTS 48
      6.5.1 Waste Package Component Properties 48
      6.5.2 Single Component Water Vapor Condensation Model Inputs 50
      6.5.3 Multi-Component Ensemble Water Vapor Condensation Inputs 52
      6.5.4 Seepage Dripping Model Inputs 59
      6.5.5 Mineral Controls 63
   6.6 MODEL OUTPUT 66
      6.6.1 Commercial Spent Nuclear Fuel Output 66
      6.6.2 Codisposed N Reactor Output 73

CONTENTS (Continued)

Page

6.7 SENSITIVITY—UNCERTAINTY OUTPUT 79
6.7.1 Uncertainty Range 79
6.7.2 Limits of the In-Package Chemistry Model Abstraction 81
6.7.3 Effect of Waste Package Design 81

7. MODEL VALIDATION 82
7.1 PRODUCTION OF ALKALINE WATERS BY GLASS DISSOLUTION 85
7.2 ACID PRODUCTION FROM STEEL DISSOLUTION 85
7.3 PRODUCTION OF HIGH IONIC STRENGTH SOLUTIONS 87
7.4 SUMMARY 88

8. RESULTS AND CONCLUSIONS 88
8.1 COMMERCIAL SPENT NUCLEAR FUEL WATER VAPOR CONDENSATION IN-PACKAGE CHEMISTRY MODEL ABSTRACTION 88
8.1.1 Commercial Spent Nuclear Fuel Water Vapor Condensation pH Abstraction 88
8.1.2 Commercial Spent Nuclear Fuel Water Vapor Condensation Ionic Strength Abstraction 89
8.2 COMMERCIAL SPENT NUCLEAR FUEL SEEPAGE DRIPPING MODEL IN-PACKAGE CHEMISTRY MODEL ABSTRACTION 92
8.2.1 Commercial Spent Nuclear Fuel Seepage Dripping Model 25°C pH Abstraction 92
8.2.2 Commercial Spent Nuclear Fuel Seepage Dripping Model 50°C pH Abstraction 96
8.2.3 Commercial Spent Nuclear Fuel Seepage Dripping Model pH Temperature Dependence 97
8.2.4 Commercial Spent Nuclear Fuel Seepage Dripping Model 25°C Ionic Strength Abstraction 98
8.2.5 Commercial Spent Nuclear Fuel Seepage Dripping Model 50°C Ionic Strength Abstraction 101
8.2.6 Commercial Spent Nuclear Fuel Seepage Dripping Model Ionic Strength Temperature Dependence 102
8.2.7 Commercial Spent Nuclear Fuel Seepage Dripping Model 25°C and 50°C Fluoride Abstractions 104
8.2.8 Commercial Spent Nuclear Fuel Seepage Dripping Model 25°C and 50°C Chloride Abstractions 105
8.3 CODISPOSED N REACTOR WATER VAPOR CONDENSATION IN-PACKAGE CHEMISTRY MODEL ABSTRACTION 106
8.3.1 Codisposed N Reactor Water Vapor Condensation pH Abstraction 106
8.3.2 Codisposed N Reactor Water Vapor Condensation Ionic Strength Abstraction 108
8.3.3 Codisposed N Reactor Water Vapor Condensation Fluoride Abstraction 109

CONTENTS (Continued)

Page

8.4 CODISPOSED N REACTOR SEEPAGE DRIPPING MODEL IN-PACKAGE CHEMISTRY MODEL ABSTRACTION 110
8.4.1 Codisposed N Reactor Seepage Dripping Model 25°C pH Abstraction 110
8.4.2 Codisposed N Reactor Seepage Dripping Model 50°C pH Abstraction 114
8.4.3 Codisposed N Reactor Seepage Dripping Model pH Temperature Dependence 116
8.4.4 Codisposed N Reactor Seepage Dripping Model 25°C Ionic Strength Abstraction 117
8.4.5 Codisposed N Reactor Seepage Dripping Model 50°C Ionic Strength Abstraction 119
8.4.6 Codisposed N Reactor Seepage Dripping Model Ionic Strength Temperature Dependence 121
8.4.7 Codisposed N Reactor Seepage Dripping Model 25°C and 50°C Fluoride Abstraction 121
8.4.8 Codisposed N Reactor Seepage Dripping Model 25°C and 50°C Chloride Abstraction 123
8.5 TOTAL CARBONATE ABSTRACTION 124
8.6 Eh ABSTRACTION 126
8.7 OXYGEN AND CARBON DIOXIDE PARTIAL PRESSURE RANGE OF APPLICABILITY 128
8.8 ABSTRACTION VALIDATION 128
8.9 LINKING THE WATER VAPOR CONDENSATION AND SEEPAGE DRIPPING MODEL FOR TSPA-LA 129
8.10 OUTPUT UNCERTAINTY 131
8.11 CONCLUSIONS 131

9. REFERENCES 132

INTENTIONALLY LEFT BLANK

FIGURES

Page

1. Commercial Spent Nuclear Fuel Single Component Water Vapor Condensation pH Outputs 66
2. Commercial Spent Nuclear Fuel Multi-Component Ensemble pH Profiles 67
3. Commercial Spent Nuclear Fuel Seepage Dripping Model Results for Q = 1.5 l/yr, Fuel Exposure = 10 Percent, and Three Seepage Compositions at 25°C 68
4. Commercial Spent Nuclear Fuel Seepage Dripping Model C22C25 Results at 25°C, Showing Eh, Reactant Summary, and Corrosion Products 70
5. Commercial Spent Nuclear Fuel Seepage Dripping Model Mineral phases for the Three Seepage Compositions at 25°C, Q = 1.5 l/yr, fuel exposure = 10% 70
6. Commercial Spent Nuclear Fuel Seepage Dripping Model Aqueous Species for the Three Seepage Compositions at 25°C, Q = 1.5 l/yr, fuel exposure = 10% 71
7. Commercial Spent Nuclear Fuel Seepage Dripping Model Results for Q = 1.5 l/yr, Fuel Exposure = 10 Percent, and Three Seepage Compositions at 50°C 72
8. Codisposed N Reactor Single-Component Water Vapor Condensation Results 73
9. Codisposed N Reactor Multi-Component Ensemble pH Profiles 74
10. Codisposed N Reactor Seepage Dripping Model Results for Q = 1.5 l/yr and Three Seepage Compositions at 25°C 75
11. Codisposed N Reactor Seepage Dripping Model Results for Q = 1.5 l/yr and Three Seepage Compositions at 50°C 76
12. Codisposed N Reactor Seepage Dripping Model Mineral Phases Results for Q = 1.5 l/yr and Three Seepage Compositions at 25°C 77
13. Codisposed N Reactor Seepage Dripping Model Aqueous Species Results for Q = 1.5 l/yr and Three Seepage Compositions at 25°C 78
14. Sensitivity Analysis of pH 80
15. Sensitivity Analysis of Ionic Strength 81
16. Sensitivity Analysis with Corrected A516 Guide Information 82
17. Non-Dripping Commercial Spent Nuclear Fuel Water Vapor Condensation pH Abstraction 89
18. Non-Dripping Commercial Spent Nuclear Fuel Water Vapor Condensation Ionic Strength Abstraction 91
19. Seepage Dripping Model pH Profiles for Commercial Spent Nuclear Fuel at 25°C, Showing the Three Time Periods of the Abstraction 93
20. Seepage Dripping Model pH Profiles for Commercial Spent Nuclear Fuel at 50°C, Showing the Three Time Periods of the Abstraction 96
21. Effect of Temperature on the pH of Run C22C25 98
22. Commercial Spent Nuclear Fuel Seepage Dripping Model 25°C Ionic Strength Profiles 99
23. Commercial Spent Nuclear Fuel Seepage Dripping Model 25°C 40 to 20,000-Year Ionic Strength Abstraction 100
24. Effect of Temperature on the Ionic Strength of Run C22C25 103
25. Commercial Spent Nuclear Fuel Seepage Dripping Model 25°C Fluoride Profiles and Abstraction 104

FIGURES (Continued)

Page

26. Commercial Spent Nuclear Fuel Seepage Dripping Model 25°C Chloride Profiles And Abstraction 106
27. Codisposed N Reactor Water Vapor Condensation pH Profiles and Abstraction 107
28. Codisposed N Reactor Water Vapor Condensation Ionic Strength Profiles and Abstraction 108
29. Codisposed N Reactor Water Vapor Condensation Fluoride Profiles 110
30. Codisposed N Reactor Seepage Dripping Model 25°C pH Profiles and 0 to 60 Year Abstraction Limits 111
31. Codisposed N Reactor Seepage Dripping Model 25°C pH and Abstraction for the 60 to 20,000 Year Period 112
32. Codisposed N Reactor Seepage Dripping Model 50°C pH Profiles and 0 to 60-Year Abstraction Limits 114
33. Effect of Temperature on the pH of Run D23C25 116
34. Codisposed N Reactor Seepage Dripping Model 25°C Ionic Strength Profiles and 0 to 80 Year Abstraction Limits 118
35. Codisposed N Reactor Seepage Dripping Model 50°C Ionic Strength Profiles and 0 to 80 Year Abstraction Limits 120
36. Effect of Temperature on the Ionic Strength of Run D23C25 122
37. Codisposed N Reactor Seepage Dripping Model 25°C Fluoride Profiles and Abstraction Limits 122
38. Codisposed N Reactor Seepage Dripping Model 25°C Chloride Profiles and Abstraction Limits 123
39. Plot of Total Carbonate Function at Two Temperatures Compared to Model Output 126
40. Plot of Eh Function at Two Temperatures Compared to Model Output 127
41. Commercial Spent Nuclear Fuel Water Vapor Condensation–Seepage Dripping Model Comparison 130
42. Codisposed N Reactor Water Vapor Condensation–Seepage Dripping Model Comparison 130

TABLES

Page

1. Data Input and References for In-Package Chemistry Model 18
2. Input Water Compositions 19
3. Sources for Fuel and High-Level Waste Glass Reaction Rates 21
4. Materials Nomenclature and Waste Package Breakdown 22
5. Input References for the Waste Package Components 23
6. Composition of Steel and Al Alloys 25
7. Steel and Al Alloy Densities and Corrosion Rates 25
8. Commercial Spent Nuclear Fuel and Codisposed N Reactor Fuel Compositions 26
9. High-Level Waste Glass Composition 27
10. Included FEPs for the In-Package Chemistry Model Report and their Disposition in TSPA-LA 32
11. Commercial Spent Nuclear Fuel Water Vapor Condensation Multi-Component Ensembles 39
12. Codisposed N Reactor Water Vapor Condensation Multi-Component Ensembles 40
13. EQ6 Input Guide for the CSNF Seepage Dripping Model Runs 45
14. EQ6 Input Guide for the Codisposed N Reactor Seepage Dripping Model Runs 46
15. Alternative In-Package Chemistry Conceptual Models 48
16. Metal Alloy Compositions 49
17. Metal Alloy Corrosion Rates 49
18. Commercial Spent Nuclear Fuel Transition State Theory Rate Law and Coefficients 50
19. High-Level Waste Glass Transition State Theory Rate Law and Constants and Codisposed N Reactor Rate Constants 50
20. Commercial Spent Nuclear Fuel Waste Package Single Component Water Vapor Condensation Surface Areas and Reactant Moles for 0.1-cm Thick Film at 10 Percent Cladding Failure 51
21. Codisposed N Reactor Waste Package Single Component Water Vapor Condensation Surface Areas and Reactant Moles for 0.1-cm Thick Film 51
22. Water Flux Conversion 52
23. Single-Component Water Flux Values for Commercial Spent Nuclear Fuel and Codisposed N Reactor Waste Package 52
24. Commercial Spent Nuclear Fuel Water Vapor Condensation Multi-component Ensembles 52
25. Codisposed N Reactor Water Vapor Condensation Multi-component Ensembles 53
26. Commercial Spent Nuclear Fuel Waste Package Component Surface Areas and Moles 53
27. Commercial Spent Nuclear Fuel Ensemble 1 Input Values 54
28. Commercial Spent Nuclear Fuel Ensemble 2 Input Values 54
29. Commercial Spent Nuclear Fuel Ensemble 3 Input Values 54
30. Commercial Spent Nuclear Fuel Ensemble 4 Input Values 54
31. Commercial Spent Nuclear Fuel Ensemble 5 Input Values 55
32. Commercial Spent Nuclear Fuel Ensemble 6 Input Values 55
33. Commercial Spent Nuclear Fuel Ensemble 7 Input Values 55
34. Commercial Spent Nuclear Fuel Ensemble 8 Input Values 55

TABLES (Continued)

Page

35. Commercial Spent Nuclear Fuel Ensemble 9 Input Values 56
36. Commercial Spent Nuclear Fuel Ensemble 10 Input Values 56
37. Commercial Spent Nuclear Fuel Ensemble 11 Input Values 56
38. Codisposed N Reactor Surface Area and Mole Data Used to Generate the Inputs for the Multi-Component Ensemble Runs 57
39. Codisposed N Reactor Ensemble 1 Input Values 57
40. Codisposed N Reactor Ensemble 2 Input Values 57
41. Codisposed N Reactor Ensemble 3 Input Values 58
42. Codisposed N Reactor Ensemble 4 Input Values 58
43. Codisposed N Reactor Ensemble 5 Input Values 58
44. Codisposed N Reactor Ensemble 6 Input Values 58
45. Codisposed N Reactor Ensemble 7 Input Values 59
46. Codisposed N Reactor Ensemble 8 Input Values 59
47. Commercial Spent Nuclear Fuel Unscaled Surface Areas and Normalization Factors 59
48. Commercial Spent Nuclear Fuel Unscaled Reactant Moles 60
49. Scaled EQ6 Inputs, Commercial Spent Nuclear Fuel Surface Areas, and Reactant Moles for 0.25-cm Thick Film at Three Fuel Exposure Values 60
50. EQ6 input water flux values for the Commercial Spen Nuclear Fuel Seepage Dripping Model 60
51. EQ6 Input Water Flux Values for the Codisposed N Reactor Seepage Dripping Model 60
52. Codisposed N Reactor Unscaled Surface Areas and Moles and Normalization Factor 61
53. EQ6 Inputs, Codisposed N Reactor Surface Areas, and Reactant Moles for 0.35-cm Thick Film 61
54. EQ6 Input Fluid Compositions 62
55. Minerals Suppressed in In-Package Chemistry Model EQ6 Runs 64
56. Major Mineral Phases Formed in EQ6 Runs 65
57. Non-Dripping Commercial Spent Nuclear Fuel pH Abstraction 90
58. Non-Dripping Commercial Spent Nuclear Fuel Ionic Strength Cumulative Distribution Parameters 91
59. Criteria Used to Define the pH for Each Abstracted Time Period 93
60. Input Matrix for the Commercial Spent Nuclear Fuel Seepage Dripping Model, 0 to 50 year pH Response Surface 94
61. Total System Performance Assessment Input pH Input Parameters for the Response Surfaces at 25°C 95
62. Flux and Fuel Exposure Limits for the Commercial Spent Nuclear Fuel Seepage Dripping Model 25°C pH Abstraction 95
63. Total System Performance Assessment Input pH input Parameters for the Response Surfaces at 50°C 96
64. Flux and Fuel Exposure Limits for the Commercial Spent Nuclear Fuel Seepage Dripping Model 50°C pH Abstraction 97
65. Ionic Strength Criteria for the Commercial Spent Nuclear Fuel Seepage Dripping Model Runs at 25°C 99

TABLES (Continued)

Page

66. Commercial Spent Nuclear Fuel Seepage Dripping Model 25°C 0 to 40-year Ionic Strength Cumulative Distribution for TSPA-LA 100
67. Commercial Spent Nuclear Fuel Seepage Dripping Model 25°C Ionic Strength 40 to 20,000-Year Abstraction 101
68. Commercial Spent Nuclear Fuel Seepage Dripping Model 25°C Ionic Strength Flux Limits for 40 to 20,000-Year Abstraction 101
69. Commercial Spent Nuclear Fuel Seepage Dripping Model 50°C 0 to 40-Year Ionic Strength Cumulative Distribution for TSPA-LA 102
70. Commercial Spent Nuclear Fuel Seepage Dripping Model 50°C Ionic Strength 40 to 20,000-Year Abstraction 102
71. Commercial Spent Nuclear Fuel Seepage Dripping Model 50°C Ionic Strength Flux Limits for 200 to 20,000 Year Abstraction 102
72. Commercial Spent Nuclear Fuel Seepage Dripping Model 25° and 50°C Fluoride Abstraction 105
73. Commercial Spent Nuclear Fuel Seepage Dripping Model 25° and 50°C Chloride Abstractions 105
74. Codisposed N Reactor Water Vapor Condensation pH Abstraction 108
75. Codisposed N Reactor Water Vapor Condensation Model Ionic Strength Cumulative Distribution 109
76. Codisposed N Reactor Water Vapor Condensation Model Fluoride Abstraction 110
77. Codisposed N Reactor Seepage Dripping Model 25°C pH Abstraction, 0 to 60 Years 112
78. Codisposed N Reactor Seepage Dripping Model 25°C pH Abstraction, 60 to 20,000 Years 113
79. Codisposed N Reactor Seepage Dripping Model 25°C pH Abstraction Flux Limits for 60 to 20,000 Year Abstraction 113
80. Codisposed N Reactor Seepage Dripping Model 50°C pH Abstraction, 0 to 60 Years 114
81. Codisposed N Reactor Seepage Dripping Model 50°C pH Abstraction, 60 to 20,000 Years 115
82. Codisposed N Reactor Seepage Dripping Model 50°C pH Abstraction Flux Limits for 60 to 20,000 Year Abstraction 115
83. Codisposed N Reactor Seepage Dripping Model 25°C Ionic Strength 0 to 80 Years Cumulative Distribution 117
84. Codisposed N Reactor Seepage Dripping Model 25°C Ionic Strength 80 to 20,000 Year Abstraction 118
85. Codisposed N Reactor Fuel Seepage Dripping Model 25°C Ionic Strength Flux Limits for 80 to 20,000 Year Abstraction 119
86. Codisposed N Reactor Seepage Dripping Model 50°C Ionic Strength Abstraction 0 to 80 Years 119
87. Codisposed N Reactor Seepage Dripping Model 50°C Ionic Strength 80 to 20,000 Year Abstraction 120

TABLES (Continued)

Page

88. Codisposed N Reactor Seepage Dripping Model 50°C Ionic Strength Flux Limits for 80 to 20,000 Year Abstraction 121
89. Codisposed N Reactor Seepage Dripping Model 25° and 50°C Fluoride Abstraction Limits....123
90. Codisposed N Reactor Seepage Dripping Model 25° and 50°C Chloride Abstraction Limits....124
91. Expression for Total Carbonate as a Function of pH to be Used in the Total System Performance Assessment....124
92. Log K Values for the Carbonate Species at Temperature....125
93. Log K Temperature Interpolation Functions for Use in the Total Carbonate Abstraction 125
94. Expression for Eh as a Function of pH, Oxygen Partial Pressure, and Absolute Temperature for use in the TSPA-LA 127
95. Gas Abstraction Information....128

ACRONYMS

B&W	Babcock and Wilcox
CDNR	codisposed N reactor
CSNF	commercial spent nuclear fuel
DOE	U. S. Department of Energy
DTN	Data Tracking Number
EBS	engineered barrier system
FEPs	Features, Events, and Processes
HLWG	high-level waste glass
PWR	pressurized water reactor
Q	water flux through the waste package
SNF	spent nuclear fuel
TSPA-LA	Total Systems Performance Assessment–License Application
TSPA-SR	Total Systems Performance Assessment–Site Recommendation

INTENTIONALLY LEFT BLANK

1. PURPOSE

The work associated with the development of this model report was performed in accordance with the requirements established in *Technical Work Plan for Waste Form Degradation Modeling, Testing, and Analyses in Support of SR and LA* (BSC 2002a). The in-package chemistry model and in-package chemistry model abstraction are developed to predict the bulk chemistry inside of a failed waste package and to provide simplified expressions of that chemistry. The purpose of this work is to provide the abstraction model to the Performance Assessment Project and the Waste Form Department for development of geochemical models of the waste package interior.

The scope of this model report is to describe the development and validation of the in-package chemistry model and in-package chemistry model abstraction. The in-package chemistry model will consider chemical interactions of water with the waste package materials and the waste form for commercial spent nuclear fuel (CSNF) and codisposed high-level waste glass (HLWG) and N Reactor spent fuel (CDNR). The in-package chemistry model includes two sub-models, the first a water vapor condensation (WVC) model, where water enters a waste package as vapor and forms a film on the waste package components with subsequent film reactions with the waste package materials and waste form—this is a no-flow model, the reacted fluids do not exit the waste package via advection. The second sub-model of the in-package chemistry model is the seepage dripping model (SDM), where water, water that may have seeped into the repository from the surrounding rock, enters a failed waste package and reacts with the waste package components and waste form, and then exits the waste package with no accumulation of reacted water in the waste package. Both of the submodels of the in-package chemistry model are film models in contrast to past in-package chemistry models where all of the waste package pore space was filled with water. The current in-package chemistry model is a film model where both dripping and non-dripping cases of water ingress/egress are considered.

The scope of the model documentation includes detailed descriptions of the process models and their inputs and outputs, as well as derivation of the in-package chemistry abstractions and their limitations.

In neither the water vapor condensation model nor the seepage dripping model is the failure mode of the waste package specified. The in-package chemistry model and resulting in-package chemistry model abstraction are general and independent of waste package failure mode.

The output from the in-package chemistry model include time series concentrations of the elements and their aqueous complexes constituting the waste package, waste form, seepage, and gas composition. Also, output will be time series values of pH, ionic strength, and mineralogical phase abundance. The in-package chemistry model abstraction simplifies the in-package chemistry model outputs for pH, ionic strength, Eh, total carbonate concentration, chloride, and fluoride concentration into a Performance Assessment Project compatible format.

To maximize the applicability while accounting for the uncertainties of the model inputs, a series of scenarios were run with variations in temperature, seepage composition, and water distribution within the waste package. The abstractions of in-package chemistry are applicable over the

water volumetric flux (hereafter referred to as "flux") range from 0.15 l/yr to 1000 l/yr, a temperature range from 15°C to 95°C and carbon dioxide partial pressure range of 10^{-4} to 10^{-2} atmospheres. Spatially, the applicability of the in-package chemistry model and in-package chemistry model abstraction is limited to the waste package interior.

Temporally, the in-package chemistry model starting time refers to the time of waste package breach, or if the waste package should fail while its temperature is above the boiling temperature of water, then the starting time refers to when the temperature in the waste package falls below the boiling temperature. Therefore, in the remainder of the model report, the term "time" will be relative to signal either of the two cases noted above. Note that the in-package chemistry abstraction does not provide information regarding the temperature history of the waste packages, therefore, TSPA must decide if the waste package temperature is above or below boiling.

Limitations on the availability of thermodynamic data for certain elements that constitute the waste package and SNF (transition metals and radionuclides) prohibited using high-ionic strength solutions as initial starting compositions for the in-package chemistry model. This data limitation also influenced the boundary conditions used in the model where constant relative humidity was required to maintain non-evaporative conditions inside the waste package.

Further data limitations include the lack of long-term metal alloy corrosion information. Another data limitation is the lack of knowledge regarding the change in the surface area of the waste package components and SNF as these components degrade in an aqueous environment. The specifics of the model limitations will be discussed in Sections 6 and 8.

This in-package chemistry model abstraction is planned to be used as input to the Total Systems Performance Assessment (TSPA)–License Application (LA) where the relationships developed in this model report will be linked to the principle factors: waste form degradation, dissolved concentrations, waste package degradation, cladding degradation, and colloid generation. In addition, the in-package chemistry model output may be used as one of the source terms for the chemistry in the invert.

2. QUALITY ASSURANCE

QA Program Applicability: Development of this model report has been determined to be subject to the Yucca Mountain Project's quality assurance program because it will be used to support performance assessments; it does not affect any items on the Q-List (BSC 2002a, Attachment I).

Electronic Management of Data: The technical work plan contains the Process Control Evaluation used to evaluate the control of electronic management of data (BSC 2002a, Attachment III) during the modeling and documentation activities, and this evaluation determined that the methods identified in the implementing procedures are adequate. No deviations from these methods were performed.

3. COMPUTER SOFTWARE AND MODEL USAGE

3.1 COMPUTER SOFTWARE

The software used in this analysis includes:

- EQ3/6 v7.2b (EQ3/6 V7.2b, STN: LLNL: UCRL-MA-110662) is qualified on the Windows 95 and HP-UX 10.20B operating systems. The EQ3/6 software is composed of three component programs, EQPT, EQ3NR, and EQ6. EQPT is used to transform a specially formatted thermodynamic database from a text format (data0.* file) to a binary format (data1.* file) which is used by EQ3NR and EQ6. EQ3NR is a geochemical speciation code which uses as input a water composition and the aforementioned thermodynamic database. Output from EQ3NR (*.3o file) provides information regarding the saturation state of various minerals and gases and the concentrations of aqueous chemical species. EQ3NR also outputs a "pickup" file (*.3p file) which contains the initial water composition in a format that is appended to the end of an EQ6 input file to set the initial condition for the EQ6 run. The software was obtained from Bechtel SAIC Company Software Configuration Management organization and installed on the IBM-compatible computer identified below. It is appropriate for the application and is used only within the range of validation in accordance with AP-SI.1Q, *Software Management*.

- EQ6 V7.2b LV (EQ6 V7.2bLV, STN: 10075-7.2bLV-02) is qualified on the Windows 95, 98, NT and 2000 operating systems. EQ6 is a geochemical reaction-path modeling code that is used to simulate complex systems such as the in-package chemical environment. Inputs for EQ6 include the EQ3 pickup file (*.3p), the thermodynamic database (data1.*), and reactant information such as surface area, number of moles, and reaction rate. Output from EQ6 includes a reaction history or time history of the solid and aqueous chemical environment (*.6o, *.txt, *.bin files). The software was obtained from Bechtel SAIC Company Software Configuration Management organization and installed on the IBM-compatible computer identified below. It is appropriate for the application and is used only within the range of validation in accordance with AP-SI.1Q, *Software Management*.

- Microsoft Excel 2000, a commercially available spreadsheet software package: Applications of this software in the current document are restricted to tabulation, visual display of results, and use of intrinsic functions (SUM, MAXIMUM, MINIMUM, AVERAGE), as well as use of the regression analysis and curve fitting routines which are both described in Section 8. No macros or software routines were developed for, or used by, this software, and consequently it is an exempt software application in accordance with Section 2.1 of AP-SI.1Q.

- GetEQData, version 1.0.1 (GetEQData V1.0.1, STN: 10809-1.0.1-0) is a Microsoft Visual Basic 6.0 macro post-processor, embedded inside a Microsoft Excel 2000 spreadsheet. This macro was used to extract output from EQ6 (*.6o files) into Microsoft Excel 2000 spreadsheets. GetEQData is qualified on Windows NT and Windows 2000

operating systems. This software was obtained and implemented under AP-SI.1Q, and was only used within the range of validation.

The EQ6 simulations and GetEQData were executed on the following machine using the Microsoft Windows 2000 operating system:

- A Dell Latitude C610, Framatome ANP Inc. Tag# 632MT11 in Albuquerque, New Mexico.

The EQ3NR and EQPT (EQ3/6 V7.2b) simulations were executed on the following machine using the Microsoft Windows 95 operating system:

- A Dell Optiplex GX300 #117728 (Bechtel SAIC Company) in Las Vegas, Nevada.

4. INPUTS

4.1 DATA AND PARAMETERS

All of the information in the following subsections are used as direct input to the in-package chemistry model.

4.1.1 Data

Table 1 lists the data used in the in-package chemistry model. These data include the thermodynamic database used by the EQ3/6 codes and three water compositions.

Table 1. Data Input and References for In-Package Chemistry Model

Identifier	Input	Reference	Used in Section:
Data0.ymp.R2	Thermodynamic database	DTN: MO0302SPATHDYN.000	6.5.4
J-13 Well Water	Water Composition	DTN: MO0006J13WTRCM.000	6.5.4
Ca-porewater	Water Composition	DTN: GS020408312272.003	6.5.4
Na-porewater	Water Composition	DTN: GS020408312272.003	6.5.4

4.1.1.1 Thermodynamic Database

The in-package chemistry model used a version of the thermodynamic database Data0.ymp.R2 (DTN: MO0302SPATHDYN.000) as a necessary component in the execution of the EQ3/6 software. This database used in the in-package chemistry model contains data for temperatures up to 200°C. This database is appropriate for the in-package chemistry model because it includes the elements that constitute the waste package, waste form, seepage, and gas compositions in the temperature range needed for the model.

The CSNF and HLWG (compositions given in Tables 8 and 9, respectively) were added to the database in order to take advantage of EQ3/6's ability to use a pH-dependent and carbonate-dependent rate law, using the EQ6 transition state theory formalism to describe the degradation. Only reactants entered as “minerals” (solids contained in the database) can specify a range of

degradation rates based on pH; "special reactants" (reactants not contained in the database) must have a constant or fixed degradation rate.

The thermodynamic data for the following aqueous species and one gas were unverified: $(NH_4)_2Sb_2S_4$(aq); $NpSO_4^{2+}$(aq); $NpO_2H_2PO_4^{+}$(aq); and NO_2(g). However, the presence of these species did not have any impact on the results of the in-package chemistry model because their concentrations were too low to be of any consequence on the results.

4.1.1.2 Input Water Compositions

Table 2 summarizes the input water compositions used in the in-package chemistry model as direct input.

Table 2. Input Water Compositions

Parameter	Units	"Ca-porewater" ECRB-SYS-CS1000/7.3-7.7/UC[a]	"Na-porewater" ECRB-SYS-CS2000/16.3-16.5/UC[b]	J-13[c]
Ca	mg/L	94	81	13.0
Mg	mg/L	18.1	3.3	2.01
Na	mg/L	39	120	45.8
K	mg/L	7.6	6.1	5.04
Si	Mg/L	N/A	N/A	61.0
SiO_2	mg/L	42	42	N/A
NO_3	mg/L	2.6	0.41	8.78
HCO_3	mg/L	397	362	See Section 6.5.4
Cl	mg/L	21	24	7.14
F	mg/L	3.4	6	2.18
SO_4	mg/L	36	31	18.4
pH	pH	7.6	7.4	7[d]

Sources: [a] Sample: ECRB-SYS-CS1000/7.3-7.7/UC; DTN: GS020408312272.003
[b] Sample: ECRB-SYS-CS2000/16.3-16.5/UC; DTN: GS020408312272.003
[c] DTN: MO0006J13WTRCM.000
[D] Harrar et al. 1990, pp. 4 to 9

For simplicity, and based on their calcium and sodium concentrations, samples ECRB-YS-S1000/7.3-7.7/UC and ECRB-SYS-CS2000/16.3-16.5/UC were termed "Ca-porewater" and "Na-porewater," respectively.

These three water compositions were used as the initial condition(s) in the seepage dripping model of the in-package chemistry model for water entering a failed waste package. The decision to use these water compositions was based on several lines of reasoning. Although it is not expected to enter the repository, the J-13 composition was used for comparison purposes, i.e., to maintain continuity between the current work and past in-package chemistry analyses. The Ca- and Na-porewater compositions were used because they were obtained from core samples proximal to the repository. These waters could represent seepage compositions that would enter a failed waste package, especially over the long term. The compositions are contained in a DTN from the U.S. Geological Survey (DTN: GS020408312272.003), and a note in the data spreadsheet states:

> Chemical composition of pore water extracted from cores of 15 ECRB-SYS-CS Series boreholes, USW SD-9, and USW NRG-7/7a, 04/26/2001 to 02/12/2002.

Thus, identifying the location of the boreholes from which the cores were removed. Furthermore, the recent collection date(s) of the samples provides confidence that collection and analysis methods were performed under an approved quality assurance program.

Drift-Scale Coupled Processes (DST and THC Seepage) Models (BSC 2003a, Section 6.2.2.1) uses the Ca-porewater (labeled "W5" in BSC 2003a) and another composition (labeled "W4" [ECRB-SYS-CS2000/16.5-21/UC]) also from the U.S. Geological Survey DTN (DTN: GS020408312272.003), which originates from the next interval in the same core as that from which the Na-porewater was extracted. The composition of the Na-porewater used in the in-package chemistry model only differs slightly from the "W4" composition used in *Drift-Scale Coupled Processes (DST and THC Seepage) Models* (BSC 2003a). Thus, continuity has been established for key inputs for the in-package chemistry model and the drift scale processes models.

Compared to the J-13 composition, and with the exception of aqueous silica, the porewater compositions are significantly more concentrated (Table 2). Two anions, chloride and fluoride, which may be important with regard to steel corrosion are concentrated in the pore waters by factors of approximately 2 to 3 compared to J-13. *Drift-Scale Coupled Processes (DST and THC Seepage) Models* (BSC 2003a) states that "W5" (Ca-porewater) has the highest (Ca + Mg)/(Na + K) ratio of the ECRB samples, and that "W4" (Na-porewater) has the lowest (Ca + Mg)/(Na + K) ratio of the ECRB samples and has higher fluoride than other samples. Thus, the two porewater represent compositional end members and capture the spread of the porewater compositions. A Piper diagram (BSC 2003a, Figure 6.2-4) clearly shows that these two samples represent compositional end members.

Since these samples cover the spectrum of observed porewater compositions sampled, and there is a possibility that waters of similar composition may potentially enter a drift and contact a failed waste package, the use of these compositions is well justified. Furthermore, use of these data in the in-package chemistry model, and, thus, the in-package chemistry model abstraction, ensures the feeds to the TSPA-LA model, will reflect the compositional variation of the initial water composition.

4.1.2 Parameters

Table 3 summarizes the parameters and their references used in the in-package chemistry model.

Table 3. Sources for Fuel and High-Level Waste Glass Reaction Rates

Identifier	Input	Reference	Used in Section:
HLWG	Reaction Rate	BSC 2001a, Section 6.2.3.3, Equations 7 and 8	6.5.1.2
CDNR	Reaction Rate	DOE 2000a, Equation 2-39; BSC 2001b, Section 6.3.7	6.5.1.2
CSNF	Reaction Rate	CRWMS M&O 2000a, Equations 16 and 18	6.5.1.2
Water Diffusion Flux	Water Flux	BSC 2003b, Section 6.6.2	6.3.2
Nitric Acid Production Rate	Reaction Rate	BSC 2002b, Table 21, p. 33	Attachment III
G value of Nitric Acid Production	Used to Calculate hydrogen peroxide production	BSC 2002b, p. 27	Attachment III
G value of Hydrogen Peroxide Production		IAEA 1998, Table 8.2, p. 214	Attachment III

NOTE: All inputs used in Attachment III are listed in Attachment III.

4.1.2.1 High-Level Waste Glass Rate Expression

For HLWG a transition state theory rate law is recommended (BSC 2001a, Section 6.2.3.3, Equations 7 and 8) in which the moles of dissolved glass are a function of the pH:

for pH < 7.1 (BSC 2001a, Section 6.2.3.3, Equation 7)

$$\log_{10} \text{rate} = (14.0 \pm 0.5) + (-0.6 \pm 0.1) \bullet \text{pH} + \log_{10}(\exp((-80 \pm 10)\ \text{kJ/mol}/(RT)))$$

and for pH ≥ 7.1 (BSC 2001a, Section 6.2.3.3, Equation 8)

$$\log_{10} \text{rate} = (6.9 \pm 0.5) + (0.4 \pm 0.1) \bullet \text{pH} + \log_{10}(\exp((-80 \pm 10)\ \text{kJ/mol}/(RT)))$$

The rate laws are in units of g/m^2-day.

4.1.2.2 CDNR Rate Expression

For CDNR, a linear (i.e., constant reaction rate) is used to describe the dissolution of the N Reactor fuel. This is the best estimate dissolution rate recommended by *DSNF and Other Waste Form Degradation Abstraction* (BSC 2001b, Section 6.3.7), which is five times the constant U-metal rate contained in *Review of Oxidation Rates of DOE Spent Nuclear Fuel, Part 1: Metallic Fuel* (DOE 2000a, Equation 2-39):

$$k_1 = 5.03 \cdot 10^9 \exp\left[\frac{-66.4 \pm 2.0\text{kJ/mol}}{RT}\right] \text{mg U/cm}^2\text{-h}$$

4.1.2.3 CSNF Rate Expression

The pH, O_2 partial pressure, and carbonate-dependent best estimate rate law used for CSNF in this analysis is that recommended in *CSNF Waste Form Degradation: Summary Abstraction* (CRWMS M&O 2000a, Equations 16 and 18) evaluated at 50°C.

for pH > 7 (CRWMS M&O 2000a, Equation 16)

$$\log_{10} \text{rate} = 4.69 + (-1085)/T + (-0.12) \bullet pCO_3 + (-0.32) \bullet pO_2$$

and for pH ≤ 7 (CRWMS M&O 2000a, Equation 18)

$$\log_{10} \text{rate} = 7.13 + (-1085)/T + (-0.32) \bullet pO_2 + (-0.41) \bullet pH.$$

Where, $pCO_3 = -\log_{10}$(total carbonate species concentration), $pO_2 = -\log_{10}$(oxygen partial pressure), and temperature in Kelvin. Rate is in units of mg/m^2-day.

4.1.2.4 Diffusion Flux

The diffusion flux of water vapor into a waste package was calculated (BSC 2003b, Section 6.2.2) for ingress of water vapor through stress corrosion cracks. The calculated value of 43.88 mol H_2O/yr (0.79 l/yr) through 25 stress corrosion cracks was used as the water flux term in water vapor condensation model runs.

4.1.3 Other Input

Table 4 contains the names and shorthand names used in this model and waste package type for the metal alloys used throughout this document.

Table 4. Materials Nomenclature and Waste Package Breakdown

Material Nomenclature	Shorthand	Waste Package Type	
		CSNF	CDNR
Alloy 22, UNS N06022	Alloy 22	✓	✓
SA-240 S31600 Stainless Steel [a]	S31600	✓	✓
SA-240 S30403 UNS N06625 Stainless Steel	304L		✓
SA-516 Grade 70 Carbon Steel	A516	✓	✓
SB-209 6061 T4	Al-6061	✓	
Aluminum Alloy-1100	Al-1100		✓
Neutronit A976™	Neutronit	✓	

NOTE: [a] There are additional chemistry controls applied to the compositional ranges specified for "S31600" stainless steel in the ASME Standard.

Table 5 summarizes the other direct inputs for the in-package chemistry model and provides the references for them.

Table 5. Input References for the Waste Package Components

Material/Property	Input	Reference	Used in Section:
21-PWR CSNF WP geometric information	WP Component Dimensions	BSC 2002c, Attachment III; BSC 2003c; Punatar 2001, p. 2-5	Attachment I "CSNF.xls"
CDNR WP geometric information	WP Component Dimensions	BSC 2003c; DOE 2000b, Section 3	Attachment I "CDNR.xls"
Periodic Table of the Elements and Mass List of Radioactive Isotopes	Atomic Weight of the Elements and Isotopes	Audi and Wapstra 1995; Parrington et al. 1996	Attachment I "CSNF.xls" "CDNR.xls"
S31600	Corrosion rate	DTN: MO0303SPAMCRAQ.000	6.5.1.1
	Density	ASTM G 1-90 1999, Table XI, p. 7	Attachment I "CSNF.xls" "CDNR.xls"
	Composition	ASME 1998, Section II, SA-240, Table 1, p. 366, for composition of 316; ASM International 1987, p. 931, for C and N content of 316	6.5.1.1
304L	Corrosion rate	DTN: MO0303SPAMCRAQ.000	6.5.1.1
	Density	ASTM G 1-90 1999, Table XI, p. 7	Attachment I "CDNR.xls"
	Composition	ASTM A 240/A 240M-99b 2000, Table 1, p. 2	6.5.1.1
A516	Corrosion rate	DTN: MO0303SPAMCRAQ.000	6.5.1.1
	Density	ASTM A 20/A 20M-95a 1995, p. 21	Attachment I "CSNF.xls" "CDNR.xls"
	Composition	ASME 1998, Section II, SA-516/SA-516M, Table 1, p. 925	6.5.1.1
Al-6061	Corrosion rate	ASM International 1987, Table 12, p. 603	6.5.1.1
	Density	ASTM G 1-90 1999, Table X1.1	Attachment I "CSNF.xls"
	Composition	ASME 1998, Section II, SB-209, Table 1, p. 236	6.5.1.1
Al-1100	Corrosion rate	ASM International 1987, Table 12, p. 603	6.5.1.1
	Density	ASTM G 1-90 1999, Table XI, p. 7	Attachment I "CDNR.xls"
	Composition	ASTM B 209-96 1996, Table 1, p. 7	6.5.1.1
Neutronit	Corrosion rate	DTN: MO0303SPAMCRAQ.000	6.5.1.1
	Density	DTN: MO0109RIB00049.001 "Material Properties of Neutronit A976/A978" for B content; ASTM A 887-89 2000, Table 1, S30463, S30464, and S30466	Attachment I "CSNF.xls"
	Composition		6.5.1.1
HLWG	Density	BSC 2003c; Stout and Leider 1994, Table 6.4	Attachment I "CDNR.xls"
	Composition	BSC 2003c; Baxter 1988, Table 10	6.5.1.2
N-Reactor Fuel	Composition	BSC 2003c; DOE 2000b, Table 3-1	6.5.1.2
CSNF	Isotopic Inventory	BSC 2003c; BSC 2001c, Attachment III Disk 1 of 9, ATT III/ LPM1/ uniform_profile/ 3.5/ ft71-case10.N04	6.5.1.2

NOTE: PWR = pressurized water reactor; WP = waste package.

4.1.3.1 Waste Package Geometric Information

Dimensional information about the geometry of the waste package components allows the volume and surface area of the waste package components to be calculated. With knowledge of the alloy density(s) and the waste package component volumes, the mass for each component is calculated, which is converted to moles that are used as input for EQ6.

The sketch SK-0219 Rev 02 (BSC 2002c, Attachment III) was used as a source for some of the 21-pressurized water reactor (PWR) CSNF waste package geometry, rather than the baseline drawing (BSC 2001d; BSC 2003d). The dimensions used in the model report are tabulated in Attachment II, Table II-1. The sketch was used in this model report since it gives more detail about the waste package interior geometry, specifically the fuel basket, than the baseline drawing. The differences in dimensions between the sketch and the baseline drawing for waste package components common to both are insignificant. For example, the dimensions of the inner vessel were taken from the sketch, but the only difference from the drawing is in the thickness of the inner vessel top and bottom lids with a combined difference of only 5 cm. Such small differences in waste package component dimensions should not impact the results of this model report as illustrated by the sensitivity analyses (Attachment II).

Since the interior geometry of these waste packages is complex, the dimensions of the individual waste package components will not be included in the text of the document; however, this information is available in Attachment I, in "CSNF.xls" for the CSNF waste package, and "CDNR.xls" for the CDNR waste package. In converting waste package dimensional information to quantities that were used as input in the in-package chemistry model, it was necessary to use the equations for the calculation of the area of a circle, area of a square, area of a rectangle, and surface area of a cylinder.

4.1.3.2 Atomic Weights

Atomic weights of the elements and radionuclide isotopes used were taken from Audi and Wapstra (1995) and Parrington et al. (1996, p. 50). These references have been used as a source for this information throughout the Yucca Mountain Site Characterization Project (CRWMS M&O 2001, Section 5.1.1.5; BSC 2002c, Section 4.1.1.6; BSC 2002d, Section 5.1.6) and are appropriate as a source for atomic weights in this analysis. As explained in Section 6.5.1.1, the atomic weights of the elements are used to convert the weight percent of the elements in the metal alloys to moles of elements in the metal alloys, which are used as input in the EQ6 files.

4.1.3.3 Waste Package Materials Properties

Table 6 summarizes the composition of the steel and aluminum alloys present in the CSNF and CDNR waste packages. While there may be some variability in the composition of the alloys used in the construction of the waste packages, they are used in the in-package chemistry model as single-value inputs, i.e., the compositions are not varied in the model. In Sections 6.3.4 and 6.7, variation in the composition of the A516 steel is discussed and a sensitivity analysis presented to show the effect on the model response. The alloy compositions represent the best available information on the materials that will be used in the construction of the waste package.

Table 6. Composition of Steel and Al Alloys

Element	A516 wt%	Neutronit wt%	Al-6061 wt%	S31600 wt%	Al-1100 wt%	304L wt%
C	0.28	0.04	—	0.02	—	0.03
Mn	1.045	—	0.15	2.00	—	2.00
P	0.035	—	—	0.045	—	0.05
S	0.035	—	—	0.03	—	0.03
Si	0.29	—	0.60	0.75	0.45	0.75
Cr	—	18.5	0.195	17.00	—	19.00
Ni	—	13	—	12.00	—	10.00
Co	—	0.2	—	—	—	—
Mo	—	2.2	—	2.50	—	—
N	—	—	—	0.08	—	0.10
Fe	98.3	64.82	0.7	65.58	0.50	68.05
B	—	1.245	—	—	—	—
Zn	—	—	0.25	—	—	—
Cu	—	—	0.275	—	0.05	—
Mg	—	—	1.0	—	—	—
Ti	—	—	0.15	—	—	—
Al	—	—	96.68	—	99.00	—
Total	100.0	100.0	100.0	100.0	100.0	100.0

Source: See Table 5

Table 7 provides the densities and corrosion rates for the waste package metal alloys described in Table 6. The density values are used, as explained in Section 6.5.2, to convert alloy volumes to moles, which are used as input in the EQ6 input files. The density values are also used in converting the corrosion rates, as explained in Section 6.5.1, to units appropriate for EQ6 input.

Table 7. Steel and Al Alloy Densities and Corrosion Rates

	A516	Neutronit	Al-6061	S31600	Al-1100	304L
Density (g/cm^3)	7.85	7.76	2.70	8.00	2.71	7.94
Corrosion Rate (μm/year)	72	0.1	3.0	0.1	3.0	0.1

Source: See Table 5.

The corrosion rates listed in Table 7 fall within the ranges provided in DTN: MO0303SPAMCRAQ.000 for temperatures of 25 to 90°C. Furthermore, to maintain consistency, the use of these corrosion rates is corroborated by Table 6 of *Geochemistry Model Abstraction and Sensitivity Studies for the 21 PWR CSNF Waste Packages* (BSC 2002d).

4.1.3.4 CSNF, N-Reactor, and HLWG Compositions

The sources for the composition of the PWR fuel that is used for the CSNF in the in-package chemistry model are *Repository Design Project, Repository/PA IED Emplacement Drift Committed Materials 1 of 2* (BSC 2003c) and Attachment III of *PWR Assembly End-Effect Reactivity Evaluation* (BSC 2001c, Disk 1 of 9, ATT III/ LPM1/ uniform_profile/ 3.5/ ft71-

case10.N04). The calculation (BSC 2001c) starts with fresh fuel (UO_2) and calculates the composition of the irradiated fuel when it is discharged from the reactor (specified by burnup) and at specified times after discharge. The calculations are performed using the SAS2H sequence and the ORIGEN sequence of the SCALE computer code system. The calculation covers initial enrichment of 2 to 5 weight percent (fuels less than 2 percent enriched are bounded by this calculation) U-235, and burn-up of 0 to 50 GWd/MTU. The quantity of fuel in one assembly is based on the Babcock and Wilcox (B&W) 15×15 assembly design with the mass of type MK-B2. The MK-B2 design contains the greatest mass of U per assembly (CRWMS M&O 1998, p. 26). The B&W 15×15 fuel assembly is one of the most reactive (B&W Fuel Company 1991, p. II 6-6).

For EQ6 runs, the CSNF was specified to have 3.5 weight percent U-235 enrichment, 40 GWd/MTU fuel burnup, and 10,000 years of decay time. The number of elements in the fuel composition was reduced to allow EQ6 to run more efficiently. EQ6 run time increases rapidly and non-linearly as the number of elements are increased. Therefore, the moles of Ru in Table 8 includes the moles of Ru, Rh, Pd, and Ag, and the moles of Gd in Table 8 includes the moles of Gd, Y, Pr, Nd, Pm, Sm, Eu, and Ho in the CSNF composition from *PWR Assembly End-Effect Reactivity Evaluation* (BSC 2001c). The elements not included in the fuel composition used in the model are Th, Pa, Am, Cm, Li, Be, As, Kr, Nb, and Xe. The concentration of the elements excluded from the CSNF composition are estimated to be below levels which have influence over the calculated in-package chemistry, thus their exclusion does not impact the results of the in-package chemistry model.

The sources for the CDNR (N Reactor) fuel composition used in the in-package chemistry model are *Repository Design Project, Repository/PA IED Emplacement Drift Committed Materials 1 of 2* (BSC 2003c) and Table 3-1 of *N Reactor (U-Metal) Fuel Characteristics for Disposal Criticality Analysis* (DOE 2000b).

Table 8 summarizes the composition of the CSNF and CDNR fuels, respectively. The CSNF is an oxide fuel while the CDNR fuel is a uranium metal type of fuel.

Table 8. Commercial Spent Nuclear Fuel and Codisposed N Reactor Fuel Compositions

Element [a]	CSNF Moles/100g	CDNR Moles/100g
U	0.3617	0.420
Np	0.0009	N/A
Pu	0.0027	N/A
Zr	0.0005	N/A
Mo	0.0009	N/A
Tc	0.0008	N/A
Ru	0.0020	N/A
Cs	0.0013	N/A
Ba	0.0010	N/A
Gd[b]	0.0035	N/A
O	0.7385	N/A

The sources for the "raw" HLWG chemical composition used in the in-package chemistry model are *Repository Design Project, Repository/PA IED Emplacement Drift Committed Materials 1 of 2* (BSC 2003c) and *Defense Waste Processing Facility Wasteform and Canister Description* (Baxter 1988, Table 10). Table 3 of *EQ6 Calculations for Chemical Degradation of N Reactor (U-metal) Spent Nuclear Fuel Waste Packages* (CRWMS M&O 2001), which uses *Repository Design Project, Repository/PA IED Emplacement Drift Committed Materials 1 of 2* (BSC 2003c) and *Defense Waste Processing Facility Wasteform and Canister Description* (Baxter 1988, Table 10) as its source, provides the HLWG composition in an EQ6-compatible format. Table 9 gives the simplified molar composition of the HLWG used in the models as reported in Table 3 of *EQ6 Calculations for Chemical Degradation of N Reactor (U-metal) Spent Nuclear Fuel Waste Packages* (CRWMS M&O 2001). The Savannah River glass composition was used in the model to maintain continuity with other analyses (e.g., CRWMS M&O 2001). Furthermore, the Savannah River glass has a higher concentration of potassium, about 23 times more than the Hanford glass, and potassium contributes to high pH conditions (BSC 2003c; CRWMS M&O 2000b, p. 8, Table 5-1). Therefore, use of the Savannah River glass is well justified in this model.

For input into EQ6, several elements in the glass composition from *Repository Design Project, Repository/PA IED Emplacement Drift Committed Materials 1 of 2* (BSC 2003c) and *Defense Waste Processing Facility Wasteform and Canister Description* (Baxter 1988, Table 10) were:

- Decayed to other elements (Pu-238 to U-234)
- Combined with other elements (e.g., Li added to Na) or
- Excluded to reduce the number of elements for ease in running EQ6.

The elements not included in the model of the glass composition were Ag, Cs, Cu, Li, Mn, Cl, Ni, Pb, Th, and Ti. These minor changes were made to the basic composition to increase the efficiency of the calculations, to decrease the EQ6 run time, and to allow the use of a pH dependent rate law. The resulting simplified HLWG formula based on 100 g is in Table 9.

Table 9. High-Level Waste Glass Composition

Element	Moles/100g HLWG
O	2.70E+00
U	7.82E-03
Ba	1.08E-03
Al	8.63E-02
S	4.01E-03
Ca	1.62E-02
P	4.89E-04
Si	7.76E-01
B	2.91E-01
F	1.66E-03
Fe	1.72E-01
K	7.51E-02
Mg	3.33E-02
Na	5.77E-01

The simplified glass composition was included in the EQ6 database as a mineral named 'SRL_Bulk.' These simplifications were necessary because the amounts of any element in the composition of minerals added to the database have to exceed 0.0001 moles/100g of glass.

4.2 CRITERIA

Project Requirements Document (Canori and Leitner 2003) contains three criteria that are relevant to the work documented in this report. They are:

- PRD-002/T-014 Performance Objectives for the Geologic Repository After Permanent Closure
- PRD-002/T-015 Requirements for Performance Assessment
- PRD-002/T-016 Requirements for Multiple Barriers.

Work described in this document will support these requirements, but more specific criteria exist in *Yucca Mountain Review Plan, Information Only* (NRC 2003). Selected acceptance criteria (NRC 2003) are presented in order to supplement or clarify the citation from *Project Requirements Document* (Canori and Leitner 2003).

The following acceptance criteria from *Yucca Mountain Review Plan, Information Only* (NRC 2003) were identified as applicable to this technical product:

1. Quantity and Chemistry of Water Contacting Waste Packages and Waste Forms, Acceptance Criteria (NRC 2003, Section 2.2.1.3.3)

1.1 AC1: System Description and Model Integration are Adequate

1.2 AC2: Data are Sufficient for Model Justification

1.3 AC3: Data Uncertainty is Characterized and Propagated Through the Model Abstraction

1.4 AC4: Model Uncertainty is Characterized and Propagated Through the Model Abstraction

1.5 AC5: Model Abstraction Output is Supported by Objective Comparisons

Technical Work Plan for Waste Form Degradation Modeling, Testing, and Analyses in Support of SR and LA (BSC 2002a) does not contain any criteria relevant to this activity.

4.3 CODES AND STANDARDS

ASTM C 1174-97 (1998), *Standard Practice for Prediction of the Long-Term Behavior of Materials, Including Waste Forms, Used in Engineered Barrier Systems (EBS) for Geological Disposal of High-Level Radioactive Waste*, is used to support the model development methodology, categorize the models developed with respect to their usage for long-term total

system performance assessment, and relate the information/data used to develop the model to the requirements of the standard. See Table 5 for other ASTM standards.

5. ASSUMPTIONS

5.1 INERT WASTE PACKAGE COMPONENTS

It is assumed that Alloy 22 and the structural components (non-fuel materials) of the fuel assembly are inert. The rationale for this assumption is that the Zircaloy is virtually non-reactive, and the amount of non-Zircaloy materials in the fuel assembly (such as the 304L springs, for example) are of negligible mass when compared to the total mass of the waste package. It is assumed that the outer shell of the waste package (Alloy 22) is inert. The basis for the Alloy 22 assumption is that Alloy 22 corrodes slowly compared to other reactants in the waste package. The probability of Alloy 22 corroding quickly is low as shown in Figure 51 of *General Corrosion and Localized Corrosion of Waste Package Outer Barrier* (CRWMS M&O 2000c, p. 109). This assumption does not require further confirmation because the effects on in-package chemistry would be small and would not significantly alter the results of the in-package chemistry model. This assumption is used throughout Sections 6.3 and 6.6.

5.2 WATER FILM

It is assumed that there is no time delay between waste package failure and the establishment of a continuous film of liquid water on the waste package internals and the chemical reactions, which accompany film formation. It is likely that a finite amount of time will be required to establish a stable film of water on the internal components of the waste package. Since the in-package chemistry model does not determine the amount of time required to establish a liquid water film after a waste package fails, this assumption is the only practical approach to apply and one that leads to the earliest release of reacted water from the waste package. Since this assumption leads to the earliest release of reacted water from the waste package, it is conservative and requires no further confirmation. This assumption is used throughout Sections 6.3 and 6.6.

5.3 FILM THICKNESS

In the water-vapor condensation model the film thickness is 0.1-cm thick for CSNF and 0.2-cm thick for CDNR. In the seepage-dripping model the film thickness is 0.25-cm thick for CSNF and 0.35-cm thick for CDNR. These film thickness values were chosen based on iterative model runs, the goal of which was to minimize the film thickness. EQ6 is an aqueous geochemical code; as such it requires the presence of sufficient liquid phase water to run, i.e., the ratio of the aqueous phase to the surface area of the solid reactants must exceed some critical value before the code executes in an efficient manner and outputs readily reproducible results for a series of run scenarios (water flux, temperature, and fuel exposure). While these film thickness values may be high with regard to adsorbed layers of water molecules on a solid surface, it was not the intent of this model report to examine chemical reactions at such a fine scale. Application of the assumed film thickness values is justified because they result in conservative in-package chemistry estimates, therefore, no further confirmation is required. This assumption is used throughout Sections 6.3 and 6.6.

5.4 TRANSLATION OF MODEL RESPONSE

It is assumed that variations in a model input will translate to the model output independent of the modeled scenario. To clarify, take the example of varying the corrosion rate of the steels used in the waste package. If the corrosion rate is decreased for one fuel exposure/flux scenario and this decrease has the effect of delaying the timing of a pH response, then it is assumed that an equivalent model response will occur for a different fuel exposure/flux scenario. The purpose of this assumption is that it allows the use of sensitivity analyses as a method of determining uncertainty ranges for parameters defined in the in-package chemistry model abstraction. Application of this assumption is justified and therefore needs no further confirmation because it is logical that a variation in an input value of a modeled chemical system will cause a similar response in a alternate but similar system. This assumption is used in Section 6.7.

6. MODEL

6.1 OBJECTIVES

The objective of the in-package chemistry model and, ultimately, the in-package chemistry model abstraction is to predict the chemistry inside of a failed waste package and to provide simplified expressions of that chemistry for use by the Performance Assessment Project. The outputs from the in-package chemistry model will be used as inputs for the in-package chemistry model abstraction, i.e., to generate abstractions of the in-package chemistry parameters of pH, ionic strength, Eh, total carbonate, chloride, and fluoride concentration. The in-package chemistry model abstraction will be implemented by the Performance Assessment Project in the TSPA-LA code, so that the dissolved concentrations, waste package colloid, and the spent nuclear fuel (SNF) sub-model abstractions will have their necessary input chemistry parameters. Thus, the in-package chemistry model and in-package chemistry model abstraction directly address FEP 2.1.09.01.0B Chemical characteristics of water in the waste package.

The in-package chemistry model simulates the chemistry inside of a failed waste package—the chemistry of the fluid that has reacted with the waste package components and SNF. For the in-package chemistry model, two different water ingress models are used:

- Water vapor ingress and subsequent condensation with film formation (i.e., the water vapor condensation model)
- The seepage dripping model where seepage enters a waste package forming a film, reacts with the waste package components and SNF, and exits the waste package.

Both the water vapor condensation and the seepage dripping model have separate process models and separate abstraction models, thus allowing for the implementation of non-dripping (water vapor condensation) and dripping (seepage dripping model) models in the TSPA-LA. Thus, model uncertainty is propagated through the abstractions to TSPA.

For both of these models the chemical reaction of the waste package components with a liquid phase was simulated as a function of time. The time-dependency of the in package chemistry is simulated by assigning kinetic rates to the reactants (i.e., the SNF and waste package components).

While the in-package chemistry model simulates in-package chemistry, the in-package chemistry model abstraction uses the output from the in-package chemistry model and derives simplified expressions, either parameter distributions or regression equations, of the in-package chemistry for use by total system performance assessment.

Model inputs for the in-package chemistry model encompass data (e.g., thermodynamic data and measured water compositions), parameters (e.g., waste form reaction rates and simulated water compositions), and other inputs (e.g., waste package design information and waste package component compositions). Inputs to the in-package chemistry model also include variables such as the percent of total fuel available for reaction (i.e., the cladding coverage for CSNF).

The N Reactor codisposal waste package is used as the representative U.S. Department of Energy (DOE) SNF in the in-package chemistry model. The rationale for this decision is that examination of the dissolution rate literature for other DOE SNF waste forms (DOE 2002, Section 6) indicates that the degradation rate of N Reactor fuel generally exceeds that of the other types of DOE SNF and that N Reactor SNF comprises approximately 85 percent of the total metric ton heavy metal of DOE SNF (DOE 2002, Appendix D).

6.2 FEATURES, EVENTS, AND PROCESSES

The development of a comprehensive list of features, events, and processes (FEPs) potentially relevant to postclosure performance of the Yucca Mountain repository is an ongoing, iterative process based on site-specific information, design, and regulations. The approach for developing an initial list of FEPs, in support of *Total System Performance Assessment for the Site Recommendation* (CRWMS M&O 2000d), was documented by Freeze et al. (2001). The initial FEP list contained 328 FEPs of which 176 were included in TSPA-SR models (CRWMS M&O 2000d, Tables B-9 through B-17). To support TSPA-LA, the FEP list was re-evaluated in accordance with *The Enhanced Plan for Features, Events, and Processes (FEPs) at Yucca Mountain* (BSC 2002e, Section 3.2). Table 10 provides a list of FEPs that are included in TSPA-LA models described in this model report, summarizes the details of their implementation in TSPA-LA, and provides specific references to sections within this model report.

6.3 BASE-CASE CONCEPTUAL MODEL

The base-case conceptual model is composed of two conceptual models, the water vapor condensation and the seepage dripping model, which collectively are referred to as the in-package chemistry model. These conceptual models differ from previous versions of the in-package chemistry model (BSC 2001e; CRWMS M&O 2000e; CRWMS M&O 2000f) where it was assumed that all of the void space within a waste package is filled with liquid. In essence the base-case conceptual model presented herein is a “film” model and that in previous model reports was a “bathtub” model. In the film model the void space inside of a failed waste package is partially occupied by liquid water in thermodynamic equilibrium with atmospheric gases both explicitly interacting in the solid-water-gas chemical system inside of a waste package. Therefore, the FEP 2.1.02.09.0A, Chemical effects of void space in waste, is addressed in the in-package chemistry model and as such in the in-package chemistry model abstraction and therefore in TSPA-LA.

Table 10. Included FEPs for the In-Package Chemistry Model Report and their Disposition in TSPA-LA

FEP No.	FEP Name	Section where Disposition is Described	Summary of Disposition in TSPA-LA
2.1.01.02.0B	Interactions between codisposed waste	6.3.2 6.3.3 6.6.2.1 6.6.2.2	Included. Interactions of condensed water and seepage with DOE SNF and HLWG is simulated in the IPCM, and abstractions of the resulting chemistry are provided for use by TSPA. HLWG tends to generate high pH solutions (Section 6.6.2) while DOE SNF generates neutral pH solutions (Section 6.6.2), and together combined with the waste package materials the high pH values are buffered to lower values. The interactions between codisposed waste is passed to TSPA explicitly via separate abstractions depending on the waste package type. The TSPA parameters (pH, ionic strength, total carbonate, Eh, chloride, and fluoride) are all impacted by this FEP.
2.1.02.09.0A	Chemical effects of void space in waste package	6.3 6.3.1 6.3.2 6.3.3 6.6.1.1	Included. The IPCM accounts for the unfilled void space in the WP, and thus its impact on the in-package chemistry. Void space in the WP is gas filled which has the effect of putting the gas phase in close contact with the liquid and solid phase reactants in the system, and is in fact the basis of the conceptual model implemented herein. Thus, the increased void space in the waste package decreases distance that gas must diffuse to maintain equilibrium with the liquid phase, this is contrast to the “bathtub” model (section 6.3.1) where all of the void space is liquid-filled and the gas phase must diffuse much longer distances to maintain equilibrium. It is included in the abstractions passed to TSPA via the oxygen and carbon dioxide equilibrium with the in-package chemistry solution. The TSPA parameters (pH, ionic strength, total carbonate, Eh, chloride, and fluoride) are all impacted by this FEP.
2.1.09.01.0B	Chemical Characteristics of Water in the Waste Package	6.3 6.3.2 6.3.3 6.6.1.1	Included. The chemical characteristics of water in the waste package is included in the TSPA-LA in-package chemistry model abstraction. The IPCM is a fully coupled reaction-path chemical model which includes the effects of waste form dissolution, metal alloy corrosion/dissolution, precipitation of metal oxide corrosion products, precipitation of complex mineral phases, reaction kinetics, thermal effects, interior WP void space, interactions of co-disposed waste forms, oxidation–reduction reactions, heterogeneous chemical reactions, and seepage composition on the resulting fluid chemistry. The output of the IPCM are time varying aqueous inventories of fluid composition, reactant abundances, product abundances, and solution properties. Solution parameters are abstracted into a TSPA compatible format in the IPCMA; therefore, all of the processes included in the IPCM are reflected in the IPCMA and thus in the TSPA. The parameters abstracted in the IPCMA include pH, ionic strength, total carbonate, Eh, chloride, and fluoride.
2.1.09.06.0A	Reduction-oxidation potential in EBS	6.6.1.2 6.6.2.2	Included. A partial treatment of this FEP is provided herein. The oxidation-reduction processes inside of the WP is explicitly modeled in the IPCM and thus implicitly included in the IPCMA. Oxidation of the metal waste package components is the primary process by which the waste packages corrode and the initial water composition is altered. Thus, in the absence of redox reactions there would be little alteration of the water inside of a failed waste package. The redox potential and its effect on the in-package chemistry is implicitly included in the abstractions passed to TSPA. The TSPA parameters (pH, ionic strength, total carbonate, Eh, chloride, and fluoride) are all impacted by this FEP.

FEP No.	FEP Name	Section where Disposition is Described	Summary of Disposition in TSPA-LA
2.1.09.07.0A	Reaction kinetics in EBS	6.3.2 6.3.3 6.6.1.1 6.6.1.2 6.6.2.2 6.7	Included. Reaction kinetics in the EBS, i.e., waste package, are included in the TSPA-LA in-package chemistry model abstraction. The IPCM uses kinetic reactants to represent the SNF (Section 4.1.2) and the WP components (Section 4.1.3.3). The kinetic rates used in the model were either linear, where a fixed amount of reactant is added at each time step, or a transition-state rate law where the amount of reactant added to the system depends on chemical properties of the aqueous phase. The effect of varying the kinetics on the in-package chemistry was examined in Section 6.7 where the rates were decreased to asses the contribution to uncertainty in pH and ionic strength for inclusion in the abstractions of pH for TSPA. The variability in the kinetics of the reactants is included in the abstractions passed to TSPA both implicitly by their use in the IPCM, and explicitly via the contribution of the kinetics to output uncertainty. The TSPA parameters (pH, ionic strength, total carbonate, Eh, chloride, and fluoride) are all impacted by this FEP.
2.1.09.02.0A	Chemical interaction with corrosion products	6.3.2 6.3.3 6.6.1.1 6.6.1.2 6.6.2.2	Included. In-package corrosion products and their effect on in-package chemistry are accounted for directly in the IPCM, and thus the IPCMA. The corrosion products of the steel and aluminum alloys in the waste package and their control on the concentration of aqueous species is of primary importance in determining the pH and ionic strength of the solution. If these corrosion products were not allowed to form during the simulations, then the resulting pH and ionic strength values would be much different then the results presented through Section 6.6. The interaction with the corrosion products is implicitly included in the abstractions passed to TSPA. The TSPA parameters (pH, ionic strength, total carbonate, Eh, chloride, and fluoride) are all impacted by this FEP.
2.1.11.08.0A	Thermal effects on chemistry and microbial activity in the EBS	6.3.3 6.6.1.2 6.6.2.2 6.7	Included. A partial treatment of this FEP is provided in this model report. The thermal effects on the in-package chemistry are examined in the SDM. Where EQ6 runs were performed at various temperatures to examine the temperature effect on the in-package chemistry. In these runs the kinetic reaction rates for the SNF were recalculated for runs at 15 to 90°C, and temperature appropriate thermodynamic data (Section 4.1.1.1) were used in the simulations. For TSPA-LA the in-package chemistry abstractions of pH, ionic strength, total carbonate, and Eh are cast in terms of temperature (Sections 8.2.3,8.2.6, 8.4.3, 8.4.6, 8.5, and 8.6) such that the in-package chemistry parameters used by TSPA can be calculated over a range of temperatures.
2.2.08.12.0A	Chemistry of water flowing into the EBS	6.3.3 6.6.1.2 6.6.2.2	Included. The chemistry of the water flowing into the EBS, i.e., the waste package, is included in the TSPA-LA LA in-package chemistry model. The SDM examined various input water chemistries (Section 4.1.1.2) and their effect on the in-package chemistry. The results showed the parameters passed to TSPA-LA were unaffected by changes in the input composition. Thus, while the abstractions for TSPA were derived using the output from the three initial water compositions there is no parameter in the abstractions to distinguish the initial water composition. The variability of the incoming water composition is implicitly included in the abstractions passed to TSPA via the use of varying composition waters in the IPCM. The TSPA parameters (pH, ionic strength, total carbonate, Eh, chloride, and fluoride) are only slightly impacted by this FEP.

NOTES: SDM = seepage dripping model; TSPA = total system performance assessment; WP = waste package; IPCMA = in-package chemistry model abstraction; IPCM = in-package chemistry model.

The chemical processes considered in the film models (water vapor condensation and seepage dripping model) include the following:

- Reaction-path tracing of the in-package chemical system
- Conservation of mass
- Kinetic dissolution of the waste package components and N Reactor U-metal fuel using linear rate laws
- Kinetic dissolution of CSNF and HLWG using transition-state theory rate laws, i.e., non-linear rate laws which are dependant on the fluid chemistry
- Equilibrium precipitation and dissolution of metal corrosion products and complex mineral phases
- Thermal, i.e., temperature effects on fluid chemistry
- Equilibrium oxidation and reduction reactions
- Chemical interaction of input solution with codisposed waste
- Effect of variable input compositions on the resulting fluid composition.

The physical processes considered in the film models include the following:

- Water flow, ingress and egress, through the waste package
- Mixing of water in contact with waste package components.

6.3.1 Film versus the Bathtub Model

Models that employ the EQ6 code to simulate the chemistry inside of a failed waste package all use kinetic rate laws, both linear and non-linear, to describe the dissolution of the waste package components and require two key input parameters for each reactant: 1) the amount of the reactant (i.e., moles); and 2) the surface area of the reactant. It is the method used in the scaling of these two quantities that distinguishes between the film and bathtub model. The bathtub model uses a volume-based scaling technique, and the film model uses a surface-area-based scaling technique.

EQ6 simulates a system that is composed of 1-liter of water—the EQ6 volume. Therefore, it is necessary to scale the reactant inputs (moles and surface area) to meet this 1-liter volume criterion.

For the bathtub model, a volume scaling scheme is used, with:

$$\text{Volume-Based Scaling Factor} = \frac{\text{EQ6 volume}}{\text{waste package total void volume*}}$$

* The void volume is the space inside of the waste package not occupied by waste package components.

Multiplying the surface area and moles of each waste package component by this scaling factor normalizes these quantities to the 1-liter EQ6 volume—this model considers the total void volume of the waste package to be filled with water.

For the film model, a surface-area-based scaling scheme is used, with:

$$\text{Surface-Area-Based Scaling Factor} = \frac{\text{EQ6 volume}}{\text{film thickness} * \text{waste package total internal surface area}}$$

Thus, multiplying the surface area and moles of each waste package component by this scaling factor normalizes these quantities to both the 1-liter EQ6 volume and the film thickness. This model spreads the 1-liter EQ6 volume equally over all of the waste package components as dictated by the thickness of the film.

In the water vapor condensation model and seepage dripping model one of the model inputs is the percent of SNF exposed to corrosive processes (i.e., the surface area of the SNF). In this model where the CSNF cladding is assumed inert (i.e., it does not react with seepage or condensation, Section 5.1) the fraction of the CSNF exposed directly influences the input surface areas and moles of the other waste package components via the surface area scaling factor. The reason for this is the EQ6 volume must be conserved. For example, in the modeled system when 1 percent of the CSNF is exposed, the water that "coats the surfaces" of the remaining 99 percent of the CSNF rods must be distributed over the other waste package components because it is not possible in EQ6 to specify that a fraction of the water in the system be nonreactive (i.e., the water coating the cladding). Based on the constraints of EQ6 the cladding remains "dry" for all simulations. The effect of increasing the surface area of the non-SNF components in these simulations is that the simulated system will generate a more aggressive chemical environment than the real system where the water contacting the cladding is non-reactive.

In essence, implementing a surface-area-based scaling method increases the surface area and moles of the reactants relative to the volume-based scaling method. Thus, the 1-liter EQ6 volume has both more surface area and moles of reactants to react with, in the film model compared to the bathtub model.

What does not change as a function of the model is the life span of the reactants. The reason for this is that the life span is a function of the kinetic rate constant and the ratio of moles to surface area, and neither this ratio nor the kinetic rate constant change regardless of the scaling factor.

In addition to the reactant properties, the water flux into the waste package is also scaled by the volume or surface-area-based scaling factor.

In addition to the effect on the surface area of the reactants, the film model also reduces the distances that gases (carbon dioxide and oxygen) must diffuse to maintain equilibrium with the waste package solution, i.e., the void space in the waste package is gas filled. In a liquid filled waste package (bathtub) the diffusion distance of gases outside the waste package is great and the probability of maintaining equilibrium between the gases and the waste package solution is low. However, in a partially liquid filled waste package, where the water is present as a film, the

diffusion distance of gases is reduced to the film thickness, and thus the probability of maintaining liquid – gas equilibrium is increased. It must be noted that in the previous versions of the in-package chemistry model (BSC 2001e; CRWMS M&O 2000e; CRWMS M&O 2000f), both of which were bathtub models, it was assumed that the waste package solution was well mixed and maintained equilibrium with the gases outside of the waste package. Therefore, the results of the previous versions of the in-package chemistry model were similar to the current model in terms of the system redox potential (Eh) and carbonate species distribution.

6.3.2 Water Vapor Condensation Model

The water vapor condensation model is a film model, which examines the in-package chemistry when a waste package fails and water vapor enters the package and condenses. The subsequent chemical reactions of the condensed water vapor with the waste package components and spent nuclear fuel form the water vapor condensation model. In the water vapor condensation model a film of water covers the waste package components, the supply rate of water is equal to the diffusion rate of water vapor, and there is no advective flow out of the waste package. The in-package chemistry from the water vapor condensation model will be used by TSPA-LA for cases when a diffusion model is implemented so that radionuclides may exit a failed waste package via diffusion through a film of water. The water vapor condensation model includes scenarios that examine the chemistry resulting from water reacting with each waste package component individually as well as that resulting from reactions with ensembles of waste package components.

The key components and concepts of the water vapor condensation are summarized below:

- The water vapor condensation model is executed in EQ6 as a titration (using the "special" reactant type for the water in the EQ6 input file), that is water and reactants are added to a "reaction vessel" at their respective kinetic rate(s) or diffusion flux for water, products form and may re-dissolve, but no water exits the system (Wolery and Daveler 1992, p. 42, Figure 3).

- Water vapor only condenses and forms a continuous film at 25°C. This temperature is used as the ambient repository temperature in the in-package chemistry model, and condensation may only occur on the waste package components and SNF when their temperatures are equal to or below the ambient temperature. With the knowledge that the interior of a waste package is the source of heat for the repository, it follows that until the temperature of the waste package internal components are equal to or less than their surroundings, water vapor will not condense on their surfaces. Furthermore, as was demonstrated in *Drift-Scale Coupled Processes (DST and THC Seepage) Models* (BSC 2003a, Section 6.5.5.1, Figure 6.5-3), the waste package temperature at 20,000 years post-closure is approximately 40°C, i.e., above the dew point temperature. However, it is also recognized that for the purposes of TSPA, a model describing the in-package chemistry for non-dripping conditions may be required at temperatures exceeding 25°C, as no other model is available, and the water vapor condensation model would provide an estimate of the chemistry. Should the water vapor condensation model be applied by TSPA at temperatures other than 25°C, additional uncertainty should be included as described in Sections 8.1.1, 8.1.2, 8.3.1, and 8.3.2.

- The relative humidity in the drift and waste package environment is sufficient to maintain a film of water on the internal waste package components for the duration of the modeled period. Concurrent with the temperature falling below boiling in the repository and the surrounding rock, the matrix of the host rock rewets to just less than 100% saturation, and maintains this value for the remainder of the model period (BSC 2003a, Section 6.5.5.1, Figure 6.5-3). Thus, given that the matrix maintains high constant saturation it follows that the humidity in the drift will also remain high for the duration of the model period. While there may be unquantified deviations in the relative humidity as a function of time, which would impact the results of the water vapor condensation model, the approach of assuming constant and high relative humidity ensures that the in-package chemistry is not interrupted for the duration of the model period.

- Water that condenses and reacts with the waste package components and SNF initially contains no dissolved solutes other than carbonate species from equilibrium with atmospheric carbon dioxide. Water vapor (gaseous phase water) is distilled, i.e., contains no solutes. Upon condensation the newly formed liquid phase contains no dissolved solutes other than the aforementioned carbonate species. The minor and trace gases in the atmosphere were not included in the model because they are either inert or of such low concentration to be of no consequence on the model results. This water composition was used in the water vapor condensation model because it best represents the composition of condensed water vapor.

- The film thickness is 0.1 cm for CSNF and 0.2 cm for CDNR (Section 5.3). Variations in the film thickness in a real system compared to the modeled system could add a small degree of uncertainty. Instead, this uncertainty is already captured by the conservative nature of the uncertainty range.

- Water vapor enters the breached waste package and condenses on the waste package components at a rate equal to the water vapor diffusion rate into the waste package, which is 43.88 moles per year per waste package (BSC 2003b, Section 6.2.2).

- 10 percent of the CSNF is available for reaction; this value was chosen because it represents the median value used in the seepage dripping model simulations. Using a single value for CSNF exposure is justified because its contribution to the chemical system is relatively benign (Section 6.6.1.1 and 6.6.1.2). Although this value was not varied in the water vapor condensation model runs its contribution to the uncertainty of the model response is expected to be small.

- 100 percent of the HLWG was exposed to corrosive processes. This value is justified because HLWG dissolution can result in an aggressive chemical environment via high pH conditions (Section 6.6.2.1), and is therefore conservative. Although this value was not varied in the water vapor condensation model runs, its contribution to the model response is accounted in the abstraction for TSPA-LA (Section 8.3.1).

- 50 percent of the CDNR surface area was exposed to corrosive processes. *N Reactor (U-Metal) Fuel Characteristics for Disposal Criticality Analysis* (DOE 2000b, Section

3, Appendix C) states that only about 50 percent of the N Reactor fuel assemblies were intact due to underwater storage; thus, an even a higher percentage of the CDNR fuel is or may be exposed in the future. This value is justified because the N reactor fuel has a minor influence on the in-package chemistry (Section 6.6.2.1). Although this value was not varied in the water vapor condensation model runs, its contribution to the uncertainty of the model response is expected to be small.

- The surface area values used in the model for the SNF and waste package components are fixed and do not vary with time. The EQ6 code uses the surface area of the reactants to calculate the amount of reactant available to react at each time step (Section 6.5.1.1). The more surface area available, the faster the reactant degrades. In an actual system, as the amount of reactant decreases due to degradation, so too would its surface area. However, it is not possible to implement the actual changing surface area in the EQ6 code. Therefore, the constant surface area provides an average surface area for the reactants for the duration of their lifetime. The constant surface area approximation could contribute to the uncertainty of the model response.

- For the ensemble runs the film is well mixed and not flowing. The rationale for this concept is twofold; first, the waste package components are evenly distributed and in close proximity to one another inside of the waste package, and secondly, the water vapor condensation model is developed to examine the chemistry of solutions resulting from combinations of waste package components and SNF (i.e., the mixture of any intra-waste package flow path dependent chemistries). The results of the single component runs compared to the ensemble runs (Sections 6.6.1.1 and 6.6.2.1) show that this concept is justified.

This conceptual model addresses the following FEPs:

- 2.1.09.01.0B Chemical characteristics of water in the waste package

- 2.1.09.07.0A Reaction kinetics in EBS: The reactants that constitute the waste package and waste form are represented in the water vapor condensation model as kinetic reactants; therefore, this FEP is addressed

- 2.1.02.09.0A Chemical effects of void space in waste package: In the film model, at least some of the void space is not filled with liquid; therefore, the conceptual model directly addresses the FEP

- 2.1.01.02.0B Interactions between codisposed waste: The film model considers codisposed waste and the chemical effects resulting from the codisposal of glass-pour canisters and the multi-canister overpacks; therefore, the conceptual model directly addresses the FEP

- 2.1.09.02.0A Chemical interaction with corrosion products: Corrosion products are generated during the degradation of the metal alloys that make up the waste package components. Therefore, the effect of the corrosion products on the in-package chemistry

is directly handled by the in-package chemistry model and, thus, the in-package chemistry model abstraction that is used in the dissolved concentration calculation.

Water Vapor Condensation Model Cases—The cases that encompass the water vapor condensation model include single reactant runs and multi-component ensemble runs. The single reactant runs react a film of water with one alloy or waste form for the purpose of determining the resulting chemistry and the contribution of the reactants to the in-package chemistry for comparison with the ensemble results. The ensemble runs combine two or more reactants for the purpose of determining the effect of multiple reactants and reactant combinations on the in-package chemistry. The combination of reactants in an ensemble represents the primary source of uncertainty in the water vapor condensation model. The choice of reactant ensembles was based on two criteria: spatial proximity of a waste package component to the SNF or HLWG and reactivity/surface area of a reactant. For example, A516 carbon steel is both highly reactive (high corrosion rate) and has a high surface area in CSNF packages and is in close proximity to the waste. For these reasons A516 appears in nearly every ensemble run.

Tables 11 and 12 summarize the cases simulated in the water vapor condensation model. The EQ6 input file (*.6i) name convention followed was CS = CSNF, CD = CDNR, comp# = ensemble ID. For example:

CS_comp7.6i has the following inputs: CSNF waste package, Al-6061, A516 FBT, and A516 stiffeners as reactants.

6.3.3 Seepage Dripping Model

The seepage dripping model is a film model that examines the in-package chemistry following the ingress of seepage into the waste package. In the seepage dripping model, seepage enters and exits the waste package without accumulating or filling all of the waste package void space, as it flows the seepage reacts with the internal components of the waste package and deposits corrosion products in the waste package interior.

Table 11. Commercial Spent Nuclear Fuel Water Vapor Condensation Multi-Component Ensembles

Waste Package Component / EQ6 File	CS_comp1	CS_comp2	CS_comp3	CS_comp4	CS_comp5	CS_comp6	CS_comp7	CS_comp8	CS_comp9	CS_comp10	CS_comp11
S31600 NG inner vessel	✓					✓			✓		
Neutronit	✓	✓			✓	✓		✓			
Al-6061	✓	✓	✓		✓	✓	✓				✓
FBT (A516)	✓	✓	✓	✓	✓	✓	✓	✓	✓	✓	✓
Stiffeners (A516)	✓	✓	✓	✓	✓	✓	✓	✓	✓	✓	✓
CSNF	✓	✓	✓	✓						✓	✓

Table 12. Codisposed N Reactor Water Vapor Condensation Multi-Component Ensembles

Waste Package Component / EQ6 File	CD_comp1	CD_comp2	CD_comp3	CD_comp4	CD_comp5	CD_comp6	CD_comp7	CD_comp8
S31600 Inner vessel	✓							
Al-110	✓	✓		✓				✓
304L MCO	✓	✓	✓	✓				
304L MCO top	✓	✓	✓	✓				
304L GPC	✓	✓	✓	✓	✓	✓		
A516 plates	✓	✓	✓	✓	✓		✓	
U-Metal	✓	✓	✓					
HLWG	✓	✓	✓	✓	✓	✓	✓	✓

NOTES: MCO = multi-canister overpack; GPC = glass-pour canister.

The key model components and concepts for the seepage dripping model are summarized below:

- The seepage dripping model of the in-package chemistry model uses the solid-centered flow through option in EQ6 (using the "displacer" reactant type for the water in the EQ6 input file) which simulates a single cell batch reactor, i.e., seepage water "flows" into a cell at specified rate while reactants are added to the cell at their kinetic rate(s), chemical reactions take place, products precipitate and redissolve, and effluent exits the cell (Wolery and Daveler 1992, p. 46, Figure 5).

- Seepage drips onto the upper surface of the waste package and penetrates the waste package through an opening. The solution then flows through the waste package coating the interior components with a film reacting, mixing, and flushing the dissolved material from the waste package. There is no accumulation of water in the waste package.

- The thickness of the water film(s) is independent of the water flux into the failed waste package. For ideal film flow, to maintain a given film thickness, a certain flow rate is required. However, with the modeling tools available and the complexity of the system, it is not possible to model ideal film flow. Therefore, in this model, the film concept is used to scale the amount of water to the surface area of reactants; in essence, taking one step closer to the ideal from the previous bathtub model. The film thickness values used in the in-package chemistry model are large relative to adsorbed water on a solid surface, and depending on the geometry (curved versus planar) and orientation (horizontal versus inclined) of a waste package component's reacting surface, as well as the presence of corrosion products which would act to retain water, a relatively high flux value may be required to sustain the film thickness values used in the model. Therefore, decoupling the film thickness and the flux is a concept that is critical for the model at early time (less than about 20 to 50 years post failure), i.e., at times before a layer of corrosion products have developed on the surfaces of the waste package components. When the surfaces of the waste package components are "fresh," the water film will more easily runoff and not fully react. There will be little change in the composition of

the incoming seepage. At later times when a layer of corrosion products develops on the surfaces, a water film will be more easily sustained under low-flow conditions. Furthermore, considering waste package geometry reveals that the key waste package components (fuel basket tubes, fuel plate assemblies, and corner guides) have a planar geometry and are largely orientated horizontally with their vertical surfaces closely adjacent so that capillary forces would maintain a film of water. In the case of the CDNR package with the two multi-canister overpacks and two glass-pour canisters there are fewer horizontal surfaces as compared to the CSNF; however, the sustained water film leads to more complete reaction of the waste package components, SNF, and seepage. Since the in-package chemistry model abstraction does not provide total system performance assessment with an abstraction of water flux and the decoupling of film thickness from water flux leads to conservative estimates of in-package chemistry, this model concept is appropriate for TSPA-LA purposes.

- The inside surface area of the S31600 inner vessel is exposed to degradation within the CSNF and CDNR waste package. The rationale for this concept is that the in-package chemistry model is only concerned with the chemistry on the interior of the waste package (i.e., the chemistry of the solution that either has reacted with the SNF or has the potential to react with the SNF).

- The composition of the seepage water entering the waste package is constant with time. Three seepage compositions (Table 2) are used in the seepage dripping model to examine the effect of water composition on the resulting in-package chemistry. While it is possible that waters of alternate compositions could enter a failed waste package, and that composition could vary with time, the results (Sections 6.6.1.2 and 6.6.2.2) show that the model response is largely insensitive to the composition of the water entering a waste package. The model does not account for the possibility of seepage concentrated via evaporative processes entering the waste package, which could add a small degree of uncertainty to the model results. Instead, this uncertainty is already captured by the conservative nature of the uncertainty range.

- The water flux through the waste package varies from 0.15 to 15.0 l/y for the seepage dripping model. These values are an order of magnitude lower than the correlation between percolation flux and drip rate, also called mean seep flow rate (CRWMS M&O 2000d, Figure 3.2-15). To ensure conservatism, lower water flux terms were used, as longer residence times within the waste package and increased contact with waste package components allows for extreme chemistries to develop. In Section 6.7 sensitivity analyses were performed to expand the range of flux values that could be used in the abstraction developed in Section 8.

- The film thickness is 0.25 cm for CSNF packages, and 0.35 cm for CDNR packages (Section 5.3). Variations in the film thickness in the real system compared to the modeled system could add a degree of unquantified uncertainty to the model output.

- The CSNF surface area is 1, 10, or 100 percent exposed to corrosive processes. Although 100 percent fuel exposure may be a low probability circumstance, the broad range of surface area values was used to include all eventualities. The CSNF surface

area is used as input parameter for the CSNF pH abstractions (Section 8.2.1 and 8.2.2), thus the range used in the model is justified.

- The CDNR and HLWG are 100 percent exposed to corrosive processes; these values were used to maximize the influence of these reactants on the in-package chemistry. No parameter is passed to TSPA-LA to describe the CDNR and HLWG exposure, i.e., these fuel exposures are justified because they are the TSPA input values.

- Due to high relative humidity on the interior of the waste package the effects of evaporation inside of the waste package will have a negligible influence on the in-package chemistry. For early failures, the openings in a waste package are likely to be small and restrictive, thus water entering will quickly increase the relative humidity inside of the waste package such that evaporation will be minimized. There will be a period immediately after waste package failure (when water first enters and the relative humidity increases) where the evaporation inside of the waste package will be high; this phenomena was not included in the in-package chemistry model. Depending on the flux value of seepage into the waste package, this early time evaporation could add a degree of unquantified uncertainty to the model results. At high flux values, the effect of early time evaporative processes is likely to have a negligible impact on the model results because the humidity inside of the failed waste package would quickly increase, and the high water flux would diminish any evaporative effects on the fluid composition. At low water flux values the opposite would be true; the time required to increase the humidity would be longer, and the low water flux would have less of a dilution effect. Thus, the effect of in-package evaporation on model uncertainty is greatest at early times and at low water flux values.

- The film is well mixed. This is justified based on the results presented for the single component and ensemble water vapor condensation model (Sections 6.6.1.1 and 6.6.2.1).

- Oxygen and carbon dioxide maintain equilibrium with the waste package solution and the ambient atmosphere outside of the waste package. The partial pressure of CO_2 and O_2 of the ambient repository atmosphere are set to $10^{-3.0}$ and 0.2 atm, respectively (log fO_2 = -0.7 and log fCO_2 = -3). The rationale for the oxygen partial pressure is that it is equivalent to that in the atmosphere (Weast 1977, p. F-210). The rationale for choosing the carbon dioxide pressure to be higher than the atmospheric value is that ambient fluids drawn from boreholes near the repository horizon appear to be in equilibrium with above-atmospheric carbon dioxide levels (Yang et al. 1996, Table 8). In the film model the waste package void space is only partially occupied with water and the remaining void space is filled with gas; therefore, this model concept is well justified. In addition, a sensitivity analysis of the model response to the CO_2 partial pressure is discussed in Section 6.3.4 and the results presented in Section 6.7. The minor and trace gases in the atmosphere were not included in the model because they are either inert or of such low concentration to be of no consequence on the model results.

- The EQ3/6 results generated using the B-dot activity coefficient equation for solutions with ionic strength greater than 1 molal are sufficiently accurate for the current

calculation. The rationale for this is that experimental data (in sulfate, nitrate, and chloride solutions) shows that EQ3/6 results using the B-dot activity coefficient equation can be used qualitatively up to an ionic strength of about 4 molal to indicate the general nature of the reactions that would actually occur (CRWMS M&O 1997, Appendix D). Scenarios when the ionic strength exceeded 1 molal occurred for the low flux (0.15 l/yr) scenarios. While additional uncertainty may be introduced to the in-package chemistry when the ionic strength exceeds one molal, the primary parameter passed to TSPA (i.e., pH) does not display unusual trends for high ionic strength simulations compared to the low ionic strength simulations (Section 8.2.1). Therefore, a decision was made to include these results in the model report and carry them forward in the abstraction with no additional uncertainty for two reasons: (1) the potential need by the Performance Assessment Project to handle low flux conditions in TSPA-LA; and (2) the submodels which use the in-package chemistry abstractions are either not effected by ionic strength (CSNF degradation and HLWG dissolutions models) or have "flags" when the ionic strength (solubility and colloid model) exceeds a threshold value.

- The surface area values used in the model for the SNF and waste package components are fixed and do not vary with time. The EQ6 code uses the surface area of the reactants to calculate the amount of reactant available to react at each time step (Section 6.5.1.1).The more surface area available, the faster the reactant degrades. In an actual system, as the amount of reactant decreases due to degradation, so too would its surface area. However, it is not possible to implement the actual changing surface area in the EQ6 code. Therefore, the constant surface area provides an average surface area for the reactants for the duration of their lifetime. The constant surface area approximation could contribute to the uncertainty of the model response.

The seepage dripping model conceptual model will aid in the disposition of the following FEPs:

- 2.1.09.01.0B Chemical characteristics of water in the waste package.

- 2.1.09.07.0A Reaction kinetics in EBS: The reactants that constitute the waste package and waste form are represented in the seepage dripping model as kinetic reactants; therefore, this FEP is addressed.

- 2.2.08.12.0A Chemistry of water flowing into the EBS: The seepage dripping model addresses this FEP by using two different seepage compositions in addition to the J-13 composition.

- 2.1.11.08.0A Thermal effects on chemistry and microbial activity in the EBS: The role of elevated temperature on the in-package chemistry is examined in the seepage dripping model.

- 2.1.02.09.0A Chemical effects of void space in waste package: In the film model, at least some of the void space is not filled with liquid; therefore the conceptual model directly addresses the FEP.

- 2.1.01.02.0B Interactions between codisposed waste: The film model considers codisposed waste and the chemical effects resulting from the codisposal of glass-pour canisters and the multi-canister overpacks; therefore, the conceptual model directly addresses the FEP.

- 2.1.09.02.0A Chemical interaction with corrosion products: Corrosion products are generated during the degradation of the metal alloys that make up the waste package components. Therefore, the effect of the corrosion products on the in-package chemistry is directly handled by the in-package chemistry model and thus the in-package chemistry model abstraction that is used in the dissolved concentration calculation.

Seepage Dripping Model Cases—A matrix of model runs (Tables 13 and 14) were executed in which four key input variables were varied across their expected input range for the purpose of generating a broad range of model response. The key parameters included: water flux, fuel exposure (clad failure), initial water composition, and temperature. Systematic combinations of three input water compositions, three values of fuel exposure (clad failure) for CSNF, and three values of water flux were run for both waste package types at two different temperatures. This approach is a factorial design approach where a run matrix was implemented (Tables 13 and 14) to capture the full range of possible scenarios and model response.

For the CSNF cases the fuel exposure (clad failure) and water flux input parameters were varied because it has been shown (BSC 2001e; CRWMS M&O 2000e; CRWMS M&O 2000f) that the results of the in-package chemistry model are sensitive to these inputs, and they are input variables in the total system performance assessment to the in-package chemistry model. The temperature was varied to increase the range of applicability of the in-package chemistry model and in-package chemistry model abstraction. The input water composition was varied to determine if the in-package chemistry model response is sensitive to this input, and it answers FEP 2.2.08.12.0A Chemistry of water flowing into the engineered barrier system.

Other model inputs were also varied in sensitivity analyses (Sections 6.3.4 and 6.7) to expand the applicability of the model abstraction for TSPA implementation and to quantify model uncertainty.

The EQ6 input file naming convention is as follows: C = CSNF, D = CDNR, 1 = 0.15 l/yr, 2 = 1.5 l/yr, 3 = 15 l/yr, 1 = 1 percent clad failure, 2 = 10 percent clad failure, 3 = 100 percent clad failure (for CDNR always set to “3”), J = J-13 water; C = Ca-porewater; N = Na-porewater, 25 = 25°C; 50 = 50°C. Tables 13 and 14 summarize the CSNF and CDNR inputs, respectively. For example, for EQ6 input file, C22C25.6i, it follows: C = CSNF, 2 = 1.5 l/yr, 2 = 10% clad failure, C = Ca porewater, 25 = 25°C.

Table 13. EQ6 Input Guide for the CSNF Seepage Dripping Model Runs

EQ6 RootFile Name (*.6i)	Waste Package Type	Flux	Cladding Failure	Water Type	Temperature (°C)
C11C25	CSNF	0.15	1%	Ca-Porewater	25
C12C25	CSNF	0.15	10%	Ca-Porewater	25
C13C25	CSNF	0.15	100%	Ca-Porewater	25
C21C25	CSNF	1.5	1%	Ca-Porewater	25
C22C25	CSNF	1.5	10%	Ca-Porewater	25
C23C25	CSNF	1.5	100%	Ca-Porewater	25
C31C25	CSNF	15.0	1%	Ca-Porewater	25
C32C25	CSNF	15.0	10%	Ca-Porewater	25
C33C50	CSNF	15.0	100%	Ca-Porewater	25
C11C50	CSNF	0.15	1%	Ca-Porewater	50
C12C50	CSNF	0.15	10%	Ca-Porewater	50
C13C50	CSNF	0.15	100%	Ca-Porewater	50
C21C50	CSNF	1.5	1%	Ca-Porewater	50
C22C50	CSNF	1.5	10%	Ca-Porewater	50
C23C50	CSNF	1.5	100%	Ca-Porewater	50
C31C50	CSNF	15.0	1%	Ca-Porewater	50
C32C50	CSNF	15.0	10%	Ca-Porewater	50
C33C50	CSNF	15.0	100%	Ca-Porewater	50
C11N25	CSNF	0.15	1%	Na-Porewater	25
C12N25	CSNF	0.15	10%	Na-Porewater	25
C13N25	CSNF	0.15	100%	Na-Porewater	25
C21N25	CSNF	1.5	1%	Na-Porewater	25
C22N25	CSNF	1.5	10%	Na-Porewater	25
C23N25	CSNF	1.5	100%	Na-Porewater	25
C31N25	CSNF	15.0	1%	Na-Porewater	25
C32N25	CSNF	15.0	10%	Na-Porewater	25
C33N50	CSNF	15.0	100%	Na-Porewater	25
C11N50	CSNF	0.15	1%	Na-Porewater	50
C12N50	CSNF	0.15	10%	Na-Porewater	50
C13N50	CSNF	0.15	100%	Na-Porewater	50
C21N50	CSNF	1.5	1%	Na-Porewater	50
C22N50	CSNF	1.5	10%	Na-Porewater	50
C23N50	CSNF	1.5	100%	Na-Porewater	50
C31N50	CSNF	15.0	1%	Na-Porewater	50
C32N50	CSNF	15.0	10%	Na-Porewater	50
C33N50	CSNF	15.0	100%	Na-Porewater	50
C11J25	CSNF	0.15	1%	J-13	25
C12J25	CSNF	0.15	10%	J-13	25
C13J25	CSNF	0.15	100%	J-13	25
C21J25	CSNF	1.5	1%	J-13	25
C22J25	CSNF	1.5	10%	J-13	25
C23J25	CSNF	1.5	100%	J-13	25
C31J25	CSNF	15.0	1%	J-13	25

Table 13. EQ6 Input Guide for the CSNF Seepage Dripping Model Runs (Continued)

EQ6 RootFile Name (*.6i)	Waste Package Type	Flux	Cladding Failure	Water Type	Temperature (°C)
C32J25	CSNF	15.0	10%	J-13	25
C33J50	CSNF	15.0	100%	J-13	25
C11J50	CSNF	0.15	1%	J-13	50
C12J50	CSNF	0.15	10%	J-13	50
C13J50	CSNF	0.15	100%	J-13	50
C21J50	CSNF	1.5	1%	J-13	50
C22J50	CSNF	1.5	10%	J-13	50
C23J50	CSNF	1.5	100%	J-13	50
C31J50	CSNF	15.0	1%	J-13	50
C32J50	CSNF	15.0	10%	J-13	50
C33J50	CSNF	15.0	100%	J-13	50

Table 14 provides the CDNR run matrix, note that since there is no fuel exposure (cladding) term in the CDNR model the number of runs is greatly reduced compared to the CSNF run matrix (Table 13).

Table 14. EQ6 Input Guide for the Codisposed N Reactor Seepage Dripping Model Runs

EQ6 RootFile Name (*.6i)	Waste Package Type	Flux	Water Type	Temperature (°C)
D13C25	CDNR	0.15	Ca-Porewater	25
D23C25	CDNR	1.5	Ca-Porewater	25
D33C50	CDNR	15.0	Ca-Porewater	25
D13C50	CDNR	0.15	Ca-Porewater	50
D23C50	CDNR	1.5	Ca-Porewater	50
D33C50	CDNR	15.0	Ca-Porewater	50
D13N25	CDNR	0.15	Na-Porewater	25
D23N25	CDNR	1.5	Na-Porewater	25
D33N50	CDNR	15.0	Na-Porewater	25
D13N50	CDNR	0.15	Na-Porewater	50
D23N50	CDNR	1.5	Na-Porewater	50
D33N50	CDNR	15.0	Na-Porewater	50
D13J25	CDNR	0.15	J-13	25
D23J25	CDNR	1.5	J-13	25
D33J50	CDNR	15.0	J-13	25
D13J50	CDNR	0.15	J-13	50
D23J50	CDNR	1.5	J-13	50
D33J50	CDNR	15.0	J-13	50

6.3.4 Sensitivity Cases—Uncertainty Analyses

The base-case model inputs have “epistemic” uncertainty, that is the uncertainty is due either to simplifying assumptions regarding geometry or composition, for example, or due to minor

variations in design versus actual parameters, e.g., engineering drawing dimensions versus actual manufactured dimensions.

Sensitivity analyses were performed to meet the following objectives: (1) to determine uncertainty ranges for pH and ionic strength for use in the in-package chemistry model abstraction; (2) to expand the boundaries (temperature, flux, and CO_2 partial pressure ranges) of the in-package chemistry model abstraction without performing a large array of additional simulations; and (3) to demonstrate the effects of waste package configuration variations on the model output.

Model runs were executed using the median seepage flux/fuel exposure case (C22C25) for the seepage dripping model CSNF at 25°C as the starting point input. The underlying assumption being that input variations will cause the same response in the modeled output regardless of the scenario.

Key inputs were varied over a range of values, and the outputs were compared to the C22C25 output. The choice of inputs that were varied in these sensitivity runs was based on the analyst's knowledge of the phenomena, i.e., inputs that were known to effect the model results were chosen. The effects of carbon dioxide partial pressure, sulfur content of the A516, and steel corrosion rates were investigated in a series of simulations. Additional simulations varying the temperature and water flux values were performed to expand the boundaries of the in-package chemistry model abstraction. Finally, runs were completed for both the CSNF and CDNR waste packages to show that minor changes in the design configuration had little impact on the model response.

The results of the sensitivity analyses are presented in Section 6.7.

6.4 ALTERNATIVE CONCEPTUAL MODELS

6.4.1 Alternative Conceptual Model I

The interior of a waste package is spatially heterogeneous with respect to composition; therefore, a stream of water traveling vertically downward through the cross-sectional interior of a waste package would encounter different materials at different times. Along this flow path and at a given time, water molecules in the stream of water would react with the solid or solids to which they were immediately adjacent, resulting in a water stream that has a variable composition along its flow path. This conceptual model could be viewed as a one-dimensional column composed of *n* cells where the reactants in each cell represent the waste package components in vertical cross section of the waste package—this model would eliminate the constraint of the EQ6 solid-centered flow through mode, used in the in-package chemistry model, of a well mixed batch reactor. This alternative conceptual model would also provide spatial information on the chemistry inside of a failed waste package, information that is not used by total system performance assessment.

The water vapor condensation model results showed (Section 6.6.1.1) that the mixing model actually provides a good alternative to the more complex Alternate Conceptual Model I. The reason being that the waste package materials tend to have an overwhelming effect on the in-package chemistry regardless of mixing.

6.4.2 Alternative Conceptual Model II

Seepage entering a failed waste package is likely to vary in composition as a function of time (i.e., as the conditions that prevail in the drift and engineered barrier system (EBS) vary over time). Therefore, a conceptual model that implemented a continuously varying input fluid composition would be more realistic than the current in-package chemistry model, in which the input fluid compositions are constant over time. The seepage dripping model showed that model response was largely insensitive to input water composition because the effect of the waste package materials on the in-package chemistry exerted much more control than the input water composition (Section 6.6.1.2). The alternative conceptual models are listed in Table 15.

Table 15. Alternative In-Package Chemistry Conceptual Models

Alternative Conceptual Model	Key Features	Screening Assessment and Basis
Alternative Conceptual Model I	The WP is compositionally discrete	The WVC model showed that the resulting chemical effects of individual WP components were comparable to that of their ensembles. See Section 6.6.1.1
Alternative Conceptual Model II	The composition of seepage entering a WP is likely to vary as a function of changing conditions in the UZ and drift environments.	The SDM showed that wide compositional ranges in the seepage composition had little influence on the resulting in-package chemistry. See Section 6.6.1.2

NOTES: SDM = seepage dripping model; WP = waste package; WVC = water vapor condensation.

Although the DOE has considered alternative models, it has been determined (and demonstrated in this model report) that the current models (water vapor condensation and seepage dripping model) are sufficient, and that this in-package chemistry model is robust, fulfills the stated purpose of this model report, and adequate for licensing purposes.

6.5 BASE-CASE MODEL INPUTS

6.5.1 Waste Package Component Properties

6.5.1.1 Metal Alloy Composition and Corrosion Rates

The in-package chemistry model represents the metal alloys as “special reactants,” in the EQ6 input files, with the compositions given in Table 16. The values in Table 16 were calculated from the weight percent values in Table 6 by dividing the weight percent of each element by the respective atomic weight for each element. This method uses the convention of assigning a 100 gram/mole molecular weight for each alloy (the same convention was used for expressing the compositions of the CSNF, CDNR, and HLWG in Tables 8 and 9).

Table 17 provides the corrosion rates used in the in-package chemistry model. The corrosion rates were calculated by converting to consistent units and multiplying the corrosion values in Table 7 by their density and dividing the result by 100g per mole. The steel corrosion rates given in Tables 7 and 17 represent values that are robust in the temperature range from 25° to 50°C. The values are supported by the data in DTN: MO0303SPAMCRAQ.000, which cover a range of temperatures and corroding water compositions.

Table 16. Metal Alloy Compositions

Element	A516 moles	Neutronit moles	Al-6061 moles	S31600 moles	Al-1100 moles	304L moles
C	2.33E-02	3.33E-03		1.67E-03		2.50E-03
Mn	1.90E-02		2.73E-03	3.64E-02		3.64E-02
P	1.13E-03			1.45E-03		1.61E-03
S	1.09E-03			9.36E-04		9.36E-04
Si	1.03E-02		2.14E-02	2.67E-02	1.60E-02	2.67E-02
Cr		3.56E-01	3.75E-03	3.27E-01		3.65E-01
Ni		2.21E-01		2.04E-01		1.70E-01
Co		3.39E-03				
Mo		2.29E-02		2.61E-02		
N				5.71E-03		7.14E-03
Fe	1.76E+00	1.16E+00	1.25E-02	1.17E+00	8.95E-03	1.22E+00
B		1.15E-01				
Zn			3.82E-03			
Cu			4.33E-03		7.87E-04	
Mg			4.11E-02			
Ti			3.13E-03			
Al			3.58E+00		3.67E+00	

Table 17. Metal Alloy Corrosion Rates

	A516	Neutronit	Al-6061	S31600	Al-1100	304L
Corrosion Rate (moles/s-cm^2)	1.80E-11	2.54E-14	2.54E-13	2.53E-14	2.54E-13	2.52E-14

Source: CSNF.xls, worksheet"Rates"

The amount of metal alloy that EQ6 "adds" to the reaction during a run is the product of the coefficients in Table 17, the duration of the EQ6 time step, and the surface area of the reactant. The surface areas used in the simulations (Sections 6.5.2, 6.5.3, and 6.5.4) remain fixed for the duration of the reactants existence.

6.5.1.2 SNF and HLWG Reaction Rates

Table 18 provides the CSNF reaction rate coefficients at 25, 50, and 90°C for the equation presented in Section 4.1.2.3. The two expressions given in Section 4.1.2.3 for the dissolution of CSNF were combined into a single closed-form expression for use in EQ6 (Table 18). The CSNF reaction rate is a transition state theory rate law that is dependent on temperature, pH, and bicarbonate concentration. The bicarbonate concentration is used rather than total carbonate because CSNF rate law is insensitive to carbonate concentration in the output pH range (3 to 8) of the model. Figure II-2 of Attachment II shows the CSNF total degradation constant as a function of pH and derived in terms of both total carbonate and HCO_3^-. This figure shows that from pH 2 to about pH 10 the total degradation constant is not sensitive to carbonate, but above pH 10 the degradation constant is sensitive to carbonate.

The coefficients in Table 18 are from the "CSNF.xls" spreadsheet, in the sheet "Rates."

Table 18. Commercial Spent Nuclear Fuel Transition State Theory Rate Law and Coefficients

Total Degradation Rate Constant = $k_1[H+]^{0.41} + k_2[HCO_3-]^{0.12}$ (mole/cm^2·s)		
Temperature (Celsius)	**Rate Constant (k_1)**	**Rate Constant (k_2)**
25	2.14E-11	7.77E-14
50	4.09E-11	1.49E-13
90	9.59E-11	3.48E-13

Source: CSNF.xls, worksheet"Rates"

The glass dissolution rate law is the pH-dependent, transition state theory rate law presented in *Defense High Level Waste Glass Degradation* (BSC 2001a, Section 6.2.3.3, Equations 7 and 8). This rate, in grams/m^2·day, was converted to a format suitable for input to EQ6 (100 g-moles/cm^2-sec) in the "Rates" worksheet, of "CDNR.xls." The first rate mechanism (described with k_1) in Table 19 is dominant at pH values ≥ 7.1, while the second rate mechanism (described with k_2) is dominant at pH values below 7.1. The rate constants (those derived for degradation at 25, 50, and 90°C) are given in Table 19.

Table 19. High-Level Waste Glass Transition State Theory Rate Law and Constants and Codisposed N Reactor Rate Constants

HLWG		
Total Degradation Rate Constant = $k_1[H+]^{-0.4} + k_2[H+]^{0.6}$ (mole/cm^2·s)		
Temperature (Celsius)	Rate Constant (k_1)	Rate Constant (k_2)
25	8.86E-19	1.11E-11
50	1.08E-17	1.35E-10
90	2.86E-16	3.60E-09
CDNR		
Temperature (Celsius)	Total Degradation constant K (mole/cm^2·s)	
25	1.63E-10	
50	1.29E-09	
90	1.97E-08	

Source: CDNR.xla, worksheet:"DSNF Rates"

6.5.2 Single Component Water Vapor Condensation Model Inputs

For the single component that water vapor condensation runs it is necessary to scale the reactant's surface area and moles to the 0.1-cm film thickness.

Surface area = [EQ6 volume (1000 cm^3)] / [Film thickness (0.1 cm)]

Surface Area = 10,000 cm^2

The moles of each reactant is calculated by dividing moles reactant per waste package by its total surface area per waste package and multiplying the result by 10,000 cm^2.

Reactant Moles = [moles reactant per waste package] / [surface area reactant per waste package(cm^2)] * 10,000 cm^2

Table 20 provides the surface area (column "C") and moles (column "D") for each of the CSNF waste package components.

Table 20. Commercial Spent Nuclear Fuel Waste Package Single Component Water Vapor Condensation Surface Areas and Reactant Moles for 0.1-cm Thick Film at 10 Percent Cladding Failure

	A	B	C	D
WP Component	**10% fuel moles**	**10%CSNF SA**	**0.1-cm Film SA (cm^2)**	**EQ6 Input Values Moles/10,000 cm^2**
S31600	105313.843	241598.779	10000	4359.039
NEUTRONIT	20983.042	529130.560	10000	396.557
Al-6061	3419.418	258957.440	10000	132.046
FBT (A516)	34843.520	1777406.400	10000	196.036
Stiffeners (A516)	2011.330	27646.044	10000	727.529
CSNF	10843.178	462421.200	10000	234.487
D = A/B*C				

Source: CSNF.xls, worksheet" Single Component WVC EQ6 Inputs"

NOTE: WP = waste package.

Table 21 provides the surface area (column "C") and moles (column "D") for each of the CDNR components.

Table 21. Codisposed N Reactor Waste Package Single Component Water Vapor Condensation Surface Areas and Reactant Moles for 0.1-cm Thick Film

	A	B	C	D
WP Component	**Total Moles**	**Total Surface Area (cm^2)**	**0.1-cm Film SA (cm^2)**	**EQ6 Input Values Moles/10,000 cm^2**
S31600 Inner vessel	131890.622	269167.135	10000	4899.953
Al-110	806.883	141782.216	10000	56.910
304L MCO	27003.677	487054.703	10000	554.428
304L MCO top	29855.874	36377.355	10000	8207.269
304L GPC	14830.838	179201.621	10000	827.606
A516 plates	11457.056	334302.863	10000	342.715
U-Metal	127455.067	1639433.037	10000	777.434
HLWG	57655.304	3113959.289	10000	185.151
D = A/B*C				

Source: CDNR.xls, worksheet" Single Component WVC EQ6 Inputs"

NOTES: MCO = multi-canister overpack; GPC = glass-pour canister.

To convert to EQ6 compatible units and simplify the EQ6 calculations, a "mole" of special reactant fluid is defined as 1000 g ~ 1000 cm^3. Thus, by dividing liters per year by 3.16E+07 seconds per year the EQ6 compatible unit of moles per second result (Table 22).

Table 22. Water Flux Conversion

Water Flux	Units
0.79	(l/yr)
2.5E-08	mols/sec per WP

Source: CSNF.xls and CDNR.xls, worksheet: "Single Component WVC EQ6 Inputs"

NOTE: WP = waste package.

The water flux values for each waste package type is calculated by multiplying the flux by the normalization factor, a value unique to each package as defined in Section 6.5.3. Table 23 provides the normalization factor and water flux for CSNF and CDNR packages.

Table 23. Single-Component Water Flux Values for Commercial Spent Nuclear Fuel and Codisposed N Reactor Waste Package

Waste Package Type	Film Thickness (mm)	Normalization Factor	Water Flux (mol/sec)
CSNF	1.0	3.0E-03	7.6E-11
CDNR	1.0	1.6E-03	4.0E-11

Source: CSNF.xls and CDNR.xls, worksheet: "Single Component WVC EQ6 Inputs"

6.5.3 Multi-Component Ensemble Water Vapor Condensation Inputs

Tables 24 and 25 list the reactants included in the CSNF and CDNR ensemble runs (Tables 11 and 20). Since each ensemble has a different total surface area, they each have their own normalization factor, and it was necessary to calculate scaled inputs for each ensemble. These calculations can be found in "CSNF.xls" and "CDNR.xls."

Table 24. Commercial Spent Nuclear Fuel Water Vapor Condensation Multi-component Ensembles

Waste Package Component / EQ6 File	comp1	comp2	comp3	comp4	comp5	comp6	comp7	comp8	comp9	comp10	comp11
S31600 inner vessel	✓					✓			✓	✓	
Neutronit	✓	✓			✓	✓		✓			✓
Al-6061	✓	✓	✓		✓	✓	✓				
FBT (A516)	✓	✓	✓	✓	✓	✓	✓	✓	✓	✓	✓
Stiffeners (A516)	✓	✓	✓	✓	✓	✓	✓	✓	✓	✓	✓
CSNF	✓	✓	✓	✓						✓	✓

Table 25. Codisposed N Reactor Water Vapor Condensation Multi-component Ensembles

Waste Package Component / EQ6 File	comp1	comp2	comp3	comp4	comp5	comp6	comp7	comp8
S31600 Inner vessel	✓							
Al-110	✓	✓		✓				✓
304L MCO	✓	✓	✓	✓				
304L MCO top	✓	✓	✓	✓				
304L GPC	✓	✓	✓	✓	✓	✓		
A516 plates	✓	✓	✓	✓	✓		✓	
U-Metal	✓	✓	✓					
HLWG	✓	✓	✓	✓	✓	✓	✓	✓

NOTES: MCO = multi-canister overpack; GPC = glass-pour canister.

Table 26 contains the surface area and moles of each CSNF reactant for 100 percent CSNF exposure and 10 percent CSNF exposure. For the CSNF water vapor condensation ensemble runs only the 10 percent fuel exposure values were used (Section 6.3.2). The total surface area and total moles of each reactant were calculated in Attachment I "CSNF.xls" in the "moles and surface areas" worksheet. The surface area and volume for each component was calculated based on the geometry of the component as it is represented in Attachment III of *EQ6 Calculation for Chemical Degradation of 21 PWR CSNF Waste Packages* (BSC 2002c), *Repository Design Project, Repository/PA IED Emplacement Drift Committed Materials 1 of 2* (BSC 2003c), and *Summary Report of Commercial Reactor Criticality Data for Crystal River Unit 3* (Punatar 2001, pp. 2 to 5). The moles of each component was calculated by multiplying the volume (cm^3) of the component by its density (g/cm^3) and dividing by 100g/mole of material.

Table 26. Commercial Spent Nuclear Fuel Waste Package Component Surface Areas and Moles

WP Component	Total Surface Area(cm^2)	Total Moles	10% fuel SA	10% fuel moles
S31600	241,598.8	105,313.8	241,598.8	105,313.8
NEUTRONIT	529,130.6	20,983.0	529,130.6	20,983.0
Al-6061	258,957.4	3,419.4	258,957.4	3,419.4
FBT (A516)	1,777,406.4	34,843.5	1,777,406.4	34,843.5
Stiffeners (A516)	27,646.0	2,011.3	27,646.0	2,011.3
CSNF	4,624,212.0	108,432.0	462,421.2	10,843.2

Source: CSNF.xls, worksheet" WVC Ensemble EQ6 Inputs"

For each ensemble a normalization factor was calculated to normalize the moles and surface area of each waste package component to the film thickness (1-mm for CSNF and 2-mm for CDNR) and EQ6 volume (1000 cm^3). The water flux value was also normalized using the same factor. The normalization factor was calculated using the following formula: Normalization Factor = [EQ6 volume / film thickness / (Σensemble component surface areas)].

The following tables contains CSNF ensemble inputs consistent with Table 24.

Table 27. Commercial Spent Nuclear Fuel Ensemble 1 Input Values

Ensemble #1	Surface Area (cm^2)	Moles
S31600	732.7	319.4
NEUTRONIT	1604.8	63.6
Al-6061	785.4	10.4
FBT (A516)	5390.7	105.7
Stiffeners (A516)	83.8	6.1
CSNF	1402.5	32.9
Normalization factor	3.0E-03	
Water Flux (mol/sec)	7.6E-11	

Source: CSNF.xls, worksheet" WVC Ensemble EQ6 Inputs"

Table 28. Commercial Spent Nuclear Fuel Ensemble 2 Input Values

Ensemble #2	Surface Area (cm^2)	Moles
NEUTRONIT	1731.7	68.7
Al-6061	847.5	11.2
FBT (A516)	5817.0	114.0
Stiffeners (A516)	90.5	6.6
CSNF	1513.4	35.5
Normalization factor	3.3E-03	
Water Flux (mol/sec)	8.2E-11	

Source: CSNF.xls, worksheet" WVC Ensemble EQ6 Inputs"

Table 29. Commercial Spent Nuclear Fuel Ensemble 3 Input Values

Ensemble #3	Surface Area (cm^2)	Moles
Al-6061	1025.0	13.5
FBT (A516)	7035.2	137.9
Stiffeners (A516)	109.4	8.0
CSNF	1830.3	42.9
Normalization factor	4.0E-03	
Water Flux (mol/sec)	9.9E-11	

Source: CSNF.xls, worksheet" WVC Ensemble EQ6 Inputs"

Table 30. Commercial Spent Nuclear Fuel Ensemble 4 Input Values

Ensemble #4	Surface Area (cm^2)	Moles
FBT (A516)	7838.7	153.7
Stiffeners (A516)	121.9	8.9
CSNF	2039.4	47.8
Normalization factor	4.4E-03	
Water Flux (mol/sec)	1.1E-10	

Source: CSNF.xls, worksheet" WVC Ensemble EQ6 Inputs"

Table 31. Commercial Spent Nuclear Fuel Ensemble 5 Input Values

Ensemble #5	Surface Area (cm^2)	Moles
NEUTRONIT	2040.5	80.9
Al-6061	998.6	13.2
FBT (A516)	6854.3	134.4
Stiffeners (A516)	106.6	7.8
Normalization factor	3.9E-03	
Water Flux (mol/sec)	9.7E-11	

Source: CSNF.xls, worksheet" WVC Ensemble EQ6 Inputs"

Table 32. Commercial Spent Nuclear Fuel Ensemble 6 Input Values

Ensemble #6	Surface Area (cm^2)	Moles
S31600	852.3	371.5
NEUTRONIT	1866.6	74.0
Al-6061	913.5	12.1
FBT (A516)	6270.1	122.9
Stiffeners (A516)	97.5	7.1
Normalization factor	3.5E-03	
Water Flux (mol/sec)	8.8E-11	

Source: CSNF.xls, worksheet" WVC Ensemble EQ6 Inputs"

Table 33. Commercial Spent Nuclear Fuel Ensemble 7 Input Values

Ensemble #7	Surface Area (cm^2)	Moles
Al-6061	1254.6	16.6
FBT (A516)	8611.4	168.8
Stiffeners (A516)	133.9	9.7
Normalization factor	4.8E-03	
Water Flux (mol/sec)	1.2E-10	

Source: CSNF.xls, worksheet" WVC Ensemble EQ6 Inputs"

Table 34. Commercial Spent Nuclear Fuel Ensemble 8 Input Values

Ensemble #8	Surface Area (cm^2)	Moles
NEUTRONIT	2266.9	89.9
FBT (A516)	7614.7	149.3
Stiffeners (A516)	118.4	8.6
Normalization factor	4.3E-03	
Water Flux (mol/sec)	1.1E-10	

Source: CSNF.xls, worksheet" WVC Ensemble EQ6 Inputs"

Table 35. Commercial Spent Nuclear Fuel Ensemble 9 Input Values

Ensemble #9	Surface Area (cm^2)	Moles
S31600	1180.5	514.6
FBT (A516)	8684.5	170.2
Stiffeners (A516)	135.1	9.8
Normalization factor	4.9E-03	
Water Flux (mol/sec)	1.2E-10	

Source: CSNF.xls, worksheet" WVC Ensemble EQ6 Inputs"

Table 36. Commercial Spent Nuclear Fuel Ensemble 10 Input Values

Ensemble #10	Surface Area (cm^2)	Moles
S31600	362.2	157.9
FBT (A516)	2664.4	52.2
Stiffeners (A516)	41.4	3.0
CSNF	693.2	16.3
Normalization factor	1.5E-03	
Water Flux (mol/sec)	3.8E-11	

Source: CSNF.xls, worksheet" WVC Ensemble EQ6 Inputs"

Table 37. Commercial Spent Nuclear Fuel Ensemble 11 Input Values

Ensemble #11	Surface Area (cm^2)	Moles
Neutronit	760.4	30.2
FBT (A516)	2554.3	50.1
Stiffeners (A516)	39.7	2.9
CSNF	664.6	15.6
Normalization factor	1.4E-03	
Water Flux (mol/sec)	3.6E-11	

Source: CSNF.xls, worksheet" WVC Ensemble EQ6 Inputs"

The following table contains the surface area and moles of each CDNR reactant for 100 percent N Reactor exposure and 50 percent N Reactor exposure (Section 6.3.2). For the CDNR water vapor condensation ensemble runs only the 50 percent fuel exposure values were used. The total surface area and total moles of each reactant were calculated in Attachment I "CDNR.xls" in the "moles and surface areas" worksheet. The surface area and volume for each component were calculated based on the geometry of the component as it is represented in *Repository Design Project, Repository/PA IED Emplacement Drift Committed Materials 1 of 2* (BSC 2003c) and *N Reactor (U-Metal) Fuel Characteristics for Disposal Criticality Analysis* (DOE 2000b, Section 3). The moles of each component were calculated by multiplying the volume (cm^3) of the component by its density (g/cm^3) and dividing by 100 g/mole of material.

Table 38. Codisposed N Reactor Surface Area and Mole Data Used to Generate the Inputs for the Multi-Component Ensemble Runs

WP Component	Total Surface Area (cm^2)	Total Moles	50% N Reactor SA (cm^2)	50% N Reactor Moles
S31600 Inner vessel	269167.1	131890.6	269167.1	131890.6
Al-110	141782.2	806.9	141782.2	806.9
304L MCO	487054.7	27003.7	487054.7	27003.7
304L MCO top	36377.4	29855.9	36377.4	29855.9
304L GPC	179201.6	14830.8	179201.6	14830.8
A516 plates	334302.9	11457.1	334302.9	11457.1
N Reactor	1639433.0	127455.1	819716.5	63727.5
HLWG	3113959.3	57655.3	3113959.3	57655.3

Source: CDNR.xls, worksheet" WVC Ensemble EQ6 Inputs"

NOTES: MCO = multi-canister overpack; GPC = glass-pour canister.

Table 39. Codisposed N Reactor Ensemble 1 Input Values

Ensemble #1	Surface Area (cm^2)	Moles
S31600 Inner vessel	250.1	122.5
Al-110	131.7	0.7
304L MCO	452.5	25.1
304L MCO top	33.8	27.7
304L GPC	166.5	13.8
A516 plates	310.6	10.6
U-Metal	761.6	59.2
HLWG	2893.2	53.6
Normalization Factor	9.3E-04	
Water Flux (mol/sec)	2.3E-11	

Source: CDNR.xls, worksheet "WVC Ensemble EQ6 Inputs"

NOTES: MCO = multi-canister overpack; GPC = glass-pour canister.

Table 40. Codisposed N Reactor Ensemble 2 Input Values

Ensemble #2	Surface Area (cm^2)	Moles
Al-110	138.7	0.8
304L MCO	476.3	26.4
304L MCO top	35.6	29.2
304L GPC	175.3	14.5
A516 plates	327.0	11.2
U-Metal	801.7	62.3
HLWG	3045.5	56.4
Normalization Factor	9.8E-04	
Water Flux (mol/sec)	2.4E-11	

Source: CDNR.xls, worksheet" WVC Ensemble EQ6 Inputs"

NOTES: MCO = multi-canister overpack;
GPC = glass-pour canister.

Table 41. Codisposed N Reactor Ensemble 3 Input Values

Ensemble #3	Surface Area (cm^2)	Moles
304L MCO	489.9	27.2
304L MCO top	36.6	30.0
304L GPC	180.3	14.9
A516 plates	336.3	11.5
U-Metal	824.6	64.1
HLWG	3132.4	58.0
Normalization Factor	1.0E-03	
Water Flux (mol/sec)	2.5E-11	

Source: CDNR.xls, worksheet" WVC Ensemble EQ6 Inputs"

NOTES: MCO = multi-canister overpack; GPC = glass-pour canister.

Table 42. Codisposed N Reactor Ensemble 4 Input Values

Ensemble #4	Surface Area (cm^2)	Moles
Al-110	165.1	0.9
304L MCO	567.3	31.5
304L MCO top	42.4	34.8
304L GPC	208.7	17.3
A516 plates	389.4	13.3
HLWG	3627.1	67.2
Normalization Factor	1.2E-03	
Water Flux (mol/sec)	2.9E-11	

Source: CDNR.xls, worksheet" WVC Ensemble EQ6 Inputs"

NOTES: MCO = multi-canister overpack; GPC = glass-pour canister.

Table 43. Codisposed N Reactor Ensemble 5 Input Values

Ensemble #5	Surface Area (cm^2)	Moles
304L GPC	247.0	20.4
A516 plates	460.8	15.8
HLWG	4292.2	79.5
Normalization Factor	1.4E-03	
Water Flux (mol/sec)	3.5E-11	

Source: CDNR.xls, worksheet" WVC Ensemble EQ6 Inputs"

NOTE: GPC = glass-pour canister.

Table 44. Codisposed N Reactor Ensemble 6 Input Values

Ensemble #6	Surface Area (cm^2)	Moles
304L GPC	272.1	22.5
HLWG	4727.9	87.5
Normalization Factor	1.5E-03	
Water Flux (mol/sec)	3.8E-11	

Source: CDNR.xls, worksheet" WVC Ensemble EQ6 Inputs"

NOTE: GPC = glass-pour canister.

Table 45. Codisposed N Reactor Ensemble 7 Input Values

Ensemble #7	Surface Area (cm^2)	Moles
A516 plates	484.7	16.6
HLWG	4515.3	83.6
Normalization Factor	1.5E-03	
Water Flux (mol/sec)	3.6E-11	

Source: CDNR.xls, worksheet" WVC Ensemble EQ6 Inputs"

Table 46. Codisposed N Reactor Ensemble 8 Input Values

Ensemble #8	Surface Area (cm^2)	Moles
Al-110	217.7	1.2
HLWG	4782.3	88.5
Normalization Factor	1.5E-03	
Water Flux (mol/sec)	3.8E-11	

Source: CDNR.xls, worksheet" WVC Ensemble EQ6 Inputs"

6.5.4 Seepage Dripping Model Inputs

For the CSNF seepage dripping model inputs for three CSNF exposure values, 100, 10, and 1 percent, were generated, i.e., a scaling factor was calculated for each fuel exposure value and the reactants surface areas and moles were scaled accordingly. Also scaled were the three values of the water flux used in the simulations. The unscaled CSNF inputs for the seepage dripping model are listed in Tables 47 and 48.

Table 47. Commercial Spent Nuclear Fuel Unscaled Surface Areas and Normalization Factors

WP Component	100% Fuel Surface Area (cm^2)	10% Fuel Surface Area (cm^2)	1% Fuel Surface Area (cm^2)
S31600	241,598.779	241,598.779	241,598.779
NEUTRONIT	529,130.560	529,130.560	529,130.560
Al-6061	258,957.440	258,957.440	258,957.440
FBT (A516)	1,777,406.400	1,777,406.400	1,777,406.400
Stiffeners (A516)	27,646.044	27,646.044	27,646.044
CSNF	4,624,211.996	462,421.200	46,242.120
Total:	7,458,951.219	3,297,160.423	2,880,981.344
Film thickness (cm)	**Normalization Factor**		
2.50E-01	5.363E-04	1.213E-03	1.388E-03

Source: CSNF.xls, worksheet "SDM EQ6 Inputs."

Table 48. Commercial Spent Nuclear Fuel Unscaled Reactant Moles

WP Component	100% Fuel Moles	10% Fuel Moles	1% Fuel Moles
S31600	105,313.843	105,313.843	105,313.843
NEUTRONIT	20,983.042	20,983.042	20,983.042
Al-6061	3,419.418	3,419.418	3,419.418
FBT (A516)	34,843.520	34,843.520	34,843.520
Stiffeners (A516)	2,011.330	2,011.330	2,011.330
CSNF	108,431.784	10,843.178	1,084.318

Source: CSNF.xls, worksheet "SDM EQ6 Inputs."

The values in Table 49 are for a 0.25 cm thick film and three (100, 10, and 1 percent) fuel exposure values, and are used because they best represent the 0.25 cm film conceptualization.

Table 49. Scaled EQ6 Inputs, Commercial Spent Nuclear Fuel Surface Areas, and Reactant Moles for 0.25-cm Thick Film at Three Fuel Exposure Values

Fuel Exposure	100%		10%		1%	
WP Material	SA (cm^2)	Moles	SA (cm^2)	Moles	SA (cm^2)	Moles
FBT (A516)	953.167	18.685	2156.287	42.271	2467.779	48.377
Stiffeners (A516)	14.826	1.079	33.539	2.440	38.384	2.793
NEUTRONIT	283.756	11.253	641.923	25.456	734.653	29.133
Al-6061	138.871	1.834	314.158	4.148	359.541	4.748
S31600	129.562	56.476	293.099	127.763	335.440	146.219
CSNF	2479.819	58.149	560.993	13.155	64.203	1.505

Source: CSNF.xls, worksheet "SDM EQ6 Inputs."

NOTE: SA = surface area; WP = waste package.

Table 50 provides the water flux values for three values of fuel exposure (clad failure).

Table 50. EQ6 Input Water Flux Values for the Commercial Spent Nuclear Fuel Seepage Dripping Model

Flux(l/yr)	0.15 (l/yr)	1.5 (l/yr)	15 (l/yr)
Fuel Exposure(%)	(mol/sec)	(mol/sec)	(mol/sec)
100	2.5490E-12	2.5490E-11	2.5490E-10
10	5.7664E-12	5.7664E-11	5.7664E-10
1	6.5994E-12	6.5994E-11	6.5994E-10

Source: CSNF.xls, worksheet "SDM EQ6 Inputs."

The CDNR seepage dripping model inputs are given in Tables 51 to 53.

Table 51. EQ6 Input Water Flux Values for the Codisposed N Reactor Seepage Dripping Model

Water Flux (l/yr)	Normalized Water Flux (mol/sec)
0.15	2.190E-12
1.5	2.190E-11
15.0	2.190E-10

Source: Attachment I, CDNR.xls, worksheet "SDM EQ6 Inputs"

Table 52. Codisposed N Reactor Unscaled Surface Areas and Moles and Normalization Factor

Waste Package Component	Surface Area (cm^2)	Moles
A516 plates	334302.863	11457.056
304L MCO	487054.703	27003.677
304L MCO top	36377.355	29855.874
304L GPC	179201.621	14830.838
S31600 Inner vessel	269167.135	131890.622
Al-110	141782.216	806.883
U-Metal	1639433.037	127455.067
HLWG	3113959.289	57655.304
Total	6201278.220	
Film Thickness (cm)	0.35	
Normalization Factor	4.607E-04	

Source: CDNR.xls, worksheet "SDM EQ6 Inputs."

NOTES: MCO = multi-canister overpack; GPC = glass-pour canister.

Table 53. EQ6 Inputs, Codisposed N Reactor Surface Areas, and Reactant Moles for 0.35-cm Thick Film

Waste Package Component	Normalized Surface Area (cm^2)	Normalized Moles
A516 plates	154.025	5.279
304L MCO	224.403	12.442
304L MCO top	16.760	13.756
304L GPC	82.564	6.833
S31600 Inner vessel	124.015	60.767
Al-110	65.324	0.372
U-Metal	755.343	58.723
HLWG	1434.708	26.564

Source: CDNR.xls, worksheet "SDM EQ6 Inputs."

NOTES: MCO = multi-canister overpack; GPC = glass-pour canister.

The water compositions listed in Table 2 were input into EQ3NR and EQ3NR was executed to preprocess the water compositions and output an EQ3NR "pickup" (*.3p) file which is used as an integral part of each EQ6 input file. EQ3NR recasts the reported concentrations from Table 2 into molal units, which are the working units of EQ6. For the J-13 composition the HCO_3^- concentration was set to as the charge balance constraint in the EQ3 input file.

Table 54 provides the EQ3NR output molal concentrations of the elements used in the EQ6 input files. All of the elements with concentrations of 1.00E-16 molal were included as a necessary input in the EQ3NR input files because these elements occur in either the waste package component compositions or the waste form component compositions.

Table 54. EQ6 Input Fluid Compositions

Constituent (molal)	Ca-Porewater[a]	Na-Porewater[b]	J13[c]	Pure Water[d]
Ionic strength	0.011	0.012	0.0035	N/A
pH	7.6	7.4	7.0	5.4
O	5.55E+01	5.55E+01	5.55E+01	5.55E+01
Al	1.00E-16	1.00E-16	1.00E-16	1.00E-16
B	1.00E-16	1.00E-16	1.00E-16	1.00E-16
Ba	1.00E-16	1.00E-16	1.00E-16	1.00E-16
Ca	2.35E-03	2.02E-03	3.24E-04	1.00E-16
Cl	5.92E-04	6.77E-04	2.01E-04	1.00E-16
Co	1.00E-16	1.00E-16	1.00E-16	1.00E-16
Cr	1.00E-16	1.00E-16	1.00E-16	1.00E-16
Cs	1.00E-16	1.00E-16	1.00E-16	1.00E-16
Cu	1.00E-16	1.00E-16	1.00E-16	1.00E-16
F	1.79E-04	3.16E-04	1.15E-04	1.00E-16
Fe	1.00E-16	1.00E-16	1.00E-16	1.00E-16
Gd	1.00E-16	1.00E-16	1.00E-16	1.00E-16
H	1.11E+02	1.11E+02	1.11E+02	1.11E+02
C	6.76E-03	8.62E-03	2.49E-03	3.79E-05
P	1.00E-16	1.00E-16	1.00E-16	1.00E-16
I	1.00E-16	1.00E-16	1.00E-16	1.00E-16
K	1.94E-04	1.56E-04	1.29E-04	1.00E-16
Li	1.00E-16	1.00E-16	1.00E-16	1.00E-16
Mg	7.45E-04	1.36E-04	8.27E-05	1.00E-16
Mn	1.00E-16	1.00E-16	1.00E-16	1.00E-16
Mo	1.00E-16	1.00E-16	1.00E-16	1.00E-16
N	4.19E-05	6.61E-06	1.42E-04	1.00E-16
Na	1.70E-03	5.22E-03	1.99E-03	1.00E-16
Ni	1.00E-16	1.00E-16	1.00E-16	1.00E-16
Np	1.00E-16	1.00E-16	1.00E-16	1.00E-16
Pb	1.00E-16	1.00E-16	1.00E-16	1.00E-16
Pu	1.00E-16	1.00E-16	1.00E-16	1.00E-16
Ru	1.00E-16	1.00E-16	1.00E-16	1.00E-16
S	3.75E-04	3.23E-04	1.92E-04	1.00E-16
Si	6.99E-04	6.99E-04	1.02E-03	1.00E-16
Tc	1.00E-16	1.00E-16	1.00E-16	1.00E-16
Ti	1.00E-16	1.00E-16	1.00E-16	1.00E-16
U	1.00E-16	1.00E-16	1.00E-16	1.00E-16
Zn	1.00E-16	1.00E-16	1.00E-16	1.00E-16
Zr	1.00E-16	1.00E-16	1.00E-16	1.00E-16

Sources: [a] EQ3NR pickup file "Ca_trc.3p" (Attachment I)
[b] EQ3NR pickup file "Na_trc.3p" (Attachment I)
[c] EQ3NR pickup file "J13_trc.3p" (Attachment I)
[d] EQ3NR pickup file "pure_trc.3p" (Attachment I)

6.5.5 Mineral Controls

In the in-package chemistry model the minerals that precipitate from solution during an EQ6 run are determined by the code via consideration of the thermodynamics of the chemical system. Based on the modeled conditions, certain minerals will precipitate from solution and others will not. In using the EQ6 software the analyst must decide, on the basis of prior knowledge related to the phenomena, which mineral phases will not be allowed to form in a simulation; this is called mineral "suppression." Table 55 lists the phases suppressed in the EQ6 runs. By deciding which minerals to suppress, the analyst is implicitly deciding which minerals will form. Often trial runs are performed so that the analyst can see first hand what minerals are forming and what minerals should be suppressed. By suppressing a phase, a decision is made based on knowledge of a phase's mode of occurrence and the relative kinetics of formation. For example, amorphous silica is more soluble than quartz at low temperatures, hence, quartz reaches saturation first; however, low-temperature quartz formation is not observed. Therefore, the analyst would "suppress" quartz formation for a low-temperature simulation.

Table 56 provides a list of the major minerals, which were not suppressed and were observed to precipitate in the EQ6 runs for the in-package chemistry model. Phases in abundance in greater than 10^{-4} moles over the 20,000 year model period are included in the list.

For certain simulations, the EQ6 code was not able to converge to a solution because of difficulties related to finding a stable mineral assemblage for the particular chemical conditions of the simulation. In these cases EQ6 would give an error stating that convergence was not possible because a phase rule violation occurred, and EQ6 would list the mineral phases involved in the violation. Suppressing one of the suspect phases was used as a means of getting the EQ6 to converge.

In the following runs, C13N50.6i, C23N50.6i, and C33N50.6i, the uranium phosphate phase $(UO_2)_3(PO4)_2{:}6H_2O$ was suppressed and in its place $(UO_2)_3(PO4)_2{:}4H_2O$ formed; thus, the effect on the chemistry was negligible. In run CD_Comp6.6i the phase bunsenite (NiO) was suppressed because of a phase rule violation and in its place trevorite ($NiFe_2O_4$) formed, another phase that had an inconsequential impact on the chemistry. In all of the runs the phase PuO_2(aged, hyd) was suppressed to aid code convergence. No other plutonium phase precipitated in its place. Although plutonium is important from a dose perspective, it has no impact on the pH of the system because of its relatively low concentration compared to the major elements (Ca, Mg, Na, K, Cl, S, and C).

Table 55. Minerals Suppressed in In-Package Chemistry Model EQ6 Runs

Mineral	Chemical Formula	Justification
Quartz	SiO_2	Quartz is formed at higher temperatures (around 573°C), but its extremely simple elemental makeup makes it resistant to corrosion, allowing it to exist widespread as a detrital fragment in many sedimentary rocks, which is why it has been noted in so many sedimentary deposits. However, other forms of SiO_2 can form as primary sedimentary minerals at low temperatures (such as chalcedony) (Klein and Hurlbut 1985, pp. 441 to 442). Therefore, the mineral quartz has been suppressed in the EQ6 runs, allowing the lower temperature varieties of SiO_2 to form.
Goethite	α-FeOOH	Goethite (α-FeOOH) and hematite (α-Fe_2O_3) are the two most thermodynamically stable Fe minerals under oxidizing conditions (Schwertmann and Taylor 1995). Goethite was suppressed in EQ6 runs of the IPCM, however, suppressing goethite had no affect on the results of the IPCM since hematite is more thermodynamically stable than goethite, and EQ6 would not allow goethite to form unless hematite was suppressed.
Tridymite	SiO_2	Tridymite exists as both α and β types. The low temperature α-tridymite forms only from pre-existing β-tridymite, which forms in the temperature range of 870°C to 1470°C (Roberts et al. 1990, pp. 881 to 882).
Muscovite	$KAl_2(Si_3Al)O_{10}(OH,F)_2$	Occurs in High T and/or P mineral assemblages and as a detrital mineral in sedimentary rocks (Roberts et al. 1990, p. 586).
Celadonite	$K(Mg,Fe^{+2})(Fe^{+3},Al)Si_4O_{10}(OH)_2$	Celadonite is found in altered volcanic rocks (Roberts et al. 1990, p. 149. Celadonite can form at low temperatures, but this is due to either diagenesis of pre-existing material, low grade metamorphic processes, or concentration of the liquid environment through evaporation (Li et al. 1997).
Annite	$KFe_3^{+2}AlSi_3O_{10}(OH,F)_2$	Synthesized, natural occurrence uncertain (Roberts et al. 1990, p. 32)
Dolomite		Dolomite is usually derived by secondary mineralization, from the replacement of Ca for Mg in the calcite crystal structure in Mg rich waters (Klein and Hurlbut 1985, p. 340). Due to the fact that it rarely occurs as a primary mineral, it was also suppressed.
Andradite		Andradite is a high P/T mineral found in metamorphic and igneous rocks (Deer et al. 1966, p. 30).
Phlogopite	$KMg_3AlSi_3O_{10}(OH,F)_2$	Occurs chiefly in metamorphic limestones and ultrabasic rocks (Roberts et al. 1990, p. 671)
Talc	$Mg_3Si_4O_{10}(OH)_2$	Talc is characteristically associated with low-grade metamorphic rock and hydrothermal alteration of ultrabasic rocks (Kerr 1977, p. 450).
Ferrite-Ca Ferrite-Mg	$CaFe_2O_4$ $MgFe_2O_4$	Magnesioferrite has been found in sintered magnesite of furnace linings and other refractories (Palache et al. 1944, p. 705), not expected to form at low T.
Zircon	$ZrSiO_4$	High P/T mineral. Found in sedimentary deposits as a detrital mineral. (Roberts et al. 1990, p. 975)
PuO_2	PuO_2	The solubilities of solid Pu(IV) oxide/hydroxide scatter within several orders of magnitude because of the difficulties of establishing equilibrium of Pu(IV), polymerization and disproportionation reactions and the strong sorption capacities of Pu^{4+} (Runde 1999). Experimental Pu solution concentrations during PuO_2 or PWR SNF degradation have been shown to be between the solubility of PuO_2 and that of a more soluble phase, $Pu(OH)_4$ (or $PuO_2 \cdot 2H_2O$) (Rai and Ryan 1982; Wilson and Bruton 1989, Section 3.1 and Table 3).
Soddyite	$(UO_2)_2SiO_4:2H_2O$	Suppression of soddyite had no effect on the results of this model report, since this mineral is fairly soluble under the conditions simulated by the IPCM, and it would not have precipitated in any of the EQ6 runs even if its formation had not been suppressed.

NOTE: P = Pressure; T = Temperature; IPCM = in-package chemistry model.

Table 56. Major Mineral Phases Formed in EQ6 Runs

Mineral	Chemical Formula	Justification
Hematite	α-Fe_2O_3	Goethite (α-FeOOH) and hematite (α-Fe_2O_3) are the two most thermodynamically stable and most widespread Fe minerals under oxidizing conditions. Hematite is usually found in tropical and subtropical regions where higher temperatures and lower water activities aid in its formation. Hematite needs a precursor such as ferrihydrite from which it forms through dehydration and rearrangement. (Schwertmann and Taylor 1995).
Pyrolusite	MnO_2	Secondary mineral forming from alteration of manganite or other manganese-bearing minerals. (Roberts et al. 1990, p. 704). [Manganite forms as a low temperature hydrothermal vein mineral; in circulating meteoric water; or bog, lacustrine, or shallow marine deposits. (Roberts et al. 1990, p. 524)]. Found as a secondary mineral in the oxidation zone at the Morro do Ferro site in Brazil (Waber 1991). Formed in the system Mn-O_2-H_2O at 25°C and one atmosphere (Bricker 1965, Table 1)
Trevorite	$NiFe_2O_4$	High P/T mineral (Roberts et al. 1990, p. 881). Trevorite was allowed to form since Ni-substituted goethite, hematite and $NiFe_2O_4$ can be synthesized at low P/T (Cornell et al. 1992), and Ni-substituted iron oxides are not in the EQ6 database.
Powellite	$Ca(Mo,W)O_4$	Occurs as a secondary mineral in the oxidation zones of ore deposits (Roberts et al. 1990, p. 692). Secondary mineral, often by the alteration of molybdenite, in copper deposits, deposits encountering contact metamorphism (Palache et al. 1951, p. 1080)
Tenorite	CuO	Occurs chiefly in the oxidation zone of copper deposits, often associated with other secondary minerals. Also occurs as a sublimation product deposited on lavas in volcanic regions (Roberts et al. 1990, p. 856; Palache et al. 1944, p. 509). CuO is a component of patina formed in atmospheric and aqueous corrosion of copper alloys, though not specifically given the mineral name tenorite (Sequeira 2000)
Schoepite	UO_3:$2H_2O$	Alteration product of uraninite (UO_2); associated with bequerelite, curite and other secondary minerals of U (Palache et al. 1944, p. 628)
Gibbsite	$Al(OH)_3$	Most common $Al(OH)_3$ polymorph (Hsu 1995). AlOOH are rarer than hydroxides and are considered the product of weathering (Allen and Hajek 1995) so the $Al(OH)_3$ polymorphs will be the primary ones expected to form in the WP.
Kaolinite	$Al_2Si_2O_5(OH)_4$	Most common kaolin, formation at 25°C is usually slow, however it can crystallize easily from the alteration of smectites (Dixon 1995)
Nontronite	$Na_{0.33}Fe_2(Si,Al)_4O_{10}(OH)_2$:$nH_2O$	One of the three most common smectite minerals found in soils. Smectites are common in temperate and cold climates, but may form or be preserved in tropical environments where leaching is limited or drainage is restricted (Allen and Hajek 1995).
$GdPO_4$: 10 H_2O	$GdPO_4$:10 H_2O	Gadolinium phosphate hydrates are insoluble in near-neutral pH solutions (Firsching and Brune 1991).
$(UO_2)_3(PO_4)_2$: XH_2O	$(UO_2)_3(PO_4)_2$:XH_2O	X = 4 or 6. $(UO_2)_3(PO_4)_2$:$4H_2O$ is a stable phase under oxidizing conditions, low temperature and pH values relevant for natural water systems (Sandino 1991, pp. 16 to 17). $(UO_2)_3(PO_4)_2$:$6H_2O$ was also allowed to form since uranyl phosphates are associated with a wide range of weathered U deposits (Finch and Murakami 1999), but few uranyl phosphates are included in the EQ6 database.
Baddeleyite	ZrO_2	High P/T mineral. Found in sedimentary deposits as a detrital mineral. (Roberts et al. 1990, p. 62) also formed in metamict zircon (Deer et al. 1966, p. 15), Baddeleyite was allowed to form in the waste package since hydrolysis of Zr salts leads to precipitation of poorly crystalline oxides at low temperatures (Milnes and Fitzpatrick 1995, pp. 1189 to 1190) and soluble Zr may be incorporated in or sorb on clay mineral surfaces (Milnes and Fitzpatrick 1995, pp. 1185 to 1186). So, it is likely that some of the Zr released by degradation of WP components will precipitate or be sorbed from solution.

NOTE: P = Pressure; T = Temperature.

6.6 MODEL OUTPUT

6.6.1 Commercial Spent Nuclear Fuel Output

6.6.1.1 Water Vapor Condensation Model Results

Figure 1 displays the results of the CSNF single component simulations. The pH profiles in Figure 1 are plotted as a function of reaction progress, the EQ6 zi (ξ) variable, to avoid confusion as the profiles are not to be interpreted as time functions. This figure provides information on how each waste package component contributes to the in-package pH and shows the upper and lower pH limits for a CSNF package.

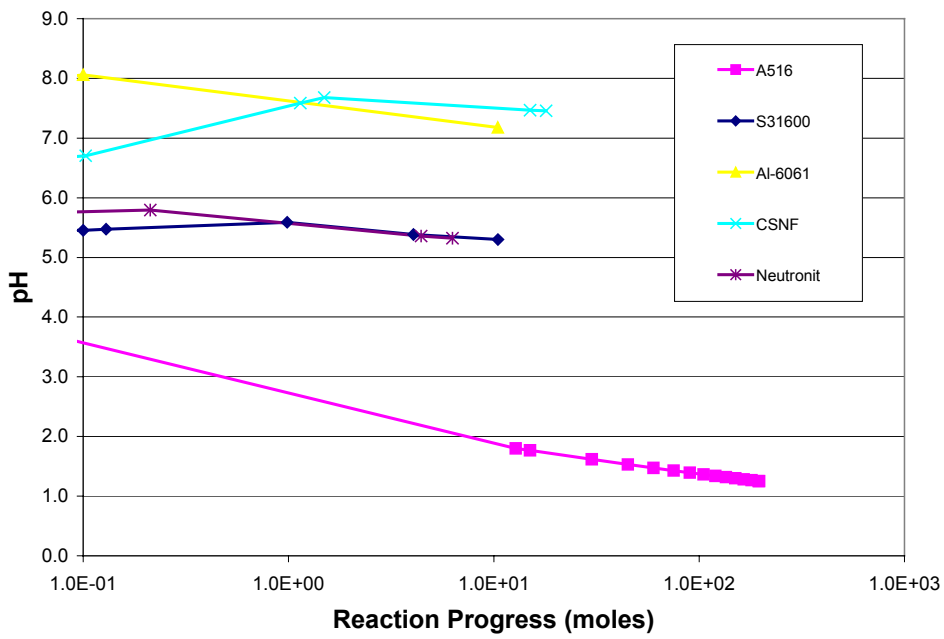

Source: Microsoft Excel Spreadsheet CSNF_WVC.xls in DTN: MO0307SPAIPCHM.001.

Figure 1. Commercial Spent Nuclear Fuel Single Component Water Vapor Condensation pH Outputs

The low pH resulting from A516 carbon steel corrosion is due to the combination of oxidation of elemental sulfur, the large quantity of A516, and its high corrosion rate relative to the other waste package components. Both the Al-6061 and the CSNF have neutral to slightly basic pH profiles, while the S31600 and Neutronit have slightly acidic pH profiles. The reasons the pH profiles are not constant is because the starting pH of the solution differs from the "pseudo" equilibrium pH of the alloy-water system, and, secondly, since the reactants are kinetic reactants their dissolution is irreversible, they can only dissolve and not re-precipitate, thus the alloy-water system is in a constant state of change as the solution chemistry and solid assemblage evolves.

The pH profiles of the water vapor condensation multi-component ensemble runs are displayed in Figure 2. Comparison of Figures 1 and 2 reveals that pH range exhibited by the single component runs (Figure 1) is also covered by the multi-component runs. The similar pH range of the two groups of simulations illustrates that the pH is dominated by the reactants and not necessarily by the conceptual model. This builds confidence in the robustness of the model.

The most acid-producing profiles include, in Figure 1, that for A516, and in Figure 2, the comp8 and comp9 profiles. The low pH observed in the comp8 and comp9 profiles is due to the lack of a buffering reactant in the ensemble. Comp8 is composed of A516 and Neutronit, while comp9 is composed of A516 and S31600, all of which are acid producing reactants (Figure 1).

The comp3 and comp7 ensembles both contain Al-6061 and A516, and comp3 also contains CSNF. For these two ensembles the early-time pH (<100 years) was controlled by A516 dissolution, the middle period (100 to 1000 years) by Al-6061 dissolution, and for greater than 1000 years the pH was controlled by equilibrium with the corrosion products. The CSNF in comp3 had a minimal effect on the system pH.

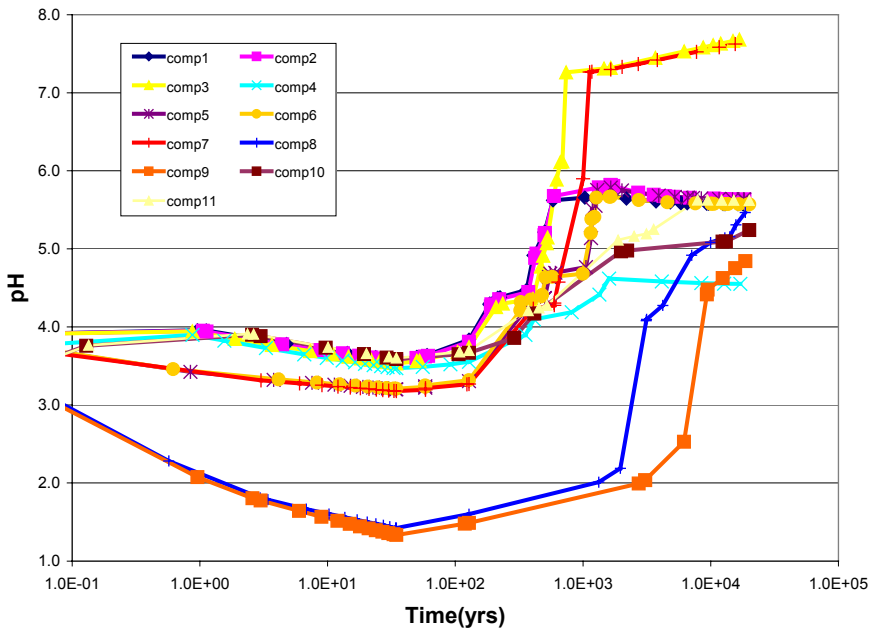

Source: Microsoft Excel Spreadsheet CS_comp_runs.xls in DTN: MO0307SPAIPCHM.001.

Figure 2. Commercial Spent Nuclear Fuel Multi-Component Ensemble pH Profiles

It must be stated that, for the purpose of total system performance assessment, only reactant combinations that include CSNF will be used in the generation of pH abstractions for the colloid, solubility, and waste form dissolution sub-models. The reason is that CSNF influences the chemistry and it would be an error to not account for its effect on the chemistry. Therefore, simulations comp5 through comp9, which do not include CSNF as part of the ensemble, are not included in the in-package chemistry model abstraction.

Furthermore, Figure 2 shows that, with the exception of comp8 and 9, the pH trends are similar in shape and magnitude. These two observations build confidence in the robustness of the conceptual model compared to Alternate Conceptual Model I (Section 6.4.1). Had the pH profiles shown a great degree of variability it would indicate that the in-package chemistry is highly path dependent, thus decreasing confidence in the robustness of the water vapor condensation model.

In the CSNF water vapor condensation model there are no fluoride or chloride abstractions because these elements are neither a constituent to the water vapor nor any of the waste package components.

The ensemble simulations and the resulting chemistry of the reacted solutions reflect interactions between CSNF, waste package components, the liquid phase water, and the atmosphere in the voids in the waste package and drift. In addition, the reactants are kinetic reactants, the metal alloys undergo oxidation and precipitate corrosion products that are in contact with the liquid phase water thereby having a first order influence on the chemistry. Because the in-package chemistry model includes all of these processes, so does the in-package chemistry model abstraction and, hence, they are included in TSPA-LA. The following FEPs are addressed by the CSNF water vapor condensation model:

- 2.1.09.01.0B Chemical characteristics of water in the waste package
- 2.1.09.07.0A Reaction kinetics in EBS
- 2.1.02.09.0A Chemical effects of void space in waste package
- 2.1.09.02.0A Chemical interaction with corrosion products

6.6.1.2 Seepage Dripping Model Results

The pH history and reactant summary for the median flux and fuel exposure seepage dripping model case at 25°C using the three different seepage compositions are displayed in Figure 3.

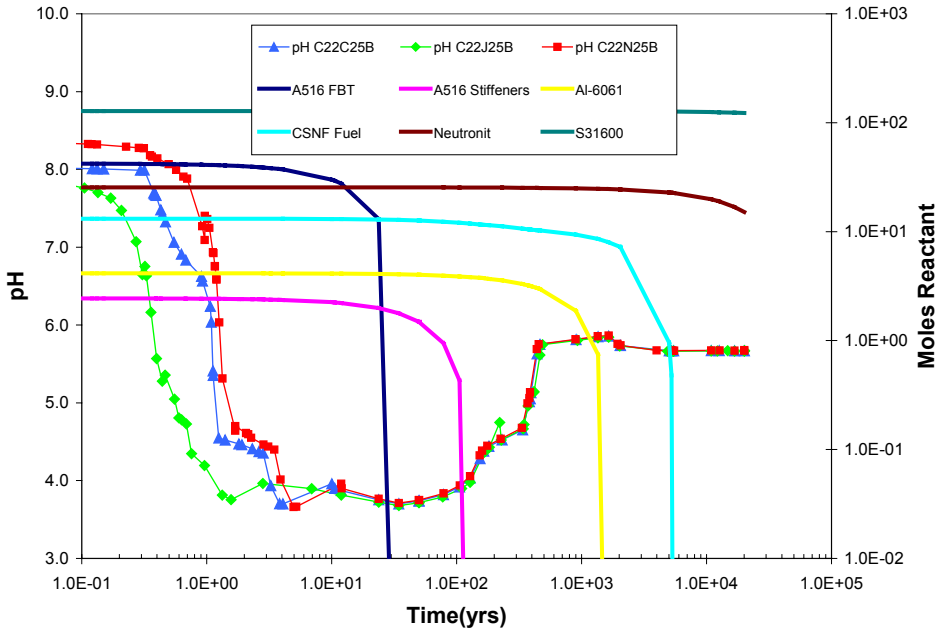

DTN: MO0307SPAIPCHM.001

Figure 3. Commercial Spent Nuclear Fuel Seepage Dripping Model Results for Q = 1.5 l/yr, Fuel Exposure = 10 Percent, and Three Seepage Compositions at 25°C

An important feature of Figure 3 is the fact that the composition of the seepage (Table 2) has virtually no effect on the pH profile. The separation in the early-time (less than approximately

0.5 years after waste package breach) pH profiles is a function of the seepage chemistry, however, this difference dissipates in approximately 10 years and the pH profiles become nearly identical. This addresses FEP 2.2.08.12.0A Chemistry of water flowing into the EBS. Thus, the composition of the water flowing into the EBS has negligible impact on the in-package chemistry pH. However, the in-package chemistry model and, thus, the TSPA-LA feed are developed using the three seepage compositions listed in Table 2; therefore, the effect of the chemistry of the water flowing into the EBS is included in the feed to total system performance assessment, although there is no parameter for the composition of the water entering the waste package. This also addresses the robustness of the in-package chemistry model with respect to Alternate Conceptual Model II. Had the seepage dripping model been sensitive to the input water composition then an alternate conceptual model with time-varying composition would be needed. This, however, was not the case, and the constant seepage assumption is justified.

Further examination of Figure 3 shows that the reactants dissolve as a function of time, i.e., they are kinetic reactants (Tables 15 and 17) and their effect on the in-package chemistry is explicitly modeled in the in-package chemistry model and thus is carried over to the feed to TSPA-LA. Therefore, FEP 2.1.09.07.0A, Reaction kinetics in EBS, is addressed by the in-package chemistry model and the in-package chemistry model abstraction and thus included in total system performance assessment.

Figure 4 displays the Eh (a measure of the redox potential), reactant summary, and oxidation products for run C22C25, the median flux and fuel exposure simulation for the Ca-porewater at 25°C. The Eh varies between approximately 0.8 to 1.0 volts, these are oxidizing conditions as the presence of metal oxide phases also indicate. Since the metal oxide corrosion products are precipitating from the solution that is in contact with the waste form and waste package components the corrosion products have a first order influence on the in-package chemistry. FEPs 2.1.09.02.0A, Chemical interaction with corrosion products, and FEP 2.1.09.06.0A, Reduction-oxidation potential in EBS, are addressed by the in-package chemistry model. The implicit inclusion of these FEPs in the in-package chemistry model, and the in-package chemistry abstraction provides confidence that these processes are included in TSPA-LA.

Figure 5 displays mineral phases that precipitated from solution for the C22 runs at 25°C for the three input water compositions. Hematite, gibbsite, schoepite, pyrolusite, and trevorite constitute the five most abundant phases, all of which are expected to form in the oxidizing waste package environment. The large amount of gibbsite ($Al(OH)_3$) that formed in these runs is due to the relatively low amount of available silica in the incoming waters and waste package components. Had more silica been available, then greater quantities of aluminum-silicate phases would have formed with proportionately less gibbsite formation. The silica phases that do form include kaolinite, nontronite-Mg, and nontronite-Ca, all of which are clay minerals. It is interesting to note that the J-13 run produced more kaolinite than the other two water compositions, the reason for this being that J-13 has a higher initial silica concentration (Table 2).

The mineral assemblage plot (Figure 5) provides further information in support of the conclusion that the composition of the seepage has little influence over which minerals formed and their amounts. The J-13 minerals show some variability compared to the other two water compositions, however, the major phases are all present in nearly identical amounts.

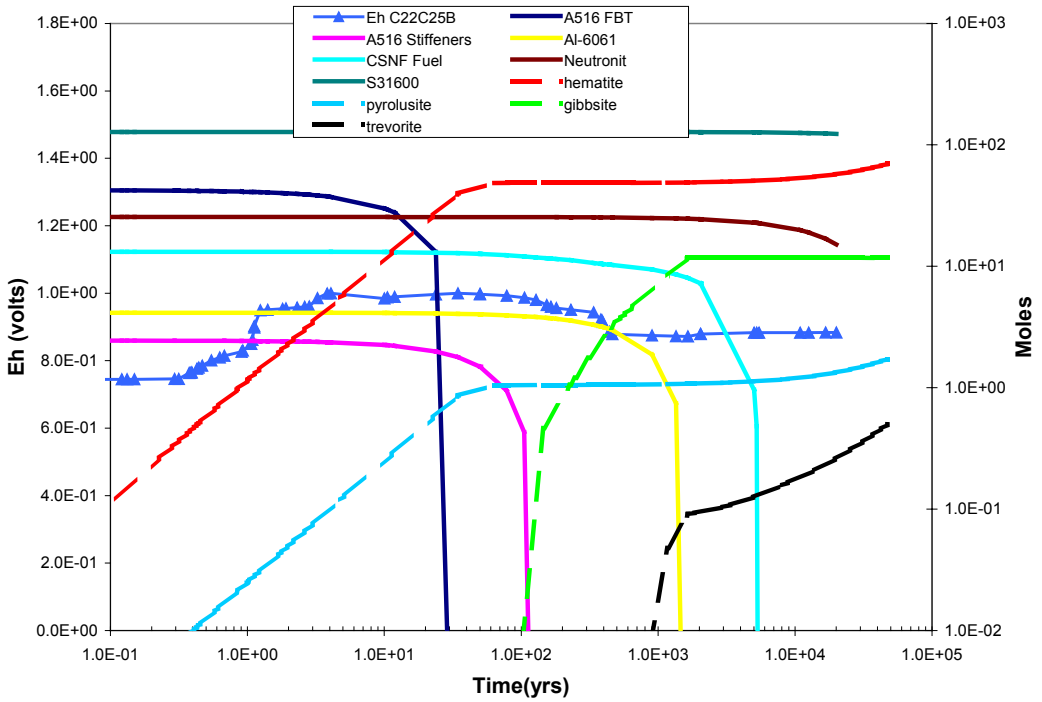

DTN: MO0307SPAIPCHM.001

Figure 4. Commercial Spent Nuclear Fuel Seepage Dripping Model C22C25 Results at 25°C, Showing Eh, Reactant Summary, and Corrosion Products

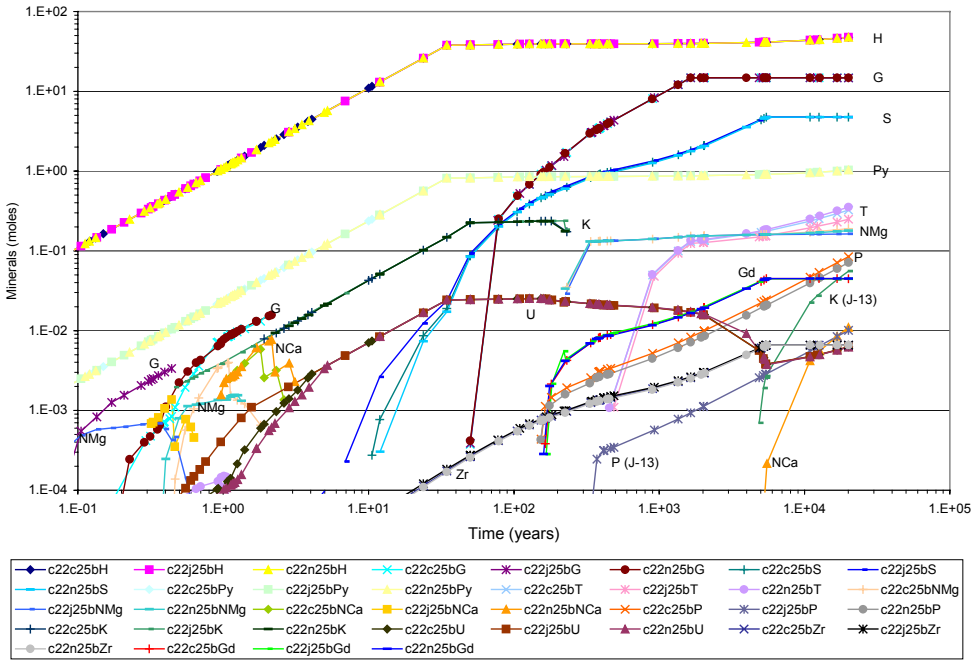

Source: Microsoft Excel Spreadsheet CSNF_Plots.xls in DTN: MO0307SPAIPCHM.001.

NOTES: H=hematite, G=gibbsite, S=Schoepite, Py=pyrolusite, T=trevorite, NMg=nontronite-Mg NCa=nontronite-Ca, K= kaolinite, P=powellite, Gd=GdPO4:10H2O, U=(UO2)3(PO4)2:6H2O, Zr=Baddeleyite

Figure 5. Commercial Spent Nuclear Fuel Seepage Dripping Model Mineral phases for the Three Seepage Compositions at 25°C, Q = 1.5 l/yr, fuel exposure = 10%

Figure 6 displays aqueous species for the C22 runs at 25°C for the three input water compositions. This plot shows that elements which were not present in the initial water compositions (Table 2). In other words, those elements that originate from the waste package and SNF have aqueous species concentrations that are nearly identical, and independent of the initial water composition, for the duration of the simulations. Examples of these elements include Ni, Cr, and B, all of which originate from oxidation of the metal waste package components. Elements which were present in the initial water composition and were also involved in reactions in the waste package also have similar aqueous species concentrations. For example, sulfur which was present in all of the water compositions as sulfate (SO_4^{2-}) shows similar concentration trends in the simulations, independent of the starting water composition, due to the sulfur contained in the A516, which dominates the sulfate concentration trends observed in Figure 6. At times great than about 5000 years, the sulfur concentration trends for the three waters shows some separation, which is due to the sulfate concentration returning to their initial values.

Figures 5 and 6 show that depending on the initial fluid composition, there is little variability in the minerals and aqueous species of the reacted fluid chemistry that may potentially exit a failed waste package. However, this variability is slight, and the pH and ionic strength of the reacted solutions is unaffected by these variations, and thus variability of the input water compositions should not impact TSPA-LA.

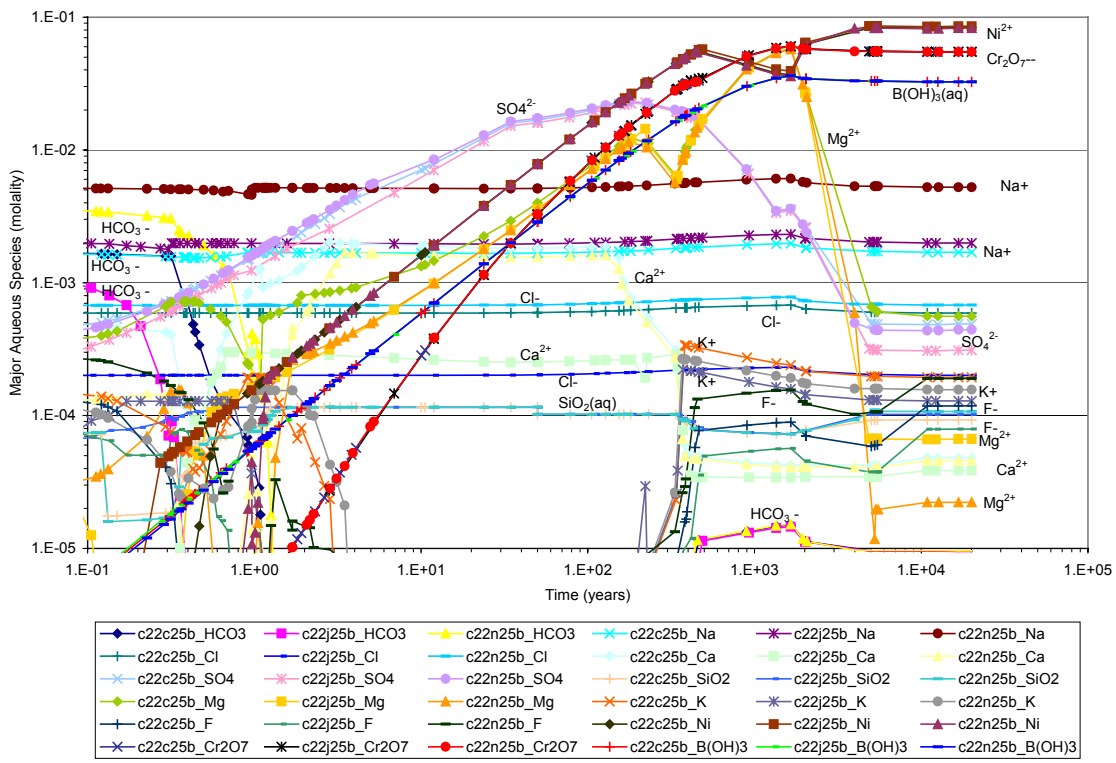

Source: Microsoft Excel Spreadsheet CSNF_Plots.xls in DTN: MO0307SPAIPCHM.001.

Figure 6. Commercial Spent Nuclear Fuel Seepage Dripping Model Aqueous Species for the Three Seepage Compositions at 25°C, Q = 1.5 l/yr, fuel exposure = 10%

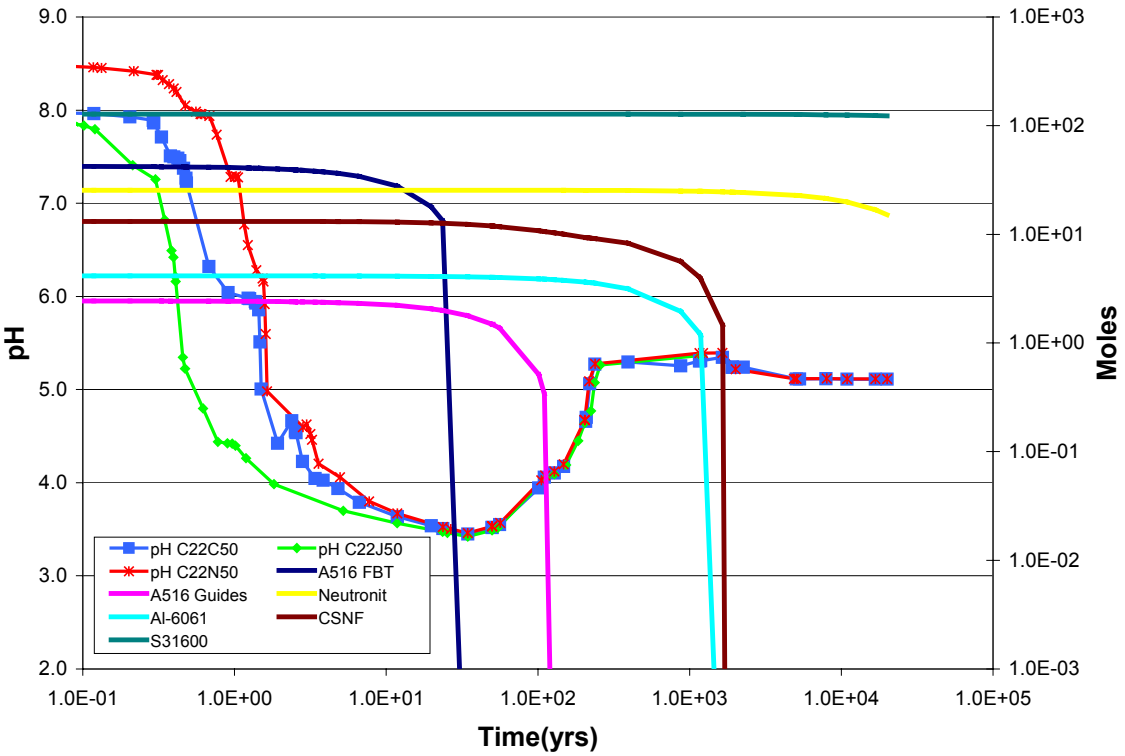

DTN: MO0307SPAIPCHM.001

Figure 7. Commercial Spent Nuclear Fuel Seepage Dripping Model Results for Q = 1.5 l/yr, Fuel Exposure = 10 Percent, and Three Seepage Compositions at 50°C

Figure 7 shows a plot of pH and reactant summary for the median seepage flux and fuel exposure values at 50°C for the three input seepage compositions. Like Figure 3 that shows the same simulations but at 25°C, the initial composition of the seepage entering the waste package has little impact on the composition of the reacted fluid composition as the contents of the waste package control the chemistry. Compared to the simulations performed at 25°C, the 50°C simulations use a CSNF degradation rate that is temperature appropriate (Table 17), while the metal alloy corrosion rates are the same as the 25°C runs (Section 5.2.5). Also, the thermodynamic database includes mineral and aqueous species data for 50°C, therefore the reacted solution chemistry and precipitated mineral phases are temperature appropriate.

The 50°C runs achieve an overall lower pH profile at long time periods and slight variations in the stable mineral assemblages compared with their 25°C counterparts. Since a suite of simulations was carried out at above ambient temperatures and the in-package chemistry model results reflect the increased thermal conditions, the TSPA-LA feed also reflects the increased thermal conditions, which means that the FEP 2.1.11.08.0A, Thermal effects on chemistry and microbial activity in the EBS, has been partially addressed. The abstraction of in-package chemistry provides a separate, i.e., different than the 25°C abstractions, set of abstractions at 50°C for TSPA-LA, as well as a means of linking the two abstractions

6.6.2 Codisposed N Reactor Output

6.6.2.1 Water Vapor Condensation Output

Figure 8 displays the pH profiles for the CDNR waste package components. The CDNR package displays a much wider variation in pH compared to the CSNF package (Figure 1). The HLW generates high pH conditions due the high concentrations of sodium and potassium. The Al-1100, S31600, and N Reactor fall in the middle of the pH range at approximately 5.7 to 6.2. The A516 and 304L steels are strong acid generators at pH of 1.5 to 2.

The results of the CDNR multi-component ensemble runs are displayed in Figure 9. The low end of the pH range in Figure 8 is not reproduced in the multi-component results (Figure 9). The ensembles include either HLWG or N Reactor fuel as a reactant because the TSPA-LA model for in-package chemistry does not take cladding credit for N reactor fuel or the glass pour canisters. Therefore, the low pH generated by 304L and A516 (Figure 8) is not observed in the ensemble runs (Figure 9) because of the pH buffering capacity that HLWG and N Reactor fuel offer.

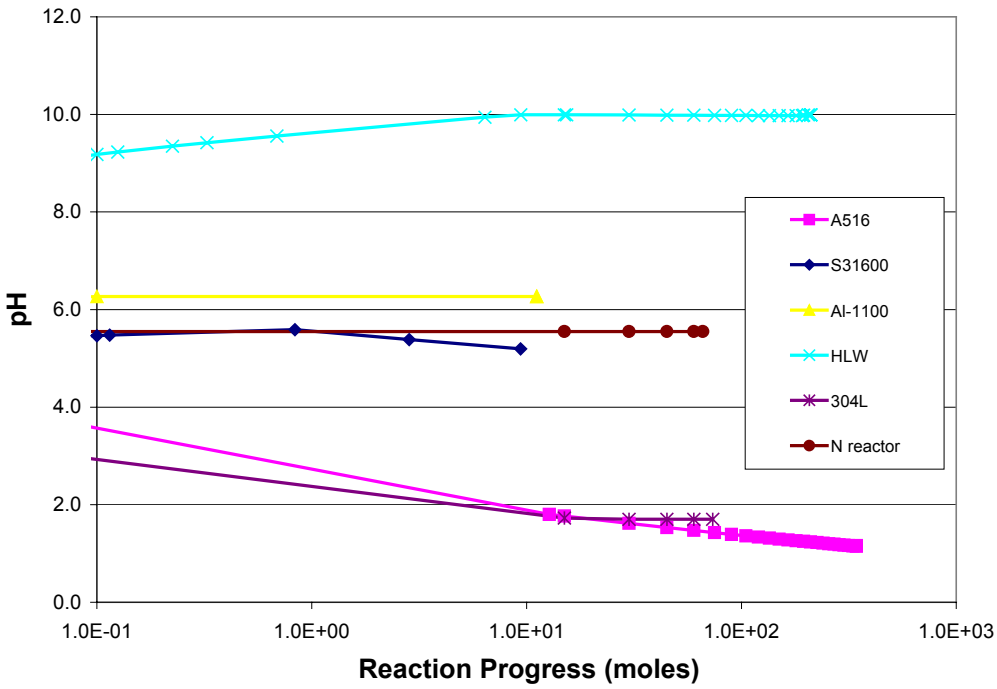

Source: Microsoft Excel Spreadsheet CDNR_WVC.xls in DTN: MO0307SPAIPCHM.001.

Figure 8. Codisposed N Reactor Single-Component Water Vapor Condensation Results

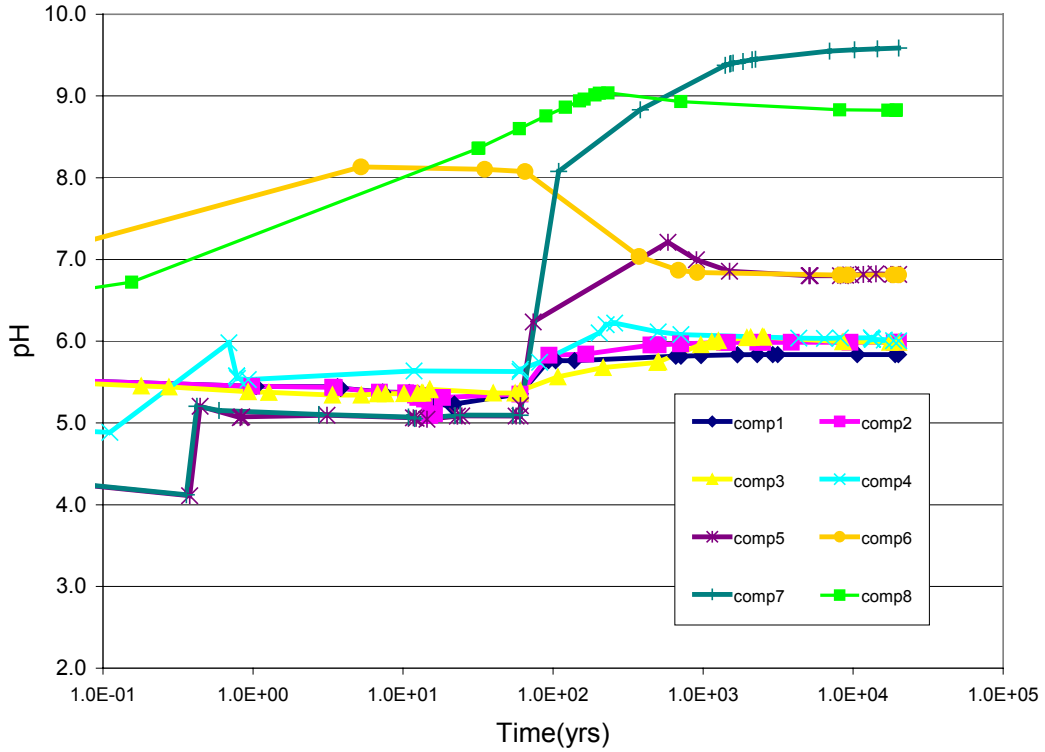

Source: Microsoft Excel Files CD_comp_runs.xls and CD_COMP_WVC.xls in DTN: MO0307SPAIPCHM.001.

Figure 9. Codisposed N Reactor Multi-Component Ensemble pH Profiles

The ensemble simulations comp1, comp2, and comp3 include both HLWG and N Reactor fuels as reactants, thus, the resulting chemistry of the reacted solutions (pH ≅ 6) reflects interactions between the co-disposed waste, the non-SNF waste package components, the liquid phase water, and the atmosphere in the voids in the waste package and drift. In addition, the fuel and metal alloys are kinetic reactants, which undergo oxidation and precipitate corrosion products that are in contact with the liquid phase water, thereby having a first order influence on the chemistry.

Since the in-package chemistry model and in-package chemistry model abstraction include all of these processes, the processes are also included in TSPA-LA. The following FEPs are addressed by the CDNR water vapor condensation model:

- 2.1.09.01.0B Chemical characteristics of water in the waste package
- 2.1.09.07.0A Reaction kinetics in EBS
- 2.2.08.12.0A Chemistry of water flowing into the EBS
- 2.1.02.09.0A Chemical effects of void space in waste package
- 2.1.01.02.0B Interactions between co-disposed waste
- 2.1.09.06.0A Reduction – oxidation potential in EBS
- 2.1.09.02.0A Chemical interaction with corrosion products.

High pH conditions are only realized in the comp7 and comp8 simulations in which HLWG is combined with A516 and Al-1100, respectively. In these two cases, the period of elevated pH

only occurs after the metal alloys have been exhausted. Because neither A516 nor Al-1100 provide long-term pH buffering like the S31600 and 304L stainless steels the pH increases when these metals are exhausted. In the Comp5 and Comp 6 simulations, where HLWG is paired with the various 304L components the resulting pH is just slightly less then pH 7. Given that the stainless steel components of the waste package have a longer predicted lifetime then the HLWG it is probable that they will moderate the basic conditions generated by HLWG dissolution and maintain neutral pH conditions inside the waste package, until the HLWG is exhausted.

6.6.2.2 Seepage Dripping Model Output

Figures 10 and 11 display the CDNR seepage dripping model pH profiles for the three seepage compositions at 25 and 50°C, respectively. Also displayed is the reactant summary. The pH profiles converge early in the simulations indicating that the model pH response is insensitive to starting water composition, which is similar to the pH profile behavior of the CSNF seepage dripping model (Figures 3 and 6).

The most outstanding feature in Figure 10 is the reactant summary for the N Reactor fuel. The figure shows that the N Reactor fuel dissolves over a short duration of just a few years. The rapidity of the N Reactor fuel dissolution diminishes its importance to the overall in-package chemistry contribution. However, the large quantity of schoepite precipitated in the waste package has the capacity to influence the in-package chemistry for an extended duration.

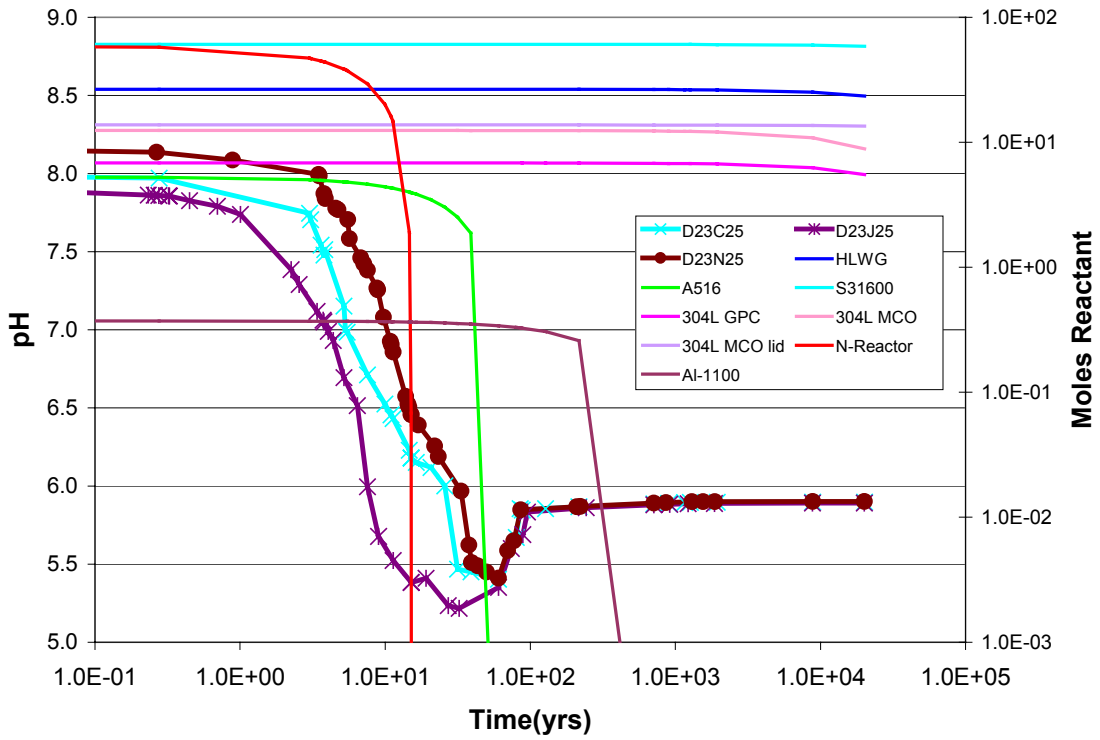

Source: Microsoft Excel Spreadsheet CDNR_SDM_25.xls in DTN: MO0307SPAIPCHM.001.

Figure 10. Codisposed N Reactor Seepage Dripping Model Results for Q = 1.5 l/yr and Three Seepage Compositions at 25°C

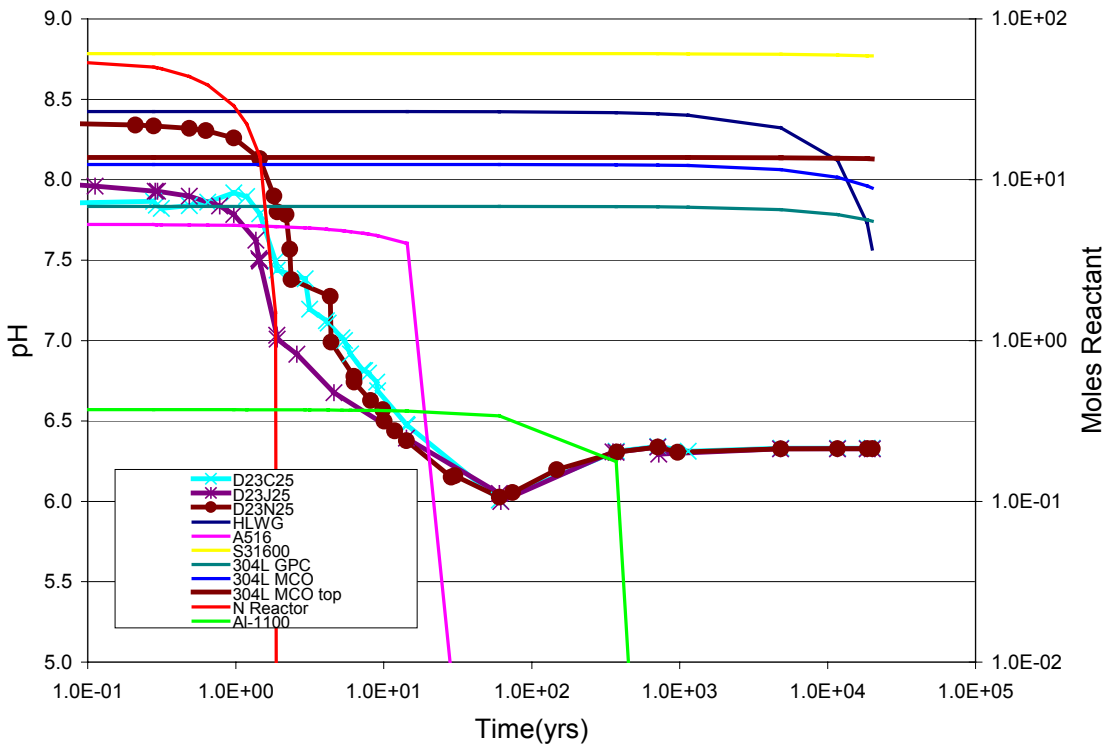

Source: Microsoft Excel Spreadsheet CD_SDM_50.xls in DTN: MO0307SPAIPCHM.001.

Figure 11. Codisposed N Reactor Seepage Dripping Model Results for Q = 1.5 l/yr and Three Seepage Compositions at 50°C

Another important feature of the pH profiles in Figures 10 and 11 is the absence of a period of sustained high pH (greater than 9) that might be expected from the dissolution of the HLWG. The CDNR water vapor condensation models, single reactant and ensemble, both predicted that high pH conditions are possible in the absence of an acid producing reactant, i.e., steel alloy. However, in the seepage dripping model, seepage is allowed to "stream" through the waste package reacting with waste package components, and it is unlikely that seepage which has reacted with HLWG could exit a waste package without contacting a steel component along its flow path.

The HLWG is more quickly depleted at 50°C then 25°C because of the higher rate constants (Table 19) at elevated temperature.

The CDNR seepage dripping model simulations include both high-level radioactive waste and N Reactor fuels as reactants, thus, the resulting chemistry of the reacted solutions reflects interactions between co-disposed waste, the non-SNF waste package components, the liquid phase water, and the atmosphere in the voids in the waste package and drift. In addition, the reactants are kinetic reactants, the fuel and metal alloys undergo oxidation and precipitate corrosion products that are in contact with the liquid phase water thereby having a first order influence on the chemistry. Since the in-package chemistry model and in-package chemistry model abstraction include all of these processes, the processes are also included in TSPA-LA.

The following FEPs are addressed by the CDNR water vapor condensation model:

- 2.1.09.01.0B Chemical characteristics of water in the waste package
- 2.1.09.07.0A Reaction kinetics in EBS
- 2.2.08.12.0A Chemistry of water flowing into the EBS
- 2.1.02.09.0A Chemical effects of void space in waste package
- 2.1.01.02.0B Interactions between co-disposed waste
- 2.1.09.06.0A Reduction – oxidation potential in EBS.

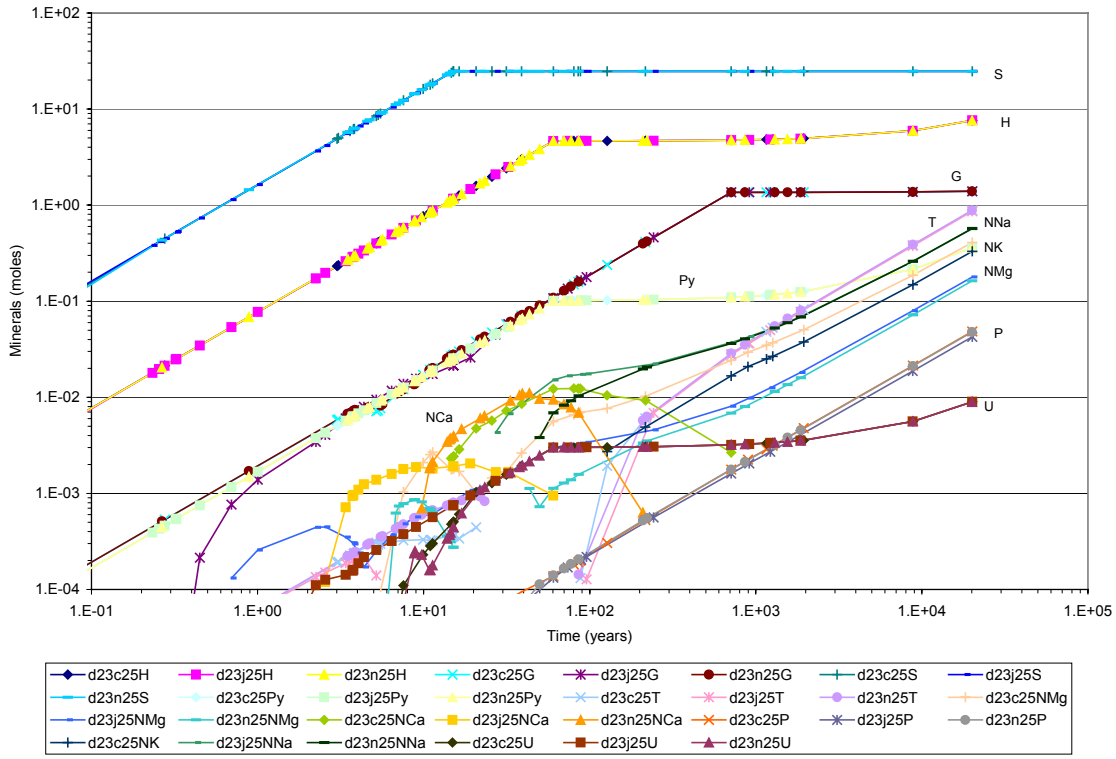

Source: Microsoft Excel Spreadsheet CDNR_Plots.xls in DTN: MO0307SPAIPCHM.001.

NOTES: H=hematite, G=gibbsite, S=Schoepite, Py=pyrolusite, T=trevorite, NMg=nontronite-Mg
NCa=nontronite-Ca, P=powellite, Gd=GdPO4:10H2O, U=(UO2)3(PO4)2:6H2O, Zr=Baddeleyite

Figure 12. Codisposed N Reactor Seepage Dripping Model Mineral Phases Results for Q = 1.5 l/yr and Three Seepage Compositions at 25°C

Figure 12 shows the minerals which formed for the CDNR seepage dripping model for the three seepage compositions at 25°C. This plot shows that schoepite, hematite, and gibbsite constitute the three most abundant mineral phases that form from the degradation of a CDNR waste package. The abundance of schoepite (UO_3:$2H_2O$) results from the complete reaction of the uranium metal N Reactor fuel, while the hematite and gibbsite are products of steel and aluminum alloys dissolution, respectively. Over the duration of the simulations, less gibbsite forms in the CDNR runs compared to the CSNF runs (Figure 5), while greater amounts of the nontronite clay minerals form in the CDNR runs compared to the CSNF runs. The reason for this is the greater availability of silica in the CDNR compared to the CSNF waste package from

the presence and degradation of the HLWG. This additional silica leads to greater amounts of nontronite formation in the CDNR waste packages.

The CDNR mineral assemblages (Figure 5) for the three seepage compositions provides further support of the conclusion that the composition of the seepage has little influence over which minerals formed and their amounts.

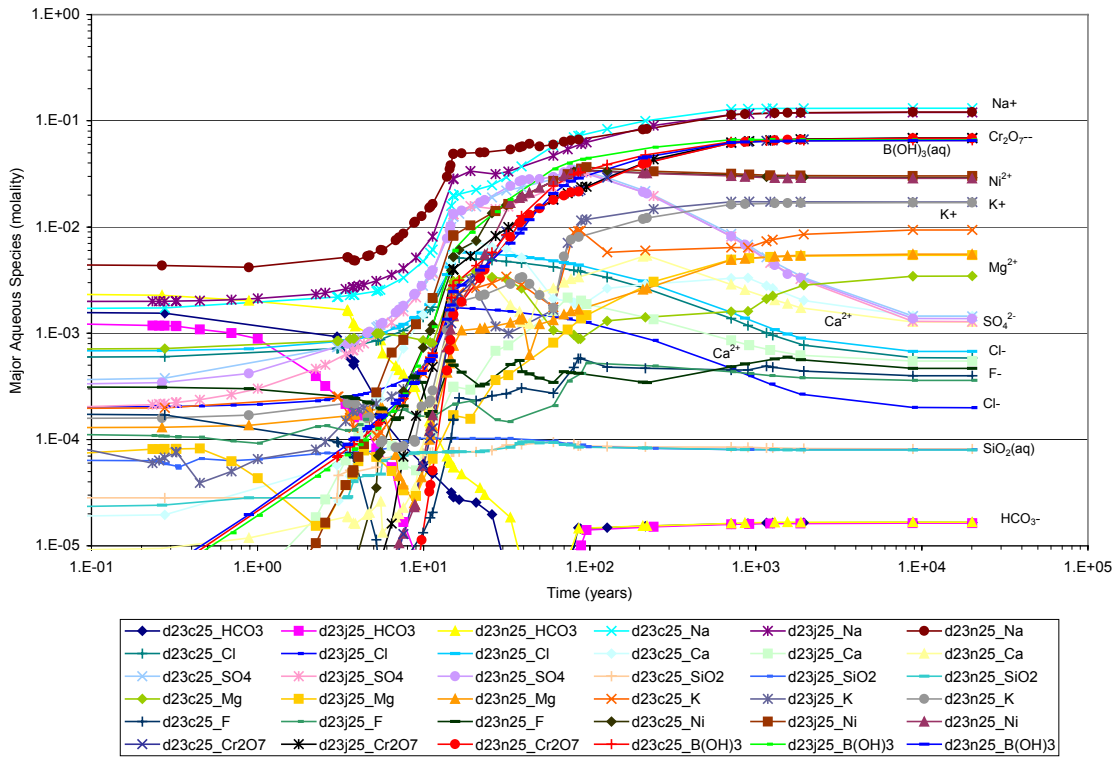

Source: Microsoft Excel Spreadsheet CDNR_Plots.xls in DTN: MO0307SPAIPCHM.001.

Figure 13. Codisposed N Reactor Seepage Dripping Model Aqueous Species Results for Q = 1.5 l/yr and Three Seepage Compositions at 25°C

Figure 13 displays the aqueous species for the CDNR runs at 25°C for the three input water compositions. Similar to CSNF, Figure 13 shows that elements which were not present in the initial water compositions (Table 2), i.e., those elements that originate from the waste package and SNF, have aqueous species concentrations that are nearly identical, and independent of the initial water composition, for the duration of the simulations. Sodium, chromium, and boron have the highest concentrations, and either originated from HLWG dissolution (in the case of the sodium) or from the oxidation of the metal waste package components (in the case of boron and chromium). While those elements that do not originate from the waste package components or SNF, and do not participate in the formation of minerals, they do have aqueous species concentrations set by the incoming water composition (e.g., chloride). However, the concentrations of the majority of aqueous species are nearly identical and independent of the seepage composition. Therefore, it may be concluded that the in-package chemistry is set by the waste package components and SNF and not the composition of the water entering the failed waste package

6.7 SENSITIVITY—UNCERTAINTY OUTPUT

Sensitivity analyses were performed to meet the following objectives: (1) to determine uncertainty ranges for pH and ionic strength for use in the in-package chemistry model abstraction; (2) to expand the boundaries (temperature, flux, and CO_2 partial pressure ranges) of the in-package chemistry model abstraction without performing a large array of additional simulations; and (3) to demonstrate the effects of waste package design configuration variations on the model output.

6.7.1 Uncertainty Range

To assess the magnitude of the model response to variability in model inputs, sensitivity analyses were performed. The inputs that were identified as potentially important included: the partial pressure of carbon dioxide (PCO_2), metal alloy corrosion rates, and the sulfur content of A516. A simple approach was taken where the median fuel exposure (cladding)/flux combination Ca-porewater CSNF seepage dripping model simulation was used as the reference case, and simulations were performed by varying these inputs independently. The results were plotted and compared to the reference case simulation and error bars were used to cover the range of the output.

The results of the sensitivity analyses are presented in Figure 14 for pH and Figure 15 for ionic strength. The sensitivity run results show that the model was not sensitive to changes in carbon dioxide partial pressure from 10^{-4} to 10^{-2} atmospheres, labeled "low PCO2" and "high PCO2," respectively, on the figures. The model was sensitive to decreases (factor of 5) in the metal alloy corrosion rates (labeled "low alloy rates" on the figures), which had the effect of delaying the pH response compared to the reference case. The metal alloy corrosion rates were not increased for the sensitivity analyses because the base-case rates are considered to be high as the steels are likely to become coated with corrosion products which would slow corrosion. Changes in the sulfur content (± a factor of five) of the A516 had the expected result of decreasing the pH when the sulfur content was increased and increasing the pH when the sulfur content was decreased.

For pH, the error bars had to meet two criteria: 1) To encompass the extreme values of pH (i.e., pH values which had the greatest deviation from neutral, which is a pH of 7); and 2) to capture the pH uncertainty over the long duration of the model period. The first criterion was set based on the reasoning that large excursions from neutral pH, either acidic or basic, are likely to have the greatest impact on the sub-models which use parameter feeds from the in-package chemistry model abstraction. The second criterion was set because the in-package chemistry tends towards stabilized conditions over long time periods and accounting for the uncertainty over long term has the potential for the greatest impact on the sub-models which use parameter feeds from the in-package chemistry model abstraction.

Figure 14 shows the reference case with error bars of ± 0.5 pH units. The error bars capture the pH low at about 20 years for the high sulfur run (yellow symbols). The high sulfur pH profile was used as the defining profile because it deviates the most from neutral. Between about 300 and 1000 years the error bars do not envelop the pH trend of the high sulfur case. Since the error bars would have had to be increased in magnitude to 1-pH unit, which over estimates the uncertainty over the long term, it was decided not to include this period in the estimation of error

bars. The period of nearly constant pH between 1000 and 20,000 years, the longest period, the low alloy corrosion rate simulation defines the error bars.

It is the recommendation based on this analysis of the variability in the model output, that for the pH abstractions (Section 8) in the in-package chemistry model abstraction a sampled uniform uncertainty range of -0.5 to 0.5 pH units be added to the abstracted pH value(s). A uniform distribution was chosen because of the equal probability of any variable contributing to the uncertainty.

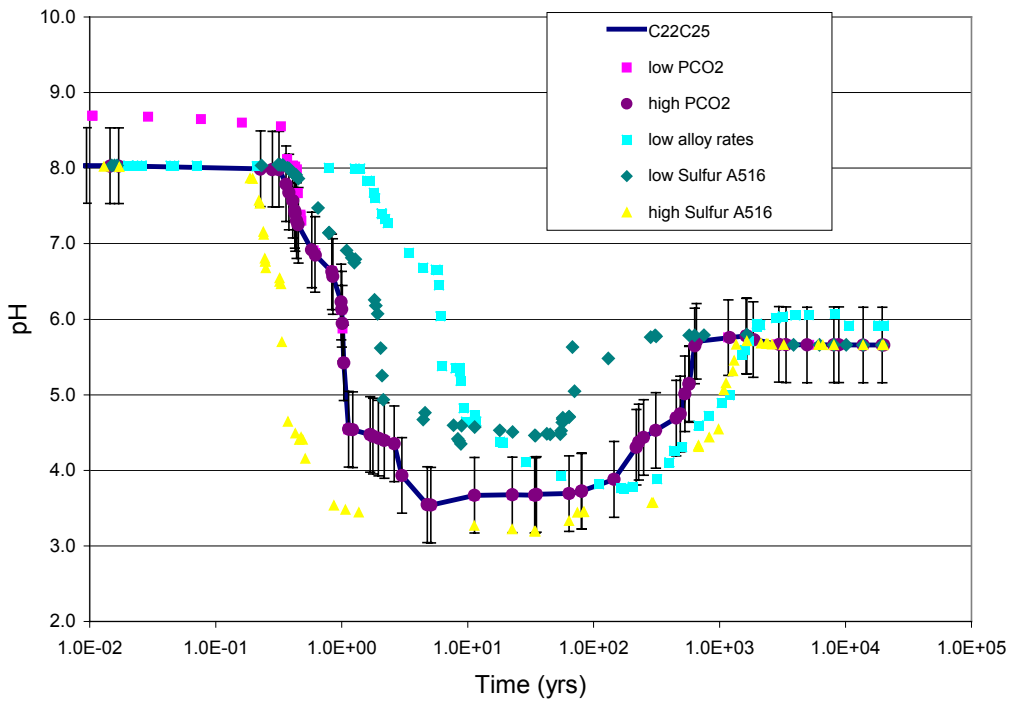

Source: Microsoft Excel Spreadsheet CS_Sensitivity.xls in DTN: MO0307SPAIPCHM.001.

Figure 14. Sensitivity Analysis of pH

For ionic strength a criterion was implemented for setting the error bars. Abstraction of the in-package ionic strength is used exclusively by the colloid sub-model in TSPA-LA. The colloid model report (BSC 2003e, Section 6.3.2.4) defines the upper limit of ionic strength for colloid stability, the value above which colloids are no longer stable as dispersed particles in solution, as 0.05 molal. Therefore, below this 0.05 molal ionic strength threshold value colloids are stable in solution and available for radionuclide adsorption. The criterion used to fit the error bars was to honor the low ionic strength (less than 0.05 molal) side of the reference case. For example, in Figure 15 the low sulfur and the low alloy rate cases tend toward lower ionic strength compared to the reference case, and the error bars cover the range of these sensitivity cases.

The ionic strength error bars are a percentage value rather than a constant additive value like that used for pH. Thus, the uncertainty range of -0.6 to 0.6 (as shown in Figure 15, is multiplied by an ionic strength value and the product is added back to the ionic strength to obtain the ionic

strength with uncertainty. This uncertainty range and its application in the TSPA-LA ionic strength abstractions is further discussed in Section 8.

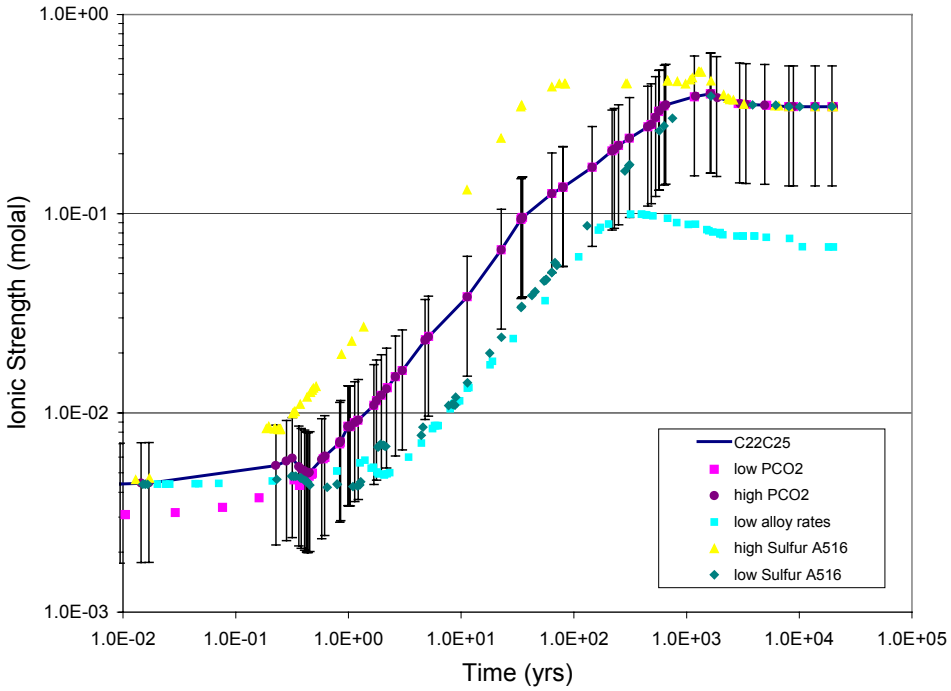

Source: Microsoft Excel Spreadsheet CS_Sensitivity.xls in DTN: MO0307SPAIPCHM.001.

Figure 15. Sensitivity Analysis of Ionic Strength

6.7.2 Limits of the In-Package Chemistry Model Abstraction

Two suites of additional simulations were performed, one using a series of elevated temperatures, and a second using a series of elevated seepage flux values. The purpose of these additional simulations was to aid in the determination of the application limits of the abstractions derived in Section 8. For the results, discussion, and application of these simulations see Sections 8.2.3, 8.2.6, 8.4.1, 8.4.3, and 8.4.6.

The runs performed at alternate carbon dioxide partial pressures (Section 6.7.1) are also used to expand the limits of the abstractions and are discussed in Section 8.8.

6.7.3 Effect of Waste Package Design

Variations in the waste package design configurations for the CSNF packages were examined to determine if the model response was sensitive. This sensitivity analysis was performed because not all of the A516 that made up the "A516_Guides" was included in the EQ6 input files, so the additional A516 was included and model runs were performed. This change affects the moles and surface area for all of the components because the additional volume of A516 changed the calculated surface area, which is used to normalize surface area of these components. The EQ6 input values are included in Attachment I, "CSNF.xls", worksheet "SDM A516 Guides." Run C11C25.6i was used as a comparison case because the effect of increased A516 on the model

response would be the greatest at low water flux and low fuel exposure. The results are shown in Figure 16.

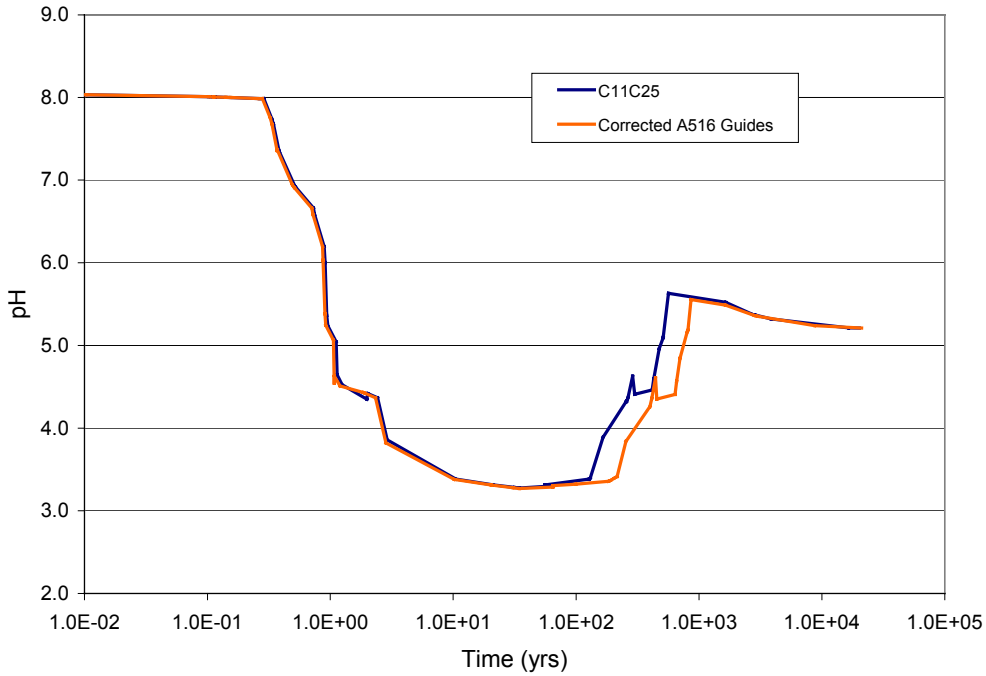

Source: Microsoft Excel Spreadsheet CS_Sensitivity.xls in DTN: MO0307SPAIPCHM.001.

Figure 16. Sensitivity Analysis with Corrected A516 Guide Information

Figure 16 shows that increasing the mass and surface area of the A516 by a factor of approximately 10 had little influence on the pH profile.

7. MODEL VALIDATION

The purpose of the in-package chemistry model and the in-package chemistry model abstraction is to predict the bulk chemistry inside of a failed waste package and to provide simplified expressions of that chemistry for use in TSPA-LA. The technical work plan (BSC 2002a, Section 2.1.4.4) states that the post-development validation of the model will focus on the two sub-models. The fuel-degradation sub-model will be validated by comparison with results from laboratory experiments published in refereed journals or literature. The types of minerals formed and the aqueous concentrations predicted by the model will be compared to experimental results to quantify the uncertainty range of the model. The steel-degradation sub-model will be validated based on results published from laboratory experiments on man-made analog materials.

The validation efforts outlined in the technical work plan and cited above were subsequently considered to provide insufficient confidence for predicting in-package chemistry over the much longer time spans to which the model is to be applied. Consequently, model validation efforts

avoided laboratory evidences and instead focused on natural analogue observation which might provide confidence in model predictions over near geologic time spans.

The primary output of the in-package chemistry model abstraction to total system performance assessment are ranges of pH and ionic strength. Adequate validation of the in-package chemistry model, therefore, entails showing, on the basis of natural analogue evidence, that the pH and ionic strength ranges are comparable.

The salient critical features of the in-package chemistry model are:

1. Production of alkaline waters ($8 < pH < 10$) by interaction of dilute solutions with waste form glass components,

2. Production of mildly acidic ($3 < pH < 5$) waters by interaction of incoming solutions with waste form metallic components (primarily A516 low-carbon and S31600 stainless steel),

3. Production of high ionic strength solutions (greater than 1 M) by reaction with waste form components.

The technical work plan (BSC 2002a, Section 2.1.4.2) indicates that the in-package chemistry model recommends a higher level of confidence (moderate or Level II) than other waste form degradation models which require a low level of confidence. The technical work plan criteria (BSC 2002a, Section 2.1.4.2) used to establish the level are:

1. The in-package chemistry model is extrapolated over long time periods.

2. The in-package chemistry model itself does not have large uncertainties, however, the in-package chemistry model must be robust enough to cover uncertain initial conditions.

3. The in-package chemistry model will be used to demonstrate compliance for licensing as it is an input to TSPA-LA.

4. The in-package chemistry model is not a primary contributor to the determination of dose.

Level II (moderate) validation, recommends satisfying Level I criteria (a) through (f) (BSC 2002f, Appendix B), and a single post-development model validation method as per AP-SIII.10Q, *Models*. The additional, single post-development model validation criterion that is addressed for each salient feature above is that of corroboration with data published in refereed journals or literature in accordance with Section 5.4.1 in AP-SIII.10Q, *Models.* Specifically, validation of the in-package chemistry model requires that the broad ranges of pH and ionic strength predicted by the model be shown to be consistent with the pH values and ionic strengths observed in natural systems and documented in refereed journals or literature, wherein the same underlying mechanisms prevail

Level I criteria recommend that model development efforts entailed:

(a) *Evaluating and selecting input parameters and data*: Section 4.1 provides the inputs used in the in-package chemistry model, which include waste package design information, material compositions, atomic weights, densities, water compositions, SNF compositions, corrosion/reaction rates, and thermodynamic data, these inputs were chosen to best represent all of the components of the in-package chemistry model. Therefore, this criterion has been met for all of the salient features.

(b) *Formulating defensible assumptions and simplifications*: Sections 5, 6.3.2 and 6.3.3 provide the assumptions (Section 5) and simplifications (Sections 6.3.2 and 6.3.3) used in the in-package chemistry model. The in-package chemistry model has been updated and subdivided into two scenario driven sub-models both of which eliminate a previous implausible conceptualization. Therefore, the in-package chemistry model assumptions and simplifications are defensible. This criterion has been met for all of the salient features of the model.

(c) *Ensuring consistency with physical principles, such as conservation of mass, energy, and momentum*: Sections 6.3, 6.3.2 and 6.3.3 provide brief discussions of the EQ6 geochemical modeling software used for the in-package chemistry model simulations. EQ6 preserves mass, both of solids and water; therefore the in-package chemistry model also conserves these properties. This criterion has been met for all of the salient features.

(d) *Representing important future state (aleatoric), parameter, and alternative model uncertainties*: Unexpected random (aleatoric) events are outside of the realm of the in-package chemistry model. However, the in-package chemistry model was designed to be robust enough to handle large changes in temperature, flux, and seepage composition. Alternate conceptual models were discussed in Section 6.4 and the current in-package chemistry model robustness eliminates the need for these alternate conceptual models. This criterion has been met for all of the salient features.

(e) *Ensuring simulation conditions have been set up to span the range of intended use and the avoidance of inconsistent outputs*: Sections 6.3.2 and 6.3.3 outline the wide range of inputs (flux, fuel exposure, temperature, reactant combinations) that were used in the in-package chemistry model. These conditions span the range of intended use in TSPA-LA for which the in-package chemistry model will be used. This criterion has been met for all of the salient features.

(f) *Ensuring that model predictions (performance parameters) adequately represent the range of possible outcomes, consistent with important uncertainties*: Sections 6.3.2 and 6.3.3 provide the input conditions which span the range of the intended use of the model; thus logic dictates that the range of outputs (performance parameters) also represents the range of possible outcomes. Additionally, sensitivity analyses have been performed to expand the performance parameters to values consistent with important conditional uncertainties. Therefore, this criterion has been met for all of the salient features.

7.1 PRODUCTION OF ALKALINE WATERS BY GLASS DISSOLUTION

Is the production of alkaline waters consistent with the peer reviewed or industry literature? Glass dissolution causes pH values greater than 7 when protons from solution exchange with alkalis, typically Na^+, K^+, or Ca^{2+}, present at the dissolving glass-solution interface, e.g.,

$$\text{Glass-Na}^+ + H^+ \leftrightarrow Na^+ + \text{Glass-H}^+$$

The general link between dissolution of alkali-bearing silicate minerals and glasses with acidity destruction (alkalinity production) is amply documented in the peer-reviewed scientific literature. Typically, large-scale weathering of alkali-bearing silicates ultimately leads to high pH values in alkali lakes (Berner and Berner 1987, pp. 280 to 281). Experiments seeking to mimic interaction of seawater with basaltic glass on the ocean floor occasionally observe alkaline pH values (note that basaltic glass is generally considered to be an appropriate natural analogue for nuclear waste glass (Ewing and Haaker 1979). The highest pH values in natural waters (up to 12) tend to be observed in deep groundwaters in contact with dissolving ultramafic rocks isolated from atmospheric CO_2 (Hem 1985, p. 64).

Values of pH above approximately 10 in fluid-mineral systems tend to be severely limited by the influx of carbon dioxide, precipitation of metal-carbonate minerals, by deprotonation of aqueous species (e.g., silica, $Al(OH)_{3aq}$, etc.), and by proton loss from mineral surface groups. Indeed it is exceedingly difficult to find natural waters with pH values of 10. Those that exhibit higher pH values do so under conditions different from those expected to prevail in the waste packages, namely they are out of contact with atmospheric carbon dioxide. For the purposes of model validation, the above discussion does two things: (1) It states the upper limit of pH to be roughly 10; and (2) it shows that the conditions in the waste form will be similar to natural systems with upper pH bounds of approximately 10.

In short, the two together indicate that the high-end pH values predicted by the in-package chemistry model are corroborated by natural observations documented in the peer-reviewed literature. This, in tandem with the satisfaction of Level I criteria (a) through (f), therefore provides sufficient justification for a medium level of confidence in this particular feature of the in-package chemistry model. On the basis of meeting the criteria for this feature, the level of confidence has been met.

7.2 ACID PRODUCTION FROM STEEL DISSOLUTION

Does the corrosion of steel and generation of acidic conditions agree with natural observations documented in the peer-reviewed literature? Oxidation of sulfur in A516 is predicted to be the primary source of acidity in the in-package chemistry model. The composition for the low carbon steel (A516) is given in Table 6. Upon complete oxidation, the form of each element that is found in natural waters will be as follows for elements present in greater than trace amounts (Hem 1985; p. 109 (C), p. 69 (Si), pp. 127 to 128 (P), pp. 84 to 88 (Mn)): C will become carbon dioxide (a weak acid), or bicarbonate; the Si will become aqueous silica; the P will form phosphoric acid, monohydrogen phosphate, or dihydrogen phosphate (weak acids) except under highly alkaline conditions; the S will become sulfate, except under highly acidic conditions. The Fe and Mn will form Mn and Fe oxides, which are largely insoluble. Note that local oxidation

will lead to local deviations from the picture outlined below. By the same token other oxidized iron phases other than those mentioned below might be observed to form for limited time periods. The assemblage may ultimately react with other components from the incoming solution (e.g., the phosphate species might react with divalent cations to form a phosphate salt such as hydroxyapatite).

For the purposes of validating acidity production by long-term steel degradation, note that for both of the metal steel components oxidation reactions involve either water, or free oxygen, or both, but that neither produces (or consumes) protons.

Oxidation of Fe, the primary component, is:

$$2Fe + 3/2O_2 \rightarrow Fe_2O_3$$

Oxidation of P under sufficiently acid conditions (i.e., pH < about 5) similarly doesn't produce acid:

$$\text{Metal-P} + 3/2H_2O + 5/4O_2 \rightarrow H_3PO_4.$$

Oxidation of S in the steel is different because it produces a strong acid, sulfuric acid, which ultimately produces protons:

$$\text{Metal-S} + H_2O + 3/2O_2 \leftrightarrow SO_4^{-2} + 2H^+$$

(Metal-P and Metal-S denote P and S, respectively, in the metal). The reaction above is constrained by two natural and experimental observations: (1) Sulfur is in reduced form in steel; and (2) sulfate is the typical oxidized form of S in oxidizing natural waters (Hem 1985, pp. 112 to 117).

The closest natural analogue for long-term low carbon steel dissolution is probably the alteration of pyrite, FeS_2, under oxidizing conditions. Pyrite oxidation is the process that generates acid mine drainage (Langmuir 1997, pp. 457 to 461) producing pH values from 2 to 5 (Drainage from coal mines show the same pH range for the same reason). There are significant differences though, the most important being that the Fe/S ratio in pyrite is orders of magnitude smaller than it is in low carbon steel. Since S oxidation produces acid, but Fe oxidation does not, this means that pH values observed in acid mine drainage would tend to be lower than those expected in the waste form. (Also the presence of alkalinity-producing glass dissolution reactions in some waste forms will drive pH higher.) The inverse connection between S content and pH in natural waters has been noted by Langmuir (1997, p. 457). Because of the predominance of iron, the principal degradation product will be some form of iron oxide or hydroxide. In either case, the reaction with acid can be characterized as dissolution of the solid with the production of Fe^{3+} and water, as in:

$$Fe_2O_3 + 6H^+ \rightarrow 2Fe^{3+} + 3H_2O$$

Addition of acid, e.g., from the oxidation of reduced sulfur, will tend to be neutralized by the iron oxide or hydroxide. Conversely, addition of alkali will be neutralized by the precipitation of the iron. Thus, over some moderate range of iron concentrations, these systems will behave as

buffers. The range is limited by the amount of ferric solid (or saturation in another ferric solid, such as ferric sulfate). The supply of dissolved iron is limited and would be depleted by excessive addition of alkali. The effective buffering range can be seen by examining Figures 12.8 and 12.10 in Langmuir (1997) to lie in the general range of pH 2 to 4 for $Fe(OH)_3$. For FeOOH the range shifts to lower pH values because of its greater thermodynamic stability. Again, since the iron to sulfur ratio is so high in low carbon steel, acidity production from sulfur oxidation below pH 3 is counteracted by acidity consumption from iron oxidation. Note lastly, that many of the reactions in the Fe-S-O-H system are microbiologically mediated. Consequently, there is likely to be a strong kinetic component to any estimations of pH control in natural systems.

For the purposes of model validation, it is sufficient to demonstrate that natural waters having pH values below 3 are rare, and below 2 exceedingly so (Langmuir 1997, pp. 410 to 411) and tend to form due to oxidation of sulfur–sometimes in the presence of fumaroles. In other words, because the conditions that would favor pH less than 3 (low acid-buffering capacity–Fe, and high S) are absent in the in-package chemistry model, the lower limit of pH approximately 3 estimated by the in-package chemistry model is corroborated by natural observations documented in the peer-reviewed literature. Moreover, this, combined with satisfaction of Level I criteria (a) through (f), provides broad support for a medium level of confidence in this feature of the in-package chemistry model. On the basis of meeting the criteria for this feature, the level of confidence has been met.

7.3 PRODUCTION OF HIGH IONIC STRENGTH SOLUTIONS

Is the production of high ionic strength solutions consistent with observations documented in the technical literature? High ionic strength solutions are predicted to occur at high pH in the in-package chemistry model and in nature, primarily because such solutions in contact with atmospheric CO_2 tend to have high levels of high charge carbonate species (Morel and Hering 1993, Chapter 3; Stumm and Morgan 1996, Chapter 3):

$$CO_2 + H_2O \leftrightarrow CO_3^{-2} + 2H^+$$

For example, a pH 10 solution in equilibrium with 10^{-3} atm of CO_2 (the in-package chemistry model carbon dioxide level in the waste package) can be roughly estimated to have an ionic strength of at least 0.45 (ignoring activity coefficient effects) corresponding to $10^{-0.7}$ M HCO_3^-, 0.1 M CO_3^{2-} with Na^+ as the charge-balancing cation (Stumm and Morgan 1996, Chapter 3). At the same time, cations such as Na^+ produced by glass dissolution, and Cs^+, precipitate from natural waters only when they become highly concentrated, as in evaporative lakes (Rai and Zachara 1984), and, therefore accumulate in solution, raising the ionic strength. The closest natural analogue to the modeled situation are alkali lakes that have high pH and are exposed to the atmosphere ($pCO_2 = 10^{-3.5}$). An example of this is Alkali Valley, Oregon, which has a pH of 10.1 and an ionic strength that exceeds 4 M (Drever 1982, p. 206). To summarize, the close linkage between extensive degradation of waste form and high ionic strengths is predicted to be most apparent when glass degradation produces high pH solutions. The high salt content of high pH solutions is corroborated by textbook documentation and natural observations documented in the peer-reviewed literature. A medium level of confidence in this feature of the in-package chemistry model is therefore justified based on both the independent corroboration from the

technical literature and satisfaction of Level I criteria (a) through (f). On the basis of meeting the criteria for this feature, the level of confidence has been met.

7.4 SUMMARY

To summarize, the in-package chemistry model is a numerical titration of water with acid-producing solids (steel components), and alkali-producing solids (glass). The outputs are time-dependent solution pH and ionic strength trajectories. Documenting that these trajectories are within the bounds of pH values and ionic strengths observed in natural situations, as documented in the peer-reviewed literature, where similar processes prevail is critical to model validation of the in-package chemistry model. Specifically, achieving a medium level of confidence requires documenting: (1) production of low-pH waters by steel degradation; (2) production of high-pH waters by glass degradation; and (3) the accumulation of dissolved salts with prolonged waste form degradation, in addition to satisfying Level I criteria (a) through (f). The evidences specifically enumerated above are believed collectively to provide broad justification for assignment of a medium level of confidence to the in-package chemistry model. The validation of in-package chemistry model meets the requirements for implementation in TSPA-LA, and does not require any further validation.

8. RESULTS AND CONCLUSIONS

The results of the in-package chemistry model are the in-package chemistry model abstractions, which are used by the Performance Assessment Project. The in-package chemistry model abstraction simplifies the detailed complex time-dependent chemistry into response surfaces and parameter distributions for the in-package chemical parameters that are to be directly implemented in the TSPA-LA.

The following subsections outline the chemical parameters, the methods and reasoning used in abstracting the parameters, the abstractions themselves, and the recommended limits of the abstractions.

8.1 COMMERCIAL SPENT NUCLEAR FUEL WATER VAPOR CONDENSATION IN-PACKAGE CHEMISTRY MODEL ABSTRACTION

For TSPA-LA the CSNF water vapor condensation model abstractions should be implemented when water vapor enters a CSNF waste package, condenses, and then reacts with the waste package components. This is a non-dripping model. There is no flux dependence in the water vapor condensation model abstractions since water does not exit the waste package.

8.1.1 Commercial Spent Nuclear Fuel Water Vapor Condensation pH Abstraction

Figure 17 displays the pH profiles and abstraction for the non-dripping water vapor condensation model for CSNF packages. Two time periods are apparent based on the sharp break in pH (0 to 1000 and 1000 to 20,000 years), and for the purpose of the abstraction, an additional transition time period was included. This transitional period (450 to 1000 years) accounts for delays in the pH response which could result from variation in the metal alloy corrosion rates (Section 6.7), and uses the minimum pH from the first period and the maximum pH from the third period as limits.

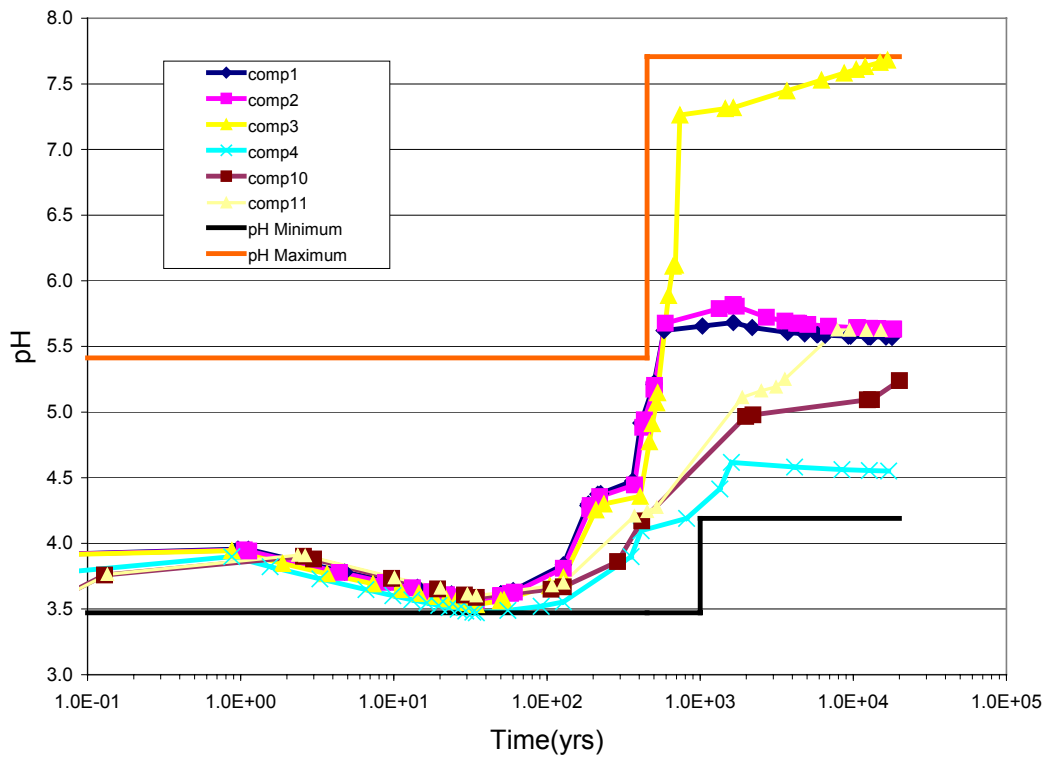

DTN: MO0307SPAIPCHM.001

Figure 17. Non-Dripping Commercial Spent Nuclear Fuel Water Vapor Condensation pH Abstraction

Note that comp5 through comp9 were not included in the abstraction because those simulations did not contain CSNF as a reactant.

In the TSPA-LA, for non-dripping CSNF, the pH should be uniformly sampled between the minimum and maximum values for the three time periods listed in Table 57. At 25°C a uniform uncertainty range of -0.5 to 0.5 pH units should be uniformly sampled and added to the sampled pH. This one pH unit uncertainty envelope accounts for variation in the EQ6 input parameters (Section 6.7). At temperatures other than 25°C a uniform uncertainty range of -2 to 2 pH units should be uniformly sampled and added to the sampled pH. The pH limits are 1 and 12, i.e., if the abstracted pH with included uncertainty is less than pH = 1, or greater than pH = 12, then the pH should be set to the limiting value.

8.1.2 Commercial Spent Nuclear Fuel Water Vapor Condensation Ionic Strength Abstraction

In an attempt to provide realistic interpretations of the ionic strength data for use in abstractions that are fed to total system performance assessment a cumulative distribution approach has been taken in abstracting this information. This approach uses the knowledge that colloids are not stable above ionic strength values of 0.05 molal, and combines the time functionality of the ionic strength as a means to assign probabilities to ionic strength ranges.

Table 57. Non-Dripping Commercial Spent Nuclear Fuel pH Abstraction

	0 - 450 years		450 to 1000 years		1000 to 20,000 years	
	Minimum	**Maximum**	**Minimum**	**Maximum**	**Minimum**	**Maximum**
Comp1	3.58	5.41	N/A	N/A	5.21	5.68
Comp2	3.57	5.41	N/A	N/A	4.94	5.82
Comp3	3.53	5.41	N/A	N/A	4.77	7.71
Comp4	3.47	5.41	N/A	N/A	4.19	4.62
Comp10	3.80	5.41	N/A	N/A	4.97	5.24
Comp11	3.82	5.41	N/A	N/A	4.24	5.63
Distribution	uniform		uniform		uniform	
Minimum	3.47	N/A	3.47		4.19	N/A
Maximum	N/A	5.41		7.71	N/A	7.71

DTN: MO0307SPAIPCHM.001

Figure 18 displays the ionic strength profiles for the non-dripping CSNF ensemble cases. The ionic strength steadily increases for approximately the first 40 years for all of the ensembles, and from 40 to 20,000 years the ionic strength is stable for most of the ensembles. Therefore, the abstraction will be divided into two periods, 0 to 40 years, and 40 to 20,000 years.

To generate realistic abstractions of ionic strength, criteria or break points for each period, were set to ensure that the cumulative distributions best reflected the model output. For example, in all cases where a cumulative distribution abstraction was implemented the minimum and maximum ionic strength for the given time period was used to set the lower and upper limits of the distribution. Additionally, the upper stability limit for colloids, 0.05 molal, was used because this value provides the cutoff for colloids. One other value, 0.01 molal, is sometimes used for the first period of the abstraction because the ionic strength is usually above 0.01 for the greater duration of the period.

Inspection of Figure 18 reveals that the ionic strength increases to greater than 0.01 molal between about one and three years, or the probability of the ionic strength being less than 0.01 molal at any point in time (between 0 and 40 years) is about 2 in 40, or 5 percent. Likewise, the probability of the ionic strength being less than 0.05 molal is about 14 in 40 or 35 percent, and finally the probability of the ionic strength being less than 0.21 (the upper limit for the 0 to 40 year period) is 100 percent.

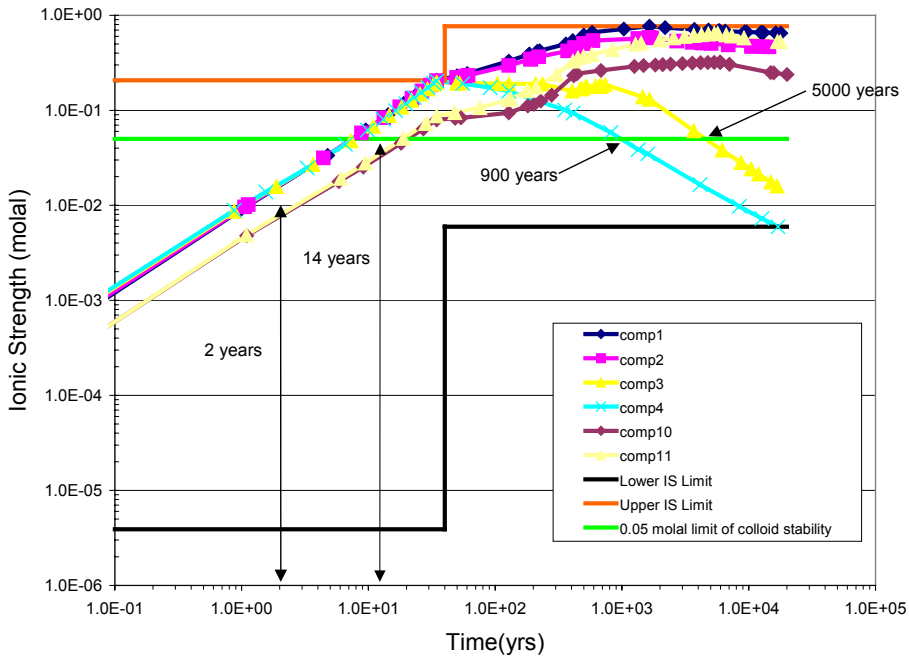

DTN: MO0307SPAIPCHM.001

Figure 18. Non-Dripping Commercial Spent Nuclear Fuel Water Vapor Condensation Ionic Strength Abstraction

For the second period from 40 to 20,000 years, four of the six simulations maintain ionic strengths greater than 0.05 molal for the entire period, while comp3 and comp4 fall below 0.05 molal at 5000 and 900 years, respectively. For a total duration of 6 × 20,000 years = 120,000 years, only 5000 to 20,000 years and 900 to 20,000 years, or 15,000 + 19,100 = 34,100 years are below the 0.05 molal value. Therefore, the probability of the ionic strength being less than 0.05 molal is 34,100/120,000 = 28 percent, and the probability of the ionic strength being less than 1.02 (the upper limit for the period) is 100 percent.

The cumulative distributions for ionic strength for the CSNF water vapor condensation model for use in TSPA-LA are recorded in Table 58.

Table 58. Non-Dripping Commercial Spent Nuclear Fuel Ionic Strength Cumulative Distribution Parameters

Time Period Post WP Breach (years)	Ionic Strength (molal)	Probability
0 to 40	3.9E-06	0.0
	0.01	0.05
	0.05	0.35
	0.21	1.0
40 to 20,000	6.4E-03	0.0
	0.05	0.28
	1.02	1.0

DTN: MO0307SPAIPCHM.001

For TSPA-LA the ionic strength should be sampled using the information in Table 58, and uncertainty should assigned to the sampled value. At 25°C a uniformly sampled uncertainty value from the range of -0.6 to 0.6 (Section 6.7) multiplied by the sampled value should be added to the sampled value. At temperatures other than 25°C, a uniformly sampled uncertainty value from the range of –0.99 to 0.99 multiplied by the sampled value should be added to the sampled value.

$$\text{Ionic strength} = IS_{sampled} + (Uncertainty_{sampled} \times IS_{sampled})$$

For example, using fictitious values, if the sampled ionic strength (IS) value is 0.72, and the sampled uncertainty is -0.04, then the ionic strength should be:

$$IS = 0.72 + (-0.04 \times 0.72)$$

$$= 0.69$$

8.2 COMMERCIAL SPENT NUCLEAR FUEL SEEPAGE DRIPPING MODEL IN-PACKAGE CHEMISTRY MODEL ABSTRACTION

For TSPA-LA the CSNF seepage dripping model abstractions should be implemented when seepage water enters a commercial spent nuclear fuel waste package and reacts with the waste package components; this is a dripping model. The seepage dripping model abstractions are organized based on parameter and temperature.

8.2.1 Commercial Spent Nuclear Fuel Seepage Dripping Model 25°C pH Abstraction

The pH profiles for the CSNF seepage dripping model are displayed in Figure 19 together with time divisions for the abstraction. The criteria used for abstraction are listed in Table 59. The time periods and the applied pH criteria were chosen based on the observed pH trends and the role of the reactants during that period. For example, during period 1 in Figure 19 all of the pH profiles achieve a minimum by 50 years, the time at which the A516 is depleted, thus the time division is set at 50 years and pH criteria are set at the minimum.

A brief discussion of the procedure used to generate the pH response surfaces will be provided using Period 1 for the CSNF seepage dripping model at 25°C as an example.

The criteria in Table 59 were chosen because they best represent the pH trend for the given time period. The minimum pH was used for the first period because the pH was low for the greatest amount of time during that period, where the log time scale exaggerates the early time pH trends even though the duration of these trends was short. The average pH was used for the second time period because this period can be characterized as transitional and the average best captures this trend. Finally, the third and longest duration period is characterized by stabilized pH, where the average was used again because it provided the best representation of the model output. Section 8.8 provides a discussion of the abstraction validation, and the Figures II-3 and II-5 display the CSNF pH abstractions at 25 and 50°C, respectively, plotted together with the model output.

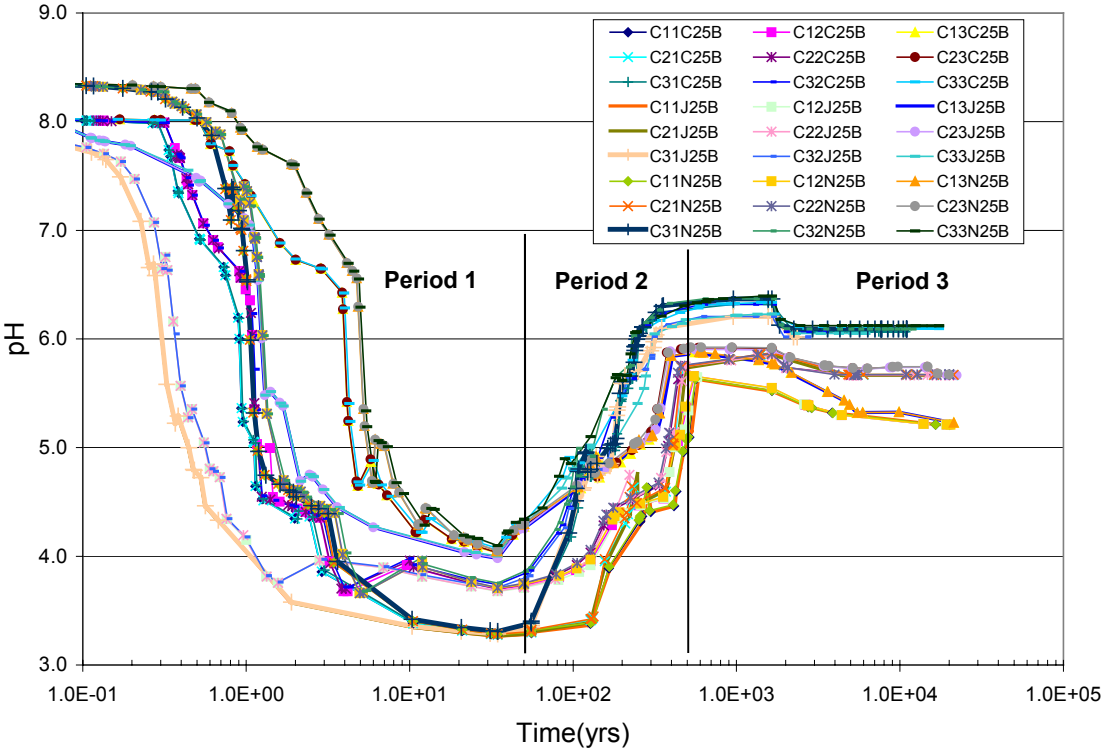

DTN: MO0307SPAIPCHM.001

Figure 19. Seepage Dripping Model pH Profiles for Commercial Spent Nuclear Fuel at 25°C, Showing the Three Time Periods of the Abstraction

Table 59. Criteria Used to Define the pH for Each Abstracted Time Period

Period	Time Period (years post waste package breach)	pH Criteria[a]
1	0 to 50	Minimum
2	50 to 500	Average
3	500 to 20,000	Average

NOTE: [a] pH criteria is the value used for each scenario to generate a point on the response surface.

The pH values for each flux/fuel exposure scenario representing each time period were compiled into three matrices in Microsoft Excel so that a response surface, since there were two independent variables, could be generated. For three-dimensional response surfaces three data columns were specified in Microsoft Excel (Table 60), where x_1 = water flux, x_2 = log fuel exposure, and y = pH, and the regression wizard was used from the "Data Analysis" – "Tools" menu tree to fit a 3-dimensional plane to the data. The output consisted of the coefficients of the equation of the plane and various goodness-of-fit statistical parameters (Table 61). Only the input matrix for the 0 to 50 year time period is included in the text, the matrices for the other time periods are included in DTN: MO0307SPAIPCHM.001.

Table 60. Input Matrix for the Commercial Spent Nuclear Fuel Seepage Dripping Model, 0 to 50 year pH Response Surface

CSNF pH Abstraction, 0 to 50 years			
EQ6 Root File Name (*.6i)	**Flux(l/yr)**	**Log (fuel exposure)**	**Minimum pH**
C11C25	0.15	-2.00	3.28
C12C25	0.15	-1.0	3.68
C13C25	0.15	0.0	4.03
C21C25	1.5	-2.0	3.28
C22C25	1.5	-1.0	3.70
C23C25	1.5	0.0	4.03
C31C25	15	-2.0	3.30
C32C25	15	-1.0	3.72
C33C25	15	0.0	4.07
C11J25	0.15	-2.00	3.26
C12J25	0.15	-1.0	3.68
C13J25	0.15	0.0	4.03
C21J25	1.5	-2.0	3.27
C22J25	1.5	-1.0	3.68
C23J25	1.5	0.0	3.98
C31J25	15	-2.0	3.29
C32J25	15	-1.0	3.71
C33J25	15	0.0	4.00
C11N25	0.15	-2.00	3.28
C12N25	0.15	-1.0	3.66
C13N25	0.15	0.0	4.05
C21N25	1.5	-2.0	3.28
C22N25	1.5	-1.0	3.66
C23N25	1.5	0.0	4.05
C31N25	15	-2.0	3.31
C32N25	15	-1.0	3.68
C33N25	15	0.0	4.10

DTN: MO0307SPAIPCHM.001

Note that the minimum, maximum, and average pH values for the time period were calculated in Microsoft Excel using either the "MIN," "MAX," or "AVERAGE" intrinsic function, respectively, for the pH values in a given time period. Note that minimum pH for the 0 to 50 year post breach is 3.3, this is also the minimum pH for all of the 25°C simulations for the entire 20,000 year model period.

Table 61 lists the pH relationships for the three time periods. The input matrices and the output data can be found in Attachment I (Microsoft Excel Spreadsheet CSNF_SDM_25.xls in DTN: MO0307SPAIPCHM.001).

Table 61. Total System Performance Assessment Input pH Input Parameters for the Response Surfaces at 25°C

$Z = y_o + ax + by$[a]				
Period	**y_o**	**a**	**b**	**R-Squared**
1	4.04	1.86E-03	3.78E-01	0.99
2	4.71	4.80E-02	2.58E-01	0.78
3	5.57	4.25E-02	5.74E-02	0.82

DTN: MO0307SPAIPCHM.001

NOTE: [a]Z = pH, × = water flux (l/yr), y =Log_{10} (Fuel Exposure (fractional value)), y_o, a, and b are coefficients of the equation.
A uniform uncertainty distribution of -0.5 to 0.5 should be added to the calculated pH values.

As the seepage flux increases, the residence time of water in a waste package decreases, which lowers the potential for reaction of that water with the waste package components. Meaning that at some upper limit of flux, seepage will enter and exit a waste package with virtually no alteration of its original composition. This upper threshold is related to the ratio of seepage flux to the kinetic rate coefficient of the most reactive reactant. A516 has both a high corrosion rate and a strong effect on the chemistry, so attempts have been made using sensitivity analyses to determine this upper flux limit by increasing the seepage flux until there is little change in the effluent chemistry. Attachment II "CS_Sensitivity.xls" shows that only minimal reaction of seepage with A516 occurs at 1000 l/yr, therefore, this is the process model limiting flux.

Table 62 provides the limits of seepage flux and fuel exposure for the regression equations in Table 61. Should the TSPA-LA seepage flux exceed the upper limit in Table 62, then the pH should be set to a constant value of 8.3, the maximum pH in Figure 19. Note that even at the limits of the abstraction the uncertainty should still be applied.

The possibility exists that in the TSPA-LA model runs the flux and fuel exposure could be less than the minimum values in Table 62. If the flux is lower than 0.15 l/yr then the pH should be calculated using 0.15 l/yr and the uncertainty range should be uniformly sampled and expanded to -1.0 to 1.0 pH units. The additional uncertainty will account for pH variations in the low flux scenarios. If the fuel exposure falls below the minimum value of 0.01, then the pH should be calculated using 0.01, and the -0.5 to 0.5 sampled uncertainty range should be applied. At low values of fuel exposure the CSNF has virtually no influence on the in-package chemistry, therefore, no additional uncertainty is required. If the both the fuel exposure and water flux fall below the minimum values, 0.01 and 0.15 l/yr, respectively, then the expanded uncertainty range of -1.0 to 1.0 pH units should be applied.

Table 62. Flux and Fuel Exposure Limits for the Commercial Spent Nuclear Fuel Seepage Dripping Model 25°C pH Abstraction

Period	**Flux Limits (l/yr)**		**Fuel Exposure Limits**	
	Lower	**Upper**[a]	**Lower**	**Upper**[a]
1	0.15	1000	0.01	1.0
2	0.15	75	0.01	1.0
3	0.15	70	0.01	1.0

NOTE: [a]Upper Limit pH = 8.3

8.2.2 Commercial Spent Nuclear Fuel Seepage Dripping Model 50°C pH Abstraction

The method outlined in Section 8.2.1 for the generation of pH response surfaces at 25°C was also applied to the 50°C abstractions. The same time periods and pH criteria were used for the 50°C abstractions as they are listed in Table 59. The pH matrices for each time period and the statistical output for the regression analyses are contained in Attachment I in "CSNF_SDM_50.xls."

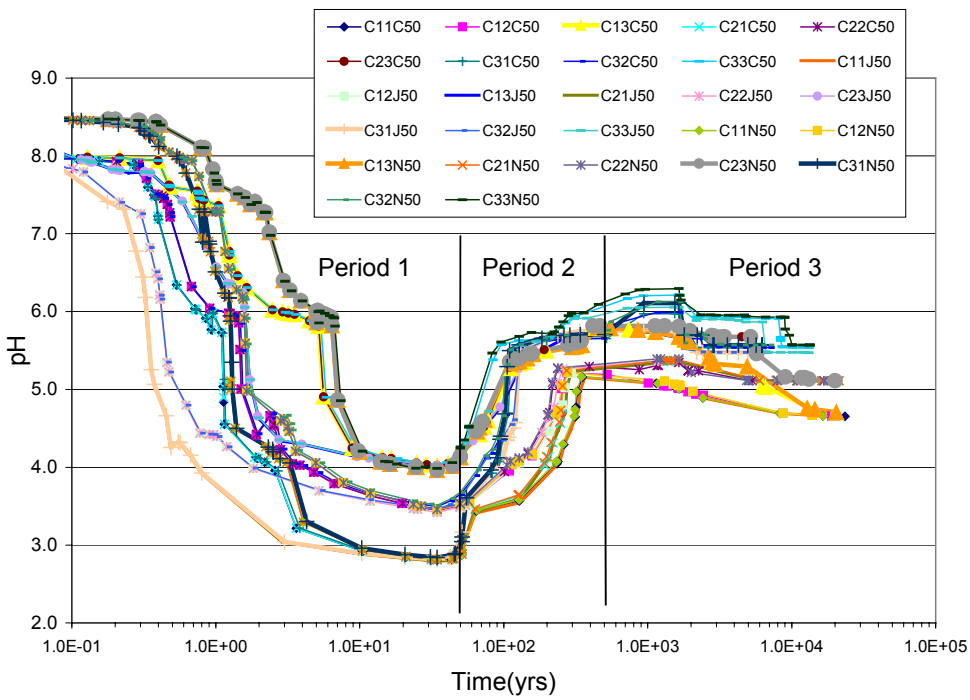

DTN: MO0307SPAIPCHM.001

Figure 20. Seepage Dripping Model pH Profiles for Commercial Spent Nuclear Fuel at 50°C, Showing the Three Time Periods of the Abstraction

The minimum pH for the 50°C CSNF simulations is 2.8, and occurs during the first 50 years post breach. Table 63 contains the TSPA-LA input parameters for the 50°C pH response surfaces.

Table 63. Total System Performance Assessment Input pH input Parameters for the Response Surfaces at 50°C

$Z = y_o + ax + by^a$				
Period	**y_o**	**a**	**b**	**R-Squared**
1	4.01	2.05E-03	5.97E-01	1.00
2	4.97	2.61E-02	4.61E-01	0.89
3	5.61	4.37E-02	2.30E-01	0.83

MO0307SPAIPCHM.001

NOTE: [a]Z = pH, × = water flux (l/yr), y =Log_{10} (Fuel Exposure (fractional value)), y_o, a, and b are coefficients of the equation.

A uniform uncertainty distribution of -0.5 to 0.5 should be added to the calculated pH values.

Table 64 provides the limits for seepage flux and fuel exposure for the regression equations in Table 63. Should the TSPA-LA seepage flux exceed the upper limit in Table 64, then the pH should be set to a constant value of 8.5, the maximum pH in Figure 20. Note that even at the limits of the abstraction the uncertainty should still be applied.

The possibility exists that in the TSPA-LA model runs the flux and fuel exposure could be less than the minimum values in Table 64. If the flux is lower than 0.15 l/yr then the pH should be calculated using 0.15 l/yr and the uncertainty range should be uniformly sampled and expanded to -1.0 to 1.0 pH units. The additional uncertainty will account for pH variations in the low flux scenarios. If the fuel exposure falls below the minimum value of 0.01, then the pH should be calculated at 0.01 with no additional uncertainty required, i.e., the -0.5 to 0.5 sampled range should be used. At low values of fuel exposure the CSNF has virtually no influence on the in-package chemistry, therefore, no additional uncertainty is required. If the both the fuel exposure and water flux fall below the minimum values, 0.01 and 0.15 l/yr, respectively, then the expanded uncertainty range of -1.0 to 1.0 pH units should be applied.

Table 64. Flux and Fuel Exposure Limits for the Commercial Spent Nuclear Fuel Seepage Dripping Model 50°C pH Abstraction

Period	Flux Limits (l/yr)		Fuel Exposure Limits	
	Lower	Upper[a]	Lower	Upper[a]
1	0.15	1000	0.01	1.0
2	0.15	135	0.01	1.0
3	0.15	65	0.01	1.0

NOTE: [a] Upper limit pH = 8.5

The flux limits provided in Table 62 and 64 differ because of the difference in the pH range of the 25°C versus 50°C simulations.

8.2.3 Commercial Spent Nuclear Fuel Seepage Dripping Model pH Temperature Dependence

Figure 21 shows the pH histories of simulations executed over the temperature range from 15° to 90°C using the initial input of C22C25. The CSNF rate law coefficients were recalculated for this temperature range. These sensitivity analyses show that for CSNF (Attachment II, "CS_sensitivity.xls") the pH varies systematically with temperature, this however does not legitimize the abstraction up to 90°C without increasing the uncertainty with the temperature. The high-temperature simulations shown in Figure 21 do not account for the effects of evaporation on the composition of the seepage, which would increase the ionic strength of the reacting solution while decreasing the flux out of the waste package. While the general trends displayed in Figure 21 for the high-temperature runs are expected to be preserved, the level of uncertainty is increased compared to the low-temperature simulations.

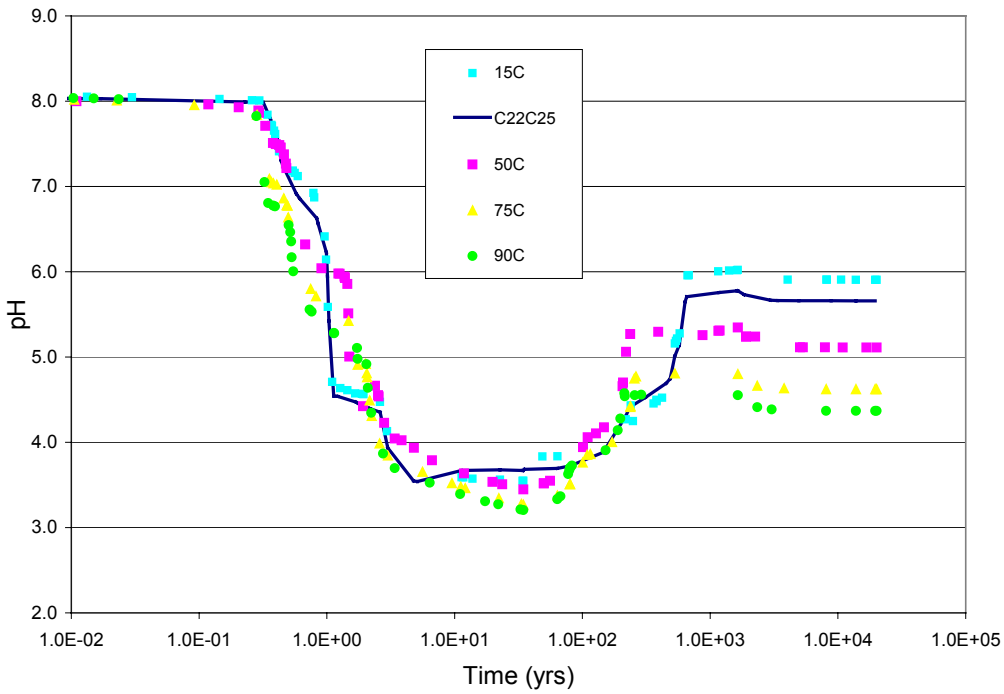

Source: Microsoft Excel Spreadsheet CS_sensitivity.xls in DTN: MO0307SPAIPCHM.001.

Figure 21. Effect of Temperature on the pH of Run C22C25

To implement a temperature functionality into the pH abstraction a linear interpolation should be applied between 25°C and 50°C, this interpolation may be used to extrapolate the pH down to 15°C and up to 95°C. However, it is recommended that the uncertainty range for temperatures greater than 50°C be expanded to -2.0 to 2.0 pH units, sampled uniformly and added to the abstracted pH value. For temperatures above 95°C and below 100°C, the pH calculated at 95°C should be used.

For certain combinations of fuel exposure (clad failure), water flux, and temperature, it may be possible for TSPA to calculate pH values of approximately 2. Likewise if the sampled uncertainty were equal to –2, then the pH would be zero. Therefore, it is necessary to set a lower limit on pH for TSPA purposes, that pH value is 1. If the TSPA calculates a pH value less than one, then TSPA must set the pH equal to one. Likewise the upper limit of pH should be set not to exceed 12.

8.2.4 Commercial Spent Nuclear Fuel Seepage Dripping Model 25°C Ionic Strength Abstraction

The ionic strength abstractions are a hybrid of cumulative distributions and regression curves. The 25°C CSNF seepage dripping model ionic strength abstraction will be presented as an example.

Figure 22 displays the ionic strength profiles for the CSNF seepage dripping model runs at 25°C. The period from 0 to 40 years is characterized by increasing ionic strength and is best

represented by a cumulative distribution type of abstraction. The period from 40 to 20,000 years can be represented as a function, where ionic strength is a function of seepage flux. It should be noted that for the low end seepage flux (0.15 l/yr) the ionic strength exceeds 1 molal, due to the accumulation of aqueous chromium species in the waste package effluent. These high chromium concentrations occur in the EQ6 simulations because there is no chrome bearing mineral phase in the thermodynamic database available to precipitate under the conditions of the simulation. Since the ionic strength abstraction is used strictly by the colloid sub-model in the TSPA-LA and colloidal suspensions are unstable at ionic strength values much less than 1 molal the significance of exceeding the limits of the B-dot activity coefficient equation is diminished.

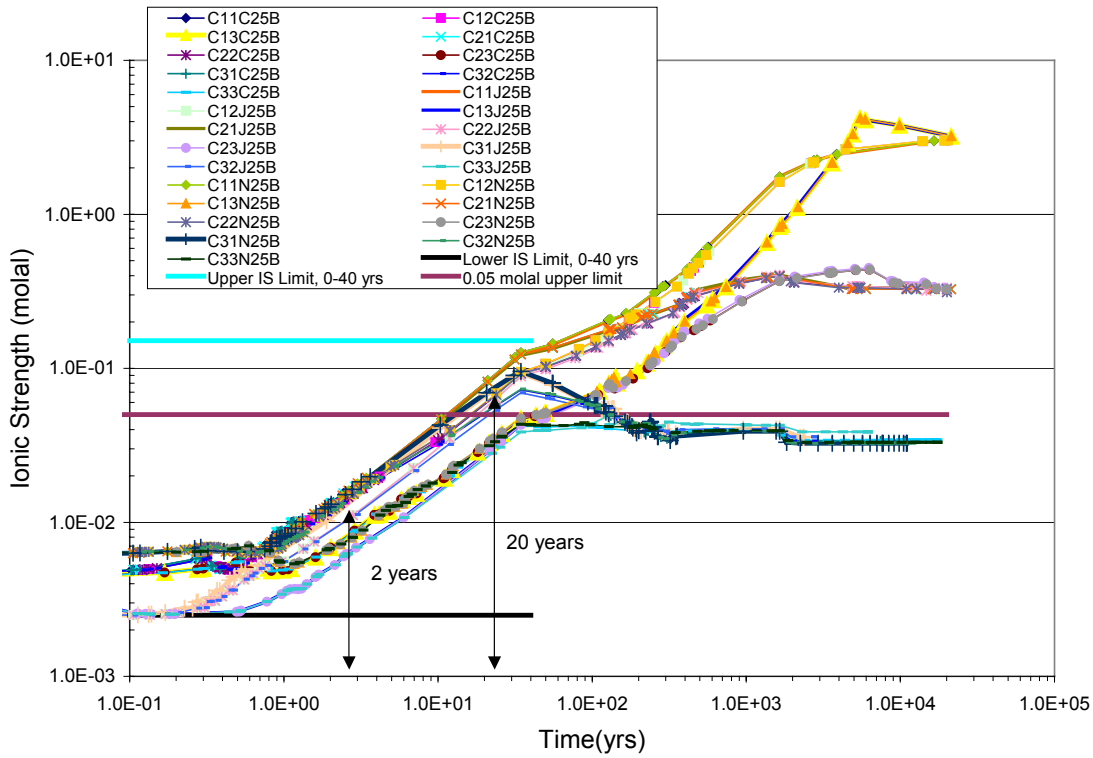

DTN: MO0307SPAIPCHM.001

Figure 22. Commercial Spent Nuclear Fuel Seepage Dripping Model 25°C Ionic Strength Profiles

Table 65 lists the criteria used in setting the ionic strength ranges.

Table 65. Ionic Strength Criteria for the Commercial Spent Nuclear Fuel Seepage Dripping Model Runs at 25°C

Period post WP breach	Ionic Strength Criteria
0 - 40 years	Min, 0.01, 0.05, Max
40 to 20,000 years	Max

Inspection of Figure 22 reveals that the ionic strength increases to greater than 0.01 molal between about one and three years, or the probability of the ionic strength being less than 0.01 molal at any point in time (between 0 and 40 years) is about 2 in 40, or 5 percent. Likewise, the probability of the ionic strength being less than 0.05 molal is about 20 in 40 or 50 percent, and

finally the probability of the ionic strength being less than 0.13 (the upper limit for the 0 to 40 year period) is 100 percent.

Table 66 provides the cumulative distribution of the ionic strength for the period from 0 to 40 years, which should be used as input for TSPA-LA.

Table 66. Commercial Spent Nuclear Fuel Seepage Dripping Model 25°C 0 to 40-year Ionic Strength Cumulative Distribution for TSPA-LA

Time Period post WP Breach (years)	Ionic Strength (molal)	Probability
0 - 40	2.5E-03	0.0
	0.01	0.05
	0.05	0.50
	1.3E-01	1.0

DTN: MO0307SPAIPCHM.001

Figure 23 displays the ionic strength abstraction for the CSNF seepage dripping model at 25°C, for the period from 40 to 20,000 years. This abstraction, and the ionic strength abstractions to follow, were all generated by plotting in Microsoft Excel the maximum ionic strength for the specified period versus the base ten logarithm of seepage flux and then using the "Add Trendline" from the "Chart" submenu to fit the exponential function to the data.

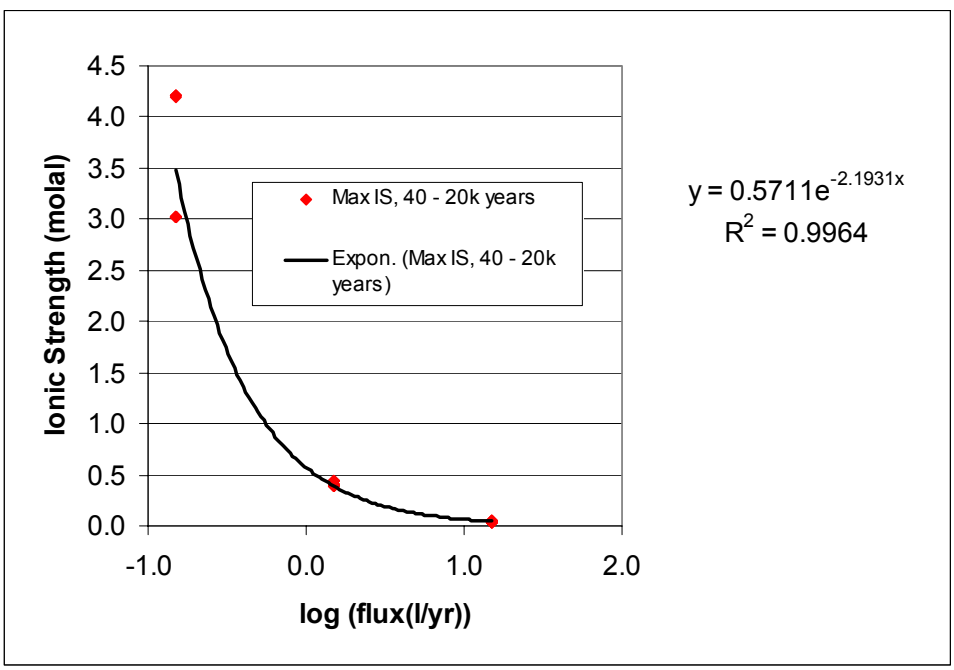

DTN: MO0307SPAIPCHM.001

Figure 23. Commercial Spent Nuclear Fuel Seepage Dripping Model 25°C 40 to 20,000-Year Ionic Strength Abstraction

The ionic strength abstraction for the CSNF seepage dripping model at 25°C from 40 to 20,000 years is given in Table 67.

Table 67. Commercial Spent Nuclear Fuel Seepage Dripping Model 25°C Ionic Strength 40 to 20,000-Year Abstraction

y = aEXP(bx)[a]	
a	**b**
0.5711	-2.1931
R^2	0.9964

DTN: MO0307SPAIPCHM.001

NOTE: [a]y = ionic strength, × = $\log_{10}$(flux(l/yr))

An uncertainty factor such as that applied in Section 8.1.2 should also be used here for TSPA-LA purposes for both the 0 to 40 year and 40 to 20,000 year abstractions. A uniform uncertainty range of -0.6 to 0.6 multiplied by the sampled value should be added to the sampled value. Ionic strength = $IS_{sampled}$ + ($Uncertainty_{sampled}$ × $IS_{sampled}$).

The limits of flux for the abstraction are given in Table 68. The upper flux limit was calculated using the ionic strength of J-13 (Table 54), i.e., at flux values greater than 210 l/yr the abstracted ionic strength would be less than that of the J-13. Note that even at the limits of the abstraction the uncertainty should still be applied.

Table 68. Commercial Spent Nuclear Fuel Seepage Dripping Model 25°C Ionic Strength Flux Limits for 40 to 20,000-Year Abstraction

Flux Limits (l/yr)	
Lower	**Upper[a]**
0.15	210

DTN: MO0307SPAIPCHM.001

NOTE: [a]Upper Limit set by J-13 at 0.0035 molal

If the flux is less than the minimum, then the ionic strength should be evaluated using the lower flux limit from Table 68. Likewise, if the flux is greater than the upper limit, then the ionic strength should be evaluated using the upper limit value from Table 68.

8.2.5 Commercial Spent Nuclear Fuel Seepage Dripping Model 50°C Ionic Strength Abstraction

The CSNF seepage dripping model 50°C ionic strength abstraction takes the same form as the 25°C abstraction.

Table 69. Commercial Spent Nuclear Fuel Seepage Dripping Model 50°C 0 to 40-Year Ionic Strength Cumulative Distribution for TSPA-LA

Time Period post WP Breach (years)	Ionic Strength (molal)	Probability
0 - 40	2.3E-03	0.0
	0.01	0.05
	0.05	0.50
	1.3E-01	1.0

DTN: MO0307SPAIPCHM.001

Table 70. Commercial Spent Nuclear Fuel Seepage Dripping Model 50°C Ionic Strength 40 to 20,000-Year Abstraction

y = aEXP(bx)[a]	
a	b
0.5551	-2.2731
R^2	0.988

DTN: MO0307SPAIPCHM.001

NOTE: [a]y = ionic strength, × = $\log_{10}$(flux(l/yr)).

An uncertainty factor such as that applied in Section 8.1.2 should also be used here for TSPA-LA purposes for both the 0 to 40 year and 40 to 20,000 year abstractions. A uniform uncertainty range of -0.6 to 0.6 multiplied by the sampled value should be added to the sampled value. Ionic strength = $IS_{sampled}$ + ($Uncertainty_{sampled} \times IS_{sampled}$).

The flux limits for the CSNF seepage dripping model 50°C ionic strength abstraction are listed in Table 71.

Table 71. Commercial Spent Nuclear Fuel Seepage Dripping Model 50°C Ionic Strength Flux Limits for 200 to 20,000 Year Abstraction

Flux Limits (l/yr)	
Lower	Upper[a]
0.15	170

NOTE: [a]Upper Limit set by J-13 at 0.0035 molal

If the flux is less than the minimum, then the ionic strength should be evaluated using the lower flux limit from Table 71. Likewise, if the flux is greater than the upper limit, then the ionic strength should be evaluated using the upper limit value from Table 71.

8.2.6 Commercial Spent Nuclear Fuel Seepage Dripping Model Ionic Strength Temperature Dependence

Figure 24 shows the ionic strength results of EQ6 simulations at progressively higher temperatures. The results plotted in Figure 24 show that temperature had a minor influence on ionic strength. Although evaporation from the interior of the waste package is not expected to be great, due to high humidity in the waste package interior, evaporation could still influence the

ionic strength as the temperature increases. Therefore, fully decoupling the temperature and ionic strength could result in misleading ionic strength values.

For TSPA-LA at temperatures from 15°C to 50°C the 0 to 40 year abstraction should use the cumulative distribution in Table 69 (50°C abstraction), which covers a slightly broader range of ionic strength than the 25°C abstraction. For the 40 to 20,000 year abstraction in the same temperature range, a linear relationship should be established between the values calculated using the relationships provided in Tables 67 and 70, honoring the limits of these relationships as defined in Tables 68 and 71. An uncertainty factor such as that applied in Section 8.1.2 should also be used here, for TSPA-LA purposes, for both the 0 to 40 year and 40 to 20,000 year abstractions. A uniform uncertainty range of -0.6 to 0.6 multiplied by the sampled value should be added to the sampled value. Ionic strength = $IS_{sampled} + (Uncertainty_{sampled} \times IS_{sampled})$.

For TSPA-LA, at temperatures greater than 50°C, implementation of a cumulative distribution that encompasses the range of ionic strength values displayed in Figure 22, of 2E-03 to 4 molal, with the following ionic strength – probability pairs: (2E-03, 0), (0.05, 0.33), and (4.0, 1.0). A uniform uncertainty range of -0.6 to 0.6 multiplied by the sampled value should be added to the sampled value. Ionic strength = $IS_{sampled} + (Uncertainty_{sampled} \times IS_{sampled})$.

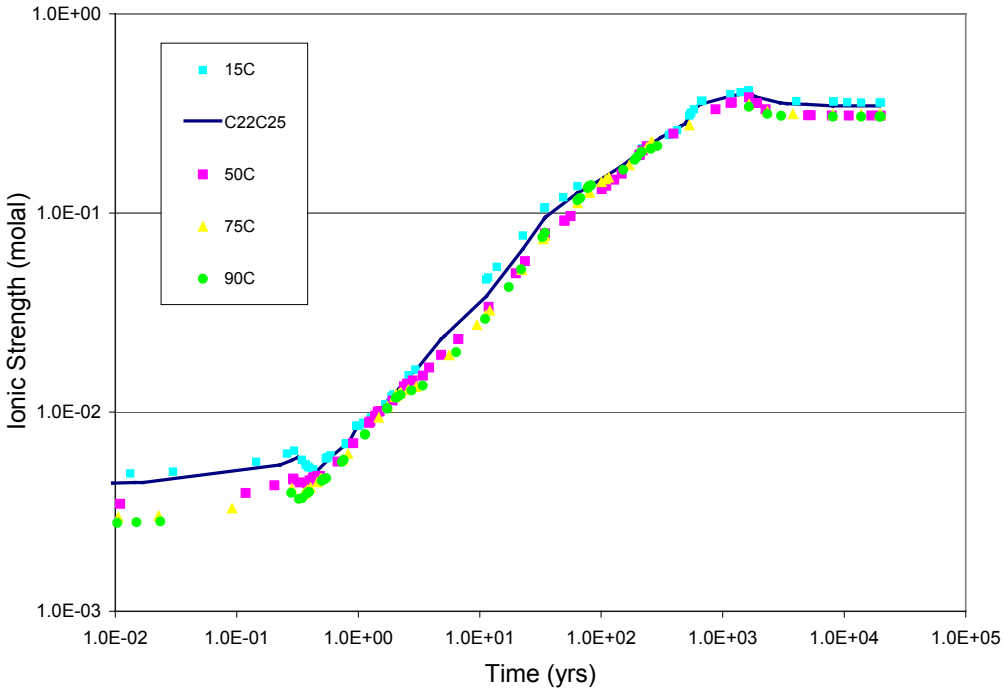

Source: Microsoft Excel Spreadsheet CS_sensitivity.xls in DTN: MO0307SPAIPCHM.001.

Figure 24. Effect of Temperature on the Ionic Strength of Run C22C25

8.2.7 Commercial Spent Nuclear Fuel Seepage Dripping Model 25°C and 50°C Fluoride Abstractions

The fluoride profiles for the 25°C CSNF seepage dripping model simulations are plotted in Figure 25 together with the limits of the abstraction. Note that other than the input seepage compositions, there are no other sources of fluorine in the CSNF waste package. The dip in fluoride concentration at about one year (Figure 25) is the result of fluorapatite precipitation with subsequent dissolution as the concentration recovers to approximately 1E-04 molal. This early fluoride minimum was not considered for the abstraction because it occurs so early, and the minimum of the average fluoride concentrations was set as the lower bound of the abstraction instead.

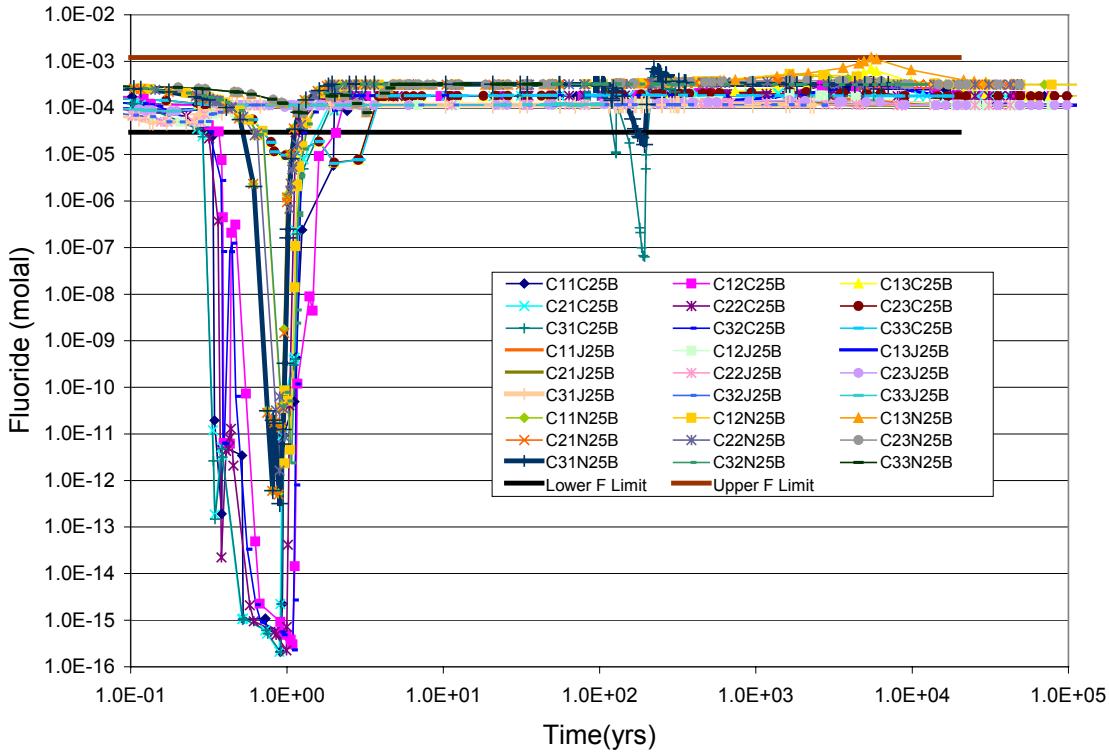

DTN: MO0307SPAIPCHM.001

Figure 25. Commercial Spent Nuclear Fuel Seepage Dripping Model 25°C Fluoride Profiles and Abstraction

If the fluoride abstraction is implemented in TSPA-LA then the fluoride values should be uniformly sampled within the range specified in Table 72. Given that the abstraction covers a wider range than what Figure 25 suggests, it is not necessary to apply an uncertainty value to the sampled fluoride value.

Table 72. Commercial Spent Nuclear Fuel Seepage Dripping Model 25° and 50°C Fluoride Abstraction

Temperature	Lower F Limit	Upper F Limit
Distribution	Uniform	
(°C)	Mol/kg	
25	3.01E-05	1.21E-03
50	1.05E-04	1.83E-03

DTN: MO0307SPAIPCHM.001

Table 72 also provides the range of fluoride concentrations for the CSNF seepage dripping model 50°C abstraction. Like the 25°C fluoride profiles, there is a low concentration dip at early time, which has been omitted from the abstraction. No temperature functionality is included for the fluoride abstraction.

8.2.8 Commercial Spent Nuclear Fuel Seepage Dripping Model 25°C and 50°C Chloride Abstractions

Figure 26 shows the CSNF seepage dripping model 25°C chloride profiles and abstraction limits. The CSNF seepage dripping model 50°C chloride profiles are not plotted because they show the same trends as the 25°C profiles.

Table 73. Commercial Spent Nuclear Fuel Seepage Dripping Model 25° and 50°C Chloride Abstractions

Temperature	Lower Cl Limit	Upper Cl Limit
Distribution	Uniform	
(°C)	Mol/kg	
25	2.01E-04	2.60E-03
50	2.01E-04	3.93E-03

DTN: MO0307SPAIPCHM.001

The chloride abstractions for 25° and 50°C are provided in Table 73. No temperature functionality is provided for the chloride abstractions.

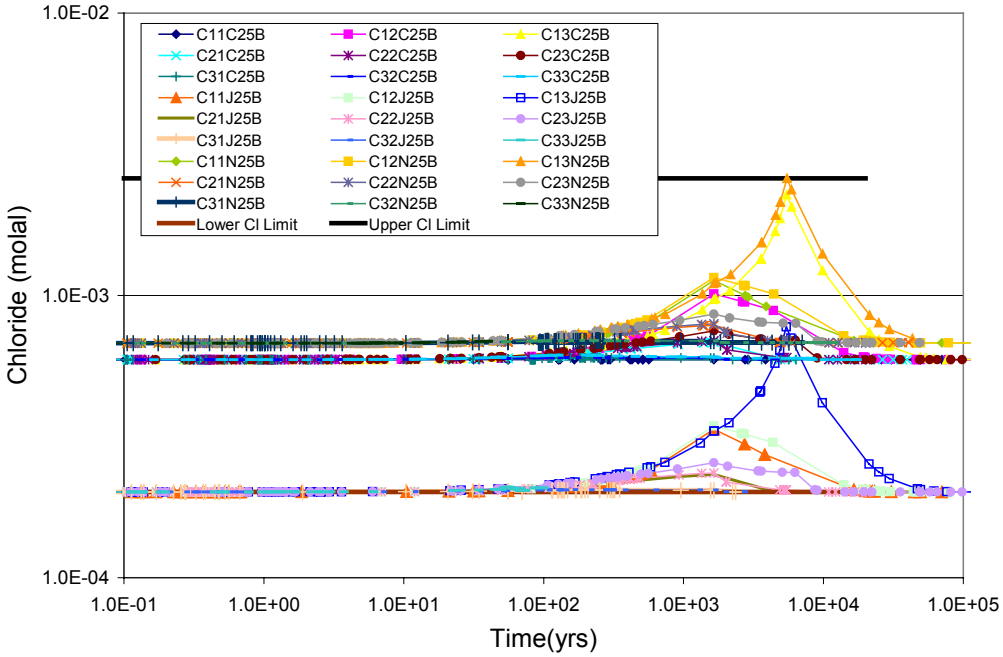

DTN: MO0307SPAIPCHM.001

Figure 26. Commercial Spent Nuclear Fuel Seepage Dripping Model 25°C Chloride Profiles And Abstraction

8.3 CODISPOSED N REACTOR WATER VAPOR CONDENSATION IN-PACKAGE CHEMISTRY MODEL ABSTRACTION

For TSPA-LA the CDNR water vapor condensation model abstractions should be implemented when water vapor enters a codisposal waste package and condenses and reacts with the waste package components-this is a non-dripping model. There is no flux dependence in the water vapor condensation model abstractions since water does not exit the waste package.

8.3.1 Codisposed N Reactor Water Vapor Condensation pH Abstraction

Figure 23 displays the CDNR water vapor condensation model pH profiles and abstraction.

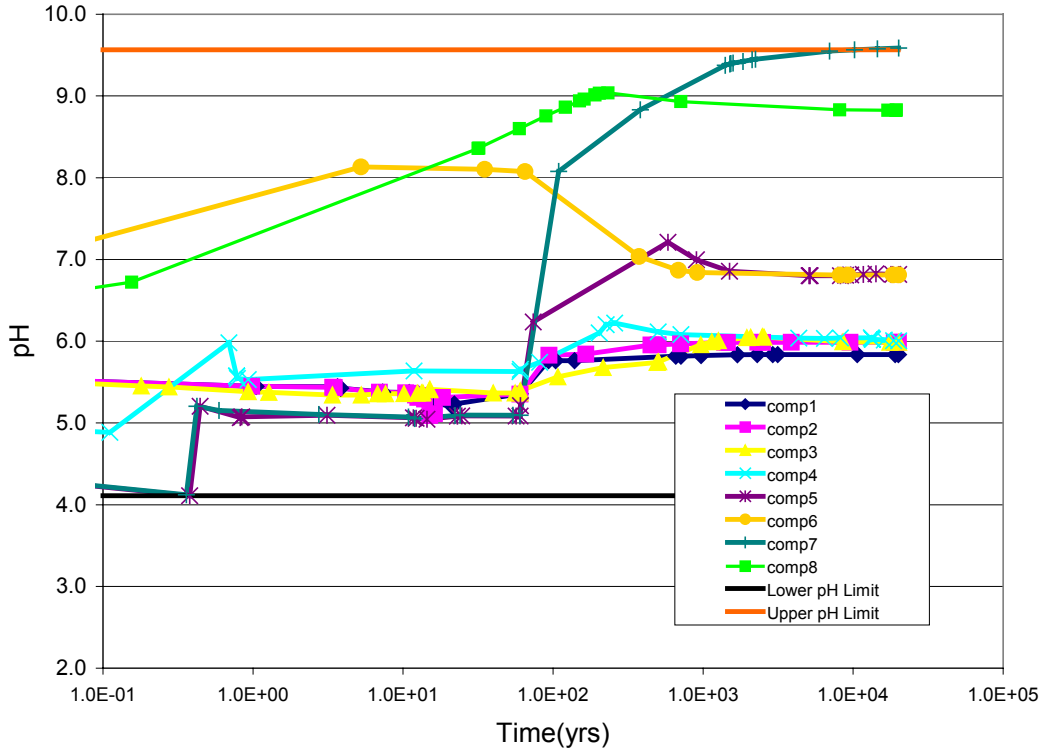

DTN: MO0307SPAIPCHM.001

Figure 27. Codisposed N Reactor Water Vapor Condensation pH Profiles and Abstraction

The pH range in the abstraction is not discretized in time because the relative time when waste package components will interact is unknown. Thus, in TSPA-LA the entire pH range specified in Table 74 should be uniformly sampled, and at 25°C a uniformly distributed uncertainty range of -0.5 to 0.5 should be added to the sampled value of pH. At temperatures other than 25°C a uniform uncertainty range of -2 to 2 pH units should be uniformly sampled and added to the sampled pH. The pH limits are 1 and 12, i.e., if the abstracted pH with included uncertainty is less than pH = 1, or greater than pH = 12, then the pH should be set to the limiting value.

Table 74. Codisposed N Reactor Water Vapor Condensation pH Abstraction

	Minimum pH	Maximum pH
Comp1	5.20	5.84
Comp2	5.09	5.99
Comp3	5.34	6.05
Comp4	4.88	6.22
Comp5	4.11	7.21
Comp6	4.11	7.21
Comp7	4.12	9.56
Comp8	5.41	9.04
TSPA-LA Input Range		
Uniform Distribution		
Maximum		9.56
Minimum	4.11	

DTN: MO0307SPAIPCHM.001.

8.3.2 Codisposed N Reactor Water Vapor Condensation Ionic Strength Abstraction

The ionic strength profiles for the CDNR water vapor condensation model are displayed in Figure 28, as are the break points used in defining the cumulative distribution. The lower limit of the range is not plotted in Figure 28 because it is less than the minimum value of the Y-axis. The ionic strength abstraction for the CDNR water vapor condensation model was broken into three periods due to the large spread in the data, e.g., the profiles cross the 0.05 threshold from 12 to 300 years.

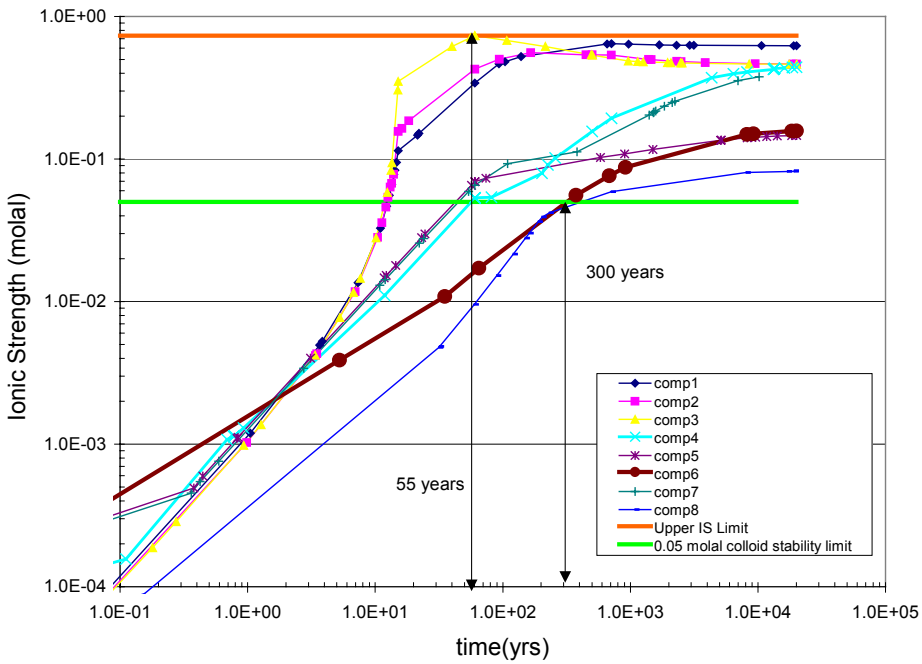

DTN: MO0307SPAIPCHM.001

Figure 28. Codisposed N Reactor Water Vapor Condensation Ionic Strength Profiles and Abstraction

The first period runs from 0 to 55 years, the second period from 55 to 300 years, and the third from 300 to 20,000 years. The probability was calculated using the number of simulations that were below the threshold rather the duration below the threshold. For example, for the 0 to 55 year period, three simulations, comp4, comp5, and comp8 were all less than 0.05 molal, so that the probability of encountering an ionic strength value less than 0.05 molal is 3/8 or 0.38. For the 55 to 300 year period the probability of encountering an ionic strength value between 0.01 and 0.05 molal is 2/8 or 0.25. The parameters for the cumulative distributions for the three periods are listed in Table 75.

Table 75. Codisposed N Reactor Water Vapor Condensation Model Ionic Strength Cumulative Distribution

Time Period post WP Breach (years)	Ionic Strength (molal)	Probability
0 to 55	3.9E-06	0.0
	0.05	0.38
	0.85	1.0
55 to300	0.01	0.0
	0.05	0.25
	0.85	1.0
300 to 20,000	0.05	0
	0.1	0.13
	0.85	1.0

DTN: MO0307SPAIPCHM.001.

An uncertainty factor, as described in Section 8.1.2, should be applied to the CDNR water vapor condensation model ionic strength abstraction. At 25°C a uniformly sampled uncertainty value from the range of -0.6 to 0.6 (Section 6.7) multiplied by the sampled value should be added to the sampled value. At temperatures other than 25°C, a uniformly sampled uncertainty value from the range of –0.99 to 0.99 multiplied by the sampled value should be added to the sampled value. Ionic strength = $IS_{sampled} + (Uncertainty_{sampled} \times IS_{sampled})$.

8.3.3 Codisposed N Reactor Water Vapor Condensation Fluoride Abstraction

Although there is no dissolved fluoride in the water vapor, the HLWG does contain fluorine (Table 9), therefore, a fluoride abstraction is provided for the CDNR water vapor condensation model. Figure 29 displays the fluoride profiles for the CDNR ensembles. The variation in the fluoride concentration (Figure 29) is due to precipitation/dissolution reactions of minor fluoride bearing phases (fluorite and fluorapatite).

Table 76 provides the minimum and maximum fluoride concentrations. The minimum fluoride concentration is set by the incoming water, which by convention, is set to 1E-16 molal. If the fluoride abstraction should be implemented in TSPA-LA, then the range between the minimum and the maximum fluoride values (Table 76) should be uniformly sampled. Since the range to be sampled encompasses 12 orders of magnitude, it is unnecessary to include any further uncertainty on the estimated fluoride concentration.

Table 76. Codisposed N Reactor Water Vapor Condensation Model Fluoride Abstraction

Lower F Limit	Upper F Limit
Minimum	Maximum
(mol/kg)	
1.0E-16	8.3E-04

DTN: MO0307SPAIPCHM.001.

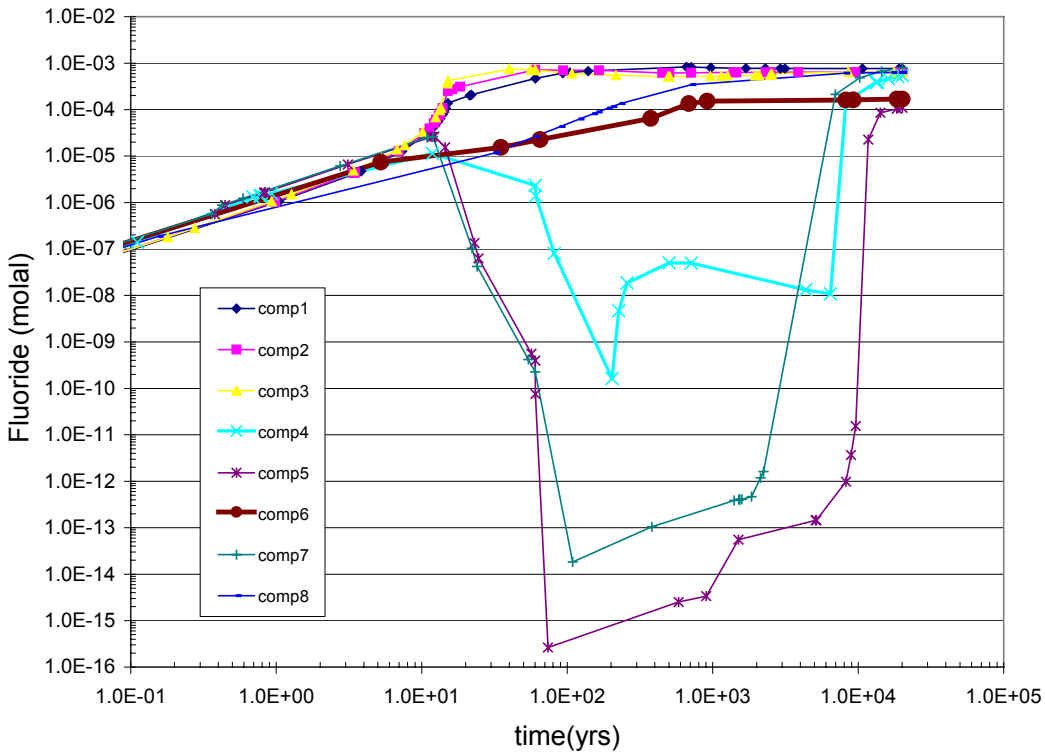

DTN: MO0307SPAIPCHM.001

Figure 29. Codisposed N Reactor Water Vapor Condensation Fluoride Profiles

8.4 CODISPOSED N REACTOR SEEPAGE DRIPPING MODEL IN-PACKAGE CHEMISTRY MODEL ABSTRACTION

In the TSPA-LA model the CDNR seepage dripping model abstractions should be implemented when seepage enters a codisposal waste package, reacts with the waste package components, and then exits the waste package-this is a dripping model.

8.4.1 Codisposed N Reactor Seepage Dripping Model 25°C pH Abstraction

Figure 30 displays the CDNR pH profiles for the seepage dripping model at 25°C, also displayed is the 0 to 60 years pH abstraction range. The pH abstraction was split into two time periods, 0 to 60 years, and 60 to 20,000 years. Since the low end of the pH range for first time period was relatively high (approximately pH = 5.2, Figure 30) compared to that observed for the CSNF (approximately pH = 3.2, Figure 17) a decision was made to not parameterize the early-time CDNR pH abstraction. Instead, the maximum and minimum pH for the 0- to 60-year period was

calculated for each simulation and a range was set. Table 77 provides the minimum and maximum pH values and the values to be uniformly sampled in TSPA-LA. A uniform uncertainty range of -0.5 to 0.5 pH units should be sampled and added to the sampled pH value.

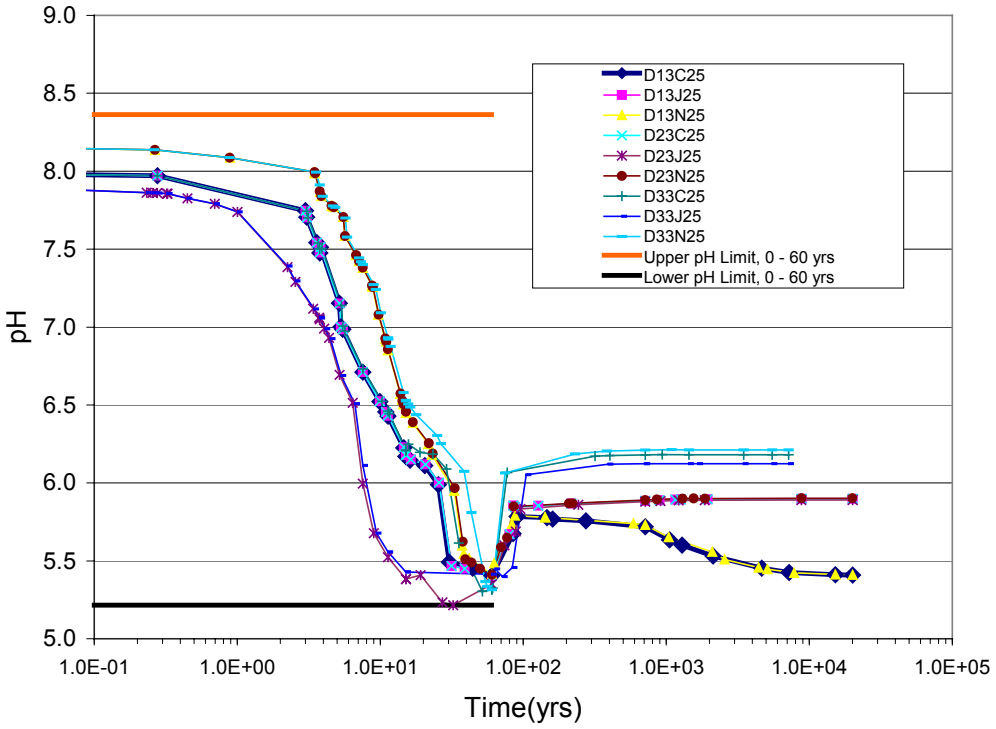

DTN: MO0307SPAIPCHM.001

Figure 30. Codisposed N Reactor Seepage Dripping Model 25°C pH Profiles and 0 to 60 Year Abstraction Limits

Table 77. Codisposed N Reactor Seepage Dripping Model 25°C pH Abstraction, 0 to 60 Years

	Flux (l/yr)	Minimum	Maximum
D13C25	0.15	5.45	8.09
D23C25	1.5	5.40	8.09
D33C50	15	5.30	8.09
D13J25	0.15	5.22	8.09
D23J25	1.5	5.22	8.09
D33J50	15	5.41	8.09
D13N25	0.15	5.41	8.36
D23N25	1.5	5.41	8.36
D33N50	15	5.31	8.36
TSPA-LA Input Range			
Uniform Distribution			
	Minimum	5.22	
	Maximum		8.36

DTN: MO0307SPAIPCHM.001

Figure 30 shows three distinct groups in the pH profiles for the 60 to 20,000 year time period, these groupings are independent of the initial seepage composition but are a function of the flux. Figure 31 is a plot of the stabilized pH versus the $\log_{10}$ of the flux (l/yr), and the regression line. Rather than use the maximum or minimum pH as the guiding criteria the stable pH for the 60- to 20,000-year period was used in generating the abstraction.

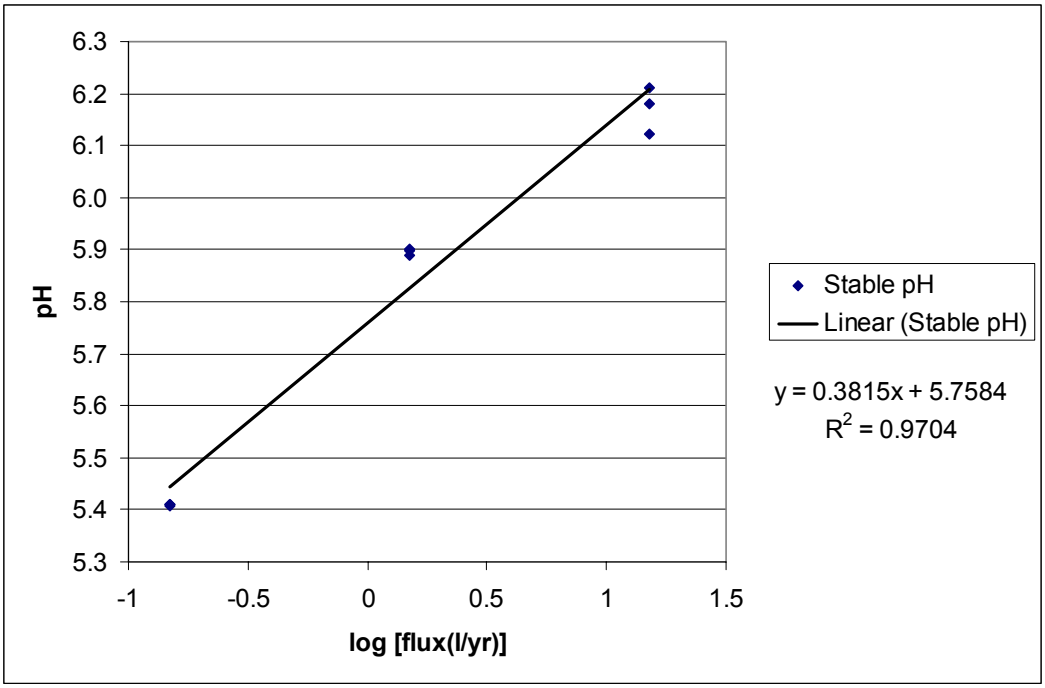

DTN: MO0307SPAIPCHM.001

Figure 31. Codisposed N Reactor Seepage Dripping Model 25°C pH and Abstraction for the 60 to 20,000 Year Period

The pH abstraction (Table 78) was generated by plotting the stabilized pH versus the log10 of the flux and selecting the "Add Trendline" from the "Chart" submenu and picking the type as linear. The results are the regression line, equation and R-squared value displayed in Figure 31. A uniform uncertainty range of -0.5 to 0.5 pH units should be sampled and added to the calculated pH value.

Table 78. Codisposed N Reactor Seepage Dripping Model 25°C pH Abstraction, 60 to 20,000 Years

$y = mx + b$[a]	
m	**b**
0.3815	5.7584
$R^2 = 0.9704$	

DTN: MO0307SPAIPCHM.001.

NOTE: [a]$y = pH$, $\times = \log_{10}(flux(l/yr))$

Examination of Figures 8 and 9 shows that the CDNR water vapor condensation model has the potential to generate pH values near 10. Although the output from the CDNR seepage dripping model (Figure 30) for the 60 to 20,000 year period shows the pH does not exceed approximately 6.3, it is possible that high pH values (8 to 10) could also result from the CDNR seepage dripping model should seepage contact the HLWG and exit the waste package without contacting metal components. This scenario also includes the possibility that a waste package may contain only HLWG, which would have a much greater potential for generating high-pH solutions.

Therefore, to include the possibility of occurrence of high-pH conditions in the TSPA-LA model, a mixed-relationship type abstraction is recommended, where 85 percent probability is assigned to the relationship in Table 78, and 15 percent probability is assigned to the 6 to 11 pH range. The 6 to 11 pH range should be sampled uniformly, and no uncertainty term should be added to this sampled range.

Table 79 provides the flux limits for the pH abstraction. At flux values greater than 1000 l/yr the pH should be set to a constant value of 8.3. The upper flux limit was set by the sensitivity analysis (Attachment II, "CS_Sensitivity.xls") which showed that above 1000 l/yr the seepage chemistry was largely unchanged.

The possibility exists that in the TSPA-LA model runs the flux could be less than the minimum value in Table 79. If the flux is lower than 0.15 l/yr then the pH should be calculated using 0.15 l/yr and the uncertainty range should be uniformly sampled and expanded to -1.0 to 1.0 pH units. The additional uncertainty will account for pH variations in the low flux scenarios.

Table 79. Codisposed N Reactor Seepage Dripping Model 25°C pH Abstraction Flux Limits for 60 to 20,000 Year Abstraction

Flux Limits (l/yr)[a]	
Lower	**Upper**
0.15	1000

NOTE: [a]Upper Limit pH = 8.3

8.4.2 Codisposed N Reactor Seepage Dripping Model 50°C pH Abstraction

The pH profiles for the CDNR seepage dripping model simulations at 50°C are plotted in Figure 32. The 0 to 60 year pH range is provided in Table 80, this range should be sampled for TSPA-LA and an uncertainty range of -0.5 to 0.5 pH units should be sampled and added to the sampled pH value.

Table 80. Codisposed N Reactor Seepage Dripping Model 50°C pH Abstraction, 0 to 60 Years

TSPA-LA Input	
Uniform Distribution	
Lower pH Limit	**Upper pH Limit**
5.93	8.49

DTN: MO0307SPAIPCHM.001.

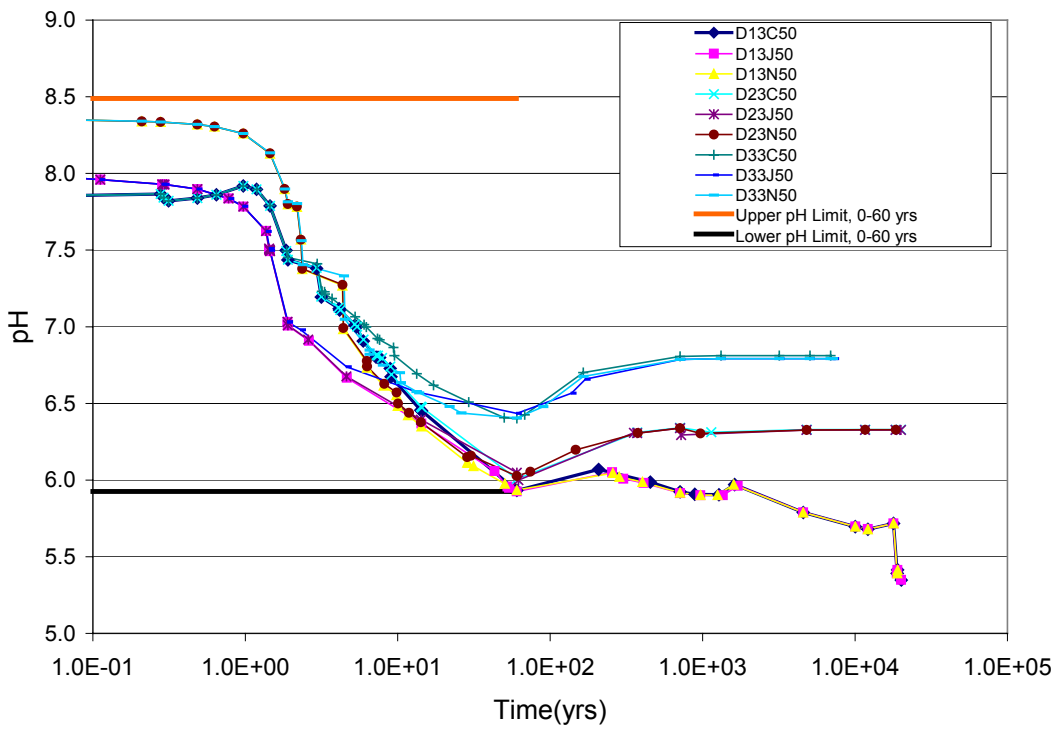

DTN: MO0307SPAIPCHM.001

Figure 32. Codisposed N Reactor Seepage Dripping Model 50°C pH Profiles and 0 to 60-Year Abstraction Limits

Note that the pH drop at 20,000 years (Figure 32) for the D13 runs results from the depletion of the HLWG, and only occurs in the low flux runs because the acid generating potential of the 304L components is more exaggerated at low flux values.

The regression equation describing the pH as a function of the $\log_{10}$ of the flux is provided in Table 81. Like the 60 to 20,000 year CDNR seepage dripping model 25°C pH abstraction the stabilized pH was also used for the 50°C abstraction to generate the regression equation. A

uniform uncertainty range of -0.5 to 0.5 pH units should be sampled and added to the calculated pH value.

Table 81. Codisposed N Reactor Seepage Dripping Model 50°C pH Abstraction, 60 to 20,000 Years

y = mx + b[a]	
M	**B**
0.4847	6.1844
R^2 = 0.9967	

DTN: MO0307SPAIPCHM.001.

NOTE: [a]y = pH, × = $\log_{10}$(flux(l/yr))

Examination of Figures 8 and 9 shows that the CDNR water vapor condensation model has the potential to generate pH values near 10. Although the output from the CDNR seepage dripping model (Figure 32) for the 60 to 20,000 year period shows the pH does not exceed approximately 6.3, it is considered possible that high pH values (8 to 10) could also result from the CDNR seepage dripping model should seepage contact the HLWG and exit the waste package without contacting metal components. This scenario also includes the possibility that a waste package may contain only HLWG, which would have a much greater potential for generating high-pH solutions.

Therefore, to include the possibility of occurrence of high-pH conditions in the TSPA-LA model, a mixed-relationship type abstraction is recommended, where 85 percent probability is assigned to the relationship in Table 81, and 15 percent probability is assigned to the 6 to 11 pH range. The 6 to 11 pH range should be sampled uniformly, and no uncertainty term should be added to this sampled range.

Table 82 provides the flux limits for the pH abstraction. At flux values greater than 1000 l/yr the pH should be set to a constant value of 8.5. The upper flux limit was set by the sensitivity analysis (Attachment II, "CS_Sensitivity.xls") which showed that above 1000 l/yr the seepage chemistry was largely unchanged.

The possibility exists that in the TSPA-LA model runs the flux could be less than the minimum value in Table 82. If the flux is lower than 0.15 l/yr then the pH should be calculated using 0.15 l/yr and the uncertainty range should be uniformly sampled and expanded to -1.0 to 1.0 pH units. The additional uncertainty will account for pH variations in the low flux scenarios.

Table 82. Codisposed N Reactor Seepage Dripping Model 50°C pH Abstraction Flux Limits for 60 to 20,000 Year Abstraction

Flux Limits (l/yr)	
Lower	**Upper[a]**
0.15	1000

DTN: MO0307SPAIPCHM.001.

NOTE: [a]Upper Limit pH = 8.5

8.4.3 Codisposed N Reactor Seepage Dripping Model pH Temperature Dependence

Figure 33 shows how the pH history for D23C25 varies as a function of temperature. Both the HLWG and N reactor fuel rate coefficients were corrected for temperature. Unlike the CSNF pH histories (Figure 21), the CDNR pH response is not systematic, i.e., it is not possible to extrapolate the regression equations beyond their range without the risk of abstracting pH values which are out of agreement with process model output. Therefore, it is recommended that only a limited temperature functionality be implemented for the CDNR seepage dripping model pH abstraction.

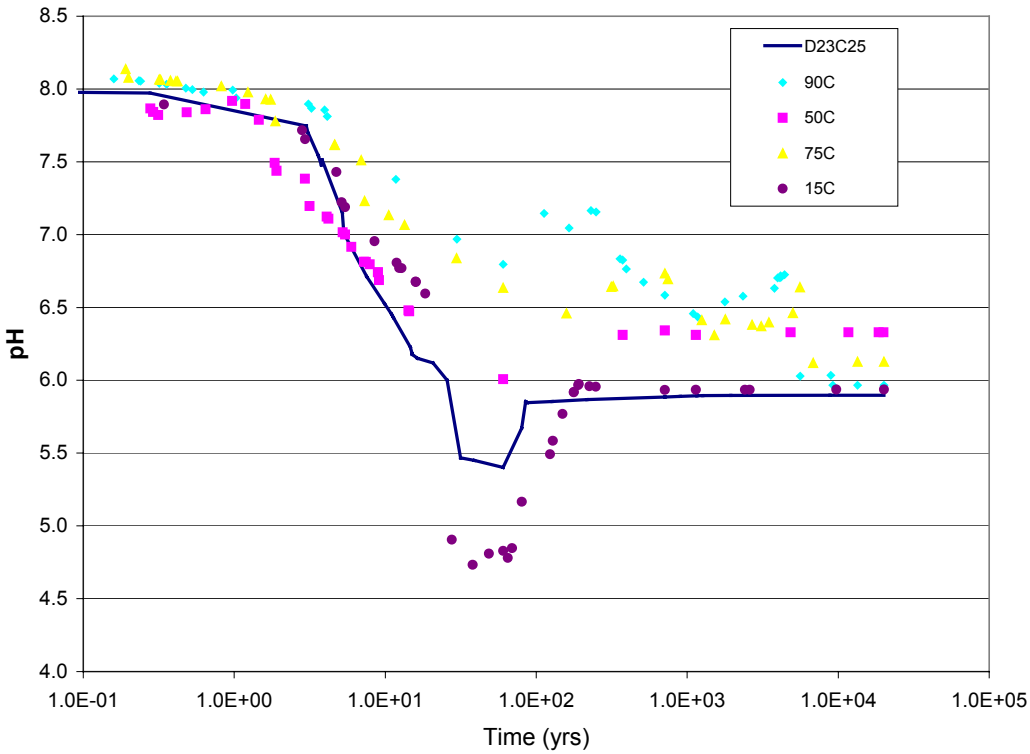

Source: Microsoft Excel Spreadsheet CDNR_sensit.xls in DTN: MO0307SPAIPCHM.001.

Figure 33. Effect of Temperature on the pH of Run D23C25

The early-time distribution (0 to 60 years post breach) should include the extreme values from Figure 33. The minimum pH value is 4.7 for the 15°C simulation, and the maximum pH is 8.1 for the 75°C simulation. Uniform sampling in the pH range from 4.7 to 8.1 will provide adequate coverage for temperatures between 15 and 95°C. For pH values sampled between 25° and 50°C. with a uniformly sampled uncertainty range of -0.5 to 0.5 should be applied. For temperatures below 25° and above 50°C a uniformly sampled uncertainty range of -2 to 2 should be applied.

For the period beyond 60 years post waste package breach, the mixed-relationship pH abstraction will be used. The TSPA-LA code should use a single selector function to choose either the pH-flux relationship (Tables 78 and 81) or a uniform distribution for the 25° and 50°C abstractions.

If the distribution is chosen, then a single distribution uniformly sampled in the pH range from 6 to 11 independent of temperature should be implemented in TSPA-LA. Using a single distribution to represent both temperatures is preferred over using two distributions and then interpolating between the sampled values because interpolating between sampled values has no basis for the temperature functionality. The expanded sampled range of 6 to 11 is sufficient to account for uncertainty and temperatures up to 95°C ; thus, it will not be necessary to include an additional uncertainty term to this sampled pH value.

If the pH-flux relationships are chosen, then the 25°C and 50°C regression equations (Tables 78 and 81) should be used, and the pH values calculated at 25°C and 50°C can define a linear (pH versus temperature) relationship to estimate the pH at temperatures between 15°C and 95°C. If the temperature is below 25°C, or above 50°C, then the extrapolated pH value should be considered as more uncertain than pH values calculated within 25°C to 50°C temperature range. Additional uncertainty should be applied to pH values extrapolated outside of the 25°C to 50°C range, and a uniformly sampled distribution in the range from -2.0 to 2.0 pH units should be applied. Application of a uniformly sampled distribution from –0.5 to 0.5 pH units should be added for pH values interpolated in the temperature range between 25°C to 50°C unless the flux is less than 0.15 l/yr in which case the uniformly sampled distribution should be expanded to -1.0 to 1.0 pH units. The lower and upper limits of pH should be set by TSPA as equal to 1 and 12, respectively. In other words, should a pH value with added uncertainty be less than one, or greater than 12, TSPA should set that pH value to its limiting value. If the temperature is less than 15°C, or greater 95°C, then the pH should be evaluated at 15°C, or 95°C, respectively.

8.4.4 Codisposed N Reactor Seepage Dripping Model 25°C Ionic Strength Abstraction

Figure 34 displays the ionic strength profiles for the CDNR seepage dripping model runs at 25°C. The period from 0 to 80 years is characterized by increasing ionic strength and is best represented by a cumulative distribution abstraction (Table 83). The period from 80 to 20,000 years can be represented by the stabilized ionic strength as a function of flux.

Table 83 provides the cumulative distribution data for the period between 0 and 80 years for the CDNR seepage dripping model 25°C abstraction. Where the 0.01 ionic strength cutoff was set to 7/80, or 0.09 probability, and the 0.05 ionic strength cutoff set to 14/80, or 0.18 probability.

Table 83. Codisposed N Reactor Seepage Dripping Model 25°C Ionic Strength 0 to 80 Years Cumulative Distribution

Time Period Post WP breach (years)	Ionic Strength (molal)	Probability
0 to 80	2.4E-03	0.0
	0.01	0.09
	0.05	0.18
	0.35	1.0

DTN: MO0307SPAIPCHM.001.

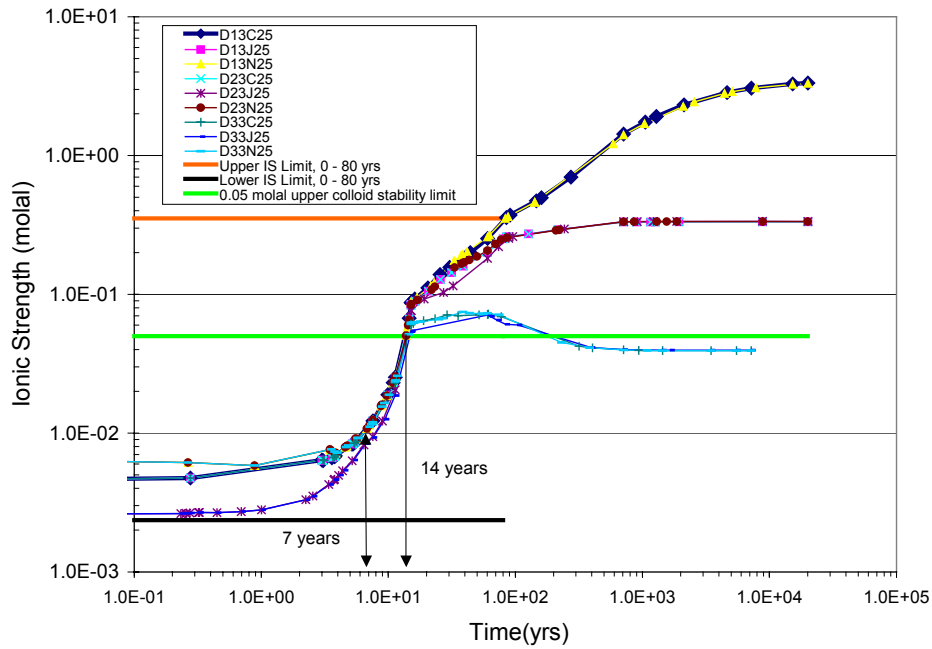

DTN: MO0307SPAIPCHM.001

Figure 34. Codisposed N Reactor Seepage Dripping Model 25°C Ionic Strength Profiles and 0 to 80 Year Abstraction Limits

The ionic strength abstraction function for the CDNR seepage dripping model at 25°C from 80 to 20,000 years is given in Table 84.

Table 84. Codisposed N Reactor Seepage Dripping Model 25°C Ionic Strength 80 to 20,000 Year Abstraction

y = aEXP(bx)[a]	
a	**b**
0.5206	-2.2168
R^2 = 0.9996	

DTN: MO0307SPAIPCHM.001

NOTE: [a]y = ionic strength, × = $\log_{10}$(flux(l/yr))

An uncertainty factor such as that applied in Section 8.1.2 should also be used here for TSPA-LA purposes for both the 0 to 80 year and the 80 to 20,000 year abstractions. A uniform uncertainty range of -0.6 to 0.6 multiplied by the sampled value should be added to the sampled value. Ionic strength = $IS_{sampled}$ + ($Uncertainty_{sampled}$ × $IS_{sampled}$).

The limits of flux for the abstraction are given in Table 85. The upper flux limit was set using the ionic strength of J-13 (Table 54) as the lower ionic strength limit, i.e., at flux values greater than 180 l/yr the abstracted ionic strength would be less than that of the most dilute input solution, in this case J-13.

Table 85. Codisposed N Reactor Fuel Seepage Dripping Model 25°C Ionic Strength Flux Limits for 80 to 20,000 Year Abstraction

Flux Limits (l/yr)	
Lower	**Upper[a]**
0.15	180

NOTE: [a] Upper Limit set by J-13 at 0.0035 molal

If the flux is less than the minimum, then the ionic strength should be evaluated using the lower flux limit from Table 85. Likewise, if the flux is greater than the upper limit, then the ionic strength should be evaluated using the upper limit value from Table 85.

8.4.5 Codisposed N Reactor Seepage Dripping Model 50°C Ionic Strength Abstraction

Figure 35 displays the ionic strength profiles for the CDNR seepage dripping model runs at 50°C. The period from 0 to 80 years is characterized by increasing ionic strength and is best represented by a cumulative distribution abstraction. The period from 80 to 20,000 years can be represented by the stabilized ionic strength as a function of flux. The ionic strength abstraction for the CDNR seepage dripping model at 50°C from 0 to 80 years is given in Table 86. Where the 0.01 ionic strength cutoff was set to 1.8/80, or 2.3E-02 probability, and the 0.05 ionic strength cutoff set to 10/80, or 0.13 probability.

Table 86. Codisposed N Reactor Seepage Dripping Model 50°C Ionic Strength Abstraction 0 to 80 Years

Time Period post WP Breach (years)	Ionic Strength (molal)	Probability
0 to 80	2.2E-03	0.0
	0.01	2.3E-02
	0.05	0.13
	0.33	1.0

DTN: MO0307SPAIPCHM.001

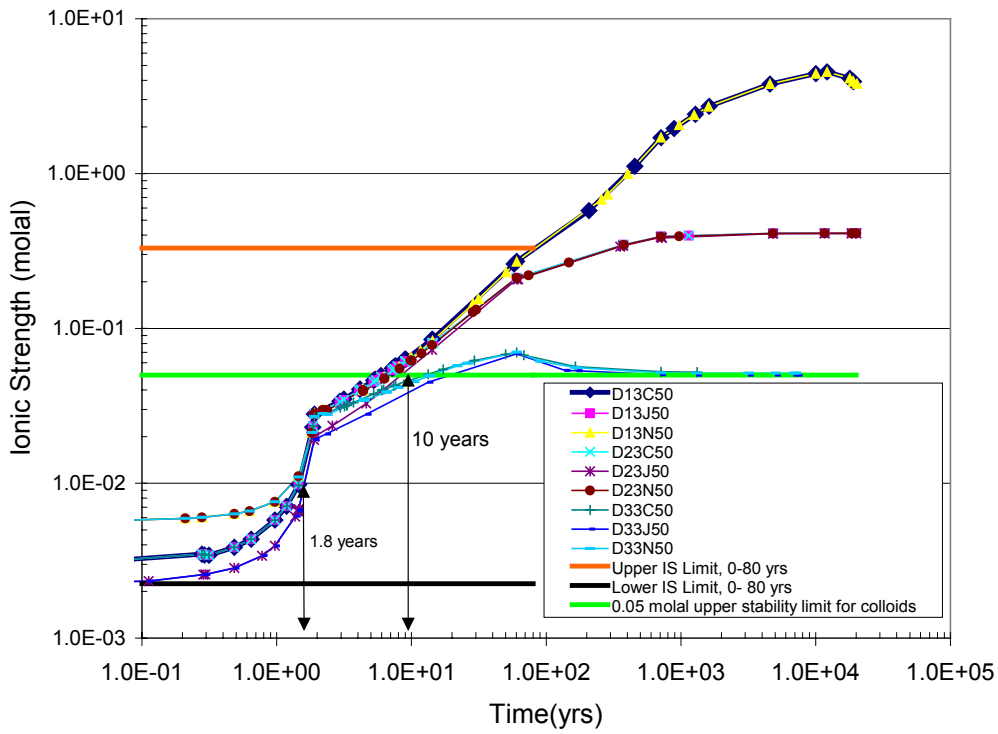

DTN: MO0307SPAIPCHM.001

Figure 35. Codisposed N Reactor Seepage Dripping Model 50°C Ionic Strength Profiles and 0 to 80 Year Abstraction Limits

The ionic strength abstraction for the CDNR seepage dripping model at 50°C from 80 to 20,000 years is given in Table 87.

Table 87. Codisposed N Reactor Seepage Dripping Model 50°C Ionic Strength 80 to 20,000 Year Abstraction

$y = aEXP(bx)^a$	
a	**b**
0.6293	-2.1549
R^2 = 0.9996	

DTN: MO0307SPAIPCHM.001

NOTE: [a]y = ionic strength, × = $\log_{10}$(flux(l/yr))

An uncertainty factor such as that applied in Section 8.1.2 should also be used here for TSPA-LA purposes for both the 0 to 80 year and the 80 to 20,000 year abstractions. A uniform uncertainty range of -0.6 to 0.6 multiplied by the sampled value should be added to the sampled value. Ionic strength = $IS_{sampled}$ + ($Uncertainty_{sampled} \times IS_{sampled}$).

The limits of flux for the abstraction are given in Table 88. The upper flux limit was set using the ionic strength of J-13 (Table 54) as the lower ionic strength limit, i.e., at flux values greater than 250 l/yr the abstracted ionic strength would be less than that of the most dilute input solution, in this case, J-13.

Table 88. Codisposed N Reactor Seepage Dripping Model 50°C Ionic Strength Flux Limits for 80 to 20,000 Year Abstraction

Flux Limits (l/yr)	
Lower	**Upper[a]**
0.15	250

DTN: MO0307SPAIPCHM.001

NOTE: [a]Upper Limit set by J-13 at 0.0035 molal

If the flux is less than the minimum, then the ionic strength should be evaluated using the lower flux limit from Table 88. Likewise, if the flux is greater than the upper limit, then the ionic strength should be evaluated using the upper limit value from Table 88.

8.4.6 Codisposed N Reactor Seepage Dripping Model Ionic Strength Temperature Dependence

Figure 36 shows that the ionic strength does not show a temperature functionality. Therefore, the 25 and 50°C abstractions should not be interpolated for intermediate temperatures. However, examination of the early time distributions (Tables 83 and 86), and the late-time flux relationships (Table 84 and 87) reveals that both the distributions and the relationships are approximately the same. Therefore, it is recommended that TSPA use the 25°C abstractions (Tables 83 and 84) for temperatures ranging from 15°C to 37.5°C, and the 50°C abstractions (Tables 86 and 87) for temperatures ranging from 37.5°C to 100°C. For temperatures between 15 and 50°C an uncertainty range of -0.6 to 0.6 should be uniformly sampled, and for temperatures greater than 50°C an uncertainty range of –0.99 to 0.99 should be uniformly sampled. For all temperatures the sampled uncertainty value should be multiplied by the ionic strength value and the result added to the ionic strength. Ionic strength = $IS_{sampled}$ + ($Uncertainty_{sampled} \times IS_{sampled}$).

8.4.7 Codisposed N Reactor Seepage Dripping Model 25°C and 50°C Fluoride Abstraction

The fluoride profiles for the CDNR seepage dripping model 25°C simulations are plotted in Figure 37. The minimum fluoride spike at about 5 years was not included in the abstraction because of its short duration. Compared to the CSNF fluoride profiles (Figure 25) the CDNR fluoride profiles are much more complex. The reason for the increased complexity is that fluorine is a component of the HLWG so that the aqueous fluorine concentration is controlled by the HLWG dissolution rate which is pH dependent (Table 19).

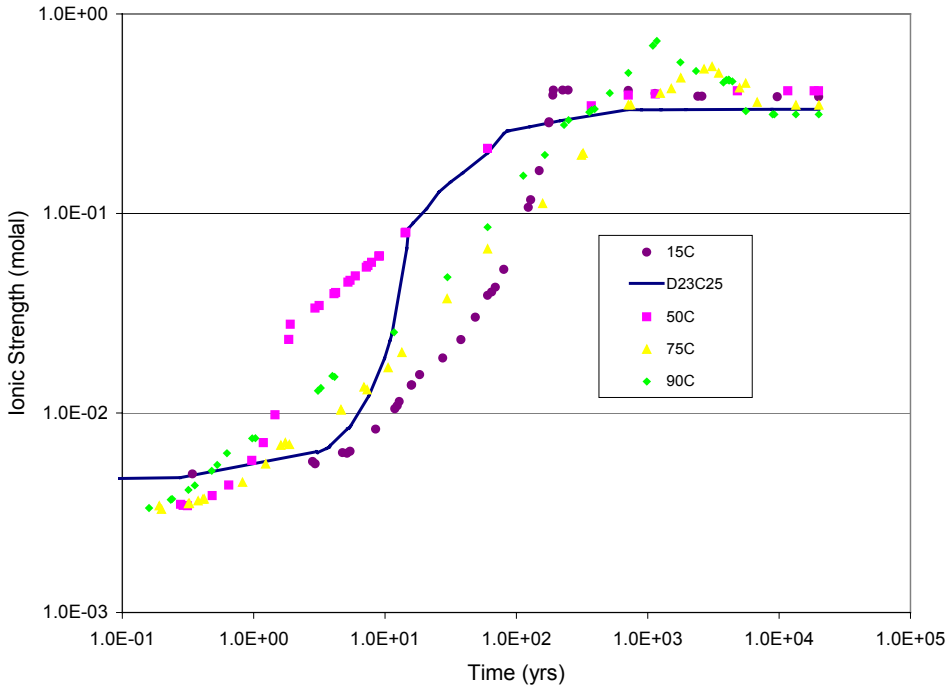

Source: Microsoft Excel Spreadsheet CDNR_sensit.xls in DTN: MO0307SPAIPCHM.001.

Figure 36. Effect of Temperature on the Ionic Strength of Run D23C25

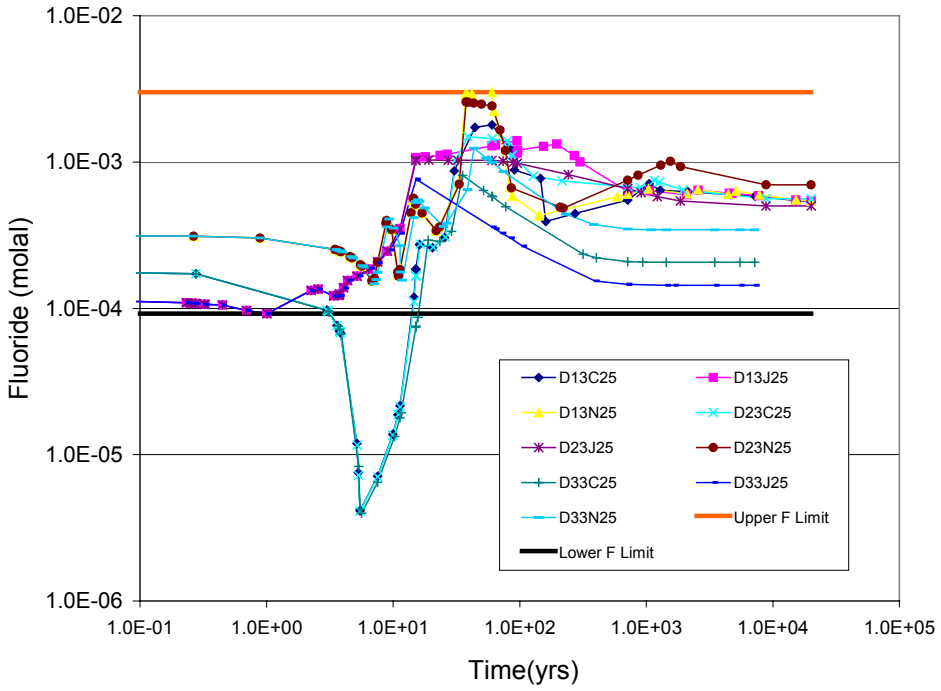

DTN: MO0307SPAIPCHM.001

Figure 37. Codisposed N Reactor Seepage Dripping Model 25°C Fluoride Profiles and Abstraction Limits

The CDNR seepage dripping model fluoride abstractions at 25 and 50°C are provided in Table 89.

Table 89. Codisposed N Reactor Seepage Dripping Model 25° and 50°C Fluoride Abstraction Limits

Temperature	Lower F Limit	Upper F Limit
Distribution	uniform	
(°C)	Mol/kg	
25	9.2E-05	3.0E-03
50	1.2E-04	2.9E-03

DTN: MO0307SPAIPCHM.001

8.4.8 Codisposed N Reactor Seepage Dripping Model 25°C and 50°C Chloride Abstraction

The CDNR seepage dripping model chloride profiles are plotted in Figure 38 together with the abstraction limits. The abstractions for 25 and 50°C are provided in Table 90.

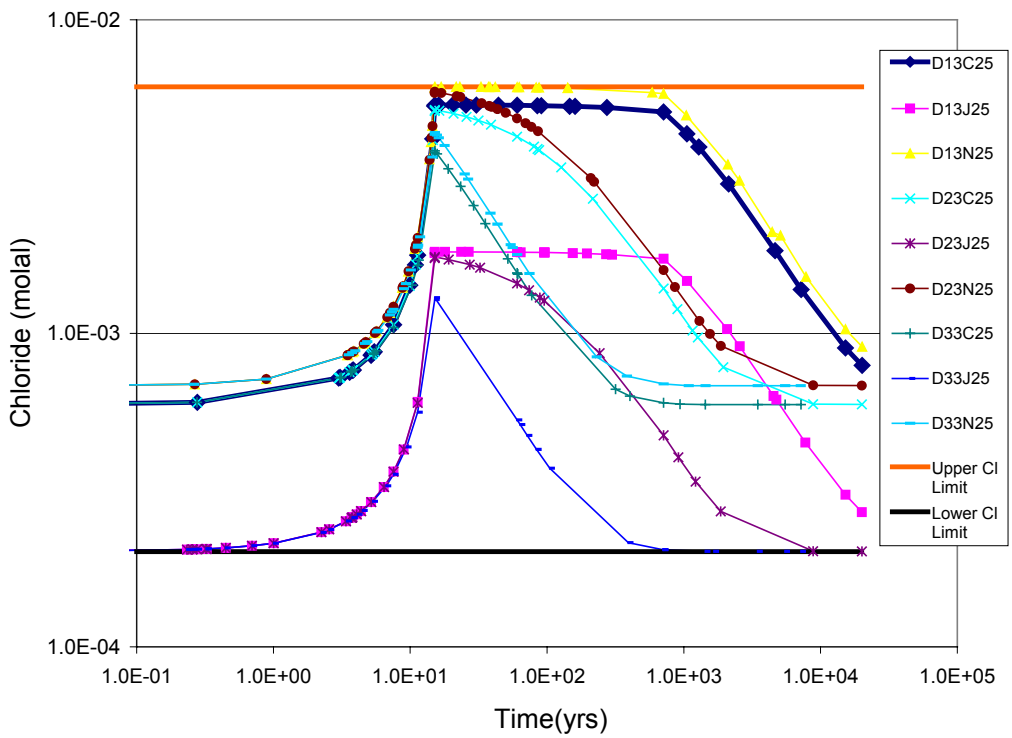

Source: Microsoft Excel Spreadsheet CDNR_SDM_25.xls in DTN: MO0307SPAIPCHM.001.

Figure 38. Codisposed N Reactor Seepage Dripping Model 25°C Chloride Profiles and Abstraction Limits

Table 90. Codisposed N Reactor Seepage Dripping Model 25° and 50°C Chloride Abstraction Limits

Temperature	Lower Cl Limit	Upper Cl Limit
Distribution	uniform	
(°C)	**Mol/kg**	
25	2.01E-04	6.11E-03
50	2.01E-04	6.16E-03

DTN: MO0307SPAIPCHM.001

8.5 TOTAL CARBONATE ABSTRACTION

Total carbonate is used in the kinetic rate expression for the dissolution of CSNF; therefore, abstracted values are needed for the TSPA-LA. In a system where the partial pressure of carbon dioxide (CO_2) is constant over the modeled period and the pH and temperature known, the total carbonate can be calculated using the equilibrium mass action expressions.

Where the total carbonate (0<pH<14) is equal to:

0) $\Sigma C = [CO_2\ (aq)] + [HCO_3^-] + [CO_3^{2-}]$

1) $CO_2(g) \Leftrightarrow CO_2\ (aq)$ $\log K = K_1$

$[CO_2\ (aq)] = PCO_{2(g)}\ 10^{K_1}$

2) $CO_2\ (aq) \Leftrightarrow H^+ + HCO_3^-$ $\log K = K_2$

$[HCO_3^-] = (PCO_{2(g)}\ 10^{K_1}\ 10^{K_2})/10^{-pH}$

3) $HCO_3^- \Leftrightarrow H^+ + CO_3^{2-}$ $\log K = K_3$

$[CO_3^{2-}] = [(PCO_{2(g)}\ 10^{K_1}\ 10^{K_2})/10^{-pH}]\ 10^{K_3}/\ 10^{-pH}$

Combining terms and substituting back into expression (0), the total carbonate for the system is equal to the expression in Table 91.

Table 91. Expression for Total Carbonate as a Function of pH to be Used in the Total System Performance Assessment

$$\text{Total C} = PCO_2(10^{K_1} + 10^{(pH + K_1 + K_2)} + 10^{(2pH + K_1 + K_2 + K_3)})$$

DTN: MO0307SPAIPCHM.001

Since the equilibrium constants for the carbonate species vary as a function of temperature it is possible to derive expressions for K_1, K_2, and K_3 that include this functionality. The thermodynamic data from 0 to 100°C for the carbonate species was extracted from Data0.ymp.R2 (DTN: MO0302SPATHDYN.000) and is compiled in Table 92. Note that log K_1 (Table 92) is the result of combined expressions.

Table 92. Log K Values for the Carbonate Species at Temperature

Log K	Reaction	Log K at temperature			
		0°C	25°C	60°C	100°C
	$CO_2(g) + H_2O = H^+ + HCO_3^-$	-7.6765	-7.8136	-8.0527	-8.3574
	$HCO_3^- + H^+ = CO_2(aq) + H_2O$	+ 6.5804	+ 6.3447	+ 6.2684	+ 6.3882
K_1	$CO_2(g) = CO_2(aq)$	-1.0961	-1.4689	-1.7843	-1.9692
K_2	$CO_2(aq) + H_2O = HCO_3^- + H^+$	-6.5804	-6.3447	-6.2684	-6.3882
K_3	$HCO_3^- = CO_3^{2-} + H^+$	-10.6241	-10.3288	-10.1304	-10.0836

Source: DTN: MO0302SPATHDYN.000.

Log K temperature expressions were derived by plotting the log K values from 0° to 100°C (Table 92) versus their respective temperatures and fitting a polynomial to the data in Microsoft Excel. This is the same method used by the EQPT code when it compiles the log K grid of an EQ3/6 data0 file (Daveler and Wolery 1992, p. 12). Therefore consistency is maintained between the approach used in the model report and that used in EQ3/6.

Table 93. Log K Temperature Interpolation Functions for Use in the Total Carbonate Abstraction

Log K	Log K expression[a]	R^2
K_1	$\text{Log } K_1 = 7E\text{-}05T^2 - 0.0159T - 1.1023$	0.9992
K_2	$\text{Log } K_2 = 5E\text{-}07T^3 - 0.0002T^2 + 0.0132T - 6.5804$	1.0
K_3	$\text{Log } K_3 = -8E\text{-}05T^2 + 0.0128T - 10.618$	0.9977

DTN: MO0307SPAIPCHM.001

NOTE: [a]T = temperature in degrees Celsius

Plots of the log K temperature interpolations are included in DTN: MO0307SPAIPCHM.001. The expressions in Table 93 are valid for temperatures in the range of 0 to 100°C. This range is larger than that for the pH abstractions (15 to 90°C) in Sections 8.1 to 8.4.

Three feeds are required for the total carbonate abstraction as it should be implemented in TSPA-LA. The first feed is the temperature, which is required to calculate the appropriate log K values. The second feed is the in-package pH, which is estimated using the relationships and conditions specified in Sections 8.1 to 8.4. The third input is the pCO_2. Once the log K values and in-package pH are calculated they can be used to calculate the total carbonate via the expression in Table 92.

Since the pH abstractions account for propagated uncertainty there is no need to introduce further uncertainty at the level of the total carbonate abstraction. Therefore, the carbonate abstraction can be used as is with no uncertainty term added to it.

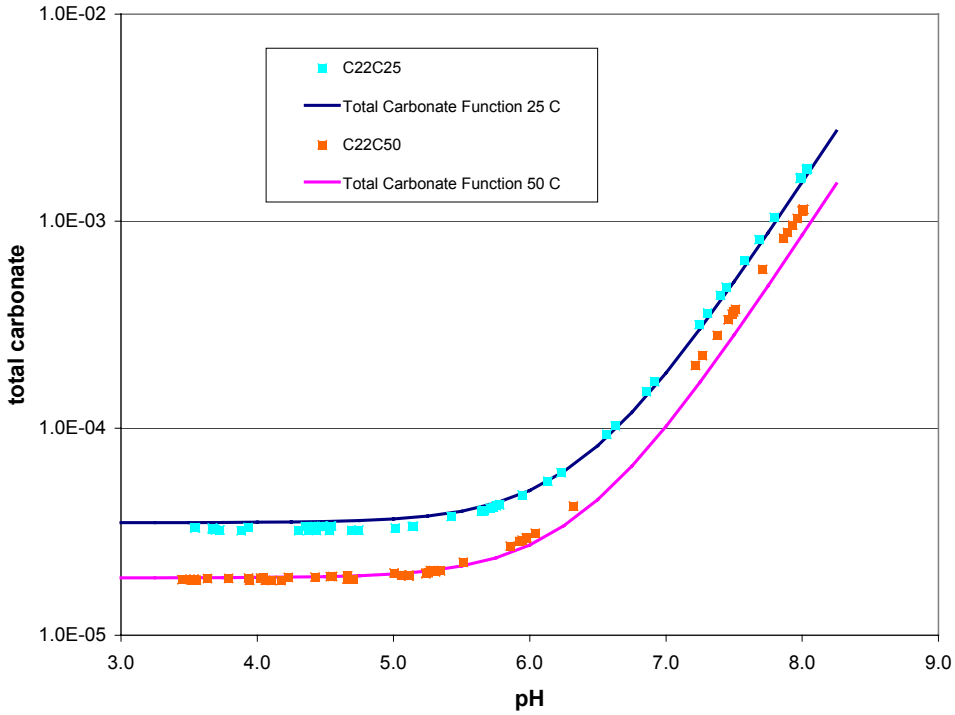

Source: Microsoft Excel Spreadsheet carbonate_Eh_abstraction.xls in DTN: MO0307SPAIPCHM.001.

Figure 39. Plot of Total Carbonate Function at Two Temperatures Compared to Model Output

Figure 39 shows the carbonate abstraction calculated at two temperatures compared to output from the model. The close agreement of the abstraction and the model output illustrates that the abstraction adequately reproduces the model output.

8.6 Eh ABSTRACTION

In aqueous systems in equilibrium with a constant partial pressure of oxygen, the Eh may be calculated directly from the pH. For the formation of water the pE° may be calculated from the following expression, where ΔG° is the Gibb's free energy of formation, F is the Faraday constant (23.06 kcal/volt-gram equivalent), Eh is the electron activity expressed in units of volts, and pE is the negative log base 10 of electron activity.

1) $1/2O_2 + 2H^+ + 2e^- = H_2O$ $\Delta G° = -56.688$ kcal/mol (DTN: MO0302SPATHDYN.000)

2) $\Delta G° = -nFEh°$ (Drever 1982, p. 254, Equation 11-6)

3) $pE = F/(2.303RT)Eh$ (Drever 1982, p. 254)

Solving (3) for Eh and substituting into (2) results in (4), establishing a relationship between ΔG° and pE°

4) $\Delta G° = -2.303nRT(pE°)$,

Where, n = number of electrons [2], R = Gas Constant (1.987E-03 kcal/mol.K), PO_2 is the partial pressure of oxygen, and T = absolute temperature (Kelvin).

Solving for pE° with temperature dependency results in:

$pE° = 6193.973/T$

Thus for the formation of water in terms of one electron mole we have:

$1/4O_2 + H^+ + e^- = 1/2H_2O$

$pE = pE° + Log(PO_2^{1/4}[H^+])$

$pE = 6193.973/T – pH + 0.25log(PO_2)$

Converting to Eh we get the expression in Table 94. The expression for Eh as a function of pH, oxygen partial pressure, and temperature (Table 94) is applicable for both CSNF and CDNR waste packages. The temperature should be input in degrees Kelvin, and the output is in volts.

Table 94. Expression for Eh as a Function of pH, Oxygen Partial Pressure, and Absolute Temperature for use in the TSPA-LA

Eh = 2.303RT/F(6193.973/T – pH + 0.25logPO2)

Figure 40 shows the Eh abstraction function plotted together with the model output from the 25° and 50°C runs for the median case. Like the carbonate abstraction, uncertainty is built in to the Eh abstraction by virtue of the input pH, which already has associated uncertainty.

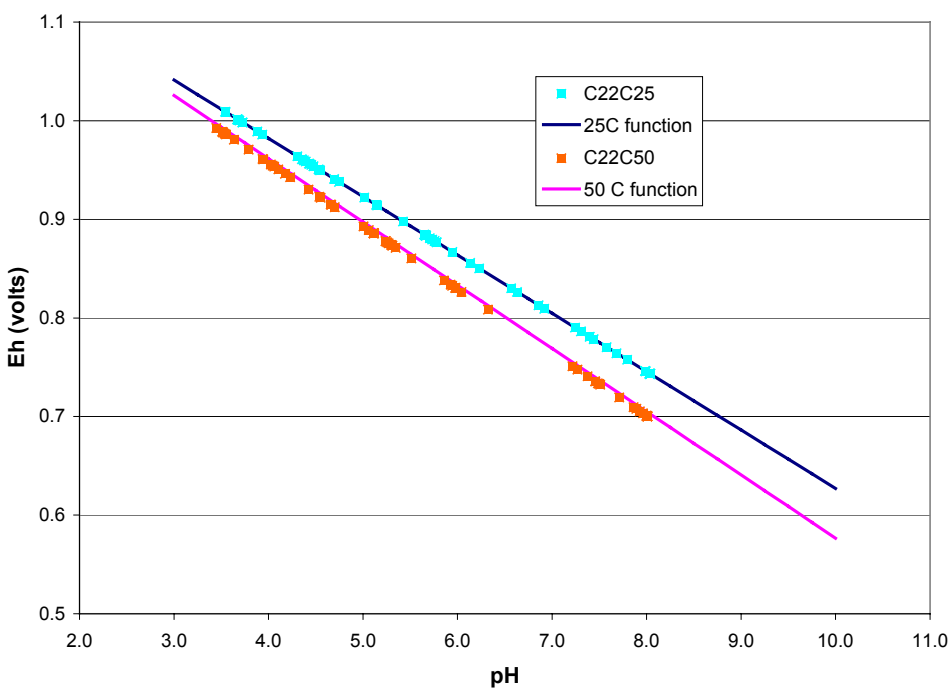

Source: Microsoft Excel Spreadsheet carbonate_Eh_abstraction.xls in DTN: MO0307SPAIPCHM.001.

Figure 40. Plot of Eh Function at Two Temperatures Compared to Model Output

8.7 OXYGEN AND CARBON DIOXIDE PARTIAL PRESSURE RANGE OF APPLICABILITY

Both oxygen and carbon dioxide partial pressures were set to constant values for the full duration of the process model simulations (Section 6). However, sensitivity analyses (Section 6.7) demonstrated that varying the PCO_2 between 10^{-4} to 10^{-2} had little or no impact on the pH and ionic strength, and furthermore, the uncertainty assigned to the abstractions incorporates this variation in CO_2 partial pressure. Therefore, the PCO_2 used in TSPA-LA may be expanded to accommodate this range (10^{-4} to 10^{-2} atmospheres) without extending beyond the uncertainty range of the abstractions. No simulations were done to determine the effects of PO_2 on the system response; therefore, TSPA-LA is limited to atmospheric conditions. Table 95 provides the gas composition.

Table 95. Gas Abstraction Information

Gas	Log partial pressure
Oxygen	-0.7
Carbon Dioxide	-4.0 to –2.0

NOTE: Partial pressure in atmospheres

8.8 ABSTRACTION VALIDATION

This abstraction model uses mathematical relationships and statistical distributions to fit product output i.e., product output is used as input for the abstraction. Thus, product output was used to generate the abstraction model, i.e., to generate the mathematical relationships and statistical distributions that will be used in TSPA-LA. Therefore, the acceptance criteria, for the abstraction relationships, is that they reflect the product output used in their generation. In other words, validation of the abstraction model requires comparison of abstracted parameter values to their corollary product output parameter values. It must be emphasized that this does not constitute validation of the product output, but only that the abstraction can reproduce a subset of the process model output through the use of mathematical relationships.

Validation of the CSNF and co-disposal pH and ionic strength abstractions is implicit in the method by which the pH response surfaces and distributions were developed. The validation process used for the pH abstractions was a comparison of the abstracted pH for each time period to the product output value for a given set of input parameters. The response surfaces are mathematical constructs whose limits were set by the process models inputs and outputs. The pH abstractions represent a best fit to the process model data, and are therefore able to reproduce the process model output for given set of input conditions within a range of uncertainty, thus rendering them self validating. The pH and ionic strength abstraction validation plots for the response surfaces, linear, and non-linear relationships are contained in Attachment II, Figures II-3 to II-9. The distributions do not require any further validation because their limits are extracted directly from the product output and as such are self validated.

The total carbonate and Eh relationships use process model input data and an abstracted pH value to calculate a total carbonate concentration and Eh values in solution at a given time. The ability for these relationships to reproduce process model output was demonstrated in Sections

8.5 and 8.6, respectively. In other words the total carbonate and ionic strength abstractions were validated by comparison to product output (Figure 39 and 40, respectively).

The remaining parameters, fluoride and chloride concentrations were set to distributions where the values were taken directly from the product output for both CSNF and co-disposal and are thus self-validated.

8.9 LINKING THE WATER VAPOR CONDENSATION AND SEEPAGE DRIPPING MODEL FOR TSPA-LA

In a potential repository situation one could imagine a scenario where a waste package could fail and water vapor would enter, condense, and react and then at some future time it is possible that seepage might also enter this same waste package and react with the remaining materials. The opposite sequence might also occur, where seepage enters a waste package and at some future time the seepage might cease and water vapor could enter the same package. This would be a scenario where the water vapor condensation model and the seepage dripping model would need to be linked. In Sections 6.6.1.2 and 6.6.2.2 it was demonstrated that the initial composition of the seepage entering a failed waste package did not exert a significant influence on the resulting in-package chemistry. As the following figures demonstrate the results of the seepage dripping model follow similar behavior as the ensemble outputs from the water vapor condensation model.

Based on the comparison of the results in Figures 41 and 42 it is recommended that for the purposes of TSPA-LA should it be necessary to link the water vapor condensation model and the seepage dripping model the change from one model to the other should occur synchronously. If a package is initially receiving water vapor and at some later time seepage begins to enter the package, then the water vapor condensation abstraction should cease and the seepage abstraction should begin at that in point in time.

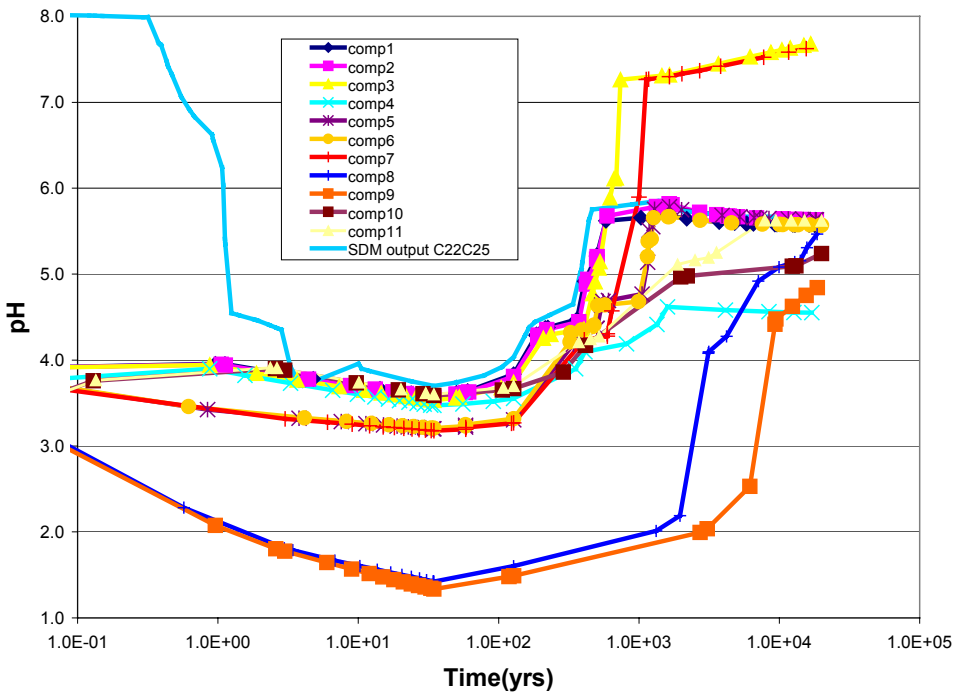

DTN: MO0307SPAIPCHM.001

Figure 41. Commercial Spent Nuclear Fuel Water Vapor Condensation–Seepage Dripping Model Comparison

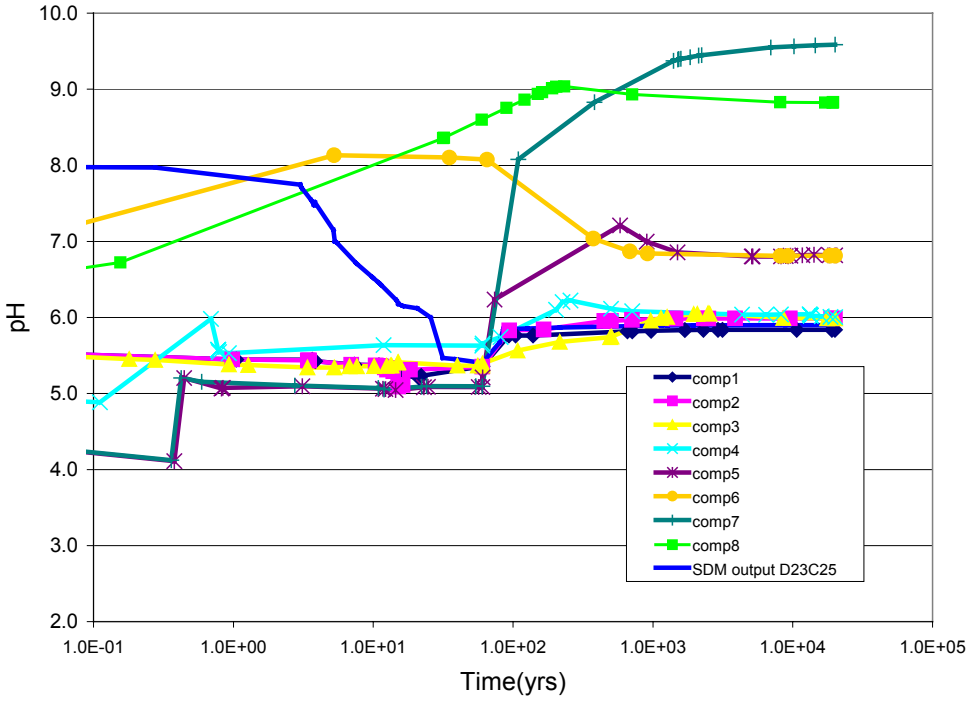

DTN: MO0307SPAIPCHM.001.

Figure 42. Codisposed N Reactor Water Vapor Condensation–Seepage Dripping Model Comparison

8.10 OUTPUT UNCERTAINTY

The in-package chemistry model combines two approaches to model uncertainty: (1) Application of a factorial design approach to account for known large potential variations in model input (reactant combinations, water flux, fuel exposure, temperature, and seepage composition; and (2) sensitivity analysis of lesser known, not as well defined input variations (carbon dioxide partial pressure, A516 sulfur content, corrosion rates, extreme temperatures and flux values). Where (1) provided the functional basis of the in-package chemistry model abstraction, (2) provided the uncertainty ranges of the abstracted parameters. Thus, the information to be used in TSPA-LA directly incorporates uncertainty exterior to the in-package environment (1) and interior to the in-package environment in a form that can be readily implemented in TSPA-LA (i.e., model uncertainty is propagated through the abstractions). Thus, the only restrictions on the subsequent use of the in-package chemistry model abstraction in TSPA-LA are that all of the abstractions presented in Section 8 must be applied within the stated limits (flux, temperature, PCO_2, and fuel exposure) as specified in this model report.

8.11 CONCLUSIONS

This model report provides the documentation of the in-package chemistry process models as well as the in-package chemistry abstractions. The abstractions are to be used as input to TSPA-LA and will feed the solubility, colloid, CSNF, and HLWG submodels. The application of the abstractions and their limits and uncertainties are documented in detail in this section.

The in-package chemistry process models are developed and documented in Section 6, and Attachment III. Based on the results of the in-package chemistry process models, it may be concluded that the following inputs and/or processes have only minor impact on the model response such that the abstractions are not affected.

- Initial water composition
- Partial pressure of carbon dioxide
- Radiolysis (Attachment III, DTN: MO0304SPAICSCR.000)
- Decreased corrosion rate of the waste package alloys
- Minor modifications to waste package design configuration
- Sulfur content of the carbon steel (A516) waste package components.

The effect of the above factors on the model response is finite and accounted for in the abstractions via applied uncertainty terms.

The following variables have a large influence on the in-package chemistry.

- Waste package type (CSNF versus codisposed)
- Water flux
- Fuel exposure (clad failure)
- Temperature.

These four parameters are used as input to the in-package chemistry abstractions, i.e., the abstractions are functions of these variables. Therefore, in TSPA-LA the in-package chemistry

is implemented as a function of external variables, which directly links the in-package chemistry to the repository environment.

The acceptance criteria from Section 4.2 relating to the quantity and chemistry of water contacting the waste packages and waste form have been met in the following sections:

- The system description and model integration were described in Sections 6.3, 6.3.1, 6.3.2, and 6.3.3.
- The sufficiency of the data is discussed in Section 4 and sub-sections of Section 4.
- The data uncertainty and its propagation through the model abstraction is described in Section 6.3.4, 6.7 and its sub-sections, and in Sections 8.1 through 8.7.
- The model uncertainty and its propagation through the model abstraction is contained in Sections 6.1 and 8.10.
- The objective comparisons of the model abstraction outputs is contained in Section 8.8.

Two DTNs were developed in this model report:

DTN: MO0307SPAIPCHM.001, which is the primary output of this model report.

DTN: MO0304SPAICSCR.000, which is developed in Attachment III and documents the effect of radiolysis on the in-package chemistry. The radiolysis analyses (Attachment III) provided an additional sensitivity study on processes that may occur and influence the in-package chemistry model results.

9. REFERENCES

9.1 REFERENCES CITED

Allen, B.L. and Hajek, B.F. 1995. "Mineral Occurrence in Soil Environments." Chapter 5 of *Minerals in Soil Environments*. 2nd Edition. Dixon, J.B. and Weed, S.B., eds. SSSA Book Series, No. 1. Madison, Wisconsin: Soil Science Society of America. TIC: 237222.

ASM International 1987. *Corrosion.* Volume 13 of *Metals Handbook.* 9th Edition. Metals Park, Ohio: ASM International. TIC: 209807.

Audi, G. and Wapstra, A.H. 1995. *Atomic Mass Adjustment, Mass List for Analysis*. Upton, New York: Brookhaven National Laboratory, National Nuclear Data Center. TIC: 242718.

B&W Fuel Company 1991. *Final Design Package Babcock & Wilcox BR-100 100 Ton Rail/Barge Spent Fuel Shipping Cask.* Volume 2. 51-1203400-01. DBABE0000-00272-1000-00014 REV 00. Lynchburg, Virginia: B&W Fuel Company. ACC: MOV.19960802.0083.

Baxter, R.G. 1988. *Defense Waste Processing Facility Wasteform and Canister Description*. DP-1606, Rev. 2. Aiken, South Carolina: E.I. du Pont de Nemours & Company, Savannah River Plant. TIC: 8704.

Berner, E.K. and Berner, R.A. 1996. *Global Environment: Water, Air, and Geochemical Cycles*. Upper Saddle River, New Jersey: Prentice Hall. TIC: 253965.

Bricker, O. 1965. "Some Stability Relations in the System Mn-O_2-H_2O at 25° and One Atmosphere Total Pressure." *American Mineralogist, 50,* 1296-1354. Washington, D.C.: Mineralogical Society of America. TIC: 238855.

BSC (Bechtel SAIC Company, LLC) 2001a. *Defense High Level Waste Glass Degradation*. ANL-EBS-MD-000016 REV 00 ICN 02. Las Vegas, Nevada: Bechtel SAIC Company. ACC: MOL.20011015.0502.

BSC 2001b. *DSNF and Other Waste Form Degradation Abstraction*. ANL-WIS-MD-000004 REV 01 ICN 01. Las Vegas, Nevada: Bechtel SAIC Company. ACC: MOL.20010316.0002.

BSC 2001c. *PWR Assembly End-Effect Reactivity Evaluation*. CAL-UDC-NU-000006 REV 00. Las Vegas, Nevada: Bechtel SAIC Company. ACC: MOL.20010412.0158.

BSC 2001d. *Repository Design, Waste Package, Project 21-PWR Waste Package with Absorber Plates, Sheet 1 of 3, Sheet 2 of 3, and Sheet 3 of 3*. DWG-UDC-ME-000001 REV A. Las Vegas, Nevada: Bechtel SAIC Company. ACC: MOL.20020102.0174.

BSC 2001e. *In-Package Chemistry Abstraction*. ANL-EBS-MD-000037 REV 01. Las Vegas, Nevada: Bechtel SAIC Company. ACC: MOL.20010315.0053.

BSC 2002a. *Technical Work Plan for Waste Form Degradation Modeling, Testing, and Analyses in Support of SR and LA*. TWP-WIS-MD-000008 REV 02. Las Vegas, Nevada: Bechtel SAIC Company. ACC: MOL.20020819.0359.

BSC 2002b. *Gamma and Neutron Radiolysis in the 21-PWR Waste Package from Ten to One Million Years*. 000-00C-DSU0-00700-000-00A. Las Vegas, Nevada: Bechtel SAIC Company. ACC: MOL.20021004.0002.

BSC 2002c. *EQ6 Calculation for Chemical Degradation of 21 PWR CSNF Waste Packages*. CAL-UDC-MD-000002 REV A. Las Vegas, Nevada: Bechtel SAIC Company. ACC: MOL.20020601.0195.

BSC 2002d. *Geochemistry Model Abstraction and Sensitivity Studies for the 21 PWR CSNF Waste Packages*. MDL-DSU-MD-000001 REV 00. Las Vegas, Nevada: Bechtel SAIC Company. ACC: MOL.20021107.0154.

BSC 2002e. *The Enhanced Plan for Features, Events, and Processes (FEPs) at Yucca Mountain*. TDR-WIS-PA-000005 REV 00. Las Vegas, Nevada: Bechtel SAIC Company. ACC: MOL.20020417.0385.

BSC 2002f. *Scientific Processes Guidelines Manual*. MIS-WIS-MD-000001 REV 01. Las Vegas, Nevada: Bechtel SAIC Company. ACC: MOL.20020923.0176.

BSC 2003a. *Drift-Scale Coupled Processes (DST and THC Seepage) Models*. MDL-NBS-HS-000001 REV 02C. Las Vegas, Nevada: Bechtel SAIC Company. ACC: MOL.20030507.0274. TBV-5120.

BSC 2003b. *EBS Radionuclide Transport Abstraction*. ANL-WIS-PA-000001 REV 01A. Las Vegas, Nevada: Bechtel SAIC Company. ACC: MOL.20030617.0222. TBV-5179.

BSC 2003c. *Repository Design Project, Repository/PA IED Emplacement Drift Committed Materials 1 of 2*. 800-IED-WIS0-00301-000-00A. Las Vegas, Nevada: Bechtel SAIC Company. ACC: ENG.20030627.0003.

BSC 2003d. *Repository Design Project, RDP/PA IED Typical Waste Package Components Assembly 1 of 9*. 800-IED-WIS0-00201-000-00A. Las Vegas, Nevada: Bechtel SAIC Company. ACC: ENG.20030702.0001.

BSC 2003e. *Waste Form and In-Drift Colloids-Associated Radionuclide Concentrations: Abstraction and Summary*. MDL-EBS-PA-000004 REV 00. Las Vegas, Nevada: Bechtel SAIC Company. ACC: DOC.20030626.0006.

Canori, G.F. and Leitner, M.M. 2003. *Project Requirements Document*. TER-MGR-MD-000001 REV 01. Las Vegas, Nevada: Bechtel SAIC Company. ACC: DOC.20030404.0003.

Christensen, H. 1995. "Remodeling of the Oxidant Species During Radiolysis of High-Temperature Water in a Pressurized Water Reactor." *Nuclear Technology, 109,* 373-382. La Grange Park, Illinois: American Nuclear Society. TIC: 253765.

Christensen, H. and Bjergbakke, E. 1982. *Radiolysis of Ground Water from Spent Fuel*. SKB TR-82-18. Stockholm, Sweden: Svensk Kärnbränsleförsörjning A.B. TIC: 205896.

Christensen, H.; Sunder, S.; and Shoesmith, D.W. 1994. *Development of a Kinetic Model to Predict the Rate of Oxidation and Dissolution of Nuclear Fuel (UO_2) by the Radiolysis of Water.* AECL-11102. Pinawa, Manitoba, Canada: Atomic Energy of Canada Limited. TIC: 242350.

Cornell, R.M.; Giovanoli, R.; and Schneider, W. 1992. "The Effect of Nickel on the Conversion of Amorphous Iron(III) Hydroxide into More Crystalline Iron Oxides in Alkaline Media." *Journal of Chemical Technology and Biotechnology, 53,* (1), 73-79. Oxford, England: Blackwell Scientific Publishing. TIC: 254448.

CRWMS M&O (Civilian Radioactive Waste Management System Management and Operating Contractor) 1997. *Degraded Mode Criticality Analysis of Immobilized Plutonium Waste Forms in a Geologic Repository.* Predecisional Document. A00000000-01717-5705-00014 REV 01. Las Vegas, Nevada: CRWMS M&O. ACC: MOL.19980422.0911.

CRWMS M&O 1998. *Summary Report of Commercial Reactor Criticality Data for Crystal River Unit 3*. B00000000-01717-5705-00060 REV 01. Las Vegas, Nevada: CRWMS M&O. ACC: MOL.19980728.0189.

CRWMS M&O 2000a. *CSNF Waste Form Degradation: Summary Abstraction*. ANL-EBS-MD-000015 REV 00. Las Vegas, Nevada: CRWMS M&O. ACC: MOL.20000121.0161.

CRWMS M&O 2000b. *Source Terms for HLW Glass Canisters.* CAL-MGR-NU-000002 REV 01. Las Vegas, Nevada: CRWMS M&O. ACC: MOL.20000823.0004.

CRWMS M&O 2000c. *General Corrosion and Localized Corrosion of Waste Package Outer Barrier*. ANL-EBS-MD-000003 REV 00. Las Vegas, Nevada: CRWMS M&O. ACC: MOL.20000202.0172.

CRWMS M&O 2000d. *Total System Performance Assessment for the Site Recommendation*. TDR-WIS-PA-000001 REV 00 ICN 01. Las Vegas, Nevada: CRWMS M&O. ACC: MOL.20001220.0045.

CRWMS M&O 2000e. *In-Package Chemistry Abstraction*. ANL-EBS-MD-000037 REV 00. Las Vegas, Nevada: CRWMS M&O. ACC: MOL.20000418.0818.

CRWMS M&O 2000f. *Summary of In-Package Chemistry for Waste Forms*. ANL-EBS-MD-000050 REV 01. Las Vegas, Nevada: CRWMS M&O. ACC: MOL.20010129.0134.

CRWMS M&O 2001. *EQ6 Calculations for Chemical Degradation of N Reactor (U-metal) Spent Nuclear Fuel Waste Packages*. CAL-EDC-MD-000010 REV 00. Las Vegas, Nevada: CRWMS M&O. ACC: MOL.20010227.0017.

Daveler, S.A. and Wolery, T.J. 1992. *EQPT, A Data File Preprocessor for the EQ3/6 Software Package: User's Guide and Related Documentation (Version 7.0).* UCRL-MA-110662 PT II. Livermore, California: Lawrence Livermore National Laboratory. TIC: 205240.

Deer, W.A.; Howie, R.A.; and Zussman, J. 1966. *An Introduction to the Rock-Forming Minerals.* New York, New York: John Wiley & Sons. TIC: 245492.

Dixon, J.B. 1995. "Kaolin and Serpentine Group Minerals." Chapter 10 of *Minerals in Soil Environments.* 2nd Edition. Dixon, J.B. and Weed, S.B., eds. SSSA Book Series, No. 1. Madison, Wisconsin: Soil Science Society of America. TIC: 237222.

DOE (U.S. Department of Energy) 2000a. *Review of Oxidation Rates of DOE Spent Nuclear Fuel, Part 1: Metallic Fuel*. DOE/SNF/REP-054, Rev. 0. Washington, D.C.: U.S. Department of Energy. TIC: 248978.

DOE 2000b. *N Reactor (U-Metal) Fuel Characteristics for Disposal Criticality Analysis*. DOE/SNF/REP-056, Rev. 0. Washington, D.C.: U.S. Department of Energy, Office of Environmental Management. TIC: 247956.

DOE 2002. *DOE Spent Nuclear Fuel Information in Support of TSPA-SR*. DOE/SNF/REP-047, Rev. 2. Idaho Falls, Idaho: U.S. Department of Energy, Idaho Operations Office. TIC: 252089.

Drever, J.I. 1982. *The Geochemistry of Natural Waters*. Englewood Cliffs, New Jersey: Prentice Hall. TIC: 240706.

Ewing, R.C. and Haaker, R.F. 1979. *Naturally Occurring Glasses: Analogues for Radioactive Waste Forms*. PNL-2776. Richland, Washington: Pacific Northwest Laboratory. ACC: NNA.19900315.0277.

Finch, R.J. and Murakami, T. 1999. "Systematics and Paragenesis of Uranium Minerals." Chapter 3 of *Uranium: Mineralogy, Geochemistry and the Environment.* Burns, P.C. and Finch, R.J., eds. Reviews in Mineralogy Volume 38. Washington, D.C.: Mineralogical Society of America. TIC: 247121.

Firsching, F.H. and Brune, S.N. 1991. "Solubility Products of the Trivalent Rare-Earth Phosphates." *Journal of Chemical Engineering, 36,* 93-95. Washington, D.C.: American Chemical Society. TIC: 240863.

Freeze, G.A.; Brodsky, N.S.; and Swift, P.N. 2001. *The Development of Information Catalogued in REV00 of the YMP FEP Database.* TDR-WIS-MD-000003 REV 00 ICN 01. Las Vegas, Nevada: Bechtel SAIC Company. ACC: MOL.20010301.0237.

Harrar, J.E.; Carley, J.F.; Isherwood, W.F.; and Raber, E. 1990. *Report of the Committee to Review the Use of J-13 Well Water in Nevada Nuclear Waste Storage Investigations.* UCID-21867. Livermore, California: Lawrence Livermore National Laboratory. ACC: NNA.19910131.0274.

Hem, J.D. 1985. *Study and Interpretation of the Chemical Characteristics of Natural Water*. 3rd Edition. Geological Survey Water-Supply Paper 2254. Washington, D.C.: U.S. Government Printing Office. ACC: NNA.19940427.0181.

Hsu, P.H. 1995. "Aluminum Hydroxides and Oxyhydroxides." Chapter 7 of *Minerals in Soil Environments.* 2nd Edition. Dixon, J.B. and Weed, S.B., eds. SSSA Book Series, No. 1. Madison, Wisconsin: Soil Science Society of America. TIC: 237222.

IAEA (International Atomic Energy Agency) 1998. *Waterside Corrosion of Zirconium Alloys in Nuclear Power Plants*. IAEA-TECDOC-996. Vienna, Austria: International Atomic Energy Agency. TIC: 248234.

Kerr, P.F. 1977. *Optical Mineralogy.* 4th Edition. New York, New York: McGraw-Hill. TIC: 252886.

Klein, C. and Hurlbut, C.S., Jr. 1985. *Manual of Mineralogy.* 20th Edition. New York, New York: John Wiley & Sons. TIC: 242818.

Langmuir, D. 1997. *Aqueous Environmental Geochemistry.* Upper Saddle River, New Jersey: Prentice Hall. TIC: 237107.

Li, G.; Peacor, D.R.; Coombs, D.S.; and Kawachi, Y. 1997. "Solid Solution in the Celadonite Family: The New Minerals Ferroceladonite, $K_2Fe^2{}_2{+}Fe^3{}_2{+}Si_8O_{20}(OH)_4$, and Ferroaluminoceladonite, $K_2Fe^2{}_2{+}Al_2Si_8O_{20}(OH)_4$." *American Mineralogist, 82,* (5-6), 503-511. Washington, D.C.: Mineralogical Society of America. TIC: 252472.

Milnes, A.R. and Fitzpatrick, R.W. 1995. "Titanium and Zirconium Minerals." Chapter 23 of *Minerals in Soil Environments.* 2nd Edition. Dixon, J.B. and Weed, S.B., eds. SSSA Book Series, No. 1. Madison, Wisconsin: Soil Science Society of America. TIC: 237222.

Morel, F.M.M. and Hering, J.G. 1993. *Principles and Applications of Aquatic Chemistry.* New York, New York: John Wiley & Sons. TIC: 248465.

NRC (U.S. Nuclear Regulatory Commission) 2003. *Yucca Mountain Review Plan, Information Only*. NUREG-1804, Draft Final Revision 2. Washington, D.C.: U.S. Nuclear Regulatory Commission, Office of Nuclear Material Safety and Safeguards. TIC: 254002.

Palache, C.; Berman, H.; and Frondel, C. 1944. *Elements, Sulfides, Sulfosalts, Oxides*. Volume I of *The System of Mineralogy of James Dwight Dana and Edward Salisbury Dana, Yale University 1837–1892*. 7th Edition. New York, New York: John Wiley & Sons. TIC: 209331.

Palache, C.; Berman, H.; and Frondel, C. 1951. *Halides, Nitrates, Borates, Carbonates, Sulfates, Phosphates, Arsenates, Tungstates, Molybdates, Etc*. Volume II of *The System of Mineralogy of James Dwight Dana and Edward Salisbury Dana, Yale University 1837–1892*. 7th Edition. New York, New York: John Wiley & Sons. TIC: 209332.

Parrington, J.R.; Knox, H.D.; Breneman, S.L.; Baum, E.M.; and Feiner, F. 1996. *Nuclides and Isotopes, Chart of the Nuclides.* 15th Edition. San Jose, California: General Electric Company and KAPL, Inc. TIC: 233705.

Punatar, M.K. 2001. *Summary Report of Commercial Reactor Criticality Data for Crystal River Unit 3.* TDR-UDC-NU-000001 REV 02. Las Vegas, Nevada: Bechtel SAIC Company. ACC: MOL.20010702.0087.

Rai, D. and Ryan, J.L. 1982. "Crystallinity and Solubility of Pu(IV) Oxide and Hydrous Oxide in Aged Aqueous Suspensions." *Radiochimica Acta, 30,* 213-216. Munchen, Germany: R. Oldenbourg Verlag. TIC: 219107.

Rai, D. and Zachara, J.M. 1984. *A Critical Review.* Volume 1 of *Chemical Attenuation Rates, Coefficients, and Constants in Leachate Migration.* EPRI EA-3356. Palo Alto, California: Electric Power Research Institute. TIC: 237846.

Roberts, W.L.; Campbell, T.J.; and Rapp, G.R., Jr. 1990. *Encyclopedia of Minerals.* 2nd Edition. New York, New York: Van Nostrand Reinhold. TIC: 242976.

Runde, W. 1999. "Letter Report on Plutonium Thermodynamic Database." Letter from W. Runde (LANL) to P. Dixon (LANL), August 1, 1999, with attachments. ACC: MOL.19991214.0624.

Sandino, A. 1991. *Processes Affecting the Mobility of Uranium in Natural Waters.* Ph.D. thesis. Stockholm, Sweden: Royal Institute of Technology. TIC: 246941.

Schwertmann, U. and Taylor, R.M. 1995. "Iron Oxides." Chapter 8 of *Minerals in Soil Environments.* 2nd Edition. Dixon, J.B. and Weed, S.B., eds. SSSA Book Series, No. 1. Madison, Wisconsin: Soil Science Society of America. TIC: 237222.

Sequeira, C.A.C. 2000. "Corrosion of Copper and Copper Alloys." Chapter 42 of *Uhlig's Corrosion Handbook.* 2nd Edition. Revie, R.W., ed. New York, New York: John Wiley & Sons. TIC: 248360.

Stout, R.B. and Leider, H.R., eds. 1994. *Preliminary Waste Form Characteristics Report, Version 1.0.* UCRL-ID-108314, Rev. 1. Livermore, California: Lawrence Livermore National Laboratory. ACC: MOL.19960314.0440.

Stumm, W. and Morgan, J.J. 1996. *Aquatic Chemistry, Chemical Equilibria and Rates in Natural Waters.* 3rd Edition. New York, New York: John Wiley & Sons. TIC: 246296.

Waber, N. 1991. *Mineralogy, Petrology and Geochemistry of the Pocos de Caldas Analogue Study Sites, Minas Gerais, Brazil. II. Morro do Ferro.* SKB TR-90-12. Stockholm, Sweden: Svensk Kärnbränsleförsörjning A.B. TIC: 206350.

Weast, R.C., ed. 1977. *CRC Handbook of Chemistry and Physics.* 58th Edition. Cleveland, Ohio: CRC Press. TIC: 242376.

Wilson, C.N. and Bruton, C.J. 1989. *Studies on Spent Fuel Dissolution Behavior Under Yucca Mountain Repository Conditions.* PNL-SA-16832. Richland, Washington: Pacific Northwest Laboratory. ACC: HQX.19890918.0047.

Wolery, T.J. and Daveler, S.A. 1992. *EQ6, A Computer Program for Reaction Path Modeling of Aqueous Geochemical Systems: Theoretical Manual, User's Guide, and Related Documentation (Version 7.0)*. UCRL-MA-110662 PT IV. Livermore, California: Lawrence Livermore National Laboratory. ACC: MOL.19980701.0459.

Yang, I.C.; Rattray, G.W.; and Yu, P. 1996. *Interpretation of Chemical and Isotopic Data from Boreholes in the Unsaturated Zone at Yucca Mountain, Nevada.* Water-Resources Investigations Report 96-4058. Denver, Colorado: U.S. Geological Survey. ACC: MOL.19980528.0216.

9.2 CODES, STANDARDS, REGULATIONS, AND PROCEDURES

AP-2.22Q, Rev. 0, ICN 1. *Classification Criteria and Maintenance of the Monitored Geologic Repository Q-List.* Washington, D.C.: U.S. Department of Energy, Office of Civilian Radioactive Waste Management. ACC: DOC.20030422.0009.

AP-SI.1Q, Rev. 05, ICN 01. *Software Management*. Washington, D.C.: U.S. Department of Energy, Office of Civilian Radioactive Waste Management. ACC: DOC.20030708.0001.

AP-SIII.10Q, Rev. 1, ICN 2. *Models*. Washington, D.C.: U.S. Department of Energy, Office of Civilian Radioactive Waste Management. ACC: DOC.20030627.0003.

ASME (American Society of Mechanical Engineers) 1998. *1998 ASME Boiler and Pressure Vessel Code.* 1998 Edition with 1999 and 2000 Addenda. New York, New York: American Society of Mechanical Engineers. TIC: 247429.

ASTM A 20/A 20M-95a. 1995. *Standard Specification for General Requirements for Steel Plates for Pressure Vessels.* West Conshohocken, Pennsylvania: American Society for Testing and Materials. TIC: 240026.

ASTM A 240/A 240M-99b. 2000. *Standard Specification for Heat-Resisting Chromium and Chromium-Nickel Stainless Steel Plate, Sheet, and Strip for Pressure Vessels.* West Conshohocken, Pennsylvania: American Society for Testing and Materials. TIC: 248529.

ASTM A 887-89 (Reapproved 2000). 2000. *Standard Specification for Borated Stainless Steel Plate, Sheet, and Strip for Nuclear Application.* West Conshohocken, Pennsylvania: American Society for Testing and Materials. TIC: 249544.

ASTM B 209-96. 1996. *Standard Specification for Aluminum and Aluminum-Alloy Sheet and Plate.* West Conshohocken, Pennsylvania: American Society for Testing and Materials. TIC: 247078.

ASTM C 1174-97. 1998. *Standard Practice for Prediction of the Long-Term Behavior of Materials, Including Waste Forms, Used in Engineered Barrier Systems (EBS) for Geological Disposal of High-Level Radioactive Waste.* West Conshohocken, Pennsylvania: American Society for Testing and Materials. TIC: 246015.

ASTM G 1-90 (Reapproved 1999). 1999. *Standard Practice for Preparing, Cleaning, and Evaluating Corrosion Test Specimens.* West Conshohocken, Pennsylvania: American Society for Testing and Materials. TIC: 238771.

9.3 SOFTWARE CODES

Software Code: EQ3/6. V7.2b. LLNL: UCRL-MA-110662.

Software Code: EQ6. 7.2bLV. PC. 10075-7.2bLV-02. Windows NT, 2000.

Software Code: GetEQData. V1.0.1. PC w/Windows 2000. 10809-1.0.1-0.

9.4 SOURCE DATA, LISTED BY DATA TRACKING NUMBER

GS020408312272.003. Collection and Analysis of Pore Water Samples for the Period from April 2001 to February 2002. Submittal date: 04/24/2002.

MO0006J13WTRCM.000. Recommended Mean Values of Major Constituents in J-13 Well Water. Submittal date: 06/07/2000.

MO0109RIB00049.001. Waste Package Material Properties: Neutron Absorbing Materials. Submittal date: 09/17/2001.

MO0302SPATHDYN.000. Thermodynamic Data Input Files - Data0.YMP.R2. Submittal date: 02/05/2003.

MO0303SPAMCRAQ.000. Materials Corrosion Rates in Aqueous Environments. Submittal date: 03/05/2003.

9.5 OUTPUT DATA, LISTED BY DATA TRACKING NUMBER

MO0304SPAICSCR.000. In-Package Chemistry Sensitivity for CSNF with Radiolysis. Submittal date: 04/10/2003.

MO0307SPAIPCHM.001. Abstractions of In-Package Chemistry for TSPA-LA. Submittal date: 03/18/2003.

ATTACHMENT I

```
Volume in drive D is 030719_1720
 Volume Serial Number is 0AC8-A9B7

 Directory of d:\

07/19/2003  10:08a          23,207,507 CDNR.zip
07/19/2003  10:08a          71,299,139 CSNF.zip
04/10/2003  10:26a             606,335 Database.zip
07/19/2003  10:03a      <DIR>          files for Attachment II
07/19/2003  03:20p      <DIR>          files for Attachment III
07/19/2003  03:21p      <DIR>          files for Attachment IV
07/19/2003  04:52p           4,395,799 spreadsheets.zip
04/10/2003  10:27a             215,216 waters.zip
04/10/2003  10:27a           1,476,546 WVC_singlereact.zip
               6 File(s)    101,200,542 bytes

 Directory of d:\files for Attachment II

07/19/2003  10:03a      <DIR>          .
07/19/2003  10:03a      <DIR>          ..
07/19/2003  03:35p          12,041,505 AttachmentII.zip
               1 File(s)     12,041,505 bytes

 Directory of d:\files for Attachment III

07/19/2003  03:20p      <DIR>          .
07/19/2003  03:20p      <DIR>          ..
04/10/2003  08:42a           4,480,834 AttachmentIII.zip
               1 File(s)      4,480,834 bytes

 Directory of d:\files for Attachment IV

07/19/2003  03:21p      <DIR>          .
07/19/2003  03:21p      <DIR>          ..
04/10/2003  08:25a             314,559 AttachmentIV.zip
               1 File(s)        314,559 bytes

     Total Files Listed:
               9 File(s)    118,037,440 bytes
               9 Dir(s)               0 bytes free
```

ATTACHMENT II

Attachment II is comprised of additional plots. The computer files are included in Attachment V.

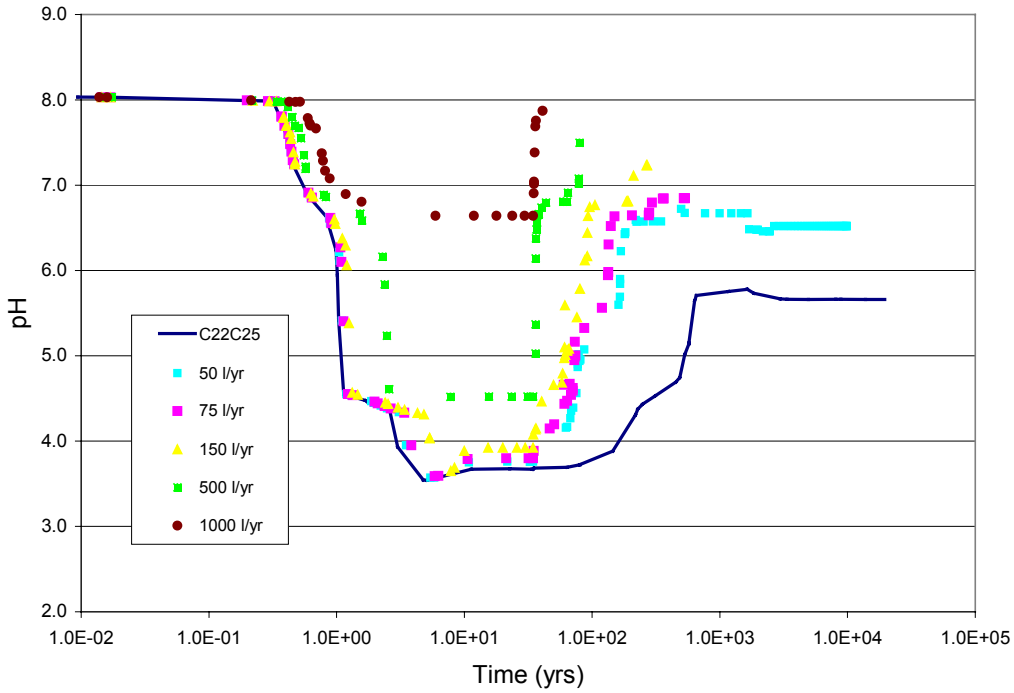

Source: Attachment V, CS_Sensitivity.xls

Figure II-1. Plot of pH Versus Time for C22C25 Showing the Effect of Increasing Flux

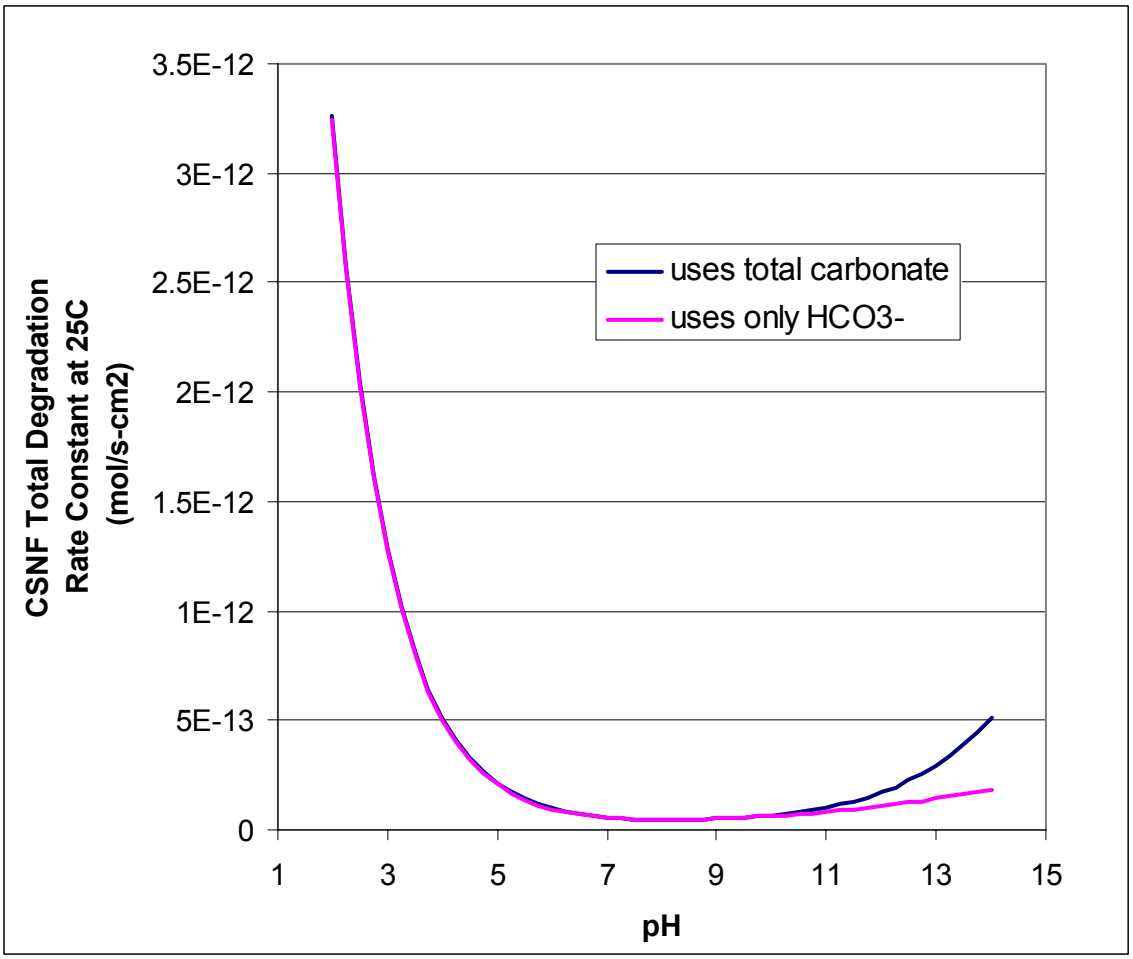

Source: Attachment V, carbonate_abstraction.xls, worksheet "CSNF Rate Sensitivity"

Figure II-2. Plot of CSNF Total Degradation Rate Constant as a function of pH

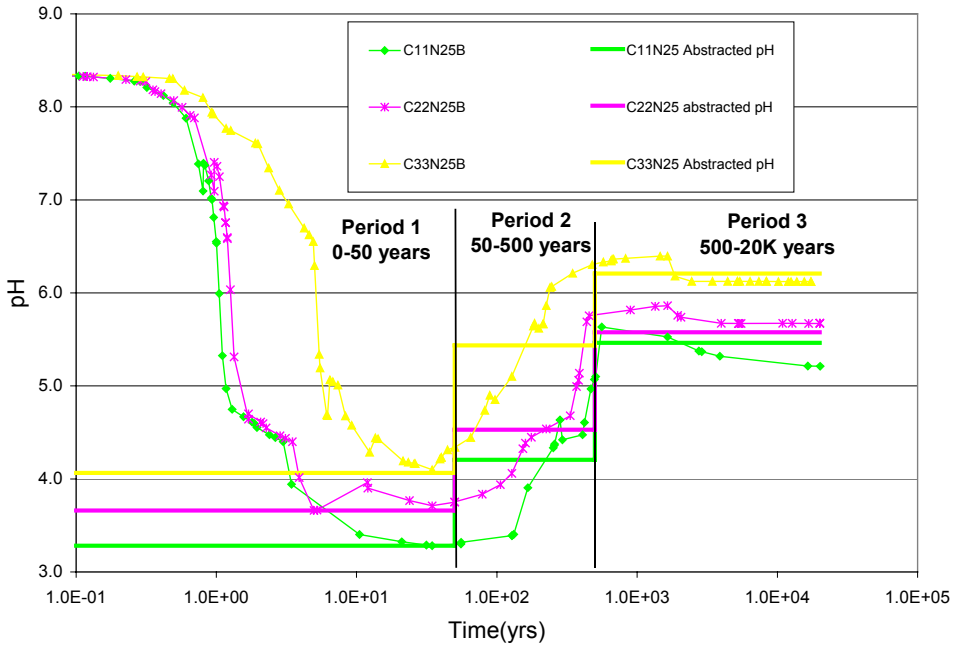

Source: Attachment V, CSNF_SDM_25.xls

Figure II-3. Validation of pH abstraction to model output for 25°C CSNF

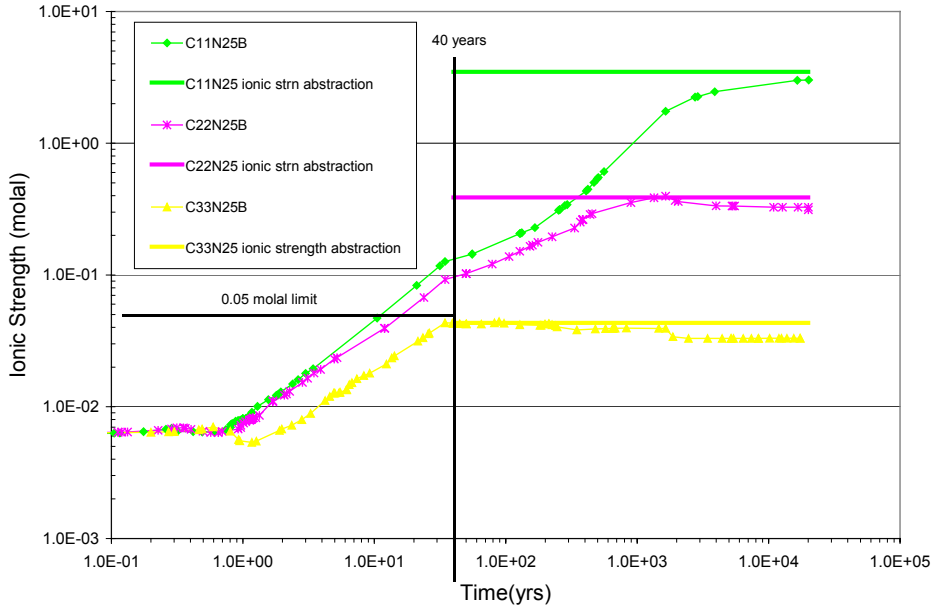

Source: Attachment V, CSNF_SDM_25.xls

Figure II-4. Validation of ionic strength abstraction to model output for 25°C CSNF

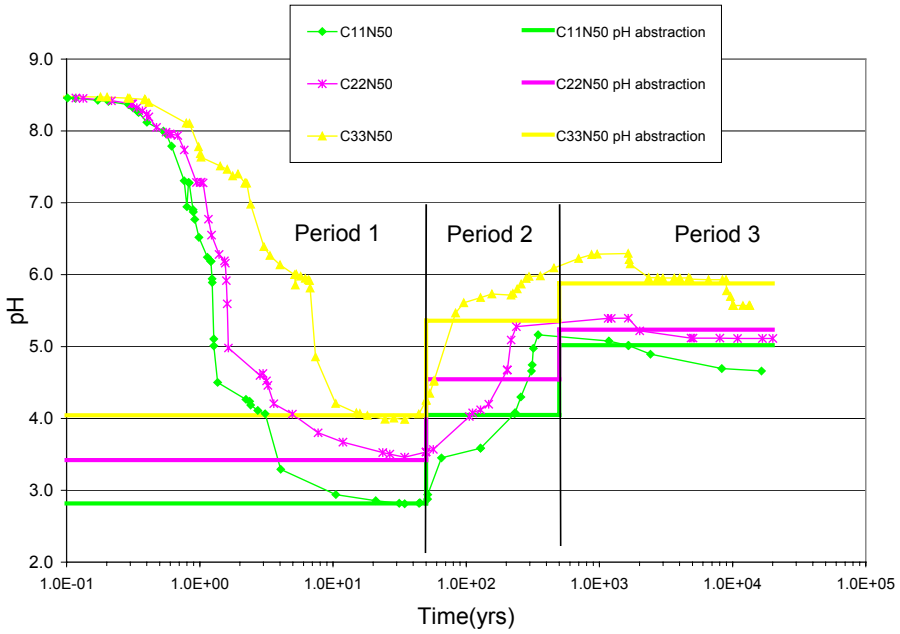

Source: Attachment V, CSNF_SDM_50.xls

Figure II-5. Validation of pH abstraction to model output for 50°C CSNF

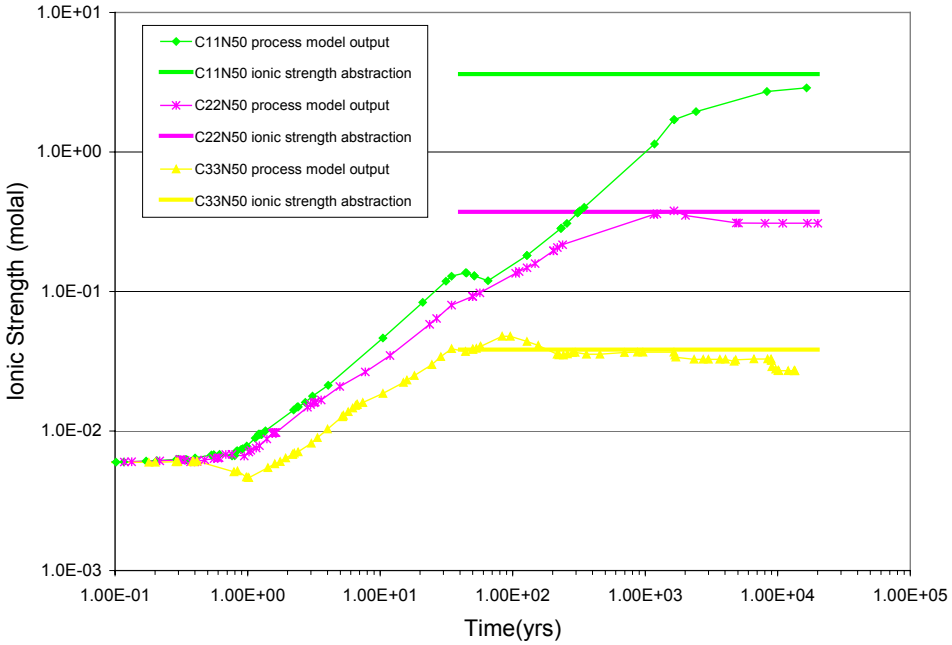

Source: Attachment V, CSNF_SDM_50.xls

Figure II-6. Validation of ionic strength abstraction to model output for 50°C CSNF

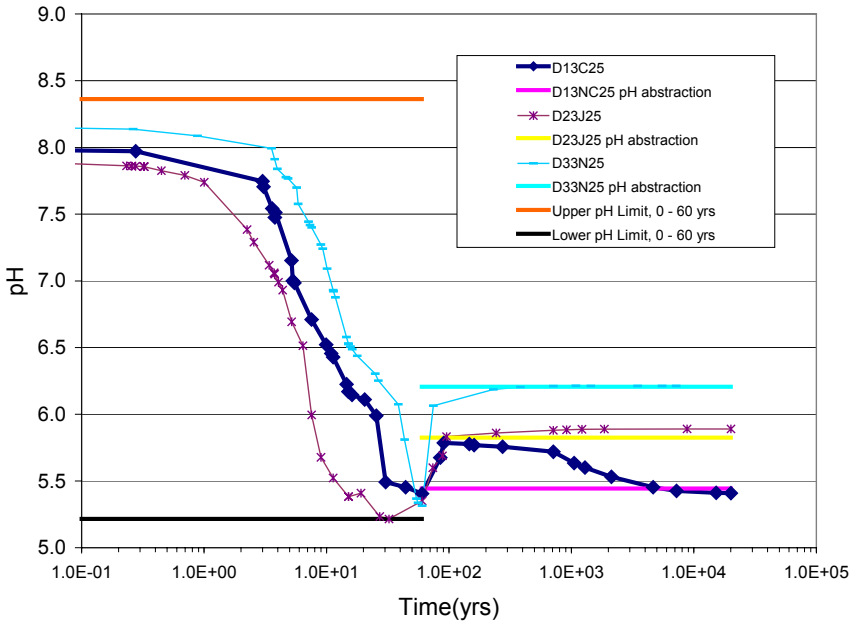

Source: Attachment V, CDNR_SDM_25.xls

Figure II-7. Validation of pH abstraction to model output for 25°C CDNR

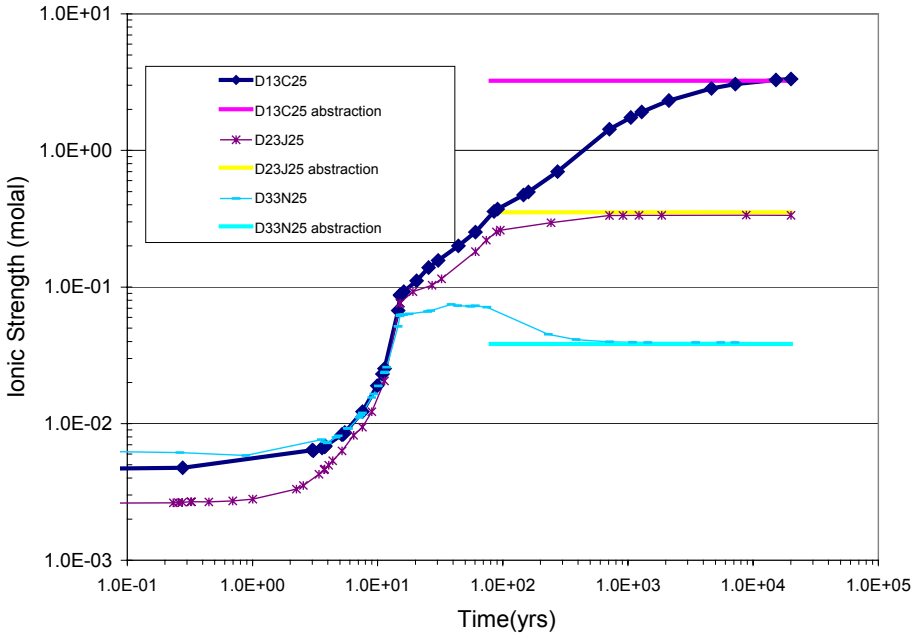

Source: Attachment V, CDNR_SDM_25.xls

Figure II-8. Validation of ionic strength abstraction to model output for 25°C CDNR

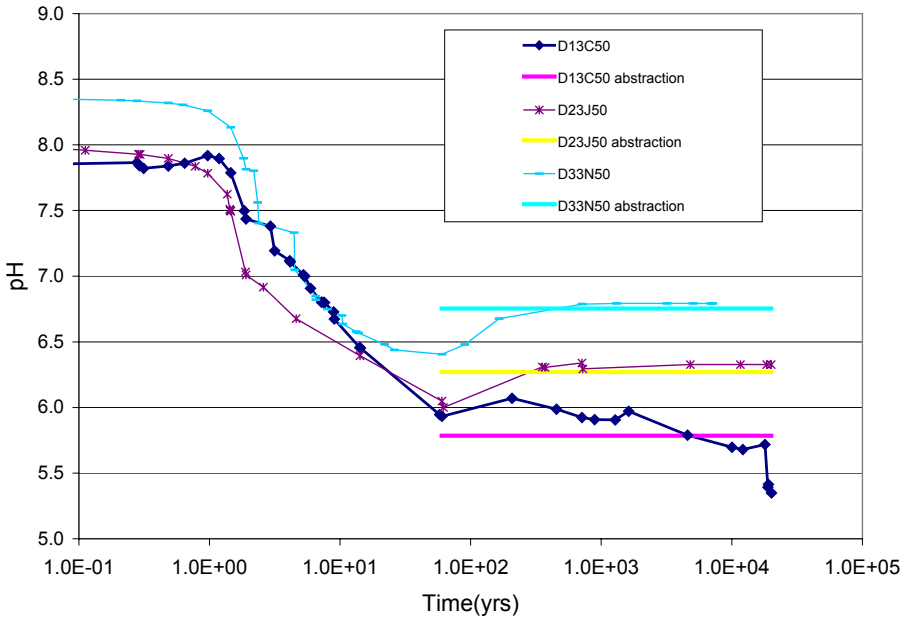

Source: Attachment V, CDNR_SDM_50.xls

Figure II-9. Validation of pH abstraction to model output for 50°C CDNR

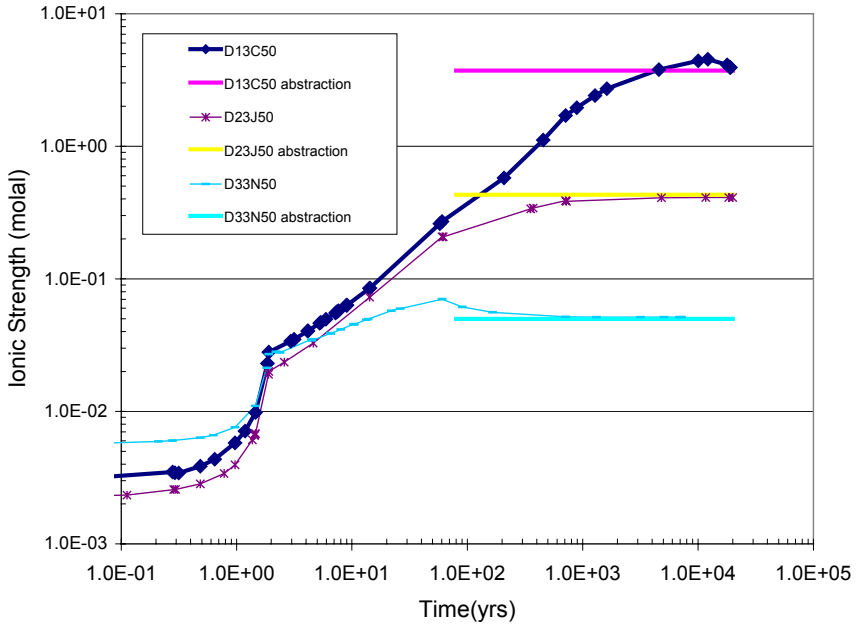

Source: Attachment V, Attachment V, CDNR_SDM_50.xls

Figure II-9. Validation of ionic strength abstraction to model output for 50°C CDNR

Table II-1. 21-PWR Waste Package Internal Component Dimensions

Component	Subcomponent	Dimension	Value (mm)
Inner Shell (1 per waste package)		Inner Diameter	1424

Component	Subcomponent	Dimension	Value (mm)
		Outer Diameter	1524
		inner height	4585
		Inner Shell Assembly height	4762
	bottom lid	thickness	88.9
	top lid	thickness	50.8
Fuel plate assembly (4 per waste package)	Fuel Basket A,B-Plate	Height	1396
	Fuel Basket A,B-Plate	Width	1134
	Fuel Basket C-Plate	Height	733.2
	Fuel Basket C-Plate	Width	1134
	Fuel Basket D,E-Plate	Height	1394
	Fuel Basket D,E-Plate	width	1132
	A,B,& C plates	thickness	7
	D & E Plates	thickness	5
Fuel Basket Tube (21 per waste package)		Length	4575
	exterior dimension	width, height	236.4
	interior dimension	width, height	226.4
Side Corner-Guide Stiffeners (4 per waste package)	Basket A Stiffener (64 per waste package)	height	77.8
		width	209.2
		thickness	10
	Basket B Stiffener (32 per waste package)	height	91.7
		width	216.4
		thickness	10
	Basket C Stiffener (32 per waste package)	height	227.3
		width	227.3
		thickness	10
Basket A-Sideguide (32 per waste package)		width	236.3
		height	89.7
		length	1134
		thickness	10
Basket B-Sideguide (16 per waste package)		width	236.4
		height	93.4
		length	1134
		thickness	10
Basket Cornerguide (16 per waste package)		width	243.4
		height	243.4
		length	1134
		thickness	10

ATTACHMENT III.

Radiolysis contribution to in-package chemistry

Radiolysis is a potentially important process which could influence the results of the in-package chemistry model. A non-mechanistic treatment in the form of a sensitivity analysis is provided here to examine how radiolysis could effect the pH and concentration of certain aqueous species. All of the pertinent computer files may be found in Attachment V.

Data and Parameters

- *Gamma and Neutron Radiolysis in the 21-PWR Waste Package from Ten to One Million Years* (BSC 2002b). Nitric acid (HNO_3) production rate at 500 years (assuming waste package failure) is 3.60E+13 molecules/yr-cm^3 (air) (BSC 2002b, Table 21, p. 33). This time was selected because it is the earliest failure, representing juvenile failure of the waste package. Figure 5 of this reference shows that the production is constant after 500 years so the selection of this time is not critical.

- Geometry of CSNF waste package: Volume = 4968751 cm^3, 10 percent fuel exposed surface area = 3297160 cm^2, void volume with 0.25-cm thick water film = 4144461 cm^3, from CSNF.xls, Attachment I.

- Surface area normalization factor for 10 percent fuel exposure = 1.213E-03, from CSNF.xls, Attachment I.

- G value for nitric acid production is 1.5 molecules/100 ev energy deposition (BSC 2003b, p. 27). The G value represents the number of molecules formed from radiolysis in a material and is linear with energy deposition. This number is used to calculate hydrogen peroxide (H_2O_2) generation by scaling (first bullet).

- Density of moist air (40 percent RH, 30°C) is 1.16E-3 gm/cm^3 (see Attachment I, Microsoft Excel file csnf_radiolysis.xls, Sheet MoistAir, Cell H14). This number is used to calculate hydrogen peroxide generation by scaling the first bullet, above.

- G value for hydrogen peroxide production is 0.72 molecules/100 ev energy deposition. This value is presented in *Waterside Corrosion of Zirconium Alloys in Nuclear Power Plants* (IAEA 1998, Table 8.2, p. 214). This value is corroborated by Christensen (1995, p. 375, Table II), Christensen et al. (1994, p. 6, Table 1) and Christensen and Bjergbakke, (1982, Table 1, p.16) G value is 0.74 molecules/100 ev energy.

Other accepted engineering numbers:

- Avogadro constant = 6.02E+23 molecules/Mole

- Density of water at 27°C = 1 gm/cm^3

Assumptions

- It is assumed that the nitric acid production and hydrogen peroxide production is represented by the production rates at 500 years. This assumption is conservative because 500 years is the earliest waste package failure time because of early failures and radiolysis generally decreases with time. Figure 5 of *Gamma and Neutron Radiolysis in the 21-PWR Waste Package from Ten to One Million Years* (BSC 2002b) shows that gamma dose and therefore most of the radiolysis is nearly constant after 500 years. This assumption needs no further validation.

- It is assumed that the nitric acid that is produced in the humid air by radiolysis is absorbed into the films of water on the fuel and none escapes the waste package through the corrosion patches. This assumption is conservative because it is the upper limit of the amount of nitric acid that can be absorbed on the fuel. This assumption is necessary because modeling of chemical diffusion rates on this scale is not available. This assumption is conservative and needs no further validation.

- It is assumed that the radiolysis production in the outer eleven fuel assemblies of the 21-PWR design can be approximated by the radiolysis in the middle nine assemblies. *Gamma and Neutron Radiolysis in the 21-PWR Waste Package from Ten to One Million Years* (BSC 2002b) gives analysis of the production in the center assembly of the waste package only. Radiation fluxes and therefore radiolysis production rates are less in the outer assemblies. This assumption is conservative and needs no further validation.

- It is assumed that other than the generation of nitric acid and hydrogen peroxide there are no other collateral chemical effects on the in-package environment. This assumption is justified because HNO_3 and H_2O_2 have the greatest potential to alter the in-package chemistry.

Model Discussion

When radiation passes through a material, some energy is deposited in the medium and chemical reactions can occur from the local deposition of energy (radiolysis). The G value represents the number of molecules of a substance that is formed when 100 ev of energy is deposited in the media. When gamma and fast neutron energy pass through moist air, nitric acid is produced. *Gamma and Neutron Radiolysis in the 21-PWR Waste Package from Ten to One Million Years* (BSC 2002b) predicts the amount of nitric acid that is produced per cm^3 of humid air in the waste package (3.6E+13 molecules/yr-cm^3 at 500 years). The amount of nitric acid formed in the waste package is calculated in EQ6 compatible input units via:

HNO_3 production rate = 3.6E+13 molecules/yr-cm^3 * (void volume waste package)

= 3.6E+13 molecules/yr-cm^3 * (4144461 cm^3)

= 1.49E+20 molecules/yr-waste package * (1 mole/6.02E+23 molecules)

= 2.48E-04 moles/yr-waste package * (1.213E-03) * (1 year/3.16E+07 seconds)

= 9.53E-15 moles/second

Where, 1.213E-03 is the normalization factor from Table 47.

When gamma and fast neutron energy pass through water, hydrogen peroxide is produced. The production rate for hydrogen peroxide (H_2O_2) in water is calculated by adjusting the nitric acid production rate by the ratio of G values and densities and converting to EQ6 compatible input units:

H_2O_2 Production Rate = PR_{HNO3} * (G_{H2O2} / G_{HNO3}) * (Density water/Density air)

= 3.6E+13 molec./yr-cm^3 * (0.72/1.5) * (1.0 gm/cm^3 / 1.16E-3 gm/cm^3)

= 1.5E+16 molec./yr-cm^3 * (4144461 cm^3)

= 6.22E+22 molecules/yr-waste package * (1 mole/6.02E+23 molecules)

= 1.03E-01 moles/yr-waste package * (1.213E-03) * (1 year/3.16E+07 seconds)

= 3.97E-12 moles/second

Where, 1.213E-03 is the normalization factor from Table 47.

EQ6 Implementation

The effect of radiolysis on the in-package chemistry was handled in a non-mechanistic manner, i.e., EQ6 does not have the facility to model the radiolysis process directly, therefore, only the products of radiolysis are included as inputs in EQ6 simulations. However, EQ6 does have the capability to model the effect of H_2O_2 and HNO_3 on the in-package chemistry.

A series of runs were performed where nitric acid and hydrogen peroxide were included as inputs in EQ6 runs and the results of these simulations were compared to their non-radiolysis counterparts.

Two base-case runs (C12C25 and C22C25, Section 6.5.4) were used to test the effects of radiolysis. These runs were chosen because they represent the median fuel exposure(clad failure) value and the low and median flux values. It would be expected that the effects of nitric acid and hydrogen peroxide additions would be greater at the low end of the flux range.

Two simulations were performed for each file, the first using the base-case nitric acid and hydrogen peroxide rates listed above, and a second where the HNO_3 and H_2O_2 rates were multiplied by a factor of ten. The EQ6 inputs are listed in Table III-1.

Table III-1. EQ6 File Names and Nitric Acid and Hydrogen Peroxide Production Rates

EQ6 Input File	HNO_3 Rate (mol/s)	H_2O_2 Rate (mol/s)
C22C25	0.0	0.0
C22CBC	9.53E-15	3.97E-12
C22BC10×	9.53E-14	3.97E-11
C12C25	0.0	0.0
C12CBC	9.53E-15	3.97E-12
C12BC10×	9.53E-14	3.97E-11

Results

The results of the simulations are displayed in Figure III-1, where the pH profiles for the various runs are displayed versus time. These results show that neither the base case nor the 10X base-case generation rates of HNO_3 and H_2O_2 had an impact on the in-package pH. Therefore, it may be concluded that if radiolysis only effects the chemistry via HNO_3 and H_2O_2 generation, then it will not be a significant process with regard to influencing the in-package chemistry.

Table III-2 provides the ferric iron, chloride and hydrogen peroxide maximum concentrations for the simulations. Again the runs with HNO_3 and H_2O_2 input show little deviation compared to the runs without HNO_3 and H_2O_2.

Table III-2. Chloride, Ferric Iron, and Hydrogen Peroxide Molality

	Maximum Molalities		
EQ6 Input File	Cl^-	Fe^{+++}	H_2O_2(aq)
C22C25	6.6E-04	8.8E-11	3.7E-19
C22CBC	6.6E-04	8.8E-11	3.7E-19
C22BC10x	6.5E-04	8.8E-11	3.7E-19
C12C25	9.7E-04	5.3E-11	3.7E-19
C12CBC	9.6E-04	5.3E-11	3.7E-19
C12BC10x	9.2E-04	5.4E-11	3.7E-19

Based on this non-mechanistic approach to modeling the effects of radiolysis on in-package chemistry it may be stated that radiolysis will not effect the in-package chemistry in a manner that would impact TSPA. The results of these analyses are compiled in DTN: MO0304SPAICSCR.000.

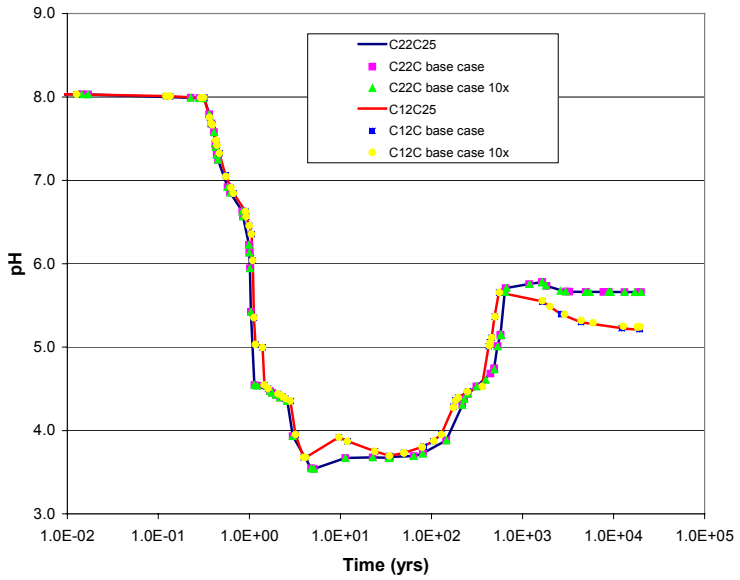

Source: csnf_radiolysis.xls, DTN: MO0304SPAICSCR.000.

Figure III-1. pH Profiles Showing how the Radiolysis Inputs Affect the pH

ATTACHMENT IV

EQ6 CSNF seepage dripping model input files for J-13 (C22J25.6i), Ca-porewater (C22C25.6i) and Na-porewater (C22N25.6i) run at three values of carbon dioxide partial pressure (10^{-4}, 10^{-3}, and 10^{-2}). The EQ6 input files and a summary excel spreadsheet are provided in Attachment V.

ATTACHMENT V.

CD-ROM